DOE/NASA/2749-79/3 Vol 3
NASA CR-159672
C00-2749-40

Conceptual Design Study of an Improved Automotive Gas Turbine Powertrain—Final Report

Edited By
C. E. Wagner and R. C. Pampreen
Chrysler Corporation
Detroit, Michigan 48288

June, 1979

Prepared for
National Aeronautics and Space Administration
Lewis Research Center
Under Contract DE-AC02-76CS52749

for
U.S. Department of Energy
Office of Conservation and Solar Applications
Division of Transportation Energy Conservation

DOE/NASA/2749-79/3 Volume 3
NASA CR-159672
C00-2749-40

Conceptual Design Study of an Improved Automotive Gas Turbine Powertrain Final Report

Edited By
C.E. Wagner and R.C. Pampreen
Chrysler Corporation
Detroit, Michigan 48288

June, 1979

Prepared for
National Aeronautics and Space Administration
Lewis Research Center
Cleveland, Ohio 44135
Under Contract DE-AC02-76CS52749

For
U.S. Department of Energy
Office of Conservation and Solar Applications
Division of Transportation Energy Conservation
Washington, D.C. 20545

Under Interagency Agreement EC-77-A-31-1040

Acknowledgement

This four volume final report covers work performed under DOE Contract No. DE-AC02-76CS52749 from November, 1972, to June, 1979. The contract was initiated by the U.S. Environmental Protection Agency, was subsequently transferred to the Energy Research and Development Administration, and was finally transferred to the Heat Engine Systems Branch, Division of Transportation Energy Conservation of the U.S. Department of Energy. Mr. Charles E. Wagner was the Chrysler Corporation Program Manager. Mr. Paul T. Kerwin, NASA-Lewis Research Center, has been the Project Officer since 1977. Previous Project Officers were David G. Evans, NASA-Lewis Research Center, and Thomas M. Sebestyen, EPA. Mr. Robert A. Mercure, DOE-Division of Transportation Energy Conservation, has been the Project Coordinator since the technical management was turned over to NASA-Lewis Research Center through an interagency agreement.

Contributors to this third volume were: R.W. Bloor, F. Dosenberger, A.A. Ladhani, D.S. Musgrave, R.C. Pampreen, L.J. Pritchard, N.W. Sparks, R. Swiatek (Design and Analysis); D.J. Bents, C.M. Elliott, C.H. Mader (Continuously Variable Transmission); C. Belleau, J.M. Corwin, W.L. Ehlers, F.A. Hagen and R.J. Warren (High-Temperature Materials); and D. Parrett (Cost Studies).

TABLE OF CONTENTS

	Page
Abstract	1
1.0 Summary	2
2.0 Introduction	4
3.0 Improved Upgraded Engine	5
3.1 Approach	5
3.2 Operating Line Change	5
3.3 Compressor Efficiency	5
3.4 Compressor - Turbine Efficiency	5
3.5 Power Turbine Efficiency	5
3.6 Parasitic Losses	5
3.7 Results	6
4.0 Advanced Powertrain Concepts	7
5.0 Advanced Powertrain Cycle Study	9
5.1 Analytical Approach	9
5.2 Compressor Efficiency Estimate	9
5.3 Axial Turbine Efficiency Estimate	10
5.4 Overall Power Turbine Efficiency Estimate	10
5.5 Radial Turbine Efficiency Estimate	10
5.6 Combuster	11
5.7 Regenerator Effectiveness	11
5.8 Pressure-Drop Losses	11
5.9 Heat Leak and Flow Leaks	11
5.10 Parasitic Engine Power	11
5.11 Transmission Characteristics	11
5.12 Two-Shaft Engine Results	12
5.13 Single-Shaft Engine Results	12
6.0 Advanced Powertrain Screening Analysis	13
6.1 Flowpath Review	13
6.1.1 Two-Shaft Engine	13
6.1.2 Single-Shaft Engine with Axial Turbines	14
6.1.3 Twin-Spool Gas Generator	14
6.2 Mechanical Design Review	14
6.2.1 Two-Shaft Engine	14
6.2.2 Single-Shaft Engine with Radial Turbine	15
6.2.3 Three-Shaft Engine	15
6.2.4 Concept Complexity Evaluation	16
6.3 Performance Review	16
6.3.1 Power-Turbine-First	17
6.3.2 Two-Shaft Engine with Interconnection	17
6.4 Summary of Results	18
7.0 Final Evaluation of Advanced Powertrain	19
7.1 Single-Shaft Engine	19
7.1.1 Operating Line	19
7.1.2 Vehicular Fuel Economy	19
7.2 Two-Shaft Engine	20
7.3 Three-Shaft Engine with Interconnection	20
7.3.1 Operating Line Determination	21
7.3.2 Operating Line Results	22
7.3.3 Turbine System Comparison	22
7.3.4 Engine Performance	23
7.3.5 Vehicular Fuel Economy	23
7.4 Three-Shaft Engine with Twin-Spool Gas Generator	23
7.4.1 Operating Line Determination	24
7.4.2 Operating Line Results	24
7.4.3 Engine Acceleration Time Estimate	25
7.4.4 Engine Performance	25

TABLE OF CONTENTS (continued)

	Page
7.5 Preliminary Turbine Rotor Stress Analysis	25
7.6 Material Review	26
7.6.1 Superalloys	27
7.6.2 Ceramic Materials	27
7.6.3 Refractory Metals	28
7.6.4 Summary	29
7.7 Cost Studies	29
7.7.1 Cost Effective Upgraded Engine	30
7.7.2 Cost Comparison of Preliminary Concepts	30
7.7.3 Cost Comparison of One-, Two-, and Three-Shaft Engines	31
7.7.4 IGT Vehicle Cost Analysis	31
7.8 Concept Selection	32
7.9 Vehicle Performance	33
7.10 Control of Belt-Drive CVT	34
7.11 Marketing Analysis for Concept Selection	36
8.0 Development Plan	37
8.1 Program Risks	37
8.2 Program Plan	39
8.3 Task Definitions	40
9.0 Conclusions	43
References	44
Tables and Figures	
Appendix A, Vehicle and Duty-Cycle Characteristics	
Appendix B, Simulated Parts List	
Appendix C, Details of Program Plan	

ABSTRACT

This is the third of four volumes of the contract final report which summarizes all of the work performed in a government-sponsored Automotive Gas Turbine Development Program (D.O.E. Contract No. DE-AC02-76CS52749). In this third volume of the contract final report, an assessment is made of the potential for developing an Improved Gas Turbine (IGT) propulsion system. The design was based on the application of current and near-term technology in a concept targeted to enter production development by 1983. The study was directed toward defining automotive gas turbine concepts with significant technological advantages over the spark ignition (SI) engine. Possible design concepts were rated with respect to fuel economy and near-term application. A program plan was prepared which outlines the development of the IGT concept that best met the goals and objectives of the study. Identified in the program plan is the research and development work needed to meet the goal of entering a production engineering phase by 1983.

The fuel economy goal of the study was to show at least a 20% improvement over a conventional 1976 SI engine/vehicle system. On the bases of achieving the fuel economy goal, of overall suitability to mechanical design, and of automotive mass production cost, the powertrain selected was a single-shaft engine with a radial turbine and a continuously variable transmission (CVT). Design turbine inlet temperature was 1150°C. Reflecting near-term technology, the turbine rotor would be made of an advanced superalloy, and the transmission would be a hydromechanical CVT. With successful progress in long-lead R&D in ceramic technology and the belt-drive CVT, the turbine inlet temperature would be 1350°C to achieve near-maximum fuel economy.

1.0 SUMMARY

This volume of the contract final report presents the results of a study of an Improved Gas Turbine (IGT) propulsion system, based on the application of current and near-term technology in a concept targeted to enter production development by 1983. This study was directed toward defining automotive gas turbine concepts with significant performance advantages over the spark-ignition (SI) engine. Possible design concepts were rated with respect to fuel economy and near-term application.

The goals and objectives for the design of the IGT were:

1. At least a 20% improvement in powertrain thermal efficiency over a conventional 1976 SI-engine/vehicle
2. Noise and exhaust-emission levels within presently or projected legal requirements.
3. Reasonable initial cost and life-cycle cost of-ownership no greater than those for the projected equivalent SI engine/vehicle system.
4. Reliability, driveability, and safety equal to or better than the projected equivalent SI engine/vehicle system.
5. Clear potential for completing prototype engine-vehicle system tests by 1983 and being at a point where a decision on production engineering could be made.

Design studies were performed to assess the potential for improving the existing Upgraded Engine design to meet or exceed the above goals and objectives. The results showed that the gain in fuel economy was only 13% or 7 percentage points below the study goal. Therefore, alternate cycles and engine concepts were investigated.

The cycle study covered a range of compressor pressure ratios from 4.2 to 10 at cycle temperatures of 1052°C and 1350°C. The calculations were performed for single-shaft and two-shaft engine configurations only. The single-shaft engine was combined with a continuously variable transmission; the two-shaft engine was combined with a three-speed automatic transmission with a lockup torque converter.

The maximum values of fuel economy were achieved with the single-shaft engine; at 1350°C, the fuel economy was 15% greater than the study goal of 23.5 mpg. The selected design pressure ratio was 4.2; this was judged to be the best compromise between fuel economy and the anticipated stress levels for the turbine

The cycle study showed that the best fuel economy for a powertrain with a single-shaft engine is obtained at a pressure ratio between 4.2 and 5.5 for a turbine inlet temperature schedule determined by operation with constant turbine exit temperature. The optimum pressure ratio depends on the component efficiency levels. The difference in fuel economy between a design pressure ratio of 4.2 and 5.5 varies from zero to 0.4 mpg. Consequently, there is only a small impact of selected design pressure ratio on the fuel economy obtained with the single-shaft engine, for the assumptions of component efficiencies used in this study.

Following the cycle study, there was a screening analysis of the most promising concepts at the design conditions selected from the cycle study. The powertrain concepts included single-shaft, two-shaft, and three-shaft engines with suitable transmission combinations. Single-stage and two-stage compressors, single-stage radial and axial turbines, and multistage axial turbines were considered. The screening study included preliminary flowpath evaluation for impact on aerodynamic and mechanical considerations.

From the results of the screening study, four concepts were selected for final evaluation of powertrain performance and mechanical design The engines selected were. the single-shaft engine with a radial turbine, the two-shaft engine with a free power turbine with variable nozzle vanes, the three-shaft engine with interconnected turbine shafts, and the three-shaft engine with a twin-spool gas generator. The review of the four concepts was characterized by component matching calculations to determine the hottest turbine inlet temperature schedule consistent with restraints on surge margin and material properties

Preliminary stress analysis was conducted to evaluate disc stresses in axial and radial turbines. The results of the stress analysis showed high risk in the design of axial turbines for an engine with a design pressure ratio of 4.2. The risk is based on the high level of disc stresses due to thermal loads and on the lack of available space to insulate the bearings from the flowpath. These risks increase as design pressure ratio increases.

The results of the final evaluation showed that only the single-shaft engine with a CVT and the three-shaft engine with interconnecting shafts and a two-speed manual transmission met and exceeded the fuel economy goal of the study. At a design-point pressure ratio of 4.2:1, the single-shaft engine could meet the goals at a turbine inlet temperature as low as 1050°C. At the same design pressure ratio, the three-shaft engine could only meet the goal at 1350°C. These results are based on the assumptions of component efficiencies, parasitic losses, and heat and flow leaks used in the powertrain performance estimates, along with the assumptions of transmission efficiencies and performance characteristics.

On the bases of fuel economy, of overall suitability to mechanical design and of automotive mass production cost, the powertrain selection is a single-shaft engine with a radial turbine and a continuously variable transmission; design turbine inlet temperature is 1150°C. This powertrain concept was judged to best meet the goals of a development program for the Improved Gas Turbine.

With advanced superalloys, a development program could be planned with a limited-life turbine designed for 1150°C. This would allow time for development of a practical CVT and for development of ceramic materials with strength properties suitable for design application to achieve maximum powertrain fuel economy at 1350°C.

The CVT configuration selected for use on the powertrain is a belt-drive CVT. This was selected as being the most practical type of CVT for automotive application, since it is simpler than the hydromechanical types and requires smaller driving forces than the traction type. The selection of the belt-drive CVT is based on the reductions in cost and noise compared to a hydromechanical CVT. Analysis indicated that a transmission based on use of variable-speed V-belt could be produced at about two-thirds the cost of a hydromechanical unit and would not likely require development to achieve acceptable noise levels.

A program plan was prepared which identified the research and development work needed to bring the single-shaft powertrain to the production engineering phase by 1983.

The engine would be designed for 77 hp (unaugmented) with a maximum power of 85 hp (augmented), a design turbine inlet temperature of 1150°C, a design pressure ratio of 4.2, and a metallic single-stage radial turbine. The CVT would be either a hydromechanical type or a belt-drive type, depending on the outcome of the transmission development. The selected vehicle has an inertia weight of 2750 lbs. with front wheel drive. The fuel economy goal is 30.4 mpg, based on gasoline.

The program would be carried out in two parts. In the first part, the design turbine inlet temperature will be 1040°C to permit development of the shafting, bearings and gears and to allow demonstration of the aerodynamic efficiency levels with metallic static parts. The maximum power would be 68 hp. In the second part of the program, the turbine will be reconfigured for a design turbine inlet temperature of 1150°C. The combustor and turbine static components will be made of ceramic materials for this temperature. The compressor will not change, but the turbine must be redesigned aerodynamically to properly match with the compressor and deliver a higher maximum output power of 85 hp.

The long-lead R and D items in the program are a ceramic radial turbine and a belt-drive CVT. To achieve the long-term ultimate fuel economy goal, it will be necessary to make the turbine out of ceramic material. To accomplish this, however, the ceramic material must have the needed mechanical properties and be capable of low-cost processing. A method of attaching ceramic material to a metal shaft must also be developed.

2.0 INTRODUCTION

This is the third of four volumes of the contract final report which summarizes all of the work performed in a government-sponsored Automotive Gas Turbine Development Program (D.O.E. Contract No. DE-AC02-76CS52749). Volume 1 presents the results of work performed with a Baseline Engine. Testing was carried out on this engine to document the state-of-the-art of the automotive gas turbine engine at the start of the program in 1972 and to conduct tests on certain component improvements. Volume 2 summarizes the design and development work on an Upgraded Engine, which incorporated the component improvements of the Baseline Engine. This third volume presents the results of a study for an Improved Gas Turbine (IGT) propulsion system which employs the development results from the Upgraded Engine and advanced concepts in materials and mechanical design. Volume 4 reviews the state-of-the-art of high temperature materials (superalloys, refractory alloys, and ceramics) as of 1978 and provides the materials technology background for the IGT study.

The purpose of the IGT study was to apply current and near-term technology to define a propulsion system configuration targeted to enter production development by 1983. This study was directed toward defining automotive gas turbine concepts with significant performance advantages over the spark-ignition (SI) engine. Possible design concepts were rated with respect to fuel economy and near-term application.

The goals and objectives for the design of the IGT were:

1. At least a 20% improvement in powertrain thermal efficiency over a conventional 1976 SI-engine/vehicle.

2. Noise and exhaust-emission levels within presently or projected legal requirements.

3. Reasonable initial cost and life-cycle cost-of-ownership no greater than those for the projected equivalent SI engine/vehicle system.

4. Reliability, driveability, and safety equal to or better than the projected equivalent SI engine/vehicle system.

5. Clear potential for completing prototype engine/vehicle system tests by 1983 and being at a point where a decision on production engineering could be made.

In carrying out the design studies, two categories of technology were considered:

1. Existing technology which had not been previously applied to this class of turbine, and

2. Currently-evolving (near-term) technology which was reasonably expected to become available in time to support the completion goal of the program.

Examples of Item 1 are: increased cycle pressure ratio (>4) and radial turbines. Examples of Item 2 are: continuously variable transmission, ceramic material, and high-temperature air bearings. In these studies, due consideration was given to the marketability in establishing design trade-offs relative to fuel consumption, costs, and performance.

Design studies were first performed to assess the potential for improving the existing Upgraded Engine design to meet or exceed the above goals and objectives. The results showed that the gain in fuel economy was only 13% or 7 percentage points below the study goal. Therefore, alternate cycles and engine concepts were investigated to achieve the fuel economy goal.

3.0 IMPROVED UPGRADED ENGINE

3.1 Approach

The evaluation of the potential for an improved Upgraded Engine to meet the IGT fuel economy goal was based on changes in TIT schedule and small increases in component efficiency targets. Although some of the targets were not realized in actual engine performance, it was assumed that the original goals could be met with changes in aerodynamic design or in engine mechanical design. These changes and the use of near-term technology are discussed in this section along with the estimated increase in fuel economy.

3.2 Operating Line Change

The maximum turbine inlet temperature was increased from 1050°C (1925°F) to 1150°C (2100°F). It was assumed that the turbine material would change from MAR-M-246 to the Pratt & Whitney RSR superalloy. At off-design, the turbine inlet temperature was increased such that off-design temperatures were closer to design-point temperature than the off-design values for the Upgraded Engine. This was accomplished by specifying constant power turbine inlet temperature instead of constant outlet temperature. A check with the steady-state surge line of the compressor allowed this. In addition, it was assumed that the combustor and vortex-chamber material would be made of ceramic material. Maximum power was reduced from 104 hp (unaugmented) to 91 hp (unaugmented) to be consistent with the specified vehicle performance goals. The compressor-turbine inlet and power turbine outlet temperature schedules are shown in Figure 1.

3.3 Compressor Efficiency

Along the engine operating line, the compressor efficiency of the Upgraded Engine ranges from 2 points above to 2 points below the goal values from 50% to 100% speed. Test data shows that this is partially attributable to installation effects of the asymmetrical collector and possible clearance effects due to housing deflections under actual engine operating conditions in contrast to thermal distortion under test rig conditions. It was expected that, upon mechanical redesign, these influences could be sufficiently eliminated. To enhance the achievement of the goal efficiencies for the Improved Gas Turbine, the specific speed was increased by 20%. The compressor efficiency variation along the engine operating line is shown in Figure 1.

3.4 Compressor-Turbine Efficiency

Analysis of engine test data shows that the efficiency of the compressor-turbine of the Upgraded Engine is 3.5 points below goal. A correlation of turbine efficiency with work coefficient (Reference 1) for small turbine blade heights (about 1.2 cm) shows that the original efficiency goal was one point above the data of existing small turbines. This puts the compressor-turbine 2.5 points below the level achieved by some of the small turbines used in the correlation. It was assumed that final design adjustments with the nozzle and rotor would permit the turbine to achieve the intended goal. Development time was not available for adjustments such as stagger changes or blade shape changes for optimum incidence angle. It was further assumed that the running clearance could be reduced in half through the use of ceramic shrouds. The build clearance is 2% of the blade height. A reduction in clearance of one-half would increase efficiency by 2 points This gives a value of turbine efficiency which is 1 point better than the goal for the Upgraded Engine turbine. To evaluate the fuel economy potential for the Upgraded Engine, therefore, the variation of compressor-turbine efficiency along the operating line was assumed to be 1 point better than the target values of the Upgraded Engine. The compressor-turbine efficiency variation along the operating line is shown in Figure 1.

3.5 Power Turbine Efficiency

Based on engine data, the efficiency of the power turbine is 4 points below goal. It was assumed that the original goal could be met with development work such as blade stagger changes or other modifications to optimize reaction and incidence angle. It was further assumed that the running clearance could be reduced with the use of ceramic shroud material and that efficiency would increase by 2 points Therefore, for the evaluation of the fuel economy potential of the Upgraded Engine, the variation of power turbine efficiency along the operating line was assumed to be 2 points better than the target values of the Upgraded Engine. The power turbine efficiency variation along the operating line is shown in Figure 1.

3.6 Parasitic Losses

Engine heat and flow losses, pressure drops, and power parasitic losses were maintained at the absolute levels of the Upgraded Engine, even though the engine size would be smaller. This assumed that there would be minor, if any, change with engine scaling.

3.7 Results

The scheduling of the component efficiencies and the TIT shown in Figure 1 and the use of the parasitic losses of the Upgraded Engine, as described above, were used to compute engine power and BSFC from 50% to 100% speed. The engine charcteristic was combined with the performance of a 3-speed automatic transmission with a lockup torque converter (1-2 upshift). The vehicle description and duty-cycle characteristics are detailed in Appendix A.

The resultant vehicular fuel economy for the combined drive cycle is 20.4 mpg. This is 13% below the value of 23.5 mpg, which was specified as the goal of the study. Consequently, alternate engine cycles (higher pressure ratio and TIT) and powertrain designs (single-shaft and 3-shaft) were investigated to achieve the fuel economy goal.

4.0 ADVANCED POWERTRAIN CONCEPTS

This section describes the advanced powertrain concepts that were considered and the method of final concept selection. The concepts consisted of single-shaft, two-shaft, and three-shaft engine configurations with appropriate transmissions. Each engine had more than one possible type of turbomachinery configuration. Figure 2 shows a schematic presentation of the basic engine concepts and shaft arrangements considered in the alternate powertrain study.

The left-hand column of Figure 2 shows the conventional two-shaft engine with a free power turbine. Variable inlet guide vanes (VIGV) are employed at the compressor inlet to augment engine power at design speed and to provide load-control at 50% speed. Variable power turbine nozzles are used to establish high inlet temperatures at off-design conditions through variable work extraction. The compressor could have one or two stages. One stage was considered for pressure ratios up to and including 5:1; two stages were considered for pressure ratios greater than 5:1. The compressor-turbine could have one or two stages, depending on the trade-off on the level of compressor work and turbine efficiency. The power turbine might have one or two stages, depending on the cycle pressure ratio and the desire for good turbine efficiency.

The next concept in the left-hand column of Figure 2 is a two-shaft engine with the power turbine placed before the compressor-turbine. This powertrain arrangement permits the turbomachinery to be supported by a single structure. This offered potential savings in size and cost relative to the conventional two-shaft engine. The variable nozzles on this concept are on the compressor-turbine.

The last concept in the left-hand column Figure 2 shows a two-shaft engine with a mechanical interconnection. Power transfer through the interconnecting shafts was investigated as an alternative to variable power turbine nozzles for possible efficiency improvement with the absence of nozzle clearance loss.

The middle column of Figure 2 shows single-shaft engine concepts. The compressor would have one or two stages depending on cycle pressure ratio, as stated above. The turbine could be a single-stage radial turbine or a two- or three-stage axial turbine, depending on cycle pressure ratio and turbine efficiency levels associated with the values of work required at high cycle pressure ratios. The engine power would be augmented at design speed and regulated at 50% speed by variable inlet guide vanes. The powertrain would require a continuously variable transmission.

Three arrangements of three-shaft engines were possible, as shown in the right-hand column of Figure 2. The first concept shows a version of the conventional two-shaft engine in which the gas generator is a twin-spool arrangement. This eliminated the need for variable inlet guide vanes, provided the potential for slightly higher cycle pressure ratio at off-design speeds (than a single-shaft gas generator), and allowed potentially higher off-design cycle temperature due to potentially higher surge margin. Compressor efficiency was expected to be higher because of the absence of the variable inlet guide vanes. In the alternate arrangement shown in the middle of the right-hand column, the inner spool could be directly coupled to the power turbine, thus eliminating the variable power turbine nozzles. However, as with the single-shaft engine, this arrangement would require a continuously variable transmission.

Lastly, a three-shaft arrangement, like that described in Reference 2, was examined. This arrangement requires variable inlet guide vanes and power turbine nozzles, but it has potentially higher turbine efficiency since the work is distributed among three stages. It also eliminates the torque-converter heat loss of the automatic transmission. The rotative speeds of the three shafts are linked together through a planetary gear set. In this arrangement, an auxiliary turbine assists the compressor-turbine and the power turbine. The latter is brought to a complete stop when the vehicle is stopped. At idle operation, the accessories are driven off the auxiliary turbine, which drives at a much more efficient rotational speed than the power turbine of the two-shaft engine. Because torque is supplied by two turbines, the vehicle acceleration normally expected from the two-shaft engine is retained and may even be better.

These concepts were reviewed for their potential fuel economy, for practicality in automotive mass production, for potential turbine stress levels, and for expected production cost. The final selection was determined from (1) a cycle study from which the design pressure ratio was selected, (2) a screening analysis which was used to eliminate some concepts based on preliminary evaluations, and (3) a detailed performance review from which the final selection was made.

The cycle study was used to determine the design-point pressure ratio best suited to achieve optimum fuel economy. It was expected that this would not necessarily be the only criterion for the pressure ratio selection. Other considerations, such as engine response, complexity, and cost, would also influence the selection of design pressure ratio. To simplify the calculations, cycle analyses were carried out for single-shaft and two-shaft engines only. The operating lines were based on constant regenerator inlet temperature, and the thermodynamic conditions along the operating line were estimated from previous operating lines determined from compressor and turbine performance matching.

In the second part of the study, a screening analysis was carried out for the various powertrain designs described above at a design-point pressure ratio selected from the cycle study. Differing from the cycle study, the evaluation was based on assumed operating lines with constant power turbine (second-stage turbine) inlet temperature for the multi-shaft engines and an equivalent operating line for the single-shaft engine. Also considered in the evaluation were preliminary estimates of mechanical complexity. Performance estimates showed that four concepts merited a detailed performance review: a single-shaft engine, a two-shaft engine, and two three-shaft engines.

The third part of the advanced engine study evaluated these four concepts in more detail. The operating lines were based on maintaining constant turbine inlet temperature until surge or material thermal limits were reached. Performance estimates were made for the components, and in contrast to the cycle studies and the screening analysis, the operating lines were computed from component matching calculations. In addition, estimates were made for turbine rotor stress levels and expected production costs.

5.0 ADVANCED POWERTRAIN CYCLE STUDY

To determine the range of design-point pressure ratio at optimum fuel economy, it was necessary to use the entire engine operating line, since as shown in Fig 3 the majority of the automotive duty cycle is spent between 50% and 70% speeds. The analytical approach to the cycle study was to use an operating line model with scheduled values of mass flow, pressure ratio, TIT and component efficiencies made from dimensionless models of available engine operating lines. Off-design operating line values were adjusted as design-point conditions were varied. The design values of pressure ratio and TIT were varied to determine the pressure ratio and TIT combination that yields optimum fuel economy when the engine is matched to an appropriate transmission. The turbine inlet temperature schedule of these operating lines were determined by holding a constant value of power turbine exit (or regenerator inlet) temperature.

5.1 Analytical Approach

The pressure ratio range covered was from 4.2:1 to 10:1. Calculations were performed at maximum cycle temperatures of 1350°C and 1052°C. The higher value was selected as the anticipated limit for the structural strength of ceramic material. The lower value provided the contrast in levels of fuel economy for the limits of material properties of superalloys currently in practice and used for uncooled turbines

Estimates were made for the variation of component efficiency with design pressure ratio. The variation of efficiency with gas generator speed was modeled after the component efficiency schedules used for the Upgraded Engine. However, the peak efficiency of a given component was adjusted to match changes in efficiency due to aerodynamic influences, such as specific speed or work coefficient, as pressure ratio increases. The other values of efficiency along the operating line were also adjusted to maintain the same variation of efficiency with speed.

5.2 Compressor Efficiency Estimate

The variation of peak compressor efficiency was based on a correlation of polytropic efficiency versus specific speed (taken from Reference 3). In the definition of specific speed of this reference, the volume flow is represented by the square root of the product of the compressor inlet and exit volume flow rates; and the compressor input head is used instead of the output head.

Figure 4 shows the correlation taken from Reference 3 with data points added from automotive-type compressors. Most of the efficiencies are based on total-total pressure ratio. The Chrysler data is based on exit-static/inlet-total pressure ratio. However, for these data points, the difference between the total-total and static-total efficiency values is within 0.5 point. A line is shown in the data band for an upper limit for compressors with values of pressure ratio equal to or greater than 4:1. The upper line of the data band in Figure 4 is defined to be a line that identifies efficiency levels that are expected to be achieved on compressors with extensive development effort. The lower line of the data band defines efficiency levels that are expected to be achieved with minimum development effort, such as, diffuser vane stagger changes, rotor leading edge cut-back and minor redesign.

Note that the Chrysler compressors have the lowest specific speed, N_S', of all the automotive types and also of all aerospace types, except for three compressors designed for pressure ratios between 9:1 and 10:1. It was decided to raise the specific speed from 48 to 58 for the Improved Gas Turbine design. Using the lower line on the data band, the polytropic efficiency increases from 0.825 to 0.84. This corresponds to a change in adiabatic efficiency from 0.78 to 0.80 at 4:1 pressure ratio and from 0.79 to 0.81 at 3:1 pressure ratio. The latter is the point of peak efficiency on a 4:1 pressure-ratio automotive compressor.

To obtain efficiency estimates at higher pressure rations, the efficiency level at a specific speed corresponding to 8:1 pressure ratio was reviewed. The change in work alone lowers the value of N_S' from 58 to 40. The lower-band level of polytropic efficiency is 0.81, which corresponds to an adiabatic efficiency of 0.73. Figure 5 shows the 4:1 and 8:1 pressure-ratio points on a plot of adiabatic efficiency versus pressure ratio for constant values of polytropic efficiency. These points are shown on a line identified as "minimum development effort". It was assumed that polytropic efficiency would not change up to 4:1 pressure ratio. Beyond 4:1, it was assumed the efficiency would fall off, as shown by the straight line joining the 4:1 and 8:1 pressure ratio points. The same logic was applied to the upper level of the data band of Figure 4, and the result is identified as the "maximum development effort" in Figure 5. The lines were then extended to 10:1 pressure ratio for the cycle study. Also included is a line identified as "current level". This line is the result of applying the same logic to the lower-level line in Figure 4, but with the use of $N_S' = 48$ as the 4:1 pressure-ratio reference.

Figure 5 also identifies "maximum" and "minimum" development levels for two-stage centrifugal compressors. It was assumed in the cycle study that two-stage compressors would be considered for pressure ratios $\geq$ 6:1. This would give the best possible levels of compressor efficiency for the cycle study. The position was taken that, if the results showed best fuel economy at a pressure ratio less than 6:1, the study could not be faulted for assuming unreasonably low values of efficiency and, consequently, being biased against the possibility of using a two-stage compressor on cost alone

A check was made on the possible effect of Reynolds Number on overall efficiency. Figure 6 shows a plot of overall compressor loss versus Reynolds Number taken from Reference 4. Shown on the figure is the range of Reynolds Number that was expected to be covered in the study. As shown on the figure, no increase in overall loss was expected, due to viscous effects.

A final check on the effect of size was made with data presented in Reference 5. Figure 7, taken from Reference 5, shows the variation of efficiency with pressure ratio as a function of flow size. Sample checks with a compressor performance-estimating computer program with self-contained loss models showed that estimated efficiencies would be consistent with this plot

5.3 Axial Turbine Efficiency Estimate

Estimates of axial turbine efficiency were taken from a correlation of total-total efficiency with work coefficient as shown in Figure 8. Data on this plot were taken from turbines with pressure ratios from 2.0:1 to 3.9:1 and with blade heights from 0.56 to 2.90 cm. It was felt that this presentation (from 11 turbines) represented the efficiency levels expected to be achieved from the small, highwork turbines expected in the engine study. All the points on or within the data band are from turbines with blade heights from 0.56 to 2.77 cm.

The majority of the data fits within the lines shown on the plot. The 3 points below the lower line were not included in the band, because higher values of efficiency existed for data points inside the band for turbines of comparable blade heights and aspect ratios. The 2 points above the band came from a supersonic turbine for a pressure ratio 3.9:1. These points were not considered in the definition of the upper line, since they were not typical of the majority of the data

In the cycle study, it was assumed metal turbine rotors would be designed for a work coefficient of 2.0 and ceramic rotors for a value of 1.5. The upper line of the data band give efficiency values of 0.835 and 0.862 for values of work coefficient of 2.0 and 1.5 respectively. Efficiency values of 0.845 and 0.882 were used in the cycle study in anticipation of better clearance control with ceramic shrouds.

In the powertrain screening analysis, preliminary flowpaths were determined from calculations for mean-radius vector diagrams. The variation of efficiency with work coefficient was taken from the dashed line on Figure 8. It was assumed that the study should reflect values of efficiency that could be achieved with component development within the time period specified in the study. Placing the dashed line 1 point below the upper line of the data band provided a small amount of conservatism in the fuel economy estimates

5.4 Overall Power Turbine Efficiency Estimate

In the cycle study, the power turbine peak efficiency was assumed to range between 0.765 and 0.815. The lower value was assumed for a single-stage turbine, and the higher value was assumed for a two-stage turbine. These efficiencies are total-static values and include losses for interstage ducts and exhaust diffusers. Efficiency was not varied as a function of design pressure ratio, because it was assumed that the work coefficient of power turbines would be between 1.0 and 1.2, consequently, power turbine efficiency would be independent of design pressure ratio. These were estimates that would be confirmed or altered as needed in the powertrain screening analysis through the use of the loss model in Figure 8 and mean-radius vector diagram calculations

5.5 Radial Turbine Efficiency Estimate

Estimates for radial turbine efficiency were taken from specific speed data from Reference 6. Figure 9 was taken from this reference, and the expected range of specific speed is indicated on the total-static efficiency plot. For conservatism in the cycle study, it was assumed the efficiency would not exceed 0.88 or be lower than 0.85. In the final engine study, a more detailed check was made on a vector-diagram computer program with self-contained loss models

The upper level was assumed to represent the efficiency that would be achieved with extensive development work, and the lower level was assumed for minimum development effort. Since the efficiency does not change over the expected range of specific speed, radial turbine efficiency was not made a function of design pressure ratio.

5.6 Combustor

Combustor efficiency varied from 0.908 at 50% speed to 0.980 at design speed. This variation was used in all cycle calculations and was independent of design pressure ratio. It is necessary to achieve these values in order to meet emission requirements. A number of combustor configurations can meet these conditions. These include (1) a lean, premixed, prevaporized combustor with torch ignitor, (2) a catalytic combustor, and (3) a variable geometry combustor. Consequently, the efficiency values used in the calculations were not dependent upon a particular combustor type.

5.7 Regenerator Effectiveness

A regenerator was selected for the alternate engine study. The performance characteristics of a recuperator were not included in the study, because of the bulk normally required to achieve high values of effectiveness and because of the lack of published data showing values of effectiveness as high as those of a regenerator. The values of regenerator effectiveness used in the study were taken from the performance characterization of the Upgraded Engine. Until engine layouts could be made with the selected powertrain, it could not be established that lower values of flow per unit area (and thus higher values of effectiveness) could be employed.

5.8 Pressure-Drop Losses

The pressure-drop fractions of engine components, such as air filter, regenerator, combustor, and exhaust duct, were varied as a function of engine speed but were independent of design pressure ratio and flow size. The flowpath complexities at the engine intake and exhaust were assumed to remain unchanged with engine size. The pressure drops for the regenerator and combustor were determined by fuel economy and emission requirements and were assumed to be independent of engine flow size and pressure ratio.

5.9 Heat Leak and Flow Leaks

The heat leaks and flow leaks were assumed to have the same values as those of the Upgraded Engine. The design massflow for the Upgraded Engine is 1.3 lbs/sec, and it was assumed that the leaks would not change below this value of design massflow. The assumption is based on the rationalization that the major sources of flow leaks are the corners or gaps of the various seal elements; thus, they do not scale appreciably with the engine size. Similarly, the heat leaks are affected by the limited insulation space available with smaller components and because engine size does not allow scaling the insulation properly. The leak paths are as shown on Figure 10 for two-shaft engines and on Figures 11 and 12 for the regenerator. The single-shaft engines were characterized without the variable turbine nozzle vanes. The leak paths are similar to those of the gas generator of the two-shaft engine; the leak paths around the power turbine are nonexistent.

5.10 Parasitic Engine Power

The power requirements for the high speed bearings, the regenerator drive, the oil pump, and the alternator drive were specified to be identical with the requirements for the same components of the Upgraded Engine. It was assumed that these requirements would be independent of design pressure ratio and flow size for mass flows below 1.3lbs/sec flow rate. For the two-shaft engines, parasitic power varied from 2.8 hp to 50% speed to 10.8 hp at design speed. For the single-shaft engines, parasitic power varied from 2.3 hp at 50% speed to 8.3 hp at design speed. The reduction in power requirements was due to the bearing arrangements selected for each engine. The two-shaft engine had an oil thrust bearing, an oil journal bearing, and a gas journal bearing on the gas generator shaft and an oil thrust bearing and two oil journal bearings on the reduction gear pinion shaft. The single-shaft engine had gas thrust and journal bearings on the engine shaft and oil thrust and journal bearings on the reduction gear pinion shaft. The single-shaft engine used a smaller oil pump since oil was only needed for the reduction gear bearings.

5.11 Transmission Characteristics

The two-shaft engine was combined with a three-speed automatic transmission with lockup torque converter. Alternate transmission concepts, such as the continuously variable transmission (CVT), offer little fuel economy advantage since the two-shaft engine is relatively insensitive to moderate engine to vehicle speed ratio changes. The fuel consumption at a given output level is not strongly dependent upon the power turbine output speed at rotational speeds near maximum efficiency.

The single-shaft engine was combined with a continuously variable transmission. One type that was chosen for powertrain analysis was the traction type with regenerative torque feedback and a positive neutral position. The mechanical configurations of the drive for this type of CVT are shown in Figures 13 and 14. The transmission features are illustrated schematically in Figure 15. The transmission efficiency characteristics are shown on Figure 16. An additional gear ratio was added to the transmission to extend the range of high transmission efficiency availability.

The second type of CVT powertrain analyzed was the hydromechanical type. The basic mechanical configuration and operation are illustrated in Figures 17, 18, and 19. The performance characteristics of 2 configurations were used in the study. Figure 20 shows the Orshansky CVT configuration; the performance curves are shown in Figures 21 to 24. The other configuration was a Sundstrand CVT. The performance characteristics are shown in Figure 25.

The third CVT considered was the belt drive type. The mechanical description is illustrated in Figure 26. A fourth type is the chain drive as illustrated in Figures 27 and 28, but vehicle performance with this type was not calculated. Figure 29 shows the performance characteristics of all CVT types used in the study. A comparison of powertrain performance with the CVT versus discrete gear changes was also made. The engine/vehicle matching characteristics for a ten-speed gear set are shown in Figure 30.

5.12 Two-Shaft Engine Results

Maximum power was 75 kw (100 hp) with full VIGV augmentation. Design-point calculations were carried out at 68 kw (91 hp) in the unaugmented mode engine operation at design speed. Fuel flow rate at idle power was computed with thermodynamic conditions established with a preswirl value of +48° at 50% speed. The study goal was to achieve a composite fuel economy of 23.5 miles per gallon.

The variation of vehicle fuel economy with design pressure ratio is shown in Figure 31 for the two-shaft engine. Results are shown for design-point temperatures of 1052°C and 1350°C and for turbine efficiency values associated with ceramic turbines (work coefficient = 1.5) and maximum turbine development effort. The upper line of each design temperature set represents the results of calculations performed with efficiency values for one- or two-stage centrifugal compressors with maximum development effort. Single-stage efficiencies were used at pressure ratios less than or equal to 5:1, and two-stage efficiencies were used for pressure ratios greater than 5.1. The lower line of each set represents the results of calculations performed with efficiency values for single-stage compressors with minimum development effort.

As the plot shows, it was not possible to achieve the goal fuel economy with maximum development effort. The turbine inlet temperature schedule along the operating line was determined by specifying constant power turbine exit temperature. In the next part of the study (screening analysis), calculations considered the use of constant power turbine inlet temperature.

5.13 Single-Shaft Engine Results

The variation of vehicle fuel economy with design pressure ratio is shown in Figure 32. Results are shown for design-point temperature sets of 1052°C and 1350°C. The lower-temperature set represents results of calculations performed with turbine efficiency values obtained with minimum development effort. The upper line on this set represents the results of calculations performed with efficiency values for one- or two-stage centrifugal compressors with maximum development effort. The lower line represents the results of calculations performed with efficiency values for single-stage compressors with minimum development. The higher-temperature sets represent results of calculations performed with efficiency values from maximum (upper set) and minimum (lower set) compressor development efforts. The upper line of each set represents the results of calculations performed with efficiency values for radial turbines with maximum development effort. The lower lines represent the results of calculations performed with efficiency values for radial turbines with minimum development effort.

The maximum values of fuel economy are significantly above the goal value. As the plot shows, the fuel economy maximizes between 4.2:1 and 5.5:1 pressure ratios in a range of development effort between minimum effort for single-stage compressors and maximum effort for two-stage compressors. The arithmetic average of the two upper curves shows a maximum value of fuel economy to occur at 5:1 pressure ratio. The gain in fuel economy over the value of 4.2:1 pressure is about one-fourth mile per gallon. It was judged that this difference might be significantly reduced due to the added acceleration fuel required for the higher-inertia shaft of the higher pressure ratio cycle. It was also judged that the structural requirements for the ceramic turbine would be eased with the lower pressure ratio. Consequently, the design pressure ratio of 4.2:1 was selected.

6.0 ADVANCED POWERTRAIN SCREENING ANALYSIS

This section discusses the screening analysis for the advanced powertrain concepts presented in Section 4.0. The engine design conditions for the study were 75 kw (100 hp) with VIGV augmentation and 68 kw (91 hp) without augmentation. The goal was to achieve a value of 23.5 mpg in combined fuel economy with a 3500-lb vehicle. Design pressure ratio was 4.2:1, and design TIT was 1350°C, with two exceptions. The two-shaft engine was also evaluated at 6:1 pressure ratio and 1350°C TIT, and the two-shaft engine with interconnection was evaluated at 4.2:1 pressure ratio but 1150°C TIT. The analysis consisted of reviews of the flowpaths, of the mechanical designs, and of the performance estimates of the various concepts. From the screening analysis, four concepts were selected for more detailed examination of powertrain performance and mechanical design.

6.1 Flowpath Review

In the screening analysis, the turbine inlet temperature schedule of the two-shaft engine was revised as a step toward trying to get the fuel economy of this powertrain to be equal to the goal. The revised schedule was based on holding a constant value of power turbine inlet temperature, in contrast to holding constant turbine exit temperature as was specified in the cycle study. The results are shown in Figure 33 and show that the goal is just barely achieved for the two-shaft engine at 6:1 pressure ratio. All the concepts outlined in Section 4.0 were evaluated at 4.2:1 pressure ratio in the screening analysis, but a preliminary evaluation was also made at 6.1 pressure for the two-shaft engine.

The turbine section was the principal area reviewed in the screening analysis. Except for the twin-spool gas generator of one of the three-shaft engines, the compressor did not have any usual impact on the engine design. The use of ceramic material for the axial turbines provided an opportunity for designing compressor-turbines with lower values of work coefficient than would be allowed with the use of superalloys, coupled with the requirement for values of polar moment of inertia that would be consistent with desired engine response time. A number of flowpaths were examined to evaluate the impact of the configuration of the ceramic turbine stages on the mechanical design of such items as the engine housing, the shaft arrangement, the bearing supports, etc.

The assumptions used in the flowpath calculations were:

1. Maximum material strength of 280 MPa, independent of temperature up to 1350°C,
2. Mean-radius nozzle exit angle $\leq 74°$,
3. Efficiency set by dashed line in Figure 8,
4. Best compromise between compressor and turbine efficiencies,
5. Last-stage exit Mach No. ≤ 0.4,
6. Exhaust diffusers area ratio = 2.5,
7. Equal work for two- or three-stage turbines on the same shaft,
8. Zero exit swirl from each stage,
9. Blade heights equal to or greater than 1.25 cm.

The material strength was modeled after data shown in Reference 7, which showed, in Figure 3 of the reference, flexural strength varying linearly from 450 MPa to 520 MPa from 0°C to 1700°C, respectively. A design level of 280 MPa was selected on the basis of choosing a design margin of 1.8 at 1350°C. This was a tentative specification until more detailed stress analysis was carried out later in the engine study.

6.1.1 Two-Shaft Engine

Flowpaths of the two-shaft engines with variable power turbine nozzles are shown in Figure 34. The design pressure ratio is 6:1; the compressor would be a two-stage centrifugal compressor. The figure shows flowpaths with the power-turbine stages placed first and second in the shafting arrangement.

Included on the figure are the values of work coefficients arrived at to satisfy the conditions outlined above and for a minimum flowpath hub dimension of 2.5 cm. This was the smallest dimension allowed for the space anticipated for bearing and insulating material. A blade taper ratio of 1.6 was used for the stress calculation, and a blade root area was estimated from an existing turbine. The root stresses are indicated above the flowpath. With two-stage turbines, all values are less than the maximum of 280 MPa allowed.

The bottom of Figure 35 shows results with single-stage turbines for the case with the power turbine first. It was necessary to increase rotational speed 40% (relative to the 2-stage turbines of Figure 34) to have similar values of work coefficient and hub radius. Consequently, blade root stresses were about doubled, and efficiencies dropped 1.5 points.

If the cycle pressure ratio were 4.2:1, Figure 35 shows that the stresses reduce slightly, but efficiency increases about 2 points or more. Furthermore, the flowpath shows more room available for bearings and insulation Consequently, for axial turbines, the design pressure ratio of 4.2:1 shows a simpler and more promising mechanical design than that for the design pressure ratio of 6:1. The fuel economy difference shown in Figure 33 for the two pressure ratios could be reduced if the heat loss can be reduced at 4.2:1 pressure ratio and increased at 6:1.

6.1.2 Single-Shaft Engine with Axial Turbines

The flowpaths for a single-shaft engine with a two-stage and a three-stage axial turbine are shown in Figure 36, for a cycle pressure ratio of 4.2:1. There is no difference in efficiency between two and three stages, because of the work coefficient selections, but the blade root stresses are lower for the three-stage turbine. The mechanical design would be encumbered with small available space for bearings and insulation. similar to the two-shaft engine.

6.1.3 Twin-Spool Gas Generator

Only the three-shaft engine with the twin-spool gas generator was selected for review, since it showed more potential complexity than the other arrangement shown at the bottom of the right-hand column of Figure 2. The compressor flowpath is shown on Figure 37. The mechanical design of the compressor is complicated by the cross-over duct diffuser, and the engine response would have to be evaluated for the higher inertia of two rotors.

The turbine flowpath is shown in Figure 38. The overall total-static efficiency would be comparable to the efficiency of the three-stage turbine of the single-shaft engine in Figure 36, if it were not for the nozzle clearance loss. The clearance loss for all variable power turbine nozzles shown in this section is assumed to be 2 points. The blade root stress levels are much lower than those for the single-shaft engine. This is a result of being able to lower rotational speed due to the specific speed changes of the individual stages of the two-stage compressor in contrast to the specific speed of the single-stage compressor. The mechanical problem for this concept is the design of a bearing in the high-temperature area between the second and third stages to support the outer spool. This was examined in detail and is discussed below.

6.2 Mechanical Design Review

Studies of a number of engine concepts and arrangements were made to evaluate and compare mechanical features Preliminary layouts were made of several engines selected as being representative of typical arrangements. For the two-shaft engine, a layout was made to evaluate turbine interconnection as an alternative to variable power turbine nozzles. However, certain mechanical design problems are discussed that are applicable to any two-shaft engine. The three-shaft engine with the twin-spool gas generator was evaluated as being typical of three-shaft engines. However, some of the problems with the turbine complexity would be typical of any three-stage assembly, whether for a three-shaft engine or a single-shaft engine. The mechanical review is concluded with evaluations of concept complexity.

6.2.1 Two-Shaft Engine

A layout study of a two-shaft arrangement with a turbine interconnection was made, as shown in Figure 39. This engine was designed for 1150°C turbine inlet temperature. This should permit the use of advanced RSR superalloys for the turbine rotor. Assuming this metal is developed to its anticipated potential strength at the required temperature level, rotors of this material would have less risk for engine development than ceramic rotors. However, the small diameter of a 75 kw engine size gives rise to a fundamental design problem associated with proximity of the flowpath to the shaft and subsequent avoidance of excessive bearing and support temperatures. This is particularly true if the rear bearing is located forward of the turbine rotor! The forward location of an air bearing also

1. does not allow space for supporting and piloting a ceramic nozzle, and

2. would result in high air-bearing loads and questionable life, if a turbine interconnection shaft were connected to the rear of the compressor-turbine rotor.

An alternate air bearing location behind the rotor is also shown in Figure 39 below the engine centerline This will allow some space forward of the turbine for piloting the ceramic nozzle and reduce loads from the interconnection shaft. It is questionable, however if adequate cooling could be provided to maintain reasonable air-bearing temperatures during operation and after shutdown (soakback).

An arrangement with the power turbine positioned forward of the compressor-turbine was also considered. This permits the turbo-machinery to be supported by a single structure which offers potential savings in size and cost relative to a conventional two-shaft engine. However, the small axial nozzles and turbine rotors, along with the concentric shafts, will have essentially the same penalty in complexity and problems with bearing location and/or cooling, as described above.

6.2.2 Single-Shaft Engine with Radial Turbine

A study layout of a single-shaft engine with a radial turbine and dual-regenerators is shown in Figure 40. The single shaft is supported on an air-lubricated bearing, located between the turbine and the impeller, and an oil-lubricated bearing forward of the impeller. An air bearing was tentatively selected for the rear location, because higher operating temperatures at the bearing are expected with the increased cycle temperatures. An air bearing would be better able to tolerate these temperatures than an oil-lubricated bearing. A relatively large diameter shaft may also be used with an air bearing for better control of critical speeds without an excessive bearing horsepower loss. Additionally, the bearing support is simpler, since oil supply and drain lines are not required. An air thrust bearing was located just behind the impeller to provide the best possible control of impeller blade-to-shroud axial clearance. Two oil-lubricated journal bearings support the reduction gear pinion to minimize deflection and resulting gear noise. The pinion is connected to the rotor through a spline to reduce noise transmitted from the pinion to the rotor, which can, in turn, be a source of air-borne noise. The reduction gear pinion is retained axially with a thrust washer.

For an arrangement with a single-stage compressor, the turbine nozzle and rotor shrouds are both piloted from the compressor housing and bearing support to maintain good tip-clearance control. The shroud piloting details for this radial turbine engine will be discussed further in the next section and compared with an axial turbine arrangement. The air intake which is integral with the reduction gear housing supports the front rotor bearing. A two-stage gear set will be adequate for reducing rotor speed to transmission input speed. The bulkhead-regenerator crossarm section of the housing can be cooled with the compressor discharge air. A single-seal ring supported from the bulkhead and seating against the ceramic rotor shroud will minimize leakage past the turbine.

The single-shaft radial turbine arrangement is shown in more detail in Figure 41. The radial inflow gas path and the single-stage turbine rotor provide some latitude in the design of a relatively straightforward support structure for simple turbine rotor shroud and nozzle geometry. The components are piloted on the compressor housing through the molybdenum-alloy bolts to the insulator, the pilot ring, and the pilot ring support. The insulator can have slotted ears on the inside diameter, which can mate with radial pins on the pilot ring to provide piloting between the low-expansion insulator and the metal pilot ring.

The molybdenum-alloy bolts were selected to pilot and retain the nozzle and shrouds in position at 1350°C inlet temperature. A detailed thermal analysis considering the geometry and thermal expansion of the bolts, shrouds, and related components will be required to assure satisfactory performance of the system. Suitable protection against oxidation must also be developed for the molybdenum material. The development risks in this area, however, still appear to be considerably less than the risk entailed in the development of axial turbomachinery in this size.

Note that the air bearing and its support, which is integral with the compressor housing, are isolated from the flowpath. This reduces the cooling requirement for the bearing significantly. However, the relatively large diameter of the flowpath (inlet plenum) for the radial turbine also results in a size and weight penalty. This factor was included in the cost evaluations.

6.2.3 Three-Shaft Engine

A three-shaft, free-power turbine arrangement is shown in Figure 42, as a representative of multi-stage axial turbines with concentric shafts. Good turbine efficiency is highly dependent on minimizing rotor tip clearance. This is especially true for small-size axial stages; this means that to attain predicted engine performance, good turbine shroud piloting must be considered a critical factor. Additionally, practical automotive turbine engines must be regenerative, implying some measure of engine housing asymmetry, whether it be geometrical, thermal, or both. Therefore, maintaining good concentricity control between the turbine rotor and its shroud becomes difficult, at best, if the turbine rotor shroud is piloted from the control bulkhead section of the engine housing, while the support for the rotor shaft bearings is piloted from the front section of the housing. Consequently, one design goal for proposed axial turbines was to pilot the turbine shroud from the structure supporting the engine shaft.

This approach is shown in Figure 42. The compressor housing pilots both the bearing support (for the inner-spool) and the front pilot ring support for the inner-spool turbine rotor shroud. The rear pilot ring support (for the outer-spool turbine rotor shroud) is bolted to the bulkhead and also pilots the rear bearing of the outer-spool. The following comments relate to the above arrangement.

- The cooling requirements of both rear rotor shaft bearings will be critical, because of the close proximity of the flowpath to the bearings. The cooling air for the outer-rotor bearing will be a leakage past both gas generator turbine rotors.

- The ceramic nozzles, rotor shrouds, and pilot ring are complex and will require extensive machining to meet design requirements. Any clearance between the nozzle shroud and pilot ring must be considered a leakage.

- The ceramic front pilot ring support for the nozzles and turbine rotor shroud utilizes struts in place of the nozzle vanes for the support structure. This eliminates the usual conduction path from the nozzle directly to the bearing area. The struts should also be more reliable as a load bearing structure than nozzle vanes. This, however, must be verified with detailed analysis.

6.2.4 Concept Complexity Evaluation

The discussion above on complexity was limited largely to the turbine section of the engine concepts, as influenced by the turbomachinery arrangement. The complexity of other portions of the engine are also influenced by the engine concept and arrangements. This is summarized on Table 3.

In addition to the other items discussed above, "Split Nozzles" are listed as a complexity item. This is a negative factor for engines with multiple-stage axial turbine rotors on one shaft. Assuming the shaft is integral with both axial rotors to minimize rotor cost, the nozzle ring must be split diametrically for assembly.

Multiple shafts and spools also increase the manufacturing complexity for gearing and shafting; rotor balancing and quality control will be critically important with a large number of high-speed components. This was considered a significant negative factor for the three-shaft engine, since gear sets operating with high-speed shafting will complicate related areas of the engine, require stringent quality control, and increase the noise level.

The complexity in transmission requirements for the various engine concepts must also be included. If the standard three-speed transmission with a lockup torque converter used for a two-shaft engine is the basis for the comparison, the low-speed gear sets required for the three-shaft engine will be less complex; however, the gear sets, plus the variable-speed transmission (CVT) for the single-shaft engines, will be somewhat more complex.

In the area of controls, all engine concepts will require VIGV's, except for the engine with the twin-spool gas generator. The variable power turbine nozzle, along with an actuator and the related control system, are required for all two- and three-shaft engine concepts. Controls are also needed for the CVT required with the single-shaft engine.

The relative complexities of the single-shaft and three-shaft engines with their transmission systems are apparent in the schematics shown in Figure 43 and 44. The three-shaft engine as shown, however, requires another reduction gear set for reducing the power turbine shaft speed to a suitable transmission input speed. Some of the performance predictions and the required quantities of some of the significant mechanical components are listed on Table 4.

6.3 Performance Review

Aerodynamic calculations were performed for the turbines of the two-shaft engines with the power-turbine-first arrangement and with the interconnection. Efficiency estimates were obtained from vector diagram computer programs with self-contained loss models. The purpose of the calculations was to evaluate the prospect of gains or losses in efficiency at off-design conditions, brought about by these powertrain arrangements. Estimates were also made of gains in powertrain fuel economy due to changes in operating-line efficiency or pressure ratio schedules brought about by the turbomachinery concepts in the two three-shaft engine concepts.

6.3.1 Power-Turbine-First

Turbine blade flow angles were established with design-point calculations. Off-design calculations were then computed at idle power. Power turbine speed was 20% of design, and compressor-turbine speed was 50% of design. These are the off-design percentage changes that occur with the conventional two-shaft arrangement.

With the same turbine inlet temperature (burner exit), as specified for the conventional arrangement, it was not possible to have enough flow to obtain the work required of the compressor-turbine. In the reversed roles of these turbines, cycle mass flow is determined by the power turbine work requirements of output and parasitic powers. This work level establishes a pressure ratio available to the compressor-turbine. The mass flow and pressure ratio may be inconsistent with the performance characteristics of the compressor-turbine.

The characteristics were better matched by reducing the turbine inlet temperature by 390°C. As temperature is reduced, the available pressure ratio across the compressor-turbine is reduced and mass flow is increased. With a temperature reduction of 390°C, it was still not possible to drive the compressor. There was no assurance that continued reduction in temperature would yield the work to drive the compressor and parasitic losses, since compressor-turbine efficiency was only 0.53 in contrast to 0.78 for the conventional arrangement.

The source of the loss was large rotor incidence angle with values up to 44°. This was a result of trying to extract the work indicated by the imposed pressure ratio with variable nozzles. The imposed pressure ratio was 1.31 in contrast to 1.19 for the standard turbine arrangement.

It appeared that it might be necessary to increase the gas generator speed to achieve sufficiently satisfactory aerothermodynamic conditions to drive the compressor and the parasitic losses. An increase in speed and the low compressor-turbine efficiency both lead to reductions in powertrain fuel economy compared to the conventional two-shaft arrangement

6.3.2 Two-Shaft Engine with Interconnection

Calculations were made to compare the change in power turbine efficiency with a mechanical interconnection substituted for variable nozzle vanes. An equivalent power turbine efficiency was computed for the interconnected turbine arrangement. Since the interconnection allows output power to be supplied by both turbines, the equivalent power turbine efficiency was computed as a work-averaged value from the efficiency and output work contributions of the respective turbines.

Computations were carried out in vector diagram computer programs with self-contained loss models. The design-point conditions were identical for both turbine arrangements. Off-design results were different because the output power was partially supplied by both turbines in the interconnection arrangement. The ratio of gas generator speed to power turbine speed at design was 1.19. At 50% speed of the gas generator, the ratio was 1.03 for the power turbine with variable nozzles and 1.36 with interconnection.

At 50% speed, the total-total efficiency of the compressor-turbine dropped from 0.80 to 0.79, and the total-total efficiency of the power turbine increased from 0.83 to 0.84, with variable nozzles replaced by an interconnecting shaft. There was no difference between the original power turbine efficiency or the equivalent power turbine efficiency with interconnection. Examination of the aerodynamic losses showed that the power turbine blade profile loss increased as much as the nozzle vane loss was reduced due to the absence of nozzle clearance space. This occurred because the off-design mass flow increased with the increase in compressor-turbine work, and consequently, the power turbine inlet and exit Mach numbers increased, which increased the blade profile loss. As a result, there was no performance gain achieved with a change in mechanical arrangement from variable nozzles to mechanical interconnection.

6.4 Summary of Results

The results of the screening analysis show that certain concepts should be eliminated from further consideration, but others should be examined in more detail. The results are summarized as follows.

Single-Shaft Engine - The cycle study showed that this concept with the CVT gives the best powertrain fuel economy. The flowpath study showed that the turbine efficiency was higher with a radial turbine than a three-stage axial turbine. The mechanical design results showed the potential for less complexity and flowpath leakage with the radial turbine than with a multi-stage axial turbine. Before the final powertrain selection could be made, the stress levels of the radial turbine and the engine response time would have to be evaluated for this concept.

Two-Shaft Engine - The cycle showed that this concept has a powertrain fuel economy that is 12.8% mpg less than that of a powertrain with a single-shaft engine. Since fuel economy was improved with a higher off-design temperature schedule, further increases would be examined for additional fuel economy gain. The impetus for the effort was the fact that this concept is competitive with the powertrain with the single-shaft engine with regard to potential turbine stress levels and the availability of the three-speed automatic transmissio Until detailed stress analysis was carried out, it was assumed that the high tip speeds of the radial turbine would incur higher blade root and disc stress levels than those for the axial turbines of the two-shaft engine. The conventional configuration of the two-shaft engine would be used, since the positioning of the power turbine in front of the compressor-turbine or the use of interconnection yielded loss of fuel economy.

Three-Shaft Engine - Preliminary estimates of fuel economy gains were made from assumed changes in turbine efficiency and off-design pressure ratio for the two three-shaft configurations. The use of the three-shaft engine with interconnected shafting would depend upon the gain in fuel economy due to the gain in turbine efficiency and the added parasitic loss of the bearings of the third shaft. It was necessary to obtain an accurate operating line to evaluate this.

The use of the twin-spool gas generator concept would depend on the actual gain in off-design pressure ratio, as well as any increase in off-design temperature due to component matching. This also would require calculations to be performed for an accurate operating line. In addition, an estimate would have to be made of the response time of the gas generator because of the additional compressor.

On the basis of this review, four concepts were selected for detailed evaluation of powertrain performance and mechanical design. The engines selected were: the single-shaft engine with a radial turbine, the two-shaft engine with a free power turbine with variable nozzle vanes, the three-shaft engine with interconnected turbine shafts, and the three-shaft engine with a twin-spool gas generator.

7.0 FINAL EVALUATION OF ADVANCED POWERTRAINS

In this section, performance results are presented for powertrains with the single-shaft, two-shaft, and three-shaft engines. Component matching calculations were performed to define operating lines for maximum off-design temperature schedules with limitations based on a surge margin of 10% and maximum regenerator seal temperature of 1150°C. Results of these calculations are presented, together with the engine performance estimates. Comparison is made of stress levels in ceramic radial and axial turbines; in radial turbines, stress levels are compared for rotors with ceramic materials and superalloys. A materials review is presented to support the use of ceramic parts, and the results of cost studies are shown for the various concepts. A final engine selection is made, and vehicle performance is calculated with the powertrain containing the selected engine. Lastly, discussions are presented on the transmission control and on a marketing analysis for the selected powertrain concept.

7.1 Single-Shaft Engine

Performance estimates were made for the compressor and turbine, and an operating line was calculated from component performance matching. The resultant engine performance was combined with CVT characteristics to calculate the vehicular fuel economy. Results are presented with four types of CVT and a geared transmission with ten discrete gear changes.

7.1.1 Operating Line

Design and off-design performance characteristics for the turbine were determined from a vector diagram computer program with internal loss models. The compressor performance characteristics were scaled from the NASA test-rig results of the compressor for the Upgraded Engine. A scaled performance map from an actual automotive compressor was considered to be a better estimate of the surge and choke characteristics than computations from a compressor vector diagram computer program. This was especially true since the design pressure ratio and rotor backsweep angle would be identical.

Operating-line calculations were performed from 50% to 100% speeds in 10%-speed increments. The operating-line goal was to maintain the design-point turbine inlet temperature of 1350°C to as low a speed as possible until the regenerator inlet temperature reached 1150°C. The turbine temperature was reduced at speeds below this point, and the regenerator inlet temperature was held constant. Another limitation was that there should be at least 10% surge margin defined as:

$$S.M. = \left\{\left(\frac{W}{P_2/P_1}\right)_{O.L.} - \left(\frac{W}{P_2/P_1}\right)_{S}\right\} \Big/ \left(\frac{W}{P_2/P_1}\right)_{O.L.}$$

where: W - Compressor mass flow, lbs/sec
P - Pressure, lbs/sq. in.

subscripts: 1 - Compressor inlet
2 - Compressor exit
O.L. - Operating line point
S - Surge point

The resulting operating line is shown on Figure 45. The turbine inlet temperature was held constant at 1350°C from design speed down to and including 70% speed. At 50% and 60% speeds, the regenerator inlet temperature was held constant at 1150°C. Plots of operating line parameters are shown in Figure 46; engine performance for these parameters is shown in Figure 47.

7.1.2 Vehicular Fuel Economy

The vehicular fuel economy was computed with a traction-drive CVT with an assumed efficiency of 0.85 for the variable-ratio drive (cf Figure 29). The variation of transmission efficiency with vehicle speed is shown in Figure 48. The computed fuel economy was 27.0 mpg. This is 15% over the study goal of 23.5 mpg.

Because of the significant margin over the goal fuel economy, additional calculations were carried out to determine the powertrain sensitivity to the selected value of design-point turbine inlet temperature and to the type of CVT configuration. In these calculations, lower values of the design-point turbine inlet temperature were held constant to progressively lower values of off-design speeds. At design temperatures of 1200°C or less, the part-load turbine inlet temperature could be held constant without exceeding the regenerator material temperature limit of 1150°C.

The results are plotted in Figure 49, which shows the variation of combined fuel economy with design-point turbine inlet temperature and CVT configuration. The variation of fuel economy with design temperature was computed with a traction-drive CVT with a variable-ratio drive efficiency of 0.85. The variation of fuel economy with CVT type was compared at a design temperature of 1038°C. The vehicle power requirements were reduced from the specification in Appendix A by an average value of 5.3% from 20 mph to 50 mph. This represented the projected improvements in vehicle aerodynamics, driveline friction, and rolling resistance. The figure shows that the goal fuel economy can be achieved with a single-shaft engine at a design-point temperature as low as 950°C with a variety of CVT configurations.

Another type of transmission investigated was one with ten sets of discrete gear ratios. Calculations with this type of transmission were performed to evaluate the possibility of approaching the characteristics of a CVT with a large number of discrete gear changes. The CVT provides engine operation at the locus of the minimum BSFC over a given range of engine speeds. Figure 50 shows the variation of BSFC with power at various engine speeds for different values of turbine inlet temperature. Included on the plot is an operating line with constant outlet temperature. If fixed engine-to-vehicle speed ratios such as shown above in Figure 30 are used, the resultant road load BSFC operation is shown in Figure 51. The fuel economy is compared to that of the powertrain with the CVT in Figure 52. The fuel economy loss is up to 30% with use of discrete gears. This confirms the need to have a CVT to provide the engine speed required for minimum BSFC at the power levels demanded by the vehicle driving requirements.

7.2 Two-Shaft Engine

Performance estimates were made for the compressor and turbines, and an operating line was calculated from component performance matching. The resultant engine performance was combined with the performance characteristic of a three-speed automatic transmission with lockup torque converter to determine vehicular fuel economy. Vehicle power requirements were those defined in Appendix A.

Design and off-design performance characteristics for the turbine were determined from vector diagram computer programs with self-contained loss models. The compressor performance chacteristics were scaled from the NASA test-rig results of the compressor for the Upgraded Engine, for the reasons stated above. Design pressure ratio was 4.2:1.

Operating line calculations were performed at 50%, 80%, and 100% speeds. Design-point turbine inlet temperature could only be maintained down to 90% speed. At 80% speed, it was necessary to reduce the turbine inlet temperature of the two-shaft engine in order to meet the 10% surge-margin requirement. With this restraint, the limit of 1150°C for the regenerator inlet temperature was never reached. Plots of operating line parameters are shown in Figure 53. Engine performance is plotted in Figure 54. The computed fuel economy is 22.6, or 4% below the goal of the study. The variation of transmission efficiency with vehicle speed is shown in Figure 55.

The difference in fuel economy between the powertrains with the single-shaft and two-shaft engines is due to power requirements for the transmission and the accessories, to bearing parasitic losses, and to heat and flow leaks. As an example, a comparison of power requirements at idle is shown on Table 5. These values typify the differences in power requirements through the engine operating range for the two powertrains. One-third of the combined fuel economy is determined by idle fuel flow. Table 6 shows the variation of turbine flow leakage for the two engines over the engine operating range. The higher values of leakage for the two-shaft engine are due to leakage down the stems of the variable nozzles, the leakage between stages, and the flow bypassing the power turbine.

7.3 Three-Shaft Engine with Interconnection

Performance estimates were made for the compressor and turbines, and an operating line was calculated from component performance matching. The resultant engine performance was combined with a two-speed manual transmission; gear ratios were 2:1 and 1:1. Vehicle power requirements were those defined in Appendix A. A schematic of the turbine arrangement was shown above in Figure 44.

7.3.1 Operating Line Determination

The three-shaft engine with interconnecting shafts differs from the two-shaft engine in that the engine mass flow is not determined by the work required of the compressor drive turbine. In the single-shaft engine, the mass flow is determined by not only the compressor work but also the output, parasitic, and accessory-load works. In the three-shaft engine arrangement with inter-connection, the auxiliary turbine assists the compressor-turbine and power turbine. Consequently, the work capacity of the compressor-turbine is less than the compressor work and the equilibrium running conditions at a given mass flow are established by the correct work split between the power turbine and auxiliary turbine. This is illustrated schematically in Figure 56, which shows the calculation paths for estimating the equilibrium running conditions for each of the engine arrangements.

Figure 56A shows the calculation path for the single-shaft engine. The compressor and turbine performance characteristics are illustrated in schematic representations of pressure ratio versus mass flow and work versus mass flow, respectively. With an assumed compressor flow, the compressor work is known. To this is added the required output work and the estimated values of bearing work and accessory load; further correction is made for flowpath leaks and the addition of fuel. For equilibrium, the total work required of the turbine must be consistent with the flow capacity of the turbine at this work level. If not, the match point on the compressor map is adjusted until convergence is achieved. Upon convergence, the mass flow of the engine is established at a given engine rotational speed.

Figure 56B shows the calculation path for the two-shaft engine. The performance characteristics of the compressor and compressor-turbine are illustrated in the same schematic representation as Figure 56A. The matching calculation proceeds in the identical manner described above except that the output and accessory works are on a second turbine. At off-design speeds, the off-design work required of the turbine for the single-shaft engine is a higher fraction of design-point work than is the off-design work required of the compressor-turbine of the two-shaft engine. As Figures 56A and 56B show, the mass flow for the two-shaft engine would be proportionately lower, and, hence, the operating line would be closer to the surge line.

Upon calculation convergence, the mass flow for the power turbine is established. The pressure ratio is also determined, since the exit total pressure from the compressor-turbine is known, and the exit static pressure at the exhaust diffuser exit has been estimated from the pressure drops in the tailpipe and regenerator core. The variable power turbine nozzle is adjusted until the vector diagram extracts the work consistent with the pressure ratio and the efficiency estimated from the computer program loss model. In the two-shaft engine, then, two iterations are required. One iteration is the compressor and compressor-turbine matching loop; the other is the selection of the correct power turbine nozzle angle setting.

Figure 56C shows the calculation path for the three-shaft engine with interconnection. The performance characteristics of the compressor and the compressor-turbine are illustrated in the same schematic representation as Figure 56A. The power turbine performance is represented with a variable power turbine nozzle, and the auxiliary turbine has the same representation as the compressor-turbine.

A compressor mass flow is assumed and sent to the compressor-turbine, along with any appropriate flow leaks. This mass flow is insufficient to allow the turbine to drive the compressor and absorb the bearing losses of the first shaft. The flow is then passed to the power turbine, and a nozzle angle is assumed. The power turbine exit total pressure and the auxiliary turbine back pressure (due to regenerator and tailpipe losses) establish the pressure ratio across the auxiliary turbine. This pressure ratio may not be consistent with the work capacity of the auxiliary turbine and the mass flow. The power turbine nozzle is then varied until the flow and work of the auxiliary turbine are consistent. The output work of this turbine is then used (1) to supply the rest of the work to drive the compressor and the first-shaft bearing losses, and (2) to drive the accesories and absorb the bearing losses of the third shaft. The remaining work is added to the power turbine shaft for output power and the bearing powerloss of the second shaft.

In the 3-shaft engine with interconnection, therefore, equilibrium is established by the correct work split between the power turbine and auxiliary turbine. At a given speed, the operating line mass flow is, therefore, determined by the variable power turbine nozzle angle setting required to obtain equilibrium at the given mass flow.

7.3.2 Operating Line Results

Figure 57 shows a comparison of the torque and power characteristics of this 3-shaft engine type and of a 2-shaft, free-power-turbine engine. Calculations for the 3-shaft engine were carried out down to 15,000 rpm and extrapolated to zero speed. The results show more power and torque developed by the 3-shaft engine at speeds below maximum-power speed. This shows that vehicle acceleration and fuel economy should improve with the 3-shaft configuration.

The reason for the performance improvement is shown in Figure 58. In this figure, the efficiencies of the two turbines are plotted against power turbine and auxiliary turbine rotational speeds. The left-hand plot shows that, at 15,000 rpm, the power turbine efficiency is 0.38, while that of the auxiliary turbine is 0.78. Because the latter maintains a high efficiency level and assists the power turbine, more output power is available than with the standard free power turbine.

The right-hand plot shows the auxiliary turbine is able to maintain a good efficiency level, because the speed reduction from peak-efficiency speed is only 36%, while that of the power turbine is 80%. Note that the efficiency of the auxiliary turbine peaks at a lower turbine speed than that of the power turbine. This efficiency match-up between the two turbines promotes good low-speed overall turbine efficiency.

Figure 59 shows this to a greater degree at 50% gas-generator-speed conditions. The figure also shows the auxiliary turbine efficiency should be about 0.62 at zero speed for the power turbine. This is in contrast to a value of about 0.35 for the power turbine of a 2-shaft engine when operating at idle. See, for example, the power turbine efficiency characteristics in the Upgraded Engine specifications in the Eighteenth Quarterly Report (Reference 9).

7.3.3 Turbine Systems Comparisons

Table 7 compares the total-static turbine efficiencies of the three engine configurations. The overall turbine efficiency of the 2-shaft and 3-shaft engines is compared to the radial turbine efficiency of the singe-shaft engine. Comparison is made at peak-power points for these engines at 50%, 80% and 100% gas generator speeds. The single-shaft and 3-shaft engines have higher turbine efficiencies than those of the 2-shaft engine. The 3-shaft engine has turbine efficiency higher than that of the single-shaft engine at design speed, comparable at 80% speed and lower at 50% speed.

If time had permitted, it might have been possible to adjust the design conditions of the turbine for the 3-shaft engine to achieve comparable efficiencies at 100% and 80% speeds to improve efficiency at 50% speed. The values on the figure suggest that 50% speed values might only differ by one point. Even if they are equal, however, the fuel economy of the single-shaft engine is still potentially better because of the reduced number of leakage paths and parasitic losses (two less bearing sets).

The torque of the 2-shaft engine is doubled by the torque converter. The dual-turbine combination of the auxiliary and power turbines preserves this torque multiplication. On Figure 57, the torque ratio for the 2-shaft engine is 1.9 (idle-power torque (16,700 rpm) divided by peak-power torque). The torque ratio for the 3-shaft engine is 3.8.

The preservation of the torque-converter torque ratio is a natural result of the auxiliary turbine torque characteristic as shown in Figure 58. The auxiliary turbine design speed is 83,333 rpm; at engine design speed and zero power turbine speed, it is 33,333 rpm. Extending the torque curve of the right-hand plot to zero speed and interpolating, the torque at the lower speed yields a torque ratio of 1.9. Computational problems did not permit calculations of zero power turbine speed. Consequently, it was not possible to obtain a more accurate value. Time did not permit making computer-code adjustments.

Nor did time permit extensive exploration of this concept. However, it is clear that higher values of torque could be achieve with a lower auxiliary turbine design speed. The gear train ratio selected for the study was 2. Further study could be conducted to check performance at other ratios.

7.3.4 Engine Performance

The operating lines determined from the component matching calculations were combined with final estimates of flow and heat leaks, bearing losses, and accesssory loads to obtain the performance characteristics and compare them with the other engine configurations. The flow leaks and total parasitic losses are compared on Table 8. The flow leaks of the three-shaft engine are unchanged from those of the two-shaft engine. It was assumed that the mechanical arrangement of the three-shaft engine would be such that the leakage across the first two stages would be the same as the leakage of the two-shaft engine; no leakage was assumed to pass across the auxiliary turbine. However, the parasitic loss of the third bearing set was accounted for.

The performance results are shown in Figure 60. The top of the figure shows the turbine inlet temperature distributions that resulted from the matching calculations. The single-shaft engine has the lowest BSFC. The BSFC of the two-shaft engine increases at intermediate powers due to lower turbine inlet temperature. There is an increase in two-shaft-engine BSFC at all power levels due to lower turbine efficiency, bearing losses of a second shaft, the flow leakage past a second turbine seal, and the subsequent thermal mix between gas flows at different temperature levels. The BSFC of the three-shaft engine would increase still further, due to the bearing loss of the third shaft. However, the increase is attenuated by higher turbine efficiency and inlet temperature, provided by better component matching. The final result is a slightly higher BSFC for the three-shaft engine than for the two-shaft engine.

The plot shows the influence of the load of the third bearing set on the BSFC of the three-shaft engine. Without the third set of bearings, the BSFC of the three-shaft engine is lower than that of the two-shaft engine. At 40 horsepower, for instance, the reduction in BSFC is due solely to slightly better turbine efficiency (cf. Table 7) and higher turbine inlet temperature. Note also at this power that the BSFC difference between single-shaft and three-shaft engines is due solely to added leakage and one more bearing set. The combination of these two (approximately 5% more leakage and 19% more parasitic loss, Table 8) is twice as effective as a turbine inlet temperature change of 100°F (two-shaft vs. three-shaft, same leakage and parasitic loss).

In conclusion, the improved component matching of the three axial turbine stages achieved the efficiency of the radial turbine of the single-shaft engine and permitted the use of the same high cycle temperature. However, these gains over the two-shaft engine component matching have been negated by the additional leak and parasitic losses to the point that the BSFC of the three-shaft engine is no better than that of the two-shaft engine above one-third of design power, and worse at lower power levels. Consequently, it must be concluded that, because of inherent losses, multiple-shaft engines cannot achieve BSFC as low as the single-shaft engine, despite the best component match.

7.3.5 Vehicular Fuel Economy

Vehicular fuel economy was estimated from the BSFC-vs-Power curve of the 3-shaft engine and the use of a two-speed manual transmission. The calculation was made from the value of fuel economy computed for the 2-shaft engine with adjustments made for the difference in BSFC-vs-Power curves and the absence of a torque converter and one gear set for the 3-shaft engine. The combined fuel economy estimated this way is 23.9 mpg. The 3-shaft engine with interconnection can therefore exceed the fuel economy goal of the study by 1.7%. However, to achieve this at a cycle pressure ratio of 4.2:1, the design-point turbine inlet temperature must be 1350°C. Consequently, the axial turbines can only be made of ceramic materials.

7.4 Three-Shaft Engine with Twin-Spool Gas Generator

The other three-shaft arrangement that was reviewed consisted of a twin-spool gas generator and a free-power turbine with variable nozzle vanes. This arrangement was reviewed to explore the possibility of performance improvement over a standard two-shaft engine with a single-spool gas generator. The performance improvement was expected to be due to higher off-design pressure ratio, and reduced fuel consumption due to lower idle speed.

Higher off-design pressure ratio yields lower specific fuel consumption. Preliminary cycle calculations showed a reduction in BSFC of 1.3% for 1% increase in 50% speed pressure ratio. It was expected that the off-design compressor pressure ratio for the twin-spool compressor would be higher than that of a single-stage compressor. The inner-spool speed would be at a proportionately higher speed than the outer spool. Final calculations showed, for instance, that the inner spool operated at 56% of its design speed when the outer spool was at 50% speed. If the compressors were on a single-shaft, the operating speed would be 50% speed for both compressors, and a lower pressure ratio would be produced.

Additional fuel economy might result at idle. With increased pressure ratio at 50% speed, the increase in engine power would require a lower rotational speed at idle power. This would lower idle fuel flow. There would, however, be a cost in engine acceleration time. It was hoped that if the outer spool were lower than 50% speed, the inner spool might be higher than 50% speed. In this way, the time to accelerate the outer spool might be made up by a smaller time to accelerate the inner spool over a smaller speed range.

7.4.1 Operating Line Determination

Figure 61 shows the calculation path for the twin-spool gas generator combined with a free-power turbine with variable nozzle vanes. The performance characteristics of the turbines and compressors are illustrated in the same schematic representation as Figure 56B.

A mass flow is assumed for the compressor of the outer spool at a specified rotational speed. This flow is used to perform a match with the second compressor at an assumed rotational speed of the inner spool. In the calculational procedure that was used, the compressor work and bearing load determined the mass flow of the turbine of the inner spool. This mass flow and the exit temperature and pressure of the first turbine determine the work of the second turbine. The off-design flow angles relative to the nozzle and rotor were assumed to be the design values. If the work of the second turbine did not match the work of the first compressor plus the bearing load of the outer spool, the rotational speed of the inner spool was adjusted. The calculations were, then, repeated until work convergence was achieved within 0.5%. Upon convergence, the mass flow of the first compressor was revised, if it differed from the mass flow of the first turbine by more than 0.5%.

Upon final calculation convergence for the gas generator, the mass flow for the power turbine is established. The pressure ratio is also determined, since the exit total pressure from the compressor-turbine is known; and the exit static pressure at the exhaust diffuser exit has been estimated from the pressure drops in the tailpipe and regenerator core. The variable power turbine nozzle is adjusted until the vector diagram extracts the work consistent with the pressure ratio and the efficiency estimated from the computer program loss model. In the twin-spool engine, therefore, three iterations are required. The first iteration is the work-split loop between the two turbines and their respective loads. The second consists of the mass flow match up between the first compressor and the first turbine. The final iteration involves the selection of the correct power turbine nozzle angle setting.

7.4.2 Operating Line Results

The compressor maps used in this study were scaled from References 10 and 11. The values of mass flow were scaled to meet the cycle-design flow requirement. The values of pressure ratio were scaled by the ratio of (required pressure ratio minus one) to (reference pressure ratio minus one). The scaled maps are shown on Figure 62. The engine-operating points are included on the maps. The turbine performance characteristics were determined from vector diagram computer programs with self-contained loss models. Discrete calculations were performed at the compressor match points rather than from the creation of complete performance maps.

Other performance parameters are shown on Figure 63 and 64. Figure 63 shows the variation of component efficiencies with outer-spool rotational speed. Figure 64 shows the variation of inner-spool speed and compressor pressure ratio with outer-spool speed. Table 9 shows the increase in off-design pressure ratio over that of a single-stage compressor.

Figure 65 shows the power turbine performance at 50% outer-spool speed and at two possible idle-point speeds. For the two-shaft engine (with a single-spool gas generator), idle power is achieved with variable inlet guide vanes deployed at +60° vane setting angle, as shown by the dashed line. This operation is nearly simulated by the twin-spool gas generator with an outer-spool speed of 46% and an inner-spool speed of 55% As with the two-shaft engine, the idle point is significantly below peak power and, hence, peak efficiency. A second possibility would be to reduce the speeds of the two spools still further until idle occurs near peak power. This occurs for the twin-spool engine at an outer-spool speed of 41% and an inner-spool speed of 50%.

7.4.3 Engine Acceleration-Time Estimate

It was felt that the latter speeds would not yield a practical idle point, because of the significant increase in acceleration time. To confirm this, calculations were performed to estimate the time to accelerate from the lower idle-point speed and from 50% outer-spool speed. The acceptable increase in response was defined to be a time increment no greater than 0.1 second greater than the time to accelerate a two-shaft engine.

The calculation of acceleration time for the twin-spool engine was to be an iterative computation to obtain the correct work split at any given time during acceleration. To begin with the procedure, the calculated acceleration times were based on the unbalanced torques at the steady-state spool-speed match points. The results of this initial calculation are shown on Table 10.

The table compares the acceleration times of each spool up to the 80% and 100% outer-spool speed values. Also shown on the table is the time to accelerate a two-shaft engine with a single-spool gas generator. The twin-spool acceleration times are significantly higher than the values for the two-shaft engine, except for the outer-spool time from 50% speed. Since the inner spool significantly lags the outer spool, the inner-spool speed must be lowered and the calculation repeated to obtain the correct work split at the time the outer spool is at 80% and 100% speeds.

In the updating of the computations, the acceleration time of the inner spool will increase even more. The acceleration time of the outer spool from either idle speed is unacceptable, since the acceleration from 50% speed is essentially comparable to the acceleration time of a standard two-shaft engine. In fact, the 45% outer-spool speed is about the same speed that the two-shaft engine must have without variable inlet guide vanes. Consequently, as with the two-shaft engine, the twin-spool arrangement does not benefit idle fuel economy unless variable inlet guide vanes are used

7.4.4 Engine Performance

The study showed that off-design pressure ratio is higher by twin-spooling, but only slightly. Without variable inlet guide vanes, idle fuel is reduced at a significant cost in acceleration time. A comparison of the resultant engine performance estimates is shown in Figure 66. The plot shows little difference in the BSFC-Power characteristics due to twin-spooling. The gain in power at intermediate speeds is due to the temperature schedule, as well as the pressure ratio increases shown in Table 9. It was possible to maintain the schedule used for the single-shaft engine, since there was adequate surge margin provided by the twin-spool compressor.

7.5 Preliminary Turbine Rotor Stress Analysis

From the variety of engine concepts studied above, the turbine arrangements of the single-shaft engine were selected for preliminary turbine stress analysis. These turbines could be a single radial turbine and a two-stage axial turbine, both assuming the use of ceramic material. Because the use of ceramic material inferred a relatively high development risk, a metal radial turbine was also considered for analysis at 1150°C. This turbine would not necessarily be intended for long-life but would allow early demonstration of engine concept feasibility in a development program.

Preliminary estimates were made from aerodynamic blade profiles, but only the stresses in the discs were calculated in any detail. The objective was to arrive at a disc shape such that the maximum combined centrifugal and thermal tensile stress would not exceed 207 MPa. This amount represents about half the modulus of rupture (MOR) strength of the sintered alpha SiC material which is being considered by the Carborundum Company for fabrication of an integral turbine rotor.

As a simulation of the thermal load, radially linear thermal gradients for steady-state operating conditions were assumed through each disc. The material temperature profile for the radial rotor, as shown in Figure 67B, was assumed to vary as the calculated relative total gas temperature, namely, from 1060°C at the tip of the disc to 960°C at the center of the disc. The gradient for the axial turbine was estimated using the Upgraded Engine turbine thermal gradient shown in Figure 67A as a reference. Note that the blade root temperature on this turbine was determined to be equal to the relative total gas temperature. On the basis of the higher thermal conductivity of ceramic materials and the size of the ceramic disc, a lower gradient is anticipated in the ceramic turbine than in the metal turbine. However, if the rim temperature for the ceramic turbine were assumed to be equal to the relative total gas temperature (1252°C), an unrealistically greater thermal gradient would result relative to the metal rotor. Therefore, the temperature was assumed to be 1120°C at the rim and 900°C at the hub of the rotor, as shown by the dashed line of Figure 67C. The corresponding 220°C-gradient thus assumed is approximately 60°C lower than that of the turbine for the Upgraded Engine.

It should be pointed out that the gradients discussed here are for steady-state conditions only and that the larger gradients occurring during transients will result in higher thermal stresses in the disc. It can be safely assumed, however, that the highest thermal stress point in the disc will not necessarily coincide with the maximum centrifugal stress point. Furthermore, it is anticipated that the maximum thermal gradient will occur at a time when the engine is running at less than the maximum operating speed. A thermal analysis will be required to effectively evaluate these transient conditions.

An axisymmetric finite element computer program was used to calculate the disc stresses. The program computes the stresses in the radial, tangential and axial directions and the shear stresses in the radial-axial plane.

The results of the stress calculations for the ceramic turbines are summarzied in Figure 68. A comparison of these results shows that the maximum combined tensile stresses in the axial turbine are appreciably higher than in radial turbine. As expected, the difference is primarily due to the increased thermal stresses in the axial turbine. The maximum combined stress at the center of the radial turbine may be reduced if the backface of the disc can be optimized to lower the centrifugal stress. The given blade stresses represent average stress estimates based on preliminary blade cross-sectional areas. Even so, the magnitude of the blade stress is reasonable.

To assess the severity of these stress levels, it is necessary to look at the strength characteristics of the material, which will require a statistical evaluation, taking into account the strength variability of ceramic materials. Such an evaluation has not been carried out for the preliminary study but must be made for a final design analysis.

The stress estimates for the 1150°C metal turbine are presented in Figure 69. Because of the lower thermal conductivity of the metal alloy, an increased thermal gradient relative to the ceramic turbine was assumed. Considering the higher density material and an assumed thermal gradient increase to 190°C, the maximum combined equivalent stress was estimated to be 450 MPa at a maximum design speed of 94,000 rpm. The estimated blade stress is 310 MPa. The impact of these stresses on the design of a metal turbine cannot be fully assessed at this time, because the candidate material, the RSR superalloy from the Pratt and Whitney Company, has not been characterized, and the material strength data are limited.

Summarizing the above results, there is evidence which indicates, that to realize such engine designs as considered here, there is a certain degree of development risk involved. For a general evaluation of the amount of risk for these turbine rotors, a set of material strength data curves, such as are shown in Figure 70, was obtained. These were derived from the Materials Review in Section 7.6 below. Strengths of ceramics and advanced metals are shown in comparison to the best current commercial superalloys and hence, were judged as moderate or high risk relative to the latter. On this basis and also on the basis of the calculated stresses, the two-stage axial-turbine ceramic design was categorized as high risk, whereas the single-stage radial-turbine designs with ceramic material and limited-life metal were considered as moderate risk.

The moderate risk metallic curve in Figure 70 is based upon preliminary properties of Pratt and Whitney's advanced RSR (rapid solidification rate) superalloys. The development goal of this material, which is a rapidly solidified superalloy with aligned grain structures, is to have a 50°C to 100°C increase in strength capabilities above currently best commercially-available superalloys. For limited-life turbine rotor application, this material appears to be adequate for development work with a moderate risk.

7.6 Material Review

As shown above the 3-shaft engine with a 2-speed manual transmission and the single-shaft engine with CVT are the only powertrain concepts capable of meeting and exceeding the fuel economy goal of the study. As shown by the preliminary stress analysis, the radial turbine is better suited to the engine than a two-stage axial turbine because of the higher thermal stresses in the discs of the axial turbines. To achieve the highest fuel economy, it is necessary to use ceramic materials. However, to achieve the goal of the study, the turbine inlet temperature for the single-shaft engine could be as low as 1050°C and have margin for the uncertainties of powertrain development. It might be possible to go as high as 1150°C with advanced superalloys. This would provide a limited-life material to be used in a development program while progress is being made in the ceramic materials and the CVT. In support of these considerations, a review of high temperature materials was conducted to establish the feasibility of the use of superalloys, ceramic materials and refractory materials. The results are discussed below.

7.6.1 Superalloys

Conventional superalloys, directionally solidfi t eutectics (DSE), oxide dispersion strengthened alloys (ODS) and tungsten fiber-reinforced superalloys were reviewed and compared on the basis of "turbine blade temperature capability". For this report, temperature capability was arbitrarily defined as the temperature to produce rupture at 138 MPa (20 KSI) in 1000 hours.

Today's best conventional cast superalloys are limited to an uncooled blade temperature of ab at 980°C (1800°F). Even with continued development and advanced processing techniques, such a directional solidification, this temperature will probably not be extended more than about 25°C (45°F). Wrought superalloys prepared by the usual forging or powder metallurgy techniques do not generally attain the strength of cast alloys in this temperature range.

Significant increases in high temperature properties have been attained by applying the directionality concept to eutectic systems and tungsten fiber superalloy composites. Directionally solidified eutectics offer the possibility of blade temperatures 60-110°C (110-200°F) above those used for conventional cast superalloys. Although tungsten fiber reinforced superalloys afford potentially the highest use temperature capability of any of the superalloy base systems studied for turbine blades, i e. about 1200°C (2200°F), their application, because of cost and fabrication problems, is most remote.

Advanced oxide dispersion strengthened alloys with elongated or fibrous grain structures appear to have a potential-use temperature of about 1040°C (1900°F) for blades and up to 1230°C (2250°F) for lower stressed stator vanes. Recently, wrought alloys produced from powder prepared by a new rapid solidification rate process have been reported that appear to have the potential of increasing the maximum temperature capability of conventional superalloys by about 50-100°C (90-180°F).

With the notable exception of some of the ODS alloys containing both chromium and aluminum, almost all of the advanced superalloy systems mentioned have relatively poor oxidation resistance and will probably require protective coatings at temperature above 1000°C (1830°F). The standard aluminide diffusion coatings provide long term protection only up to about 1040-1100°C (1900°-2000°F). Newer, more costly overlay coatings may extend this range to around 1150°C (2100°F).

Before the advanced superalloy-base materials studied in this report could be considered for a practical small automotive-size turbine rotor, many serious cost, design and fabrication problems would have to be solved. A near net shape integral rotor appears to be necessary to avoid the intolerably high fabrication and assembly costs associated with the individual blade-type construction commonly used for larger aircraft-type turbine rotors. Two processes, investment casting and isothermal superplastic forging, have the potential to produce relatively low-cost integrally bladed turbine rotors.

Politically generated uncertainties in the supply of key alloying elements, particularly chromium, and rapidly rising prices cloud the future for any large scale usage of superalloys in automotive gas turbines.

7.6.2 Ceramic Materials

It is clear that substantial increase in fuel efficiency in a gas turbine engine will be realized only if the turbine inlet temperature is increased significantly. Such temperatures would be well above those considered practical for the best available superalloys or with the refractory metals, generally because of poor oxidation resistance, undesirably high density fabrication problems, high raw material cost, and uncertain availability.

The following ceramic materials, listed in order of greatest immediate potential, were reviewed and compared for use at high-stress, high-temperature locations within a marketable gas turbine engine. It should be emphasized that none of the following have properties which have, to date, been completely optimized.

1. Hot Isostatically Pressed Silicon Nitride - offers the greatest potential for high strength and high Weibull modulus at elevated temperature, and, in principle, is capable of economical, high volume production of complex parts. Development, however, has been moving slowly

2. Sintered Alpha Silicon Carbide - Exclusive to the Carborundum Company, this material demonstrates no strength degradation through 1650°C (3000°F), and has unequaled oxidation resistance of any form of silicon carbide or silicon nitride. It is capable of being formed to shape, although injection molding is not possible at this time on cross sections greater than 12 5 mm (0 5 in) because of binder bake out cracking.

3. Sinterable Silicon Nitride - Offers the potential for low cost, complex part fabrication; however high temperature strength and oxidation resistance are limited, resulting from the addition of sintering aids to the Si_3N_4 powder.

4. Chemical Vapor Deposited Silicon Carbide - Excellent potential for high strength and oxidation resistance; however very serious fabrication problems continue to hamper developmental progress.

5. Sinterable Beta Silicon Carbide - Although this material displays many of the fine properties of sintered alpha SiC, there is no commercial source of beta SiC powder.

6. Hot Pressed Silicon Nitride - The strength of this material is exceptionally high at room temperature, falling off quite drastically by 1370°C (2500°F). The process remains prohibitively expensive and time consuming; therefore it does not lend itself to high volume production.

7. Hot Pressed Silicon Carbide - Also prohibitively expensive for high volume production.

Materials considered as medium-stress candidates were 1) Recrystallized SiC, 2) Reaction sintered silicon carbide, 3) Reaction bonded silicon nitride, 4) SiC composites, and 5) SiALON. For specialized applications, each differs in its potential for success. Each has both benefits and disadvantages.

Materials reviewed for regenerator/recuperator application in order of greatest potential for success, were 1) AS (alumium-silicate), 2) MAS/LAS (magnesium-alumino silicate/lithium-alumino silicate). Pure MAS is subject to thermal fatigue, while pure LAS is subject to chemical attack by sulphur (in fuel) and road salt ingestion.

Coatings for oxidation/corrosion protection were reviewed and found to be unnecessary on those forms of SiC containing no free silicon. Forms of SiC containing free silicon readily oxidize at high temperature, however this may be considered protective rather than destructive. It is inconclusive as to whether a surface layer of pure CVD Si_3N_4 would benefit reaction bonded silicon nitride or hot pressed silicon nitride.

Joining methods for ceramics were reviewed and grouped into four major categories: 1) Adhesive and Cements, 2) Mechanical Bonding, 3) Solid Phase Joining, and 4) Liquid Phase Joining). Specialized applications of each were discussed.

Machining methods of ceramics were reviewed. Two methods were found most effective: 1) Diamond Machining, and 2) Ultrasonic Abrasive Machining. All methods of machining ceramics are expensive, and should be avoided by forming ceramic parts as close to design tolerances as possible.

Economics of ceramics, both in regard to raw material and processing was investigated. Costs of raw materials are very low for SiC and Si_3N_4 when compared to superalloys or refractory metals, at least by an order of magnitude. Furthermore, such raw materials are in virtually unlimited supply in the United States. Processing costs and energy requirements are lower than for turbine metals, so long as final part machining is minimized. Although many economic variables are difficult to fully assess at this time, it is expected that ceramics would enjoy a cost advantage over the superalloys and the refractory metals if compared on a cost-per-part basis, owing to the lower bulk density of the ceramics.

7.6.3 Refractory Metals

Five refractory metals — chromium, columbium, molybdenum, tantalum and tungsten and their alloys were examined. Some of the alloys appeared to offer usable properties for turbine rotor application. However, they all have undesirable features that detract from their potential usefulness and final selection would, at best, be a compromise.

While tantalum and tungsten have more than adequate stress-rupture strength, their high density would impose unreasonable inertia penalties when used in rotating components. Chromium alloys, on the other hand, would be quite advantageous from the same standpoint, having a lower density than nickel-base alloys, but their extreme brittleness and sensitivity to interstitials preclude their use for such an application. From the standpoint of fabricability many refractory alloys perform rather poorly.

Chromium and tungsten base alloys (Group VI A) because of their low ductiliy are difficult to reduce mechanically to usable products. Chromium in particular requires extrusion or swaging to gross final shape. Tantalum and columbium on the other hand are very ductile (Group V A) and are readily fabricable although requiring high deformation forces. Molybdenum, while being in Group IV A, has intermediate fabricability. Tantalum and tungsten because of their extremely high melting points, have not been successfully investment cast.

Although alloys of both columbium and molybdenum are normally used in the wrought condition, several of them have recently been investment cast with extremely encouraging results. The experimental shapes produced included small integral turbine rotors and commercial engine size airfoil shapes with acceptable surface finish. In view of the small size of the projected turbine rotor, precision investment casting to net shape appears to be the only currently practical method of secondary fabrication.

In the event that the final material choice for the hot gas path components of the IGT is a refractory alloy, raw material cost will be an important consideration in mass production decisions. While the relative low cost of chromium is undoubtedly attractive, some alloy development breakthroughs are required before full advantage can be derived from that alloy system. At the other end of the scale the high cost of tantalum coupled with a high density precludes serious consideration of its use as a compressor-turbine rotor material. Tungsten-base alloys are of intermediate cost but have a high ductile-to-brittle transition temperature.

The base materials for the castable refractory alloys, columbium and molybdenum, are practically at opposite ends of the cost range, with molybdenum second only to chromium. This cost advantage holds not only for the pure metal but also for the commercial alloys which contain less than 2% additions. Availability and strategic importance, while not the primary selection criteria, strongly favor molybdenum in view of its ample domestic reserves and production capacity.

The stress-rupture properties of the various molybdenum and columbium alloys cover essentially the same range and the selection is usually governed by fabricability. In a cast turbine rotor, while property optimization by thermo-mechanical treatments is not feasible, the actual properties are expected to be in the range of recrystallized or stress-relieved alloys and will be affected by process variables. The properties of the cast columbium alloys are reported to be comparable to that of the wrought material (with similar thermal history); actual test results show cast molybdenum-base TZM alloy to be somewhat superior to the stress-relieved wrought alloy.

The creep properties of molybdenum alloy TZM, cast and wrought, are also superior to that of the strongest columbium alloys. While molybdenum alloys appear to be the best suited of the refractory alloys for the rotor of a high-temperature turbine, they have one common serious deficiency, a catastrophic oxidation behavior. In spite of that problem they remain extremely attractive because of their unique hot strength. The oxidation is partially alleviated by the use of protective coatings. However, serious consideration of the usage of molybdenum alloys in the IGT would require additional development efforts particularly in the area of coating reliability.

7.6.4 Summary

The review of materials which could be considered for the Improved Gas Turbine Engine shows the feasible potential for the use of ceramic materials and the superalloy with structural properties created by rapid solidification rate (RSR). The ceramic materials are needed to achieve the highest possible fuel economy, but the RSR superalloy could be used as an interim limited-life material during the development of the structural properties required of the ceramic material.

7.7 Cost Studies

Relative manufacturing cost was estimated for the various powertrain concepts. Many combinations of engine elements were estimated by comparing the elements to similar elements of the Upgraded Engine. More detailed estimates were made by constructing simulated parts lists, and a rationale for the confidence level of the estimates is discussed. Some general observations of the relation of similar elements are made. For comparison with standard reciprocating engines, estimates were made of overall system costs; operating and lifetime costs are also discussed.

7.7.1 Cost-Effective Upgraded Engine

The cost data on the Upgraded gas turbine engine was reviewed, analyzed, and updated for parts list changes and late vendor quotations. All hardware designs of this engine were then reviewed and sketches of more cost-effective production configurations were made, where applicable. Many of these changes were incorporated in an engine section layout, Figure 71. All of the changes were cost estimated on a production basis, and the costs provided a base against which all other concepts could be compared.

Some of the value engineering applied to the Upgraded Engine is as follows. The numbers refer to the numbers on Figure 71.

1. Eliminate: starter reduction gear, air pump, etc., since current low-emission burners do not require atomizing air for starting.
2. Simplify: costly machining of inlet flowpath replaced by injection molding.
3. Combine or separate pieces to reduce cost: make thrust bearing integral with generator drive shaft.
4. Use lower cost material: modify the configuration of the accessory drive sprockets for fabrication in powder metal.
5. Minimize material: fabricate regenerator-drive worm gearshaft from tubing instead of bar stock.
6. Use lower cost process: change the output gearshaft from a casting to a splined bar stock assembly.
7. Accomplish function at lower cost: change the oil pump drive from a flex coupling to a tang and slot.
8. Change size; change the compressor impeller hub from an I.D. to an O.D. fit.
9. Minimize use of fasteners: change the bolting of the oil trough to the housing to spot-welding the pan.

7.7.2 Cost Comparison of Preliminary Concepts

A cost summary of the concepts that were initially considered for powertrain selection is shown on Table II. The cost estimates were facilitated by categorizing the costs of the hardware items of the cost-effective Upgraded Engine into groups that would reflect changes in the new engine designs. These broad categories are:

1. Engine housing, thermal insulation and assembly costs
2. Turbomachinery costs
3. Regenerator and seals costs
4. Reduction gear and transmission costs

Costs were estimated for the four categories for each engine concept considering changes in mass flow, features used, number of turbomachinery stages and regenerators, and the complexity of the gear sets and transmission. The results indicated that the single-shaft engine with a radial turbine would be the lowest-cost concept.

An example of the method of cost estimate is as follows. The regenerator cost from the cost-effective Upgraded Engine was divided into seal, core, and cover cost. The material cost for the core and cover changes directly with the mass flow ratio of 1050°C and 1350°C engines, since the area of the items determine material cost for a given thickness. The labor and burden portion of the base cost is almost invariant for the size changes involved; so it was added back to the new calculated material cost. The material cost for the seals changes with the square root of the mass flow ratio of the 1050°C and 1350°C engines. The base labor and burden cost were added back to the new calculated seal material cost. The sum of the base labor and burden costs and the new calculated material costs form an estimate for the regenerator costs of the 1350°C engine. This estimate was compared to assessments made by independent methods which confirmed the validity of the approach.

7.7.3 Cost Comparisons of One, Two, and Three-Shaft Engines

More detailed estimates were made on the single-shaft, two-shaft, and three-shaft engine concepts selected for detailed performance study. A preliminary parts list of the single-shaft engine is given in Appendix B. The parts in this list and similar lists for the multiple-shaft engines were categorized, and the costs were summarized, as shown on Table 12. The values show close agreement with the estimates on Table 11. A breakdown of part cost distributions for the various categories is given on Table 13.

The cost confidence levels for parts groups in the engines studied are shown on Table 14. The rationale for the cost confidence levels is as follows:

- High confidence in the accuracy of the estimate:
  The item is directly comparable in technology, tooling, and material to typical automotive parts now in production. Error is estimated at ± 5%.

- Medium confidence in the accuracy of the estimate:
  The item is comparable to automotive parts that have been produced but only in limited, low volume. Error is estimated at ± 10%.

- Low confidence in the accuracy of the estimate:

  The item has not been fabricated, has not been designed, represents new technology, and requires unconventional processes. Error is estimated at +100%.

Some of the observations of interest made during this study were:

- Costs of auxiliaries and accessories are those of standard parts currently made or purchased by the Contractor and are the same for all engines.

- Multiple-shaft engines have a penalty for assembly complexity.

- The single-shaft engine with power take-off at the front of the engine has an advantage by incorporating part of the intake into the reduction gear housing.

- Estimates of costs of ceramic and metal turbines, assuming fully-developed processes, strongly indicate cost convergence.

- Estimates of regenerator costs for one-, two-, and three-shaft engines, at the same turbine inlet temperature, are nearly the same, because the cost impact of the many complex factors are compensating.

7.7.4 IGT Vehicle Cost Analysis

Customer acquisition costs of alternative engines must include the vehicle-related costs, such as brake power source costs (no vacuum with the turbine), and heater costs (no hot water with the turbine), in order to be complete. Also, since the piston engine, with equivalent low emission capability, is the base, the piston engine and its system-related costs should be the reference. The estimated 1976 variable costs for the six-cylinder and concept engines include the following:

Engine-Related Costs	Vehicle-Related Costs
Base Engine	Power Brakes
Power Steering Pump	Engine Coolers
Starter	Emission Controls
Electrical	Air Cleaners
Fuel Systems	Exhaust Ducts
Mounts and Pulleys	Heater - Air Conditioning
Transmission	

Since current burner development is expected to meet 1981 emission requirements, the emission control hardware that will be required for the piston engine to meet 1981 requirements was cost-estimated at 1976 costs.

The variable manufacturing costs were assessed in detail for the powertrain concepts reviewed for the final selection. Vehicle system costs were also evaluated and were compared to costs of vehicles powered by spark-ignition and diesel engines. The results of the analysis showed that, on the basis of high-volume production, the manufacturing cost of the vehicle with a gas turbine engine is 30% higher than the cost with a spark-ignition engine. By comparison, the cost of a diesel-powered vehicle is 20% higher than the cost of the vehicle with a spark-ignition engine. Additional factors, however, would impact on the vehicle acquisition cost or "sticker price" to the customer. For a vehicle having an entirely new type of engine, these would include the usual fixed business costs plus allowances for costs related to the introduction of a new product; capital investment, new product warranty, service training, and engineering. The sticker price will also depend on unpredictable factors, such as future emission standards and competitive considerations.

Chrysler's long-term product objective is to develop the turbine as an alternative to the diesel for the 100-horsepower-and-above car and small-truck market. Projecting over the long term when vehicle introduction costs have been absorbed, the potential would appear to be for the turbine and the diesel to have close to the same sticker price.

The life-cycle cost, however, includes operating (fuel and maintenance), financing, and insurance costs, along with the sticker price. Both the turbine and the diesel would have about the same fuel costs, and with similar initial costs, the life-cycle costs may be considered equivalent.

Although the diesel is generally regarded as a low-maintenance concept, the turbine also has good potential in this area. Lower maintenance costs are expected, because oil and filter changes should be minimal, considering that combustion gases do not contact the lubricant.

7.8 Concept Selection

Of all the powertrains reviewed, only the single-shaft engine with a CVT and three-shaft engine with interconnecting shafts and a two-speed manual transmission met and exceeded the fuel economy goal of the study. At a design-point pressure ratio of 4.2:1, the single-shaft engine could meet the goals at a turbine inlet temperature as low as 1050°C. At the same design pressure ratio, the three-shaft engine could only meet the goal at 1350°C. These results are based on the assumptions of component efficiencies, parasitic losses, and heat and flow leaks used in the powertrain performance estimates, along with the assumptions of transmission efficiencies and performance characteristics.

The cycle study showed that the best fuel economy for a powertrain with a single-shaft engine is obtained at a pressure ratio between 4.2 and 5.5 for a turbine inlet temperature schedule determined by operation with constant turbine exit temperature (Figure 32). The optimum pressure ratio depends on the component efficiency levels. The difference in fuel economy between a design pressure ratio of 4.2 and 5.5 varies from zero to 0.4 mpg. Consequently, there is only a small impact of selected design pressure ratio on the fuel economy obtained with the single-shaft engine, for the assumptions of component efficiencies used in this study.

The best fuel economy for a powertrain with a two-shaft engine varies between design pressure ratios of 5.5 and 7.0 for a turbine inlet temperature schedule determined by operation with constant power turbine exit temperature (Figure 33). This range narrows to 5.5 to 6.5 for constant power turbine inlet temperature. The optimum pressure ratio depends on the component efficiency levels. The difference in fuel economy between a pressure ratio of 4.2 and the optimum pressure ratio values ranges from 0.3 to 0.6 mpg for operation with constant power turbine exit temperature and from 0.5 to 1.2 mpg for constant power turbine inlet temperature. The lower differences are associated with minimum development effort, and the higher differences reflect maximum development effort. The difference in fuel economy is moderately significant as off-design temperature increases.

The results of the stress analysis showed high risk in the design of axial turbines for high temperature engines. The risk is based on the high level of disc stresses due to thermal loads and on the sparsity of available space to properly insulate the bearings from the flowpath. These risks increase as design pressure ratio increases (Figure 35).

On the basis of fuel economy, overall suitability to mechanical design and production cost, the powertrain selection is a single-shaft engine with a radial turbine and continuously variable transmission: design turbine inlet temperature is 1150°C. This powertrain concept was judged to best meet the goals of a development program for the Improved Gas Turbine. With advanced superalloys, a

development program could be planned with a limited-life turbine designed for 1150°C. This would allow time for development of a practical CVT and for development of ceramic materials with strength properties suitable for design application to achieve near-maximum powertrain fuel economy at 1350°C.

The CVT configuration selected for use on the powertrain is the belt-drive CVT. This was selected as being the most practical type of CVT for automotive application. It is simpler than the hydromechanical types and requires smaller driving forces than the traction type. While belt technology is being developed, the hydromechanical type could serve as an interim to demonstrate powertrain fuel economy.

An initial preliminary layout of the selected powertrain is shown in Figure 72. The engine is shown mounted transversely in a front wheel drive vehicle. Note that the engine, with its variable ratio belt drive, will fit between the vehicle frame side rails. The engine features a single regenerator located to the rear of the turbomachinery and with the axis parallel to the engine axis. This allows the turbine exit gas to flow directly into the regenerator with no turning required. Also, a more symmetrical engine housing results with this arrangement, and the engine exhaust gas may be conveniently ducted to the rear from this side location on the vehicle. The regenerator crossarm and bulkhead section of the engine housing may be adequately cooled, using air taken from the duct leading from the compressor collector to the high pressure regenerator inlet. The turbomachinery and its supporting structure will be installed as a subassembly in the forward section of the engine housing.

Figures 73A and 73B show front and side external views, respectively, of the engine, including the variable ratio belt transmission plus the accessories for both engine and vehicle. The engine turbomachinery, burner, and starter are located just below the hoodline to allow room for the transmission gear case, which is positioned forward and just above the front axle centerline.

The layout indicates no areas of interference between engine and body components. Not included in the layout, however, are the engine air intake duct and filters and the battery, which are expected to require changes in vehicle components. Also not shown are items such as the electronic control unit, exhaust system, VIGV actuator, CVT pulley controls, engine mounts, heater system components, and the windshield washer reservoir.

Section BB (of Figure 73A) on Figure 73C was taken to show the rotor shaft assembly, burner, air intake, and reduction gear. Included on the reduction gear output shaft is the variable ratio drive pulley and the sprocket for the chain driving the accessories and regenerator core.

A single-shaft engine with a front-mounted, variable-ratio belt drive is shown in Figures 74A and 74B in a pickup truck. No interference problems are apparent. A drive connecting shaft would be required to transmit power from the belt system to the gear box as shown in Figure 75.

7.9 Vehicle Performance

Calculations were performed to estimate vehicle response to operator demands with a vehicle equipped with a single-shaft engine and CVT. A control strategy that senses the vehicle operator's power demand and maximizes the engine operation for that demand can be developed. There is limited engine power available at low engine speeds, both for engine, as well as vehicle acceleration. Maximum vehicle accelerations are possible only at or near maximum engine speeds, and the proper relationship between engine and vehicle acceleration rate must be established.

A potential solution involves the use of a rate of change of accelerator-pedal-position sensor, which would indicate the operator's demands more closely than simply an accelerator-pedal-position sensor. For example, rapid movements indicate the desire for large vehicle speed changes at a quick rate, while slower movements indicate the perturbations of vehicle speed associated with normal traffic operation. The former indicates the need for maximum vehicle acceleration, thus maximum engine power, while the latter indicates a modest change in engine power requirements. The engine response to these varying demands can be optimized. Considering an initially stationary vehicle, a rapid, continuing accelerator pedal motion indicates the desire for a maximum-performance start and, thus, as much engine power availability as possible. This is obtainable by initially utilizing all of the available engine acceleration power to accelerate the engine, leaving the vehicle at rest. As the engine approaches maximum speed and power, some of the available acceleration power is delivered to the vehicle, starting it in

motion. When the engine reache[s] maximum speed, full, design power is available for vehicle acceleration. Although the notion of an initially stationary vehicle for a condition demanding maximum vehicle motion seems contradictory, results of preliminary analysis minimize this objection.

The characteristics of a vehicle powered by a single-shaft engine and responding to maximum accelerator position and accelerating from rest are shown on Figures 76 and 77. The time required to accelerate the engine to maximum speed from idle would be about 1.1 seconds. However, this power level at standstill would be simply dissipated in tire slip. Diverting 60% of the available power to the vehicle at about 75% engine speed allows the vehicle to begin moving sooner, at about 0.75 second instead of 1.1 seconds, with only a slight delay in reaching maximum engine speed. The vehicle response, compared to that of the two-shaft engine arrangement, shows the lag of the single-shaft-powered vehicle to be only about a car length. The less demanding, more normal, vehicle acceleration requirements would exhibit proportionally less vehicle lag, with the engine and vehicle accelerating together.

These calculations were performed with preliminary estimates of compressor and turbine polar moments of inertia and with an air thrust bearing. More accurate estimates were made of the turbomachinery geometry, and the air thrust bearing was replaced by a ball bearing. In the original calculations, the polar moment of inertia of the disc of the thrust bearing was approximately equal to that of the turbine, due to the size of the disc of the thrust bearing. The large size was required because the thrust load was sustained by an air film instead of an oil film.

The vehicle performance with these revisions is shown on Figures 78 to 80. The results in Figure 78 show an initial acceleration of the vehicle comparable to that of a vehicle with a spark-ignition engine of equal maximum power (100 horsepower). From 0.1 to 0.8 second, the acceleration is less than that of the vehicle with the spark-ignition engine. However, as Figures 79 and 80 show, the variation of vehicle speed and distance traveled are comparable to the values obtained with the Baseline Vehicle of the Baseline Engine Development Program, in contrast to the results shown in Figures 76 and 77. Consequently, it is possible to preserve the vehicle performance with a powertrain with a single-shaft engine and a CVT. However, care must be exercised in the engine design to minimize shaft polar moment of inertia and in the CVT design for the match and the control of engine-to vehicle characteristics.

7.10 Control of Belt-Drive CVT

This section discusses the control requirements for the belt-drive CVT. Remarks are confined to fixed-center, variable-sheave pulley systems. Position of the belt pitchlines on the drive and driven pulleys and the tension between them on each side is determined primarily by the loading of the drive and the axial forces exerted on the sheave faces to maintain belt tension. Equilibrium positions (i.e. fixed ratio conditions) can be thought of as a condition when all these forces are in dynamic balance, so that the belt tends to stay in a given pitchline configuration. The axial forces required to hold a belt drive in balance can be thought of as functions of these other variables and have been defined in this way by several authors working independently.

Most familiar applications of belt-drive hardware involve variable speed requirements which do not involve rapid or even continuous changes in drive ratio Usually the driver pulley is position-controlled rather than force-controlled. This is a convenient means of adjustment; however, it works only because the response time of the belt-drive system is much faster than the change in adjustment with most of these kinds of hardware. Attempting to control a belt drive by sheave-position changes within the response time of the drive itself does not work, because of the high transient imbalance initiated into these controlling forces. Making the belt drive respond quickly enough for the single-shaft turbine powertrain requires a careful determination and application of the forces involved.

In order to provide the correct amount of axial force on each sheave (and thus control the belt-drive ratio), the following parameters must be known:

a. tight and slack side belt tensions

b. torque transmitted

c. desired ratio

In practice, this is accomplished by monitoring the torque exerted on one of the pulleys (usually the driven) and the center-to-center separation force, which can be manipulated to yield items (a) and (b)

In many drives, the desired ratio is some function of speed and/or driver torque. A conversion must then be made, usually by some mechanical means, such as a pair of bobweights in conjunction with springs and ramps, to translate these values into the desired approximate axial forces. In most cases, the stability and life of the drive depends mostly upon how cleverly this conversion is accomplished. In drives where the ratio is either arbitrarily determined or a function of parameters not directly experienced by one of the drive components, the sheave actuating mechanism may be built to simply respond to an appropriate command signal, such as a voltage, hydraulic pressure, etc. In any case, the belt drive quantities that will be controlled are the axial force and the balance between the axial force and the separating forces at work in the running drive.

The single-shaft gas turbine engine automotive powertrain presents a control challenge over and above what is required for delivering power to a fixed load system. Typical applications of the single-shaft power plant to date have been aircraft (turboshaft) prime movers and auxiliary power units which drive fixed frequency alternators.

In both cases, the load level seen by the engine is relatively constant and is delivered over a narrow speed range. Automotive usage imposes a load schedule that is usually a small fraction of the maximum-rated power of the system. Yet that maximum power must be made instantly available on demand for acceleration, routine maneuvers such as passing, etc. The engine design reflects off-range excursions; the control system has to keep the engine and transmission in an optimum compromise operational state throughout this range and be able to change rapidly from one state to the next in response to a command input.

The engine speed is a direct, single-valued and strictly-defined function of engine output power, while the vehicle speed is an independent parameter. The CVT must interpose the matching between engine and load; the CVT control has to determine the instantaneous ratio between engine and vehicle speeds based upon conditions in the engine and the power demanded from the system. Power level demand changes have to immediately result in ratio changes; the CVT control must respond faster than the engine or the vehicle.

With the use of a CVT, there also comes the possibility of smooth exchanges of large quantities of energy back and forth between the engine and the moving vehicle. The vehicle motion, itself, can be thought of as an "energy reservoir" that can be augmented or tapped at will by minute, instantaneous changes in the transmission ratio. Changes in engine speed do not necessarily depend upon the 'engine time constant', as it has been classically defined. It may be advantageous for the control system (both engine and transmission integrated together) to be programmed to accomplish reverse flow, power reflections under certain conditions.

It is apparent that the fuel flow into the turbine must vary in conjunction with the CVT ratio for all speed and power conditions. CVT ratio essentially determines engine speed while the fuel flow into the machine determines the temperature (and, hence, the power which must be related to engine speed to prevent unwanted excursions of temperature). It is desirable to hold the turbine inlet temperature to a high upper limit to maximize the cycle efficiency.

However, the limit must be set 'hard' to prevent overheating damage to the mechanical parts of the machine. It becomes apparent that two control schemes are possible. One could arbitrarily manipulate the CVT ratio to obtain the desired speed (and power level) while maintaining closed-loop operation around turbine inlet temperature. Alternately, one could add fuel to the system arbitrarily in anticipation of the power level desired while moving the CVT ratio automatically to maintain an engine speed. Obviously, both of these philosophies must be relaxed to include overspeed and over-temperature safety limiters and the provision for functioning when the vehicle is at rest, or during engine startup

Current single-shaft engine fuel controls employ scheduling to accelerate the engine, change power levels, etc. With the CVT, the automotive powertrain gains an extra degree of freedom that could obviate the use of different, preprogrammed schedules in favor of the simpler closed-loop servo.

The control inputs required to accomplish the generalized single-shaft engine/CVT powertrain system are:

a. turbine inlet temperature, or any signal which is a known, direct, real time, and single-valued function of this temperature

b. engine speed

c. vehicle, or propshaft speed

d. system power demand

e. ambient temperature and pressure

Outputs from the control system will basically be:

a. fuel flow

b. CVT ratio

In an actual system, there are ancillary controls to perform the actuation of appropriate elements which serve to carry out these functions. The exact control methods and elements depend on the CVT selected and the translation of drive input commands to the power level demand signal

7.11 Marketing Analysis for Concept Selection

The selection of the most appropriate engine power level for incorporation into a viable vehicle marketing plan was considered next. The design point pressure ratio, component efficiencies and maximum cycle temperatures determine the gross thermal efficiency of the engine However, the engine output power level and air flow rate influence the realized brake thermal efficiency. The aerodynamic component efficiency is directly related to the engine air flow rate while the engine parasitic losses, i.e., mechanical flow and heat, determine the fraction of the gross engine output available for useful brake output. Then for decreasing design engine output power levels the lower air flows result in poorer component efficiencies, mainly due to the relative increase in size effects. The mechanical losses remain essentially constant since, although rotational speeds increase with decreasing flow size, the high speed bearings sizes can be reduced somewhat. The flow and heat leaks are also not strongly affected since the number of corners and joints involved are not changed, and, in general, the space available for insulation is somewhat reduced. Thus, on a relative basis, the parasitic losses are more significant with lower-output-power engines.

The output characteristics for design power levels of 75, 100 and 125 horsepower, shown on Figure 81 show the lower efficiency and higher BSFC of the lower-output engines. This lower efficiency would reduce the competitive fuel economy advantages of the turbine engine as compared to spark-ignition engines at lower output power levels. Referring to Figure 82, the slope of the gas-turbine-powered vehicle fuel economy, as a function of inertia-weight class, which is related to engine power level for a given vehicle performance, would be flatter than that shown for the reciprocating engines Thus the greater the engine power level, the greater the fuel economy advantage of the gas turbine

A long-range, overall projection for the total U.S. car and truck market is shown on Figure 83. As shown, the increase in the truck and small-car segment, together with the decrease in the large-car segment, is expected to level off after 1979. However, because of vehicle weight-reduction efforts and fuel-economy requirements, the market for the 100-horsepower-and-above segment is expected to diminish as shown, leveling out at a two- to three-million yearly potential, largely because of payload requirements. Diesel engines are currently being targeted for this 100-horsepower-and-above segment, but the gas turbine, developed to its potential, would be a beneficial alternative.

These considerations have resulted in the selection of 85 horsepower as the base development size for the 1150°C selected engine. This size was chosen so that when the engine is developed to its long-range 1350°C potential, it would be at a desirable 114 horsepower range without a change in shaft speeds, compressor size, or regenerator size.

At 1150°C the engine would be suitable for initial introduction in a future 2750 lb, front-wheel-drive vehicle, where it would yield a fuel economy of 30.4 mpg (gasoline) It is expected that if properly marketed, such a vehicle could initially be sold in substantial but limited volumes at a premium price while the development to the long-range, higher-power version, along with a gradual buildup of production facilities, proceeds.

8.0 DEVELOPMENT PLAN

This section describes a program plan for development of the IGT concept selection in Section 7.0. Identified in the program is the development work needed to meet the goal of entering a production engineering phase by 1983. The overall program plan includes detailed task schedules, cost estimates, and manpower requirements for each phase of the program.

The engine will be designed for 77 horsepower (unagmented) with a maximum power of 85 horsepower (augmented). Design turbine inlet temperature is 1150°C; design pressure ratio is 4.2. The cycle characterization is shown on Table 15; the station notation is defined on Table 16. The turbine is a metallic single-stage radial turbine. The CVT will be either a hydromechanical type or a belt-drive type, depending on the outcome of the CVT development. The selected vehicle has an inertia weight of 2750 lbs. and has front-wheel drive. The fuel economy goal is 30.4 mpg, based on gasoline.

The program will be carried out in two parts. In the first part, the design turbine inlet temperature will be 1040°C to permit development of the shafting, bearings, and gears and to allow demonstration of the aerodynamic efficiency levels. Compressor design mass flow is set by the design point conditions for 1150°C turbine inlet temperature and would not change. The maximum power would be 68 horsepower. In the second part of the program, the turbine will be redesigned aerodynamically and mechanically for a design turbine inlet temperature of 1150°C to deliver a higher maximum output power of 85 horsepower. The combustor and turbine static components will be made of ceramic materials for this temperature.

The long-lead R and D items are a ceramic radial turbine and a belt-drive CVT. Results of the powertrain study showed that the best fuel economy is obtained with a single-shaft engine at 1350°C turbine inlet temperature and with a belt-drive CVT. To achieve the ultimate fuel economy goal, it will be necessary to make the turbine out of ceramic material. This material must have the needed mechanical properties and be capable of low-cost processing. A method of attaching ceramic material to a metal shaft must be developed. The need for the belt-drive CVT is based on reductions in cost and noise compared to a hydromechanical CVT. Analysis indicates that a transmission based on use of variable-speed V-belt could be produced at about two-thirds the cost of a hydromechanical unit and would not likely require development to achieve acceptable noise levels.

The program is outlined schematically in Figure 84. Included on the figure are the powertrain configurations required to achieve the ultimate fuel economy and the long-lead development items. The engine will begin with all metallic parts and have an initial value of maximum power of 68 horsepower. With the introduction of ceramic-static components, the power rises to 85 horsepower. Ultimately, the engine power would increase to 114 horsepower with the introduction of a ceramic turbine rotor. The long-lead R and D items are shown on the figure. Depending on development progress, these items could be introduced in the development program. The ceramic rotor would be substituted for a metallic rotor, and the belt-drive CVT would replace the hydromechanical CVT on the powertrain.

A summary of certain design information for the powertrains of this program plan, for the powertrain with advanced development, and for the powertrains of the study is shown on Table 17. The study results show the change in fuel economy and design parameters as turbine inlet temperature increases for a fixed design power. The program plan shows the change in fuel economy and design parameters for fixed compressor mass flow as turbine inlet temperature increases with the incorporation of ceramic components. The advanced development powertrain is applied to a heavier vehicle. Depending upon the development progress in ceramic materials, the radial turbine could be made of ceramic material instead of a superalloy; hence the term back-up is used.

8.1 Program Risks

The program has been realistically structured to achieve program goals. By design, therefore, overall risk of the basic program is low. Values of compressor efficiency, turbine efficiency, and regenerator effectiveness were set at levels already shown to be achievable in tests on comparable sized components. Additionally, conservative values were selected for leakage and heat loss. As with any new design some allowance for aerodynamic, heat recovery, sealing and insulation development is being provided, but in this particular engine concept these should be no more than straight forward refinement and optimization steps.

The high speed (94,300 rpm) of the engine, however, will likely require some fundamental bearing, shaft, and reduction gear development to achieve stable operation with acceptable values of life, parasitic loss and noise level. Maximum speed of both the gas generator and power turbine rotors on the Baseline Engine was 45,000 rpm. This was successfully increased to 58,500 and 70,000 rpm respectively in the Upgraded Engine even with the inclusion of an advanced technology gas foil bearing for the compressor drive turbine journal bearing. Eaton has demonstrated a 100,000 rpm - 50 hp single-shaft engine, and turbocharger rotors currently run up to 150,000 rpm. In light of the above experience along with some preliminary design analysis, it is expected that all aspects of the proposed high speed mechanical systems can be satisfactorily developed. However, its longest lead and potentially highest risk aspect would be associated with successful development of gas lubricated journal and thrust bearings for the shaft connecting the compressor and turbine wheels. Priority, therefore, would be given to early program effort in this area.

With turbine inlet temperature up to 1150°C, prime reliance will be on the use of a metallic turbine wheel. Experimental materials exhibiting needed properties have already been demonstrated so that the risks associated with having a fully-demonstrable wheel within this five-year program appear minimal.

Similarly, risks associated with having ceramic static hot section components within this period also appear minimal. Excellent results have been achieved by Carborundum in casting SiC vortex under Task 10 of the current Chrysler contract and the application of ceramics to burners, shrouding, ducting and stator blades is being effectively demonstrated on Ford-ARPA, DDA-DOE, and Garrett-ARPA programs.

Finally, predicted values of overall vehicle performance for the proposed IGT system were based on the use of an existing hydromechanical continuously variable transmission. Efficiency values were assumed at tested levels of the Orshansky first generation units. So in this area also, fundamental development risk is minimal although some development to control noise associated with high pressure hydraulic machinery would likely be needed.

Based on the foregoing, the overall risk associated with a successful demonstration of the fundamental engine concept would be expected to be small. However, the long range purpose of the program is to save fuel by mass producing and marketing a more economical automotive engine, and in working to achieve this purpose two higher risk back-up items of the proposed program assume a vital role. One of these is the ceramic turbine and the other is a variable sheave V-belt CVT.

With respect to the ceramic turbine, response time of the basic engine with metal wheel is questionable in regard to customer acceptance. A wide open throttle acceleration would require about 1.0 second for rotor acceleration before clutching to the vehicle drive train. With a lighter ceramic wheel, the time would be reduced to a more acceptable 2 seconds. Additionally, a metallic wheel relies on the use of nickel and chromium, two materials of uncertain availability with respect to high volume automotive use. There are no supply problems in the raw materials of proposed ceramic wheels.

The risks associated with the ceramic wheel would be in achieving practical low cost processing of a material with adequate strength and a practical attachment to a metal shaft. Promising approaches have been proposed for achieving success in both of these areas, but being of a fundamental nature, development time is uncertain. This factor, along with the long range importance of the ceramic wheel warrants that efforts in this area receive program development priority.

As stated above, the hydromechanical CVT meets program performance and efficiency needs. However, our analysis indicates that a transmission based on the use of a variable speed V-belt could be produced at about two-thirds the cost of a hydromechanical unit and would not likely require development to achieve acceptable noise levels. A two-belt transmission is currently being used successfully in the 70-hp Volvo 343 passenger car and in a single-belt 70-hp Kawasaki snowmobile. Average service life for the car belts is over 40,000 miles. Also, Gates Rubber has been testing relatively small experimental belts at 100 to 130 horsepower and projects 100,000-mile service life on an automobile-duty cycle. Nevertheless, unlike the hydromechanical concept, proof of a V-belt system suitable for a 100-horsepower, single-shaft engine has yet to be shown. So, even though the system is more suitable to volume automotive use, it does carry a development risk and should, therefore, be accorded development priority.

8.2 Program Plan

The proposed development plan is made up of eleven tasks, as summarized in Figure 85. The general approach is to begin with a preliminary overall [illegible] task to define specific subsystem requirements and then concentrate major program effort on co[illegible]ent design and development, to achieve required levels of aerodynamic, mechanical, material, trans[illegible]ssion, and control performance. This effort would then phase into the design, building, and demonstration of the goal engine and vehicle system.

The development approach is to use three types of engine - a combined turbomachinery engine rig, a workhorse engine, and an experimental IGT engine. The combined turbomachinery rig is actually a nonregenerative engine which will be used to confirm the compressor and turbine performances when these components are combined to produce the sum of the required output and regenerator drive power. The workhorse engine will be a single-shaft version of the Upgraded Engine with the turbomachinery configurations and sizes of the IGT. This engine will be used for final development of the regenerator drive and seal system, of the CVT and the control system, and of the ceramic components. The experimental IGT engine design will emphasize efficient packaging and simplicity and will feature rig and workhorse-engine-developed components. The final CVT design and control system will be combined with this engine.

In the first two years, all of the development for the 1040°C-turbine and most of the development for the compressor will be completed. The turbine design will begin first, followed immediately by the compressor design. The design schedule is arranged so that the compressor design takes place during the procurement for the turbine parts. It is planned that compressor development will be sufficiently completed for successful testing of the combined turbomachinery rig, but the 1040°C-turbine development must be fully completed. The combined turbomachinery rig will operate at cycle inlet temperature and would be utilized to identify any problems caused by component interaction in an engine-type environment. Compressor testing will continue into the last three years to explore extending the state-of-the-art in diffuser performance and reducing rotor inertia, and to rectify performance penalties imposed by the regenerator inlet housing configuration of the experimental program engine. The turbine activity will consist of the design and development of the 1150°C turbine. Two design configurations are anticipated. Rig development of both compressor and turbine are scheduled through the beginning of the fourth year of the contract, with final engine development in the last two years.

The large value of design rotational speed (94,300 rpm) will require careful design of bearings and shaft. A subcontract to MTI will support this effort, mainly in the prediction of critical speeds and in the development of an air bearing system. The air bearing system is important to minimize parasitic losses associated with high-speed shafts. A test rig at the subcontractor facility should be operational by the third quarter of FY 1979, as indicated in Appendix C, to support this development.

The elastomer-mounted ring gear of the regenerator will need some development for higher temperature operation. Reduced leakage and pressure drop will also be of prime importance because of fuel economy sensitivity of these parameters. The test rig development goal will be to have a reliable regenerator system, capable of 870°C turbine exhaust temperatures, ready for workhorse engine testing in FY 1982. The workhorse engine is a single-shaft adaptation of the Upgraded Engine; see Task 7.0. The materials support effort for the workhorse regenerator system will be accomplished in Task 6.0.

The hydromechanical CVT comes closest to an ideal transmission for the single-shaft gas turbine engine. In spite of the cost penalties involved, this transmission type still represents the only truly low-risk alternative CVT in the near term of this program. Accordingly, some funds will be spent on a contract basis to allow development work on an existing-hydromechanical CVT to continue. At the beginning of the program, Chrysler will issue an RFP pertaining to development of a hydromechanical CVT and control system that can be integrated with the proposed single-shaft gas turbine engine and a conventional, rear-wheel-drive vehicle.

A belt-drive CVT test and development rig will be designed and built to subject candidate drive belts to the appropriate regime of power levels, ratio schedules, duty cycle, and environment anticipated in automotive transmission service. Basic questions pertaining to ratio control, and the influence of automotive loading conditions on tension and ratio variation must be defined and addressed. Once a satisfactory belt drive CVT has been developed, a system designed for the workhorse engine/vehicle will follow. The final belt drive CVT design for the IGT system will evolve from vehicle and test cell

development of the workhorse system. Integration of the transmission and engine control systems will first be investigated mathematically with digital and analog computer simulations. A final CVT design and control system will be defined and incorporated into the IGT experimental engine.

Development of a suitable alloy composition and processing procedure would require a joint program with P&WA. Short time tensile, creep-rupture, LCF, and hot corrosion samples would be required. The goal is to provide a metallic radial turbine ready for rig testing by late FY 1981, as shown in Appendix C.

To expedite ceramic turbine development, a concerted effort will be made to deliver a preliminary ceramic rotor design (for 1040°C) to Carborundum by mid-FY-1979. Chrysler designers will work closely with Carborundum in addressing such key design considerations as binder bake-out limitations and molding constraints during the initial months of the program. A specified number of rotors and rotor-like shapes will be supplied to Chrysler for both nondestructive evaluation and for spin testing. Consideration shall also be given to methods and problems associated with molding component parts of sintered -SiC, as per engineering drawings supplied by Chrysler. The largest part of this effort will focus, however, on the goal of successfully forming and sintering an integral radial rotor during FY-1979 and FY-1980.

A subcontract will be issued to KBI to investigate various aspects of Hot Isostatic Pressing of Silicon Nitride HIP (Si_3N_4) technology, such as canning/cladding/encapsulation methods, pressure and temperature effects on densification, the effect of sintering aids on densification and elevated temperature properties, and size/shape fabrication capability.

A test rig will be provided to simulate engine operating gas temperature levels including transients. This will allow ceramic static parts to be tested under conditions that may be varied to suit development requirements. Simulated radial rotors, as well as complete vaned rotors (to be supplied near the end of FY 1980), will be subjected to thermal shock in a modified version of the turbomachinery rig. Design changes needed for this area are scheduled to begin in mid-FY 1980. Test rig modifications will be completed near the beginning of FY 1981, which may allow a small number of parts to be tested during FY 1981.

The design of a ceramic turbine rotor for 1150°C turbine inlet temperature will begin about mid-FY 1980. The test and development work will follow the steps carried out for the 1040°C rotor. This work will be conducted in the last two years of the program.

An oxidation rig will allow for the evaluation of the chemical and high temperature effect of engine gases on ceramic parts made of alpha silicon carbide and/or various forms of silicon nitride. Effects such as surface degradation/erosion and strength after exposure will be correlated with such variables as time, temperature, gas flow rate, impurity elements in fuels, and other possible variables. Design of such a rig is to be completed by the end of FY 1979. Testing will commence in mid-FY 1980.

8.3 Task Definitions

Appendix C contains detailed charts showing task and subtask timing, and milestone points, plus effort and material cost estimates. Specific contents of the various tasks are described in the following sections.

Task 1.0 Administer Program

This task will provide for constant project review, formal reporting and provide a channel for communication in matters that may impact on the overall program. Program control will be maintained by monitoring technical progress and direction, task schedules, and financial status. Close attention to progress made toward attaining program goals and specifications will help to maintain schedules, and provide early identification of problem areas.

Task 2.0 Preliminary IGT Experimental Engine Design

Preliminary layouts of single-shaft engine arrangements will be reviewed and modifications required for installation in a subcompact, 2750 lb. vehicle will be studied. Layouts will be made showing proposed component designs (such as shaft and bearings, support structures, housing configuration, reduction gears, and regenerator and accessory drives). Revisions will be shown as detail design work progresses.

During the initial months of the project, the preliminary design will be used to define detailed engine specifications. These specifications will both define specific aerodynamic and mechanical component design constraints, and will define the type of testing, operating hours, and thermal cycles required to establish the desired component life, performance, and reliability. The specifications are expected to change as the design process continues and will be updated accordingly.

Task 3.0 Aerodynamic Component Development
This task consists of the design, procurement, test, and development of the compressor and turbine. The compressor will be designed for the flow size of an engine capable of delivering 85 hp at 1150°C turbine inlet temperature (TIT). However, it will also be used in the workhorse engine (1040°C TIT, 68 hp) and the experimental IGT engine (1150°C TIT, 85 hp), since both engines will have the same design massflow. The turbine designs will differ for each engine temperature, since the output power increases with TIT.

Task 4.0 Mechanical Component Design and Development
This task consists of the design and development of the engine shaft system, the reduction gears, and the regenerator and its seal system. The shaft and bearing arrangement will be submitted to a subcontractor for a complete dynamic analysis, including shaft stability and response. The subcontract will also provide for a test rig simulation of the shaft system to assure satisfactory shaft and bearing performance throughout the engine operating range. The reduction gear design applies only to the experimental IGT engine. Existing gear sets can be used for the combined turbomachinery rig and the workhorse engine. The regenerator drive and seal system will be developed on a test rig and on the workhorse engine.

Test 5.0 CVT and Control Design and Development
This task covers the procurement of and some development on a hydromechanical CVT,. the development of a belt drive CVT, a study of a traction drive CVT, and the mathematical modeling of the engine and transmission control systems. Development of the belt drive CVT will begin with rig testing; final development testing will come from workhorse engine testing.

Task 6.0 Develop and Utilize Improved Materials
This task covers the materials aspect of the design and development work performed for the 1150°C and 1040°C turbines, for the regenerator system, and for the insulation of the engine housing. The properties of the high temperature materials influence the heat transfer paths and the structural integrity of the parts. Items covered in this task include the design and development of metallic and ceramic versions of these turbines, methods of shaft attachment, and the evaluation of fabrication and processing alternatives. Ceramic material development will start with a preliminary rotor design, followed by the design of the 1040°C rotor and then the 1150°C rotor. This development will be assisted by heat transfer and stress analysis studies, followed by static rig tests of the stationary components in a thermal test rig, an oxidation rig, the combined turbomachinery rig, and the workhorse engine. The metallic versions of these rotors will be designed first. To obtain the necessary strength, the RSR (rapid solidification rate) process of P&WA will be considered.

Task 7.0 Evaluate and Develop Workhorse Engine
Use of this workhorse concept will allow engine experience much earlier in the program. Initial testing will be primarily steady-state performance and endurance evaluation. Endurance testing will encompass the complete engine system, including ceramic components as they become available.

Task 8.0 Design and Develop IGT Engine Regenerator System
This will be a continuation of the effort started under Tasks 4 and 6. The IGT experimental engine regenerator drive system will be finalized utilizing information gained from elevated temperature testing conducted under Task 6.

Any necessary test rig modifications will be made to accommodate IGT program components. Regenerator system components will be procured with initial tests being conducted on test rigs. Emphasis will be placed on long life, reduced system leakage, and regenerator effectiveness. Since the test rig will be configured like the engine housing, "real world" performance levels are anticipated.

Task 9.0 Develop IGT Engine Burner System

A test rig will be designed for low emission burner development. The rig configuration will be as much like the IGT engine configuration as possible. With this approach, subsequent engine emission test results should closely reflect test rig results. Both steady-state and transient emission testing will be conducted.

Burner development normally entails many iterative loops of "cutting and patching" before good temperature distribution, stability, and low emission levels can be obtained. For this reason, initial burner development (at lower temperatures) will be accomplished with metallic components (such as Lamilloy). A ceramic counterpart will follow once a successful metallic design has been established. Remaining development effort would be aimed at obtaining a successful ceramic version of the metallic burner suitable for IGT engine operation. This effort would be primarily concentrated on obtaining an acceptable level of durability.

Task 10.0 IGT Program Engine Design

The IGT experimental engine design will emphasize efficient packaging, simplicity, and will feature rig and workhorse-engine-developed components. Whether or not a ceramic turbine will be incorporated will depend on the success of the brittle materials design and development program. The ceramic rotor would have lower inertia than its metal counterpart, resulting in better rotor response. Once installed in a test vehicle, an engine with this low inertia ceramic rotor should provide improved driveability characteristics. A final CVT design and control system will be specified and incorporated into the IGT experimental engine.

Task 11.0 Design IGT Program Engine Vehicle Installation

This task will involve optimizing the engine - transmission - vehicle system driveability, fuel economy, and general customer appeal. A demonstration fleet will be prepared for vehicle system performance evaluations. The primary objective of this task is to develop an IGT vehicle system with maximum consumer acceptability.

9.0 CONCLUSIONS

A study was conducted to determine the improved gas turbine powertrain configuration best suited to achieving a fuel economy which is 20% better than the value achieved with a spark-ignition engine in a vehicle with an inertia weight of 3500 pounds. Cycle analyses and detailed performance studies were carried out to determine concepts which would achieve the study goals. One concept was selected on the basis of fuel economy, cost, and low risk. A market application was identified, and a development plan was outlined. The results are summarized as follows:

1. Best fuel economy was achieved with a single-shaft engine with a continuously variable transmission.

2. Engines with more than one shaft have less fuel economy because of parasitic losses and flow and heat leaks.

3. The highest fuel economy with a single-shaft engine is achieved at a design turbine inlet temperature of 1350°C; the study goal was met at 950°C.

4. Because of this, a development program could be planned around use of an advanced superalloy. With RSR metal, the design turbine inlet temperature could be 1150°C, and based on the calculations in the study, the fuel economy would be 9% beyond the goal of the study.

5. A development plan was outlined which would lead to a decision on production engineering by 1983. The engine would be designed for 85 hp (augmented). A hydromechanical CVT would be used, and the engine would have a metal radial turbine

6. Long-lead technology was identifed for ceramic material for the radial turbine and for a belt drive CVT. The ceramic material would be needed to increase turbine inlet temperature to 1350°C and achieve maximum fuel economy. The belt drive CVT is needed for minimum noise and cost, as well as maximum fuel economy.

All the conclusions are based on the assumptions of component efficiencies or values of regenerator effectiveness used in the study. However, the values which were used represent levels currently available in the state-of-the-art. Consequently, the study results do not require advances in the technologies of aerodynamics or regenerator effectiveness. The same conservatism was applied to estimates of parasitic losses and flow and heat leaks.

References

1. Baseline Gas Turbine Development Program - Twenty-First Quarterly Progress Report. Prepared for U.S. Department of Energy, Division of Transportation Energy Conservation, Edited by F.W. Schmidt and C.E. Wagner, January 31, 1978.

2. Kronogard, S.O.: Three-Shaft Automotive Turbine-Transmission Systems of the KTT Type - Performance and Features. ASME Paper No. 77-GT-94; March, 1977.

3. Pampreen, R.C., Firman, P.A., Erwin, J.R., and Dawson, R.W.: A Small Axial-Centrifugal Compressor Matching Study Program. USAAVLABS Technical Report 70-34; October, 1970.

4. Pampreen, R.C.: Small Turbomachinery Compressor and Fan Aerodynamics. Trans. ASME, Journal Engineering for Power; July, 1974.

5. Castor, J.G. and Riddle, B.C.: Automobile Gas Turbine Optimization Study. AiResearch Manufacturing Company of Arizona, Report AT-6100-R7, Prepared for EPA, Office of Air Programs; July, 1972.

6. Kofskey, M.G. and Nusbaum, W.J.: Effects of Specific Speed on Experimental Performance of a Radial-Inflow Turbine. NASA Technical Note TN D-6605; February, 1972.

7. Mechanical Response of High Performance Silicon Carbides. Carborundum Company, 2nd International Conference on Materials, 1976.

8. Design and Performance of Gas Turbine Power Plants. Volume XI - High Speed Aerodynamics and Jet Propulsion; pp 528-531. Edited by W.R. Hawthorne and W.T. Olson, Princeton, New Jersey, Princeton University Press, 1960.

9. Baseline Gas Turbine Development Program - Eighteenth Quarterly Progress Report, Appendix B, Page 5.5.1 Prepared for U.S. Department of Energy, Division of Transportation Energy Conse.vation, Edited by F.W. Schmidt and C.E. Wagner, April 30, 1977.

10. Nineteenth Quarterly Progress Report - Baseline Gas Turbine Development Program. Prepared for U.S. Department of Energy, Division of Transportation Energy, Conservation. Edited by F.W. Schmidt and C.E. Wagner, July 31, 1977.

11. Klassen, Hugh A.: Effect of Inducer Inlet and Diffuser Throat Areas on Performance of a Low Pressure Ratio Sweptback Centrifugal Compressor. NASA TM X-3148, January, 1975.

TABLE 1

Baseline Vehicle for Improved Automotive Gas Turbine Conceptual Design Study

**Vehicle Class	Compact
Curb Weight	3100 lbs.
Test Weight	3400 lbs.
**Frontal Area	21.5 ft.²
**Wheel Base	109.5 in.
Axle Ratio	2.70:1
Tires	ER78-14
HP/WT Ratio (reference)	0.03
Transmissions	3-Speed Automatic
1st Ratio	2.5 to 1
2nd Ratio	1.5 to 1
3rd Ratio	1.0 to 1
**0-60 MPH Acceleration Time	15.0 sec.
**Minimum Range. (Combined Federal Driving Cycle)	300 Miles
1976 Fuel Economy (Combined Federal Driving Cycle)	19.6 MPG
**Roominess Index*	273"
**Hip Room	57"
**Shoulder Room	55"
**Trunk Space	16.0 ft.³

*See Definitions Attached **IGT Characteristics

TABLE 2

Definitions

1. **Accessories** - Engine-driven components, associated with vehicle operation but not required for operation of the basic engine (e.g., air conditioner, power steering pump, etc.).

2. **Accessory Drives** - Engine power devices providing power for the accessories.

3. **Auxiliaries** - Components external to the basic engine required for proper engine operation in an automotive application (e.g., fan, cooling system, starter, fuel control system, alternator, battery, etc.).

4. **Drivetrain** - Aggregation of components necessary to transmit the engine power to the wheels (e.g., transmission, drive shaft, clutch system, axle, final reduction gears, etc.).

5. **Basic Engine** - The basic power-producing unit without auxiliaries, or accessories.

6. **Engine System** - The Basic Engine plus auxiliaries.

7. **Powertrain** - The engine system plus drivetrain, and accessory drives.

8. **Powertrain System** - The powertrain plus any vehicle system elements necessary to make the powertrain function as an automotive powerplant (e.g., fuel supply system, exhaust system, battery containment, instruments and gages, linkages, etc.).

9. **Chassis/Body** - The chassis and body elements into which the powertrain system is integrated to form an automotive vehicle (e.g. frame, sheet metal, brake system, steering system, bumpers, interior, wheels, tires, suspension system, etc.).

10. **Automotive Vehicle** - A complete self-propelled vehicle (e.g., Otto spark-ignition automotive vehicle, Stirling automotive vehicle, Gas Turbine automotive vehicle, etc.).

11. **Roominess Index** - To be furnished by the Government.

12. **Powertrain Thermal Efficiency** - The ratio of axle shaft output power to energy content of the fuel consumed with appropriate conversions for unit consistency. The fuel energy content will be based on a gasoline equivalent (133,000 BTU/gal.).

TABLE 3

Manufacturing Complexity

Turbine Section	Split Nozzles Multiple Shrouds Tip Clearance Control Proximity to Bearings
Gearing and Shafting	Multiple Spools Balancing Shaft Dynamics
Transmission	Standard C.V.T. Simplified
Controls	Variable Geometry C.V.T. Multiple Spools

TABLE 4

Comparison of Part Quantities

	Radial 1-Shaft	Interconnected 3-Shaft
Ceramic Burner and Turbine Parts	7	18
High Speed Components Shafts, Bearings, Seals, Pinions	9	20
Engine plus Transmission Gear Sets	2 Simple 2-to-3 Planetary	4 Simple 2 Planetary
Variable Speed Unit	1	0

TABLE 5

Powertrain Parasitic Power Losses

	2-Shaft Engine		Single-Shaft Engine
	Idle Power	Max Power @50% Speed	50% Speed
Bearing Power, HP			
Gas Generator	0.84	0.84	1.58
Power Turbine	0.08	0.54	
Reduction Gears	0.03	0.08	0.01
Accessory Power, HP			
Oil Pump	0.18	0.47	0.08
Regenerator Drive	0.08	0.22	0.21
Alternator	0.42	0.44	0.42
Power Steering Pump	0.21	0.52	0.26
Transmission Power, HP			
Transmission Pump	0.21	0.57	
Torque Converter (in Drive)	2.45	—	1.49*

*CVT (Pump, Gears and Bearings)

TABLE 6

Listing of Leakage and Parasitic Power Loss for Various Engine Configurations

Turbine Leakage %							
Engine Speed %	**50**	**60**	**70**	**80**	**90**	**95**	**100**
SS	4.1	4.5	4.8	5.7	5.5	5.7	5.8
2s 1st Stage	6.3	6.0	6.2	6.8	6.6	6.8	6.9
2s 2nd Stage	3.4	3.3	3.5	3.9	3.7	3.9	3.9
Total Parasitic Loss, HP							
SS	2.3	3.1	4.1	5.3	6.6	7.4	8.3
2s	2.4	3.6	5.0	6.3	8.2	9.0	9.4

SS - Single-Shaft Engine

2s - Two-Shaft Engine

$$\text{Leakage} = \frac{M_1 - M_x}{M_1}$$

M_1 = (Air + Fuel) Flow Rate

M_x = Local Inlet Flow

TABLE 7

Turbine Efficiency Comparison (Total-Static)

Gas Generator Speed %	3-Shaft Overall Turbine Efficiency	Single Stage Turbine Efficiency	2-Shaft Overall Turbine Efficiency
100	0.874	0.852	0.849
80	0.843	0.845	0.822
50	0.770	0 805	0.758

TABLE 8

Listing of Leakage and Parasitic Power Loss for Various Engine Configurations

Turbine Leakage % Engine Speed %	50	60	70	80	90	95	100
SS	4.1	4.5	4.8	5.7	5.5	5.7	5.8
3s 1st Stage	5.9	6.1	6.4	6.7	7.1	7.2	7 1
3s 2nd Stage	3.2	3.4	3.6	3.8	4.1	4.1	4.0
2s 1st Stage	6.3	6.0	6 2	6.8	6.6	6.8	6.9
2s 2nd Stage	3 4	3.3	3.5	3.9	3.7	3.9	3.9
Total Parasitic Loss, HP							
SS	2.3	3.1	4 1	5.3	6.6	7 4	8.3
2s	2.4	3 6	5.0	6 3	8 2	9.0	9 4
3s	3.2	4.8	6.6	8 4	10.9	12.1	12 8

SS - Single-Shaft Engine

2s - Two-Shaft Engine

3s - Three Shaft Engine

$$\text{Leakage} = \frac{M_I - M_X}{M_I}$$

M_I = (Air + Fuel) Flow Rate

M_X = Local Inlet Flow

TABLE 9

Pressure Ratio Comparison

Gas Generator Speed %	Twin-Spool Pressure Ratio	Single-Stage Comparison	% Increase
80	2.926	2.76	6.0
50	1.576	1.54	2.3

TABLE 10

Comparison of Acceleration Times — Single-Spool Versus Twin-Spool Gas Generator

Shaft Configuration	Time (sec.) to Accelerate to: 80%	100%
Single-Spool	0.79	1.14
Twin-Spool		
From 41% Outer-Spool Speed:		
Outer-Spool	1.42	1.82
Inner-Spool	1.85	2.42
From 51% Outer-Spool Speed:		
Outer-Spool	0.74	1.12
Inner-Spool	1.23	1.80

TABLE 11

Preliminary Estimate of Manufacturing Costs

Concept	Arrangement	Hardware Category - Cost Percentages: Housing Insulation Assembly	Turbo-Machinery	Regene-rator	Reduction Gear Trans.	Cost Ratio
Cost Effective						
Upgraded Engine 1925° F	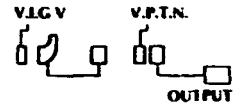	27.5	36.4	18.7	17.4	1.00
Maximum Upgrade - 2100° F						
V.P.T.N.	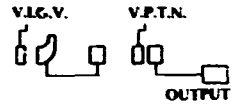	25.3	34.7	13.5	17.4	.91
Inter-Connection	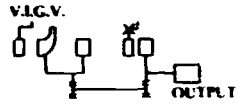	25.3	27.2	13.5	23.2	.89
Two-shaft - 2500° F						
Conventional 4:1	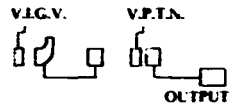	23.6	36.4	10.3	17.4	.88
Conventional 6:1	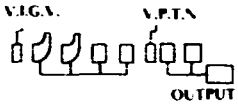	23.6	43.3	9.0	17.4	.93
P.T. First 4:1	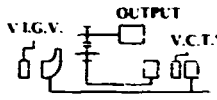	21.9	36.4	10.3	17.4	.86
P.T. First 6:1	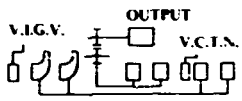	21.9	43.3	9.0	17.4	.92
Single-shaft - 2500° F						
Radial 4:1	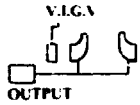	23.6	24.4	9.7	19.5	.77
Axial 4:1	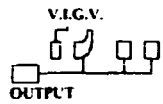	23.6	26.9	10 2	19.5	.80
Twin Spool 4:1	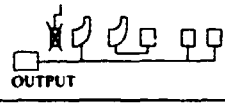	23.6	26.1	10.2	19.5	.79
Three-shaft - 2500° F						
3 Axial 4:1	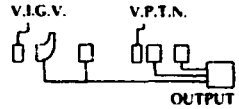	25.0	40.3	10.2	15.2	.91

TABLE 12

Estimates of Variable Manufacturing Cost Percentages By Turbine Engine and Hardware Category.

1350°C T.I.T. Except as Noted

1976 Dollars

Category	Engine			
	CEUE* 1052°C	3 Shaft	2 Shaft	Single Shaft Radial
Housing	24.6	23.1	22.7	23.5
Turbomachinery	23.0	28.4	24.8	18.3
Reduction Gear and Transmission	21.0	18.4	21.2	19.8
Regenerator	17.6	12.0	12.0	12.0
Controls	13.9	13.9	13.9	8.9
Total	100.1	95.8	94.6	82.5

*CEUE = Cost Effective Upgraded Engine

TABLE 13

Part Cost Distribution

	Base CEUE* %	3 Shaft %	2 Shaft %	1 Shaft %
Housing Assembly & Ancillaries				
Engine Housing	4.7	3.8	3.8	4.3
Insulation	8.8	6.5	6.5	7.4
Miscellaneous Items				
Mounts-Support Brackets	0.3	0.3	0.3	0.3
Dump Valve, Heater Connector	0.3	0.7	0.7	0.7
Engine Build Up	1.0	1.9	1.5	1.0
Ignition Exciter & Cable	0.4	0.4	0.4	0.4
Auxiliaries				
Alternator	1.6	1.6	1.6	1.6
Starter		2.1	2.1	2.1
Clutch Drive on Rotor				
Bendix Clutch Shaft				
Starter, Bracket, Reduction Gear Box	2.0			
Pulley, Belt, Adjusting Bolt	0.1			
Accessories				
Power Steering Pump	0.9	1.2	1.2	1.2
Burner Assembly				
Cover Assembly & Miscellaneous	0.4	0.4	0.4	0.4
Tube	3.3	3.3	3.3	3.3
Torch Chamber & Nozzle	0.3	0.3	0.3	0.3
Premixer & Injector	0.6	0.6	0.6	0.6
TOTAL	24.6	23.1	22.7	23.5
Turbomachinery				
Variable Power Turbine Nozzle	6.1	6.1	6.1	2.0
Assemble Gas Generate.	0.4	0.7	0.7	0.7
Gas Generator Support Casting	1.2	1.2	1.2	1.2
Rear Bearing Carrier	0.6	0.6	0.6	0.6
Vortex (Plenum)	5.4	5.4	5.4	5.4
Gas Generator Turbine Nozzle	1.9	1.9	1.9	1.9
Assemble Gas Generator Rotor System	0.1	0.1	0.1	0.1
Gas Generator Turbine Wheel	1.4	0.9	0.9	1.4
Sleeve	0.2	0.2	0.2	0.2
Compressor Impeller	0.5	0.5	0.5	0.5
Compressor Inducer				
Front Bearing Carrier	0.4	0.4	0.4	0.4
Compressor Cover	1.2	1.2	1.2	1.2
Variable Inlet Guide Vanes	0.5	0.5	0.5	0.5
Bolts, Oil Drain Tube	0.3	0.3	0.3	1.9
Air Intake Housing	0.2	0.2	0.2	—
Power Turbine Bearing Support Assembly	0.6	0.6	0.6	—
Power Turbine Rotor	—	4.0	4.0	—
Wheel	1.8	—	—	—
Sleeve	0.1	—	—	—
Assemble Sleeve & Pinion	0.1	—	—	—
Third Turbine Wheel & Shaft, Nozzle	—	3.5	—	—
TOTAL	23.0	28.4	24.8	18.3
Reduction Gear & Transmission				
Assemble	0.3	0.9	0.3	0.3
Housing & Cover	2.4	2.7	2.4	1.8
Housing & Cover Miscellaneous	—	0.2	0.2	—

*CEUE = Cost Effective Upgraded Engine

TABLE 13

Part Cost Distribution (continued)

	Base CEUE* %	3 Shaft %	2 Shaft %	1 Shaft %
Reduction Gear & Transmission (cont.)				
Regenerator Drive Components	—	1.2	1.2	1.1
Pinion	0.2	—	—	—
Worm	1.1	—	—	—
Gear & Shaft Assemblies	—	—	—	—
Intermediate Gear & Shaft	1.5	—	1.5	—
Pinion	0.1	—	0.1	—
Pinion Miscellaneous	0.1	—	[illegible]	—
Output Shaft & Gear	1.8	—	1.8	—
Ancillary Drive Assembly	0.7	—	0.7	—
Air-Oil Separator	0.1	0.1	0.1	0.1
Oil Pump	0.7	0.6	0.6	0.4
Air Pump Surge Tank & Miscella: eous				
Electric Clutch Assembly				
Oil Strainer, Pan, Filler, Level Indicator, Filter	0.3	0.3	0.3	0.4
Transmission	12.0	3.5	12.0	12.6
1976 Base Cost				
Input Drive Plate, Lock-Up				
TOTAL	21.0	18.4	21.2	19.8
Regenerator	—	12.0	12.0	—
Inner Rub Seals	4.8	—	—	3.6
Outer Rub Seals	2.4	—	—	1.8
Core Assembly	—	—	—	—
Core	8.8	—	—	5.3
Rim Drive	0.4	—	—	0.3
Cover & Bolts	1.2	—	—	1.1
TOTAL	17.6	12.0	12.0	12.0
Controls				
Electronic Control Unit	4.5	4.5	4.5	4.5
Actuators				
Variable Power Turbine Nozzle	4.7	4.7	4.7	—
Variable Inlet Guide Vanes	2.0	2.0	2.0	2.0
Sensors				
Gas Generator Speed	0.4	0.4	0.4	0.4
Power Turbine Speed	0.3	0.3	0.3	—
T_8 Sensor	0.7	0.7	0.7	0.7
Fuel Metering Valve	1.2	1.2	1.2	1.2
TOTAL	13.9	13.9	13.9	8.9

*CEUE = Cost Effective Upgraded Engine

TABLE 14

Engine Cost Distribution By Percent

Category	Cost Confidence Level								
	Single Shaft Engine			Two Shaft Engine			Three Shaft Engine		
	High	Med.	Low	High	Med.	Low	High	Med.	Low
Housing Assembly & Ancillaries									
Engine Housing, Accessories, Starter, Burner & Misc.	15.5			13.6			13.8		
Housing Insulation		8.9			6.9			6.8	
Silicon Carbide Burner Tube			4.0			3.5			3.5
Turbomachinery									
Nozzles, Shrouds & Plenum			11.4			12.3			12.7
Wheels			1.7**			5.1**		1.4	2.3**
Support Structure & Misc.		7.0		8.8				13.2	
Molybdenum Fasteners			2.0			—			—
Regenerator									
Core		6.7			5.8			5.8	
Spray Metal Seals & Cover	7.9			6.9			6.8		
Reduction Gears & Transmission									
Housing & Cover, Oil Pump & Miscellaneous	3.7			4.0			4.9		
Reduction Gears, Bearings, Shafts & Regenerator Drive		5.0			5.7			10.6***	
Transmission		15.3		12.7			3.7****		
Controls									
Electronic Control Unit, Actuators, Sensors & Fuel Metering Valve		10.7			14.7			14.5	
Total	27.1	53.6	19.1	37.2	41.9	20.9	29.2	52.3	18.5

* Burner Tube Listed Separately on Line Three.
** Silicon Carbide Ceramic Wheels.
*** Contains Feedback Gears and Shafts.
**** Planetary Gears, Wet Clutch and Band.

TABLE 15

Single Shaft Engine

Concep Engine Characterization

Ambient Conditions: 85°F. 14.696 PSIA

Engine Speed, RPM	47,150	56,580	66,010	75,440	84,870	89,585	94,300
Fraction	.5	.6	.7	.8	.9	.95	1.0
Compressor Pressure Ratio	1.54	1.83	2.22	2.76	3.44	3.80	4.185
Component Efficiency							
Compressor	.760	.785	.800	.800	.795	.785	.770
Turbine	.805	.815	.829	.840	.850	.852	.852
Burner	.998	.998	.999	.999	.999	.999	.999
Regenerator	.957	.948	.939	.928	.916	.911	.905
Parasitic Loss, HP	2.30	3.14	4.11	5.28	6.64	7.43	8.28
Output Power, HP Net	7.38	14.79	25.97	41.74	62.22	69.70	77.0
Fuel Flow Lb/Hr Gasoline	4.37	6.91	10.57	16.11	23.58	27.04	31.11
Specific Fuel Consumption							
Lb/Hp-Hr	.592	.467	.407	.386	.379	.388	.404
Gas Flow, Lb/Sec							
Station 1	.247	.323	.412	.534	.679	.743	.819
3	.239	.313	.399	.517	.657	.718	.791
4	.237	.310	.395	.509	.649	.709	.782
5	.239	.312	.397	.511	.652	.712	.785
8	.244	.319	.407	.527	.671	.733	.809
9	.246	.322	.411	.531	.679	.744	.820
Pressure, PSIA							
Station 1	14.67	14.66	14.63	14.60	14.54	14.51	14.48
2 = 3	22.60	26.82	32.49	40.29	50.03	55.14	60.58
4	22.43	22.63	32.28	40.06	49.80	54.91	60.35
5	22.06	26.11	31.60	39.19	48.75	53.77	59.14
8	14.98	15.10	15.26	15.48	15.79	15.97	16.17
9	14.73	14.76	14.81	14.90	15.02	15.10	15.20

TABLE 16

Engine Characterization Schematic Station Notation

Single Shaft Engine

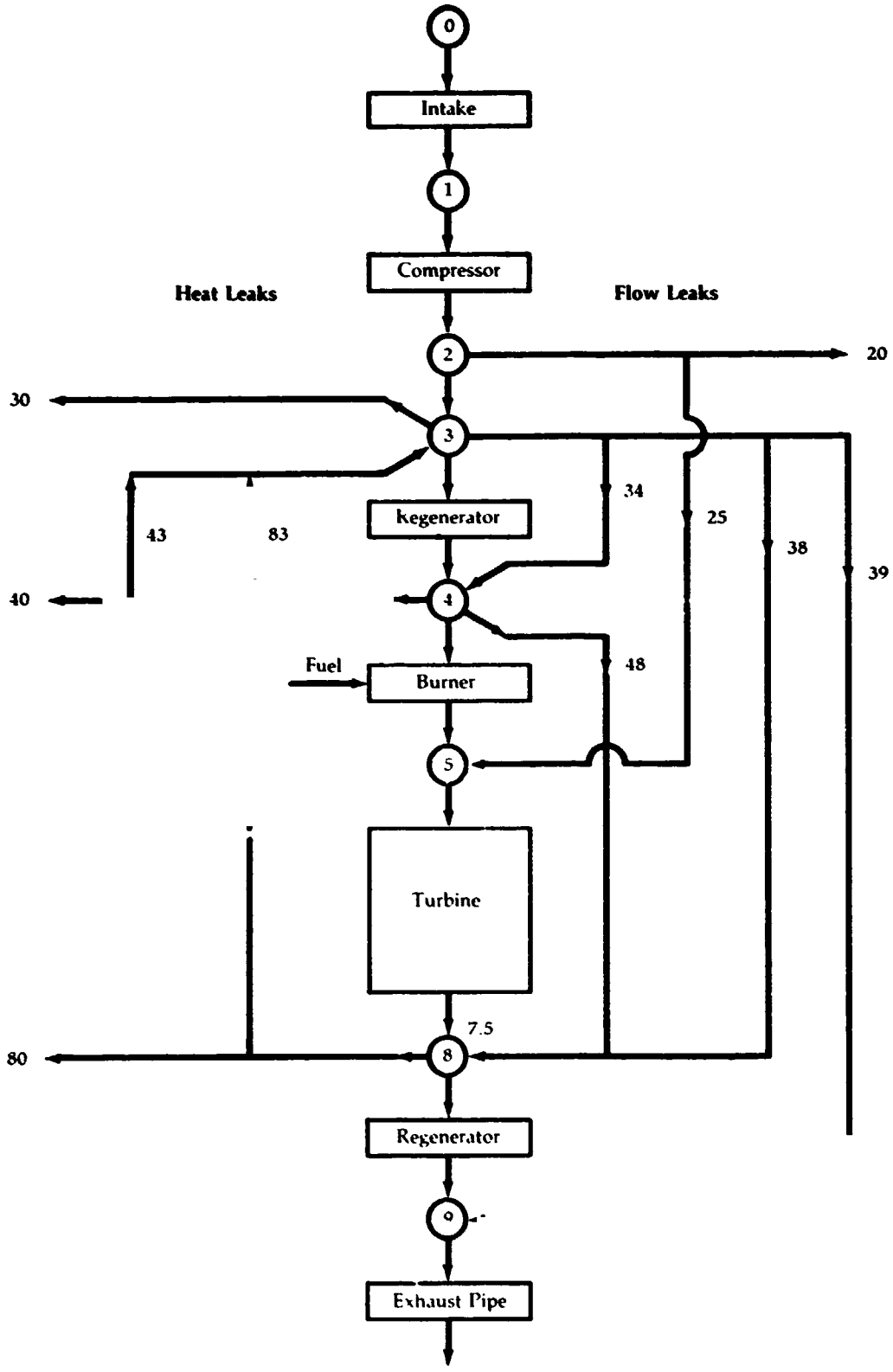

Table 17

TABLE 17
Improved Automotive Gas Turbine Study
Single Shaft Engine
4.2:1 Pressure Ratio

	Maximum Turbine Inlet Temperature		Horsepower		MPG Comb. (Gas)	Vehicle Inertia Weight Lbs.	W_{CP} Design #/S	Engine Speed RPM	Compressor		Turbine					
										Efficiency Max.		Efficiency Max.	TIP Speed		Stress	%
	°C	°F	Design	Aug.					Ns	70 - 80%‡	Ns	100%**	FPS	Material	KSI	Leak
Study Engine & Vehicle, Traction CVT, No A/C																
	1040	1900	91	100	24.9	3500	1.085	81.900	92.6	.808	68.3	.858	2075	Metal	72	4.0
	1150	2100	91	100	25.9	3500	.924	88,700	92.6	.805	68.3	.856	2155	Metal	78	4.7
	1350	2460	91	100	27.0	3500	.733	99.600	92.6	.80	68.3	.852	2300	Ceramic	40	5.9
Development Plan Engine & Vehicle (A/C, P/S, Coastdown HP)																
Derated	1040	1900	62.2	68.4	29.5	2750	.819	94.300	92.6	.80	79.1	.852	2075	Metal	72	5.3
														*Ceramic	31	
Goal	1150	2100	77	84.7	30.4	2750	.819	94.300	92.6	.80	75.8	.852	2155	Metal	78	5.3
														*Ceramic	34	
Adv Dev.	1350	2460	104	114.4	27.6	3500	.819	94.300	92.6	.80	68.3	.852	2300	Metal	40	5.3
														*Ceramic		

Aug. = Augmented
Comb. = Combined
W_{CP} = Compressor Massflow
NS = Specific Speed
‡ = Occurs Between 70 and 80% Speeds
** = Occurs at Design Speed
*Back-Up

Variation of Component Efficiencies and Turbine Inlet and Outlet Temperatures With Gas Generator Speed for Improved Upgraded Engine

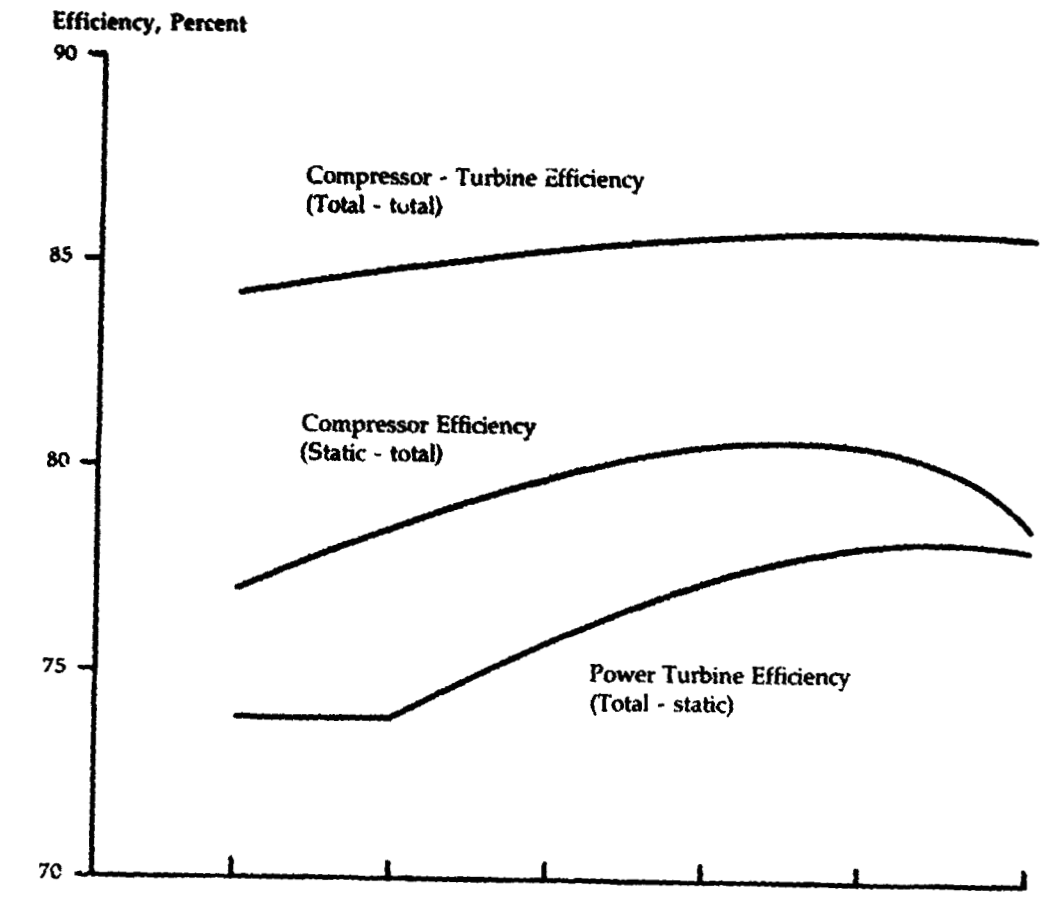

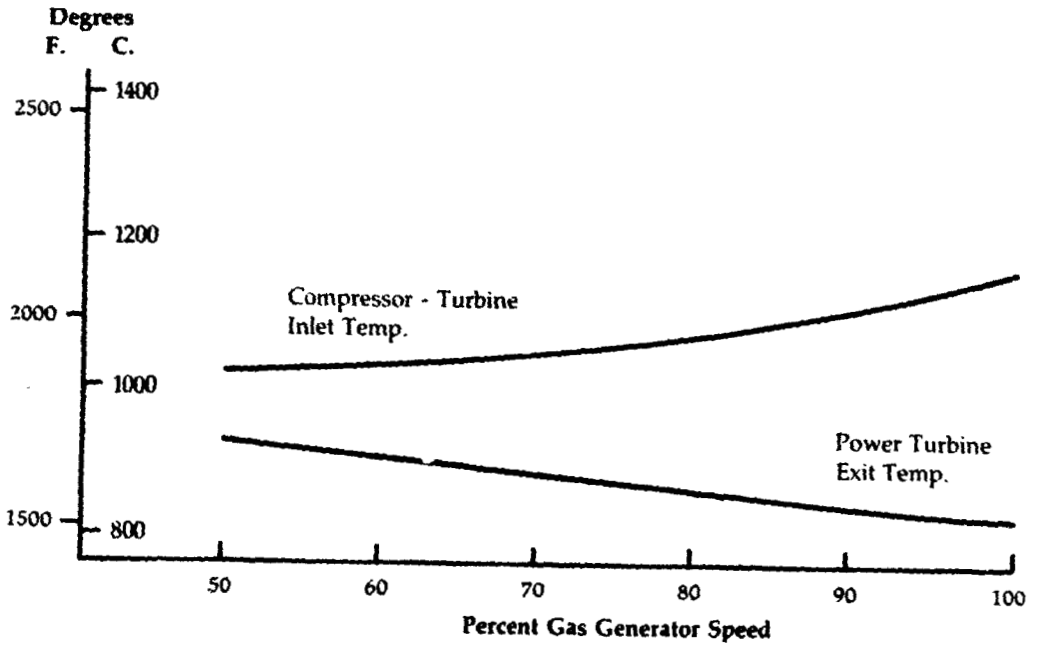

Figure 1

Figure 2

Engine Concepts And Shaft Arrangements Reviewed for IGT Study

2 Shaft	Single Shaft	Multiple Shaft
CONVENTIONAL 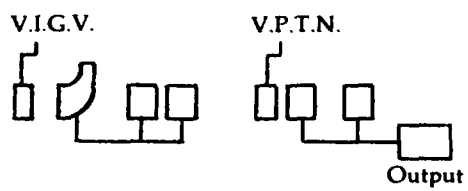 	RADIAL TURBINE 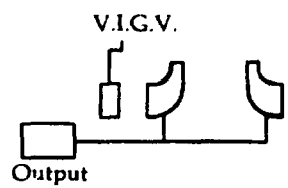 	3-SHAFT-FREE POWER TURBINE 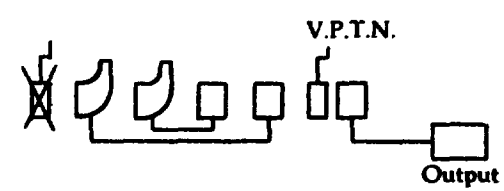
POWER TURBINE-FIRST 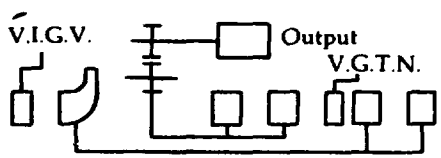 	2-STAGE AXIAL TURBINE 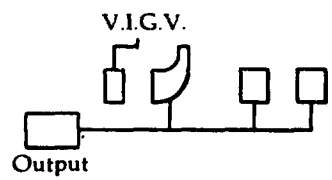 	TWIN SPOOL 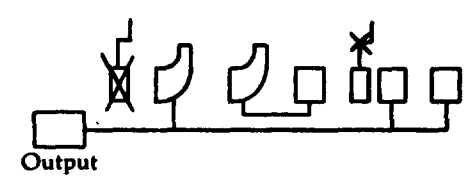
POWER TRANSFER 4:1 PR, 2100°F 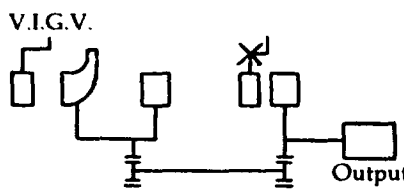 		3 SHAFT-AUXILIARY TURBINE 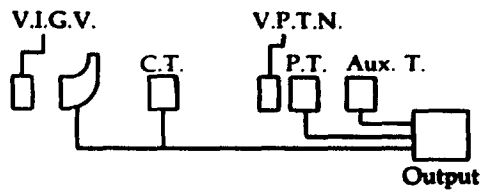

Notes:

1. Actual No. of Compressor and Turbine Stages was Varied
2. V.I.G.V. = Variable Inlet Guide Vanes.
3. V.P.T.N. = Variable Power Turbine Nozzle.
4. Output = Power to Trans., Etc.

Highway Drive Cycle

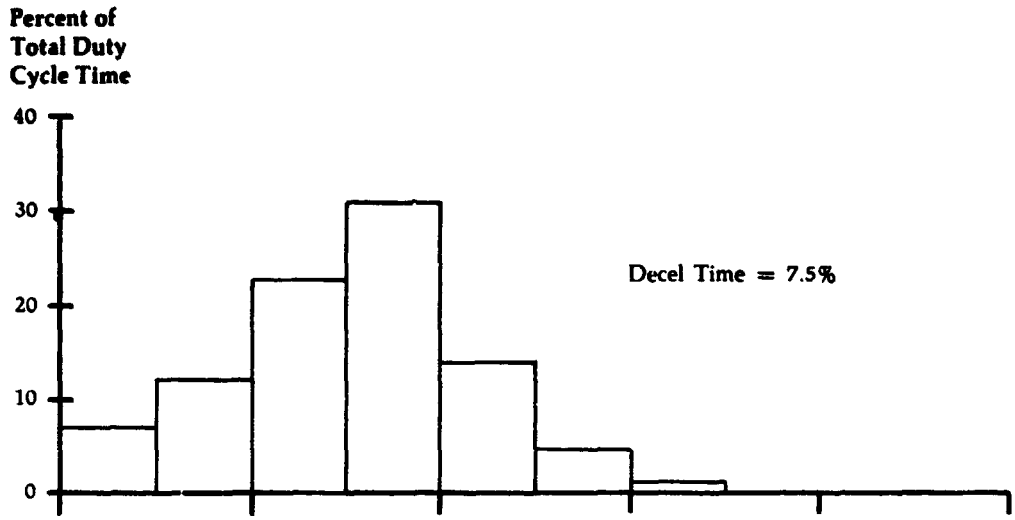

Urban Drive Cycle

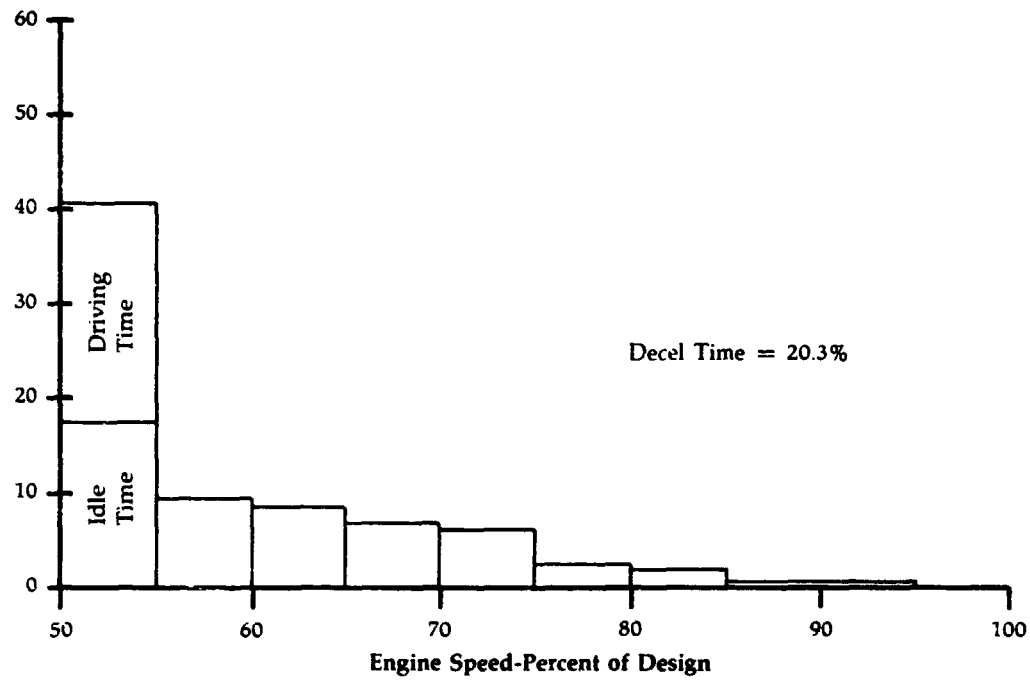

Figure 3

Figure 4

Single-Stage Centrifugal Compressor Polytropic Efficiency vs. Specific Speed

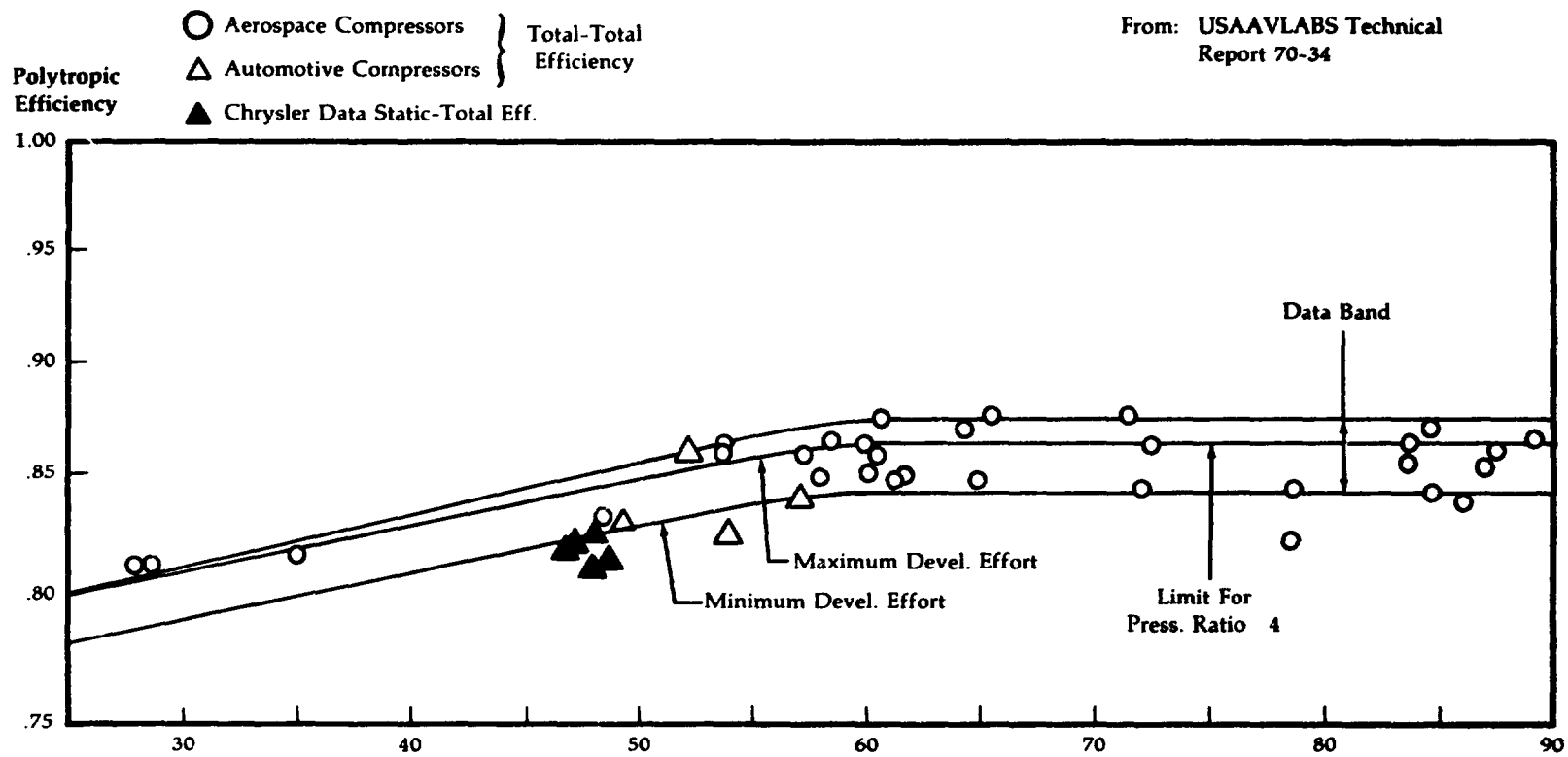

$$\text{Specific Speed} = \left[N\sqrt{W/\rho}\,/\,(\Delta H')^{3/4}\right](T_2/T_1)^{1/4}(P_2/P_1)^{1/4}\eta_{AD}^{3/4}$$

N - RPM
W - Flow, lbs/sec
ρ - Inlet Stag. Density, lb/ft^3

$\Delta H'$ - Ideal Work, ft-lbs/lb
T - Temperature, °R
P - Pressure, PSF

η_{AD} - Adiabatic Efficiency
1 - Inlet
2 - Exit

Variation Of Adiabatic Efficiency With Pressure Ratio For Constant Values Of Polytropic Efficiency

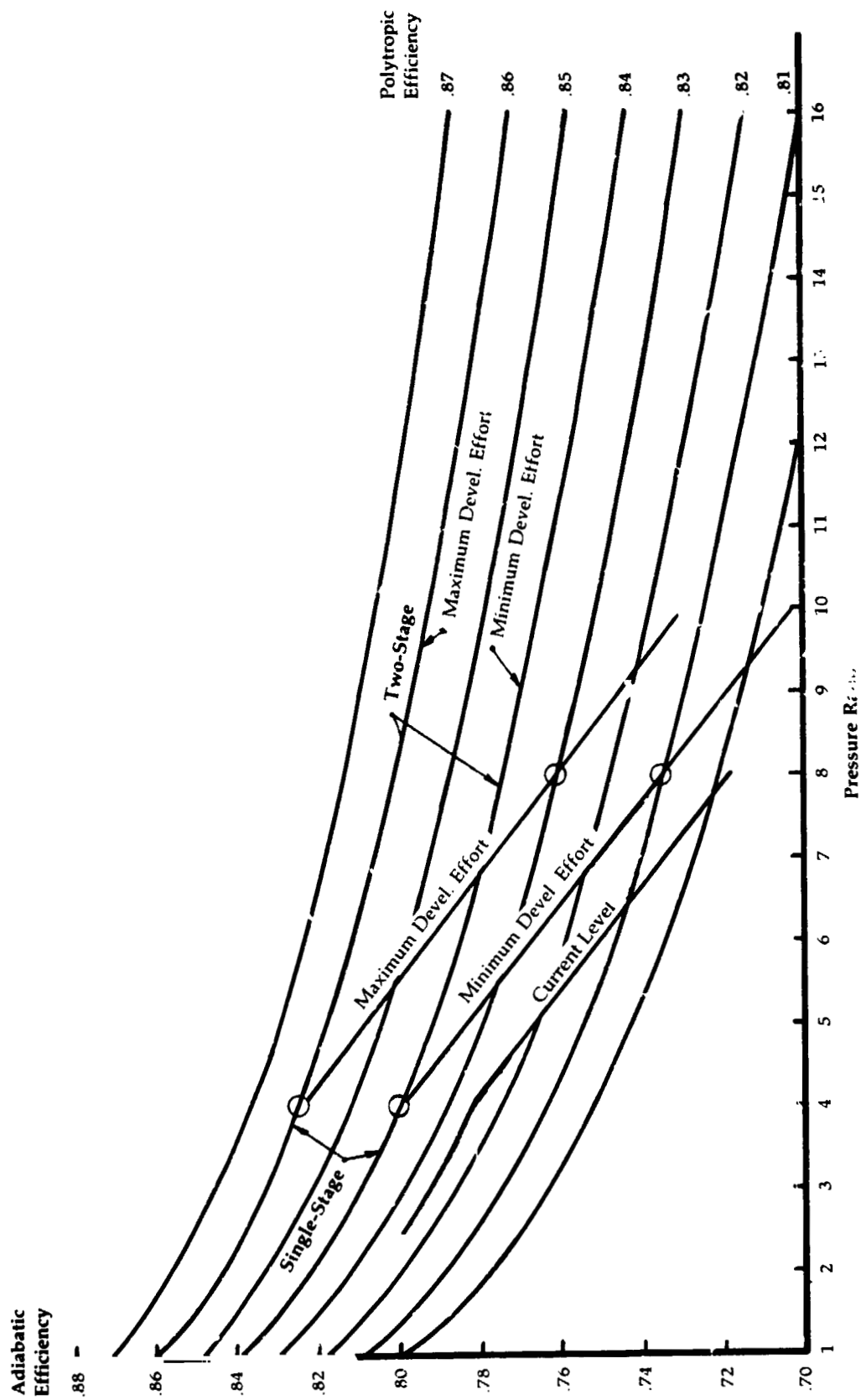

Figure 5

Variation of Centrifugal Compressor Stage Efficiency Loss With Reynolds Number

From: Trans. ASME
July, 1973

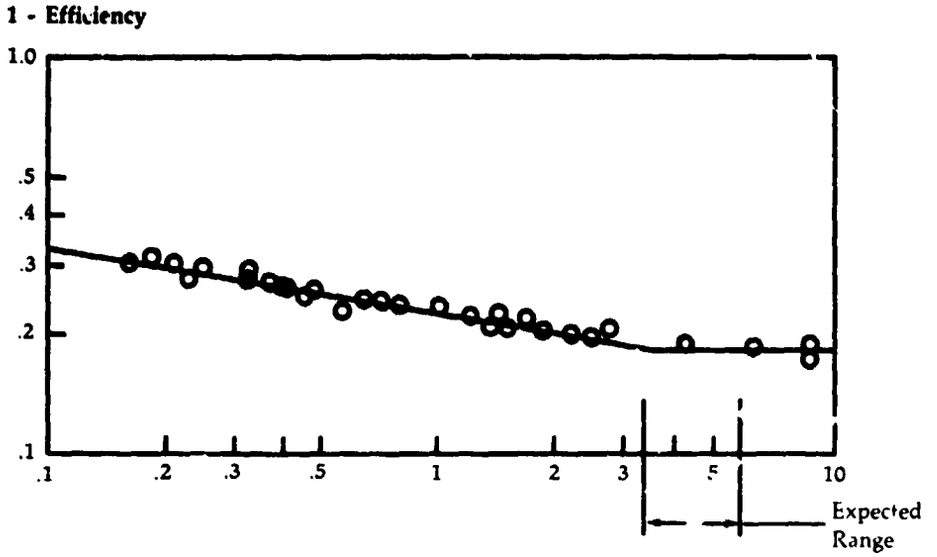

Reynolds No x 10^6

$$\text{Reynolds No.} = \frac{UD\rho}{\mu}$$

U - Rotor Tip Speed, ft/sec
D - Rotor Tip Diameter, ft
ρ - Inlet Stag. Density, Slugs/ft^3
μ - Viscosity, slugs/ft-sec

Figure 6

Single-Stage Centrifugal Compressor Efficiency Range

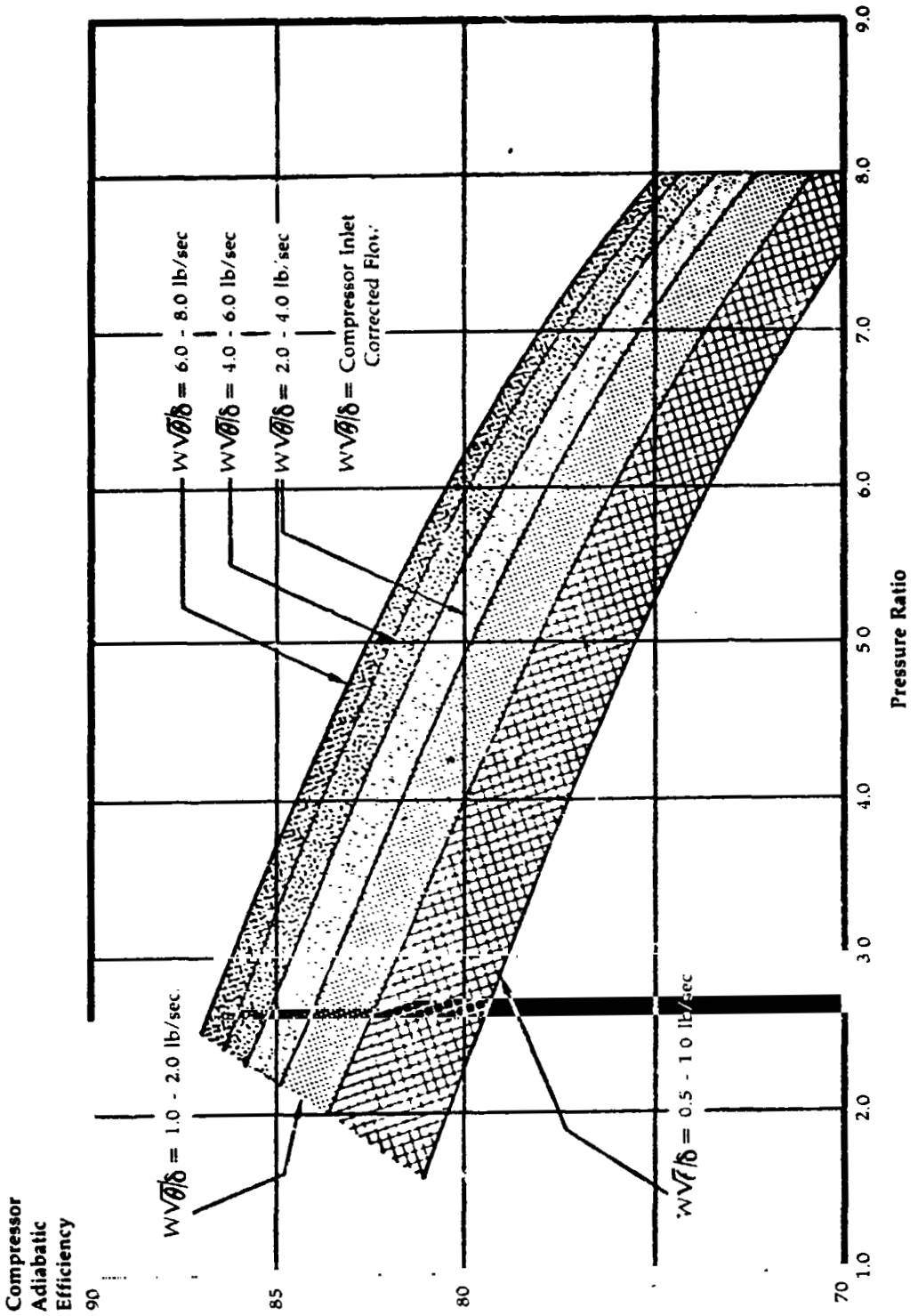

(cf AT-6100-R7)
Page 2-3

Figure 7

Variation of Design-Point and Near-Design Efficiency Values with Work Coefficient For Small High-Work Axial Turbines

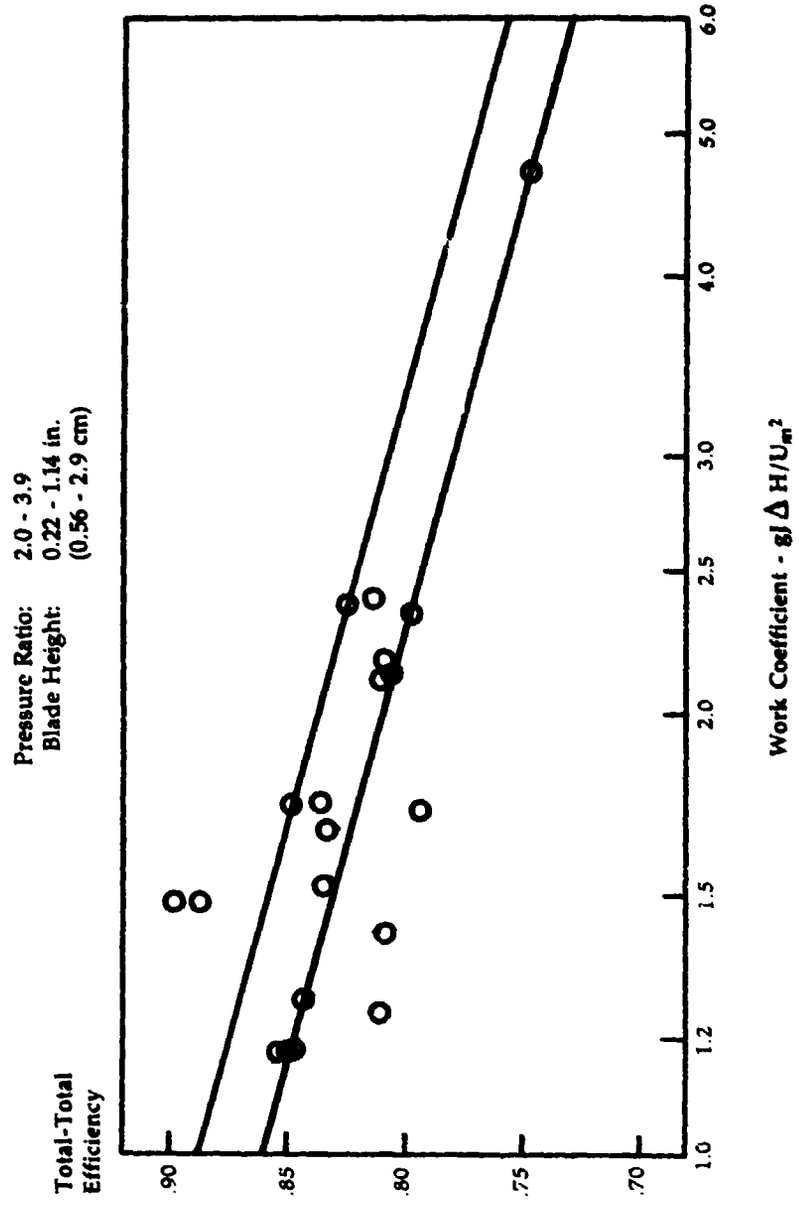

Figure 8

Variation of Efficiency With Specific Speed At Equivalent Design Speed With Best Stator-Rotor Combination

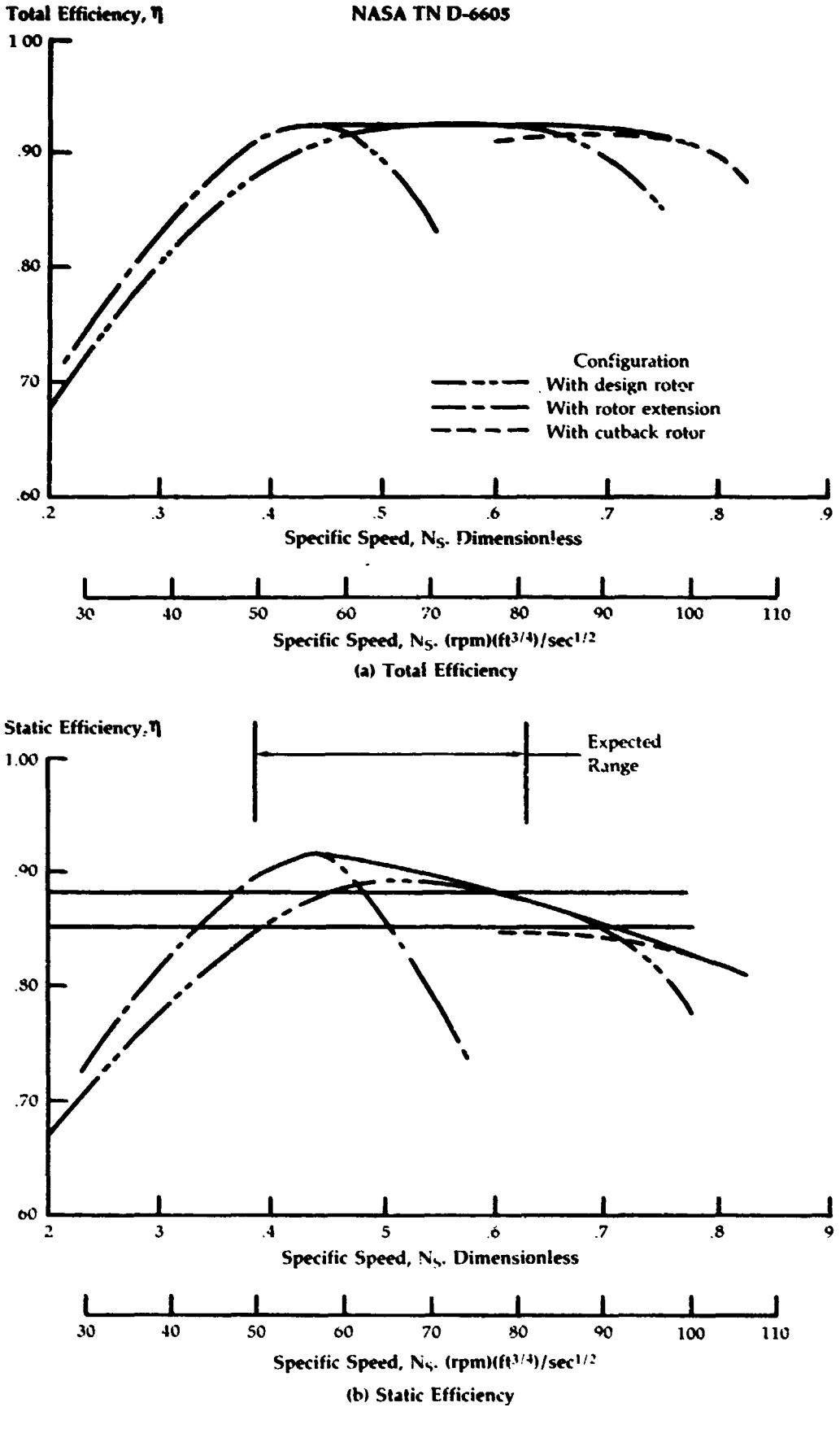

Figure 9

Engine Flow Leak Paths for 2-Shaft Engine with Free Power Turbine

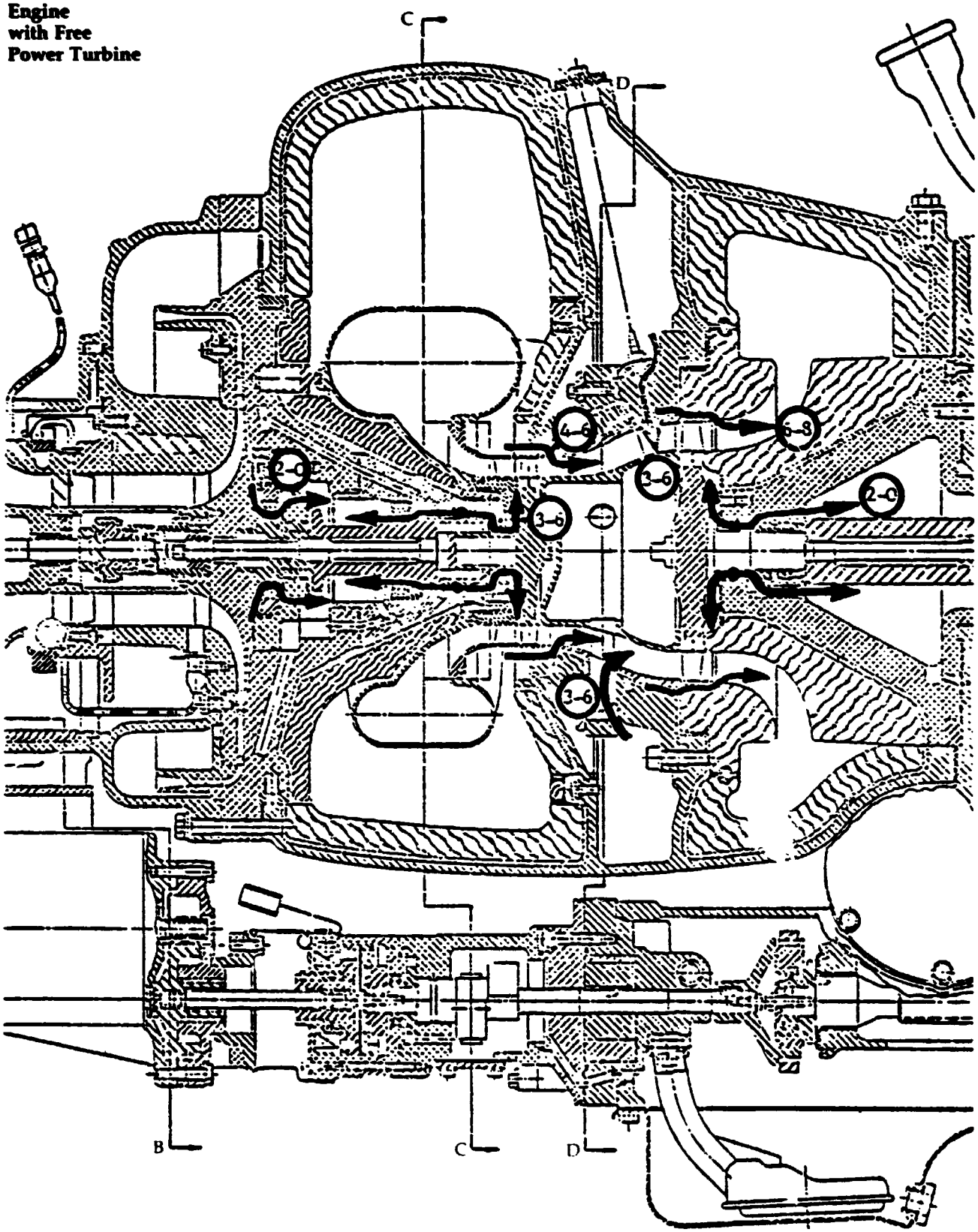

Figure 10

Regenerator Pinion
Flow Leak Path

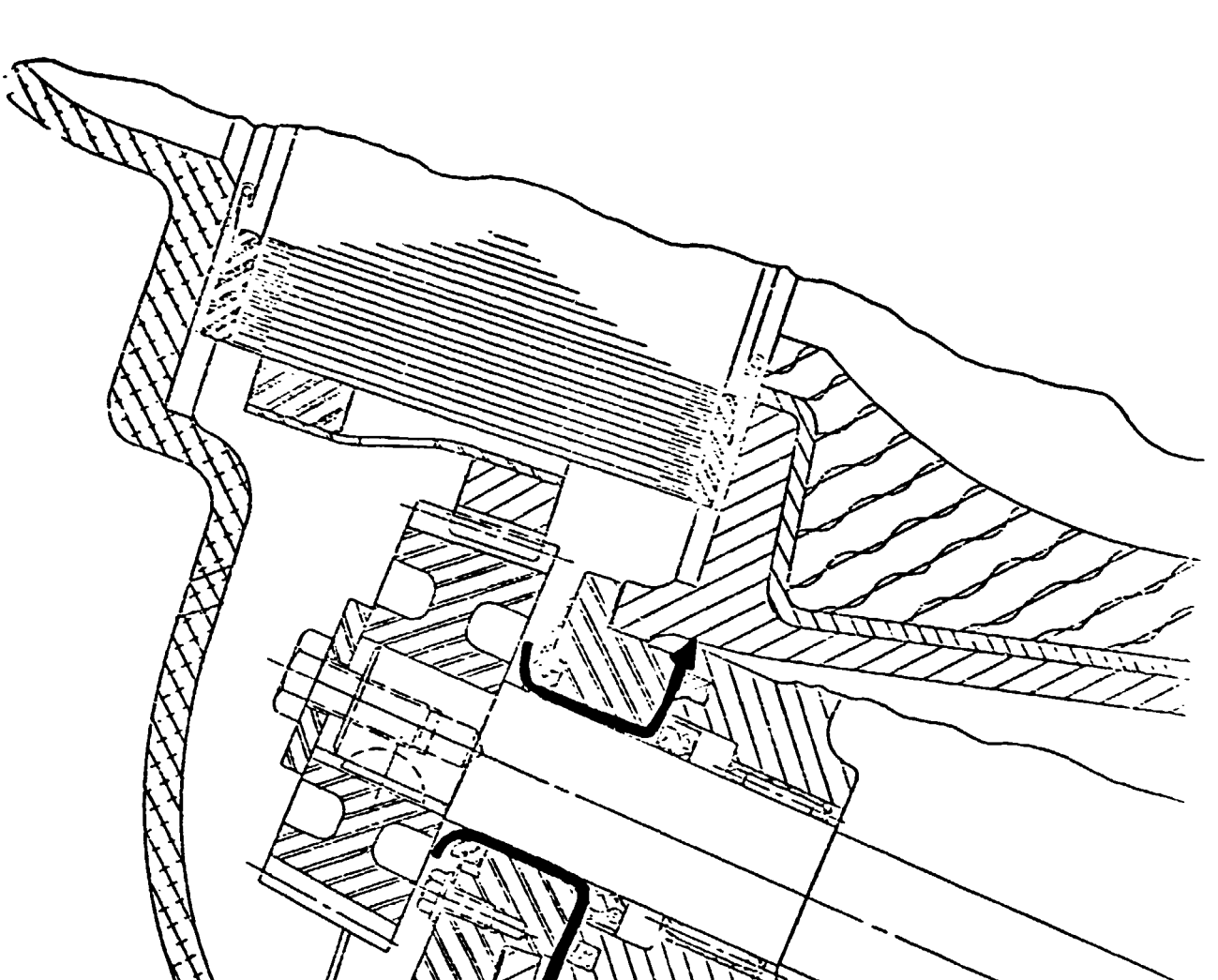

Figure 11

Regenerator Flow Leak Path

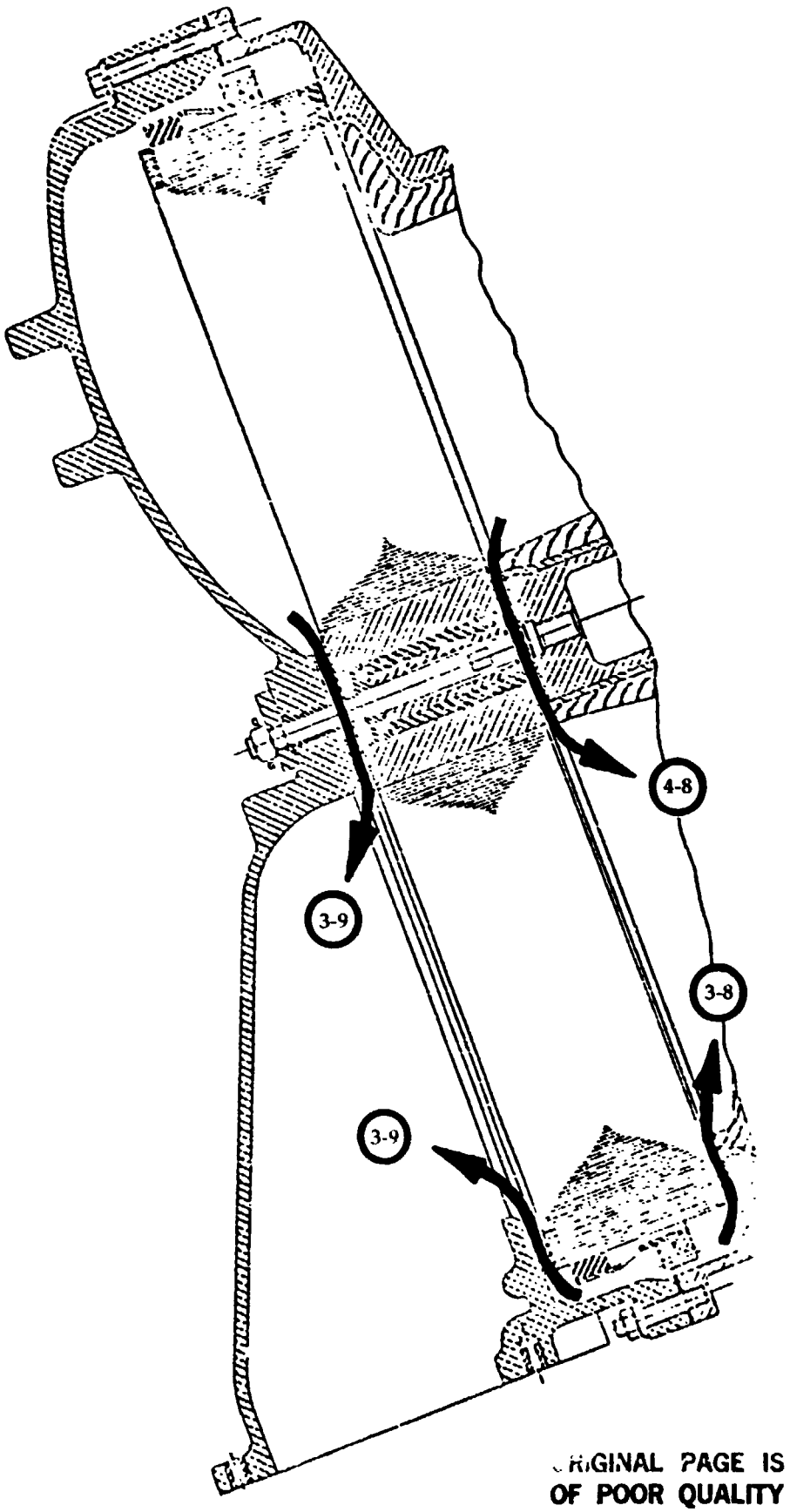

Figure 12

Basic Types of Traction Drive CVT

Ring cone with Planetary

A nonrotating metal ring makes contact with tapered rollers. Drive ends of rollers are planet members engaging a planetary ring connected to the output shaft. Zero speed may be at one end of the speed range or at mid-range, providing a reversible drive.

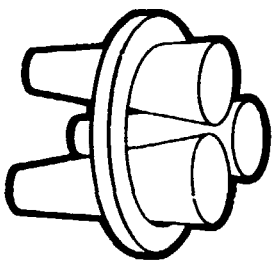

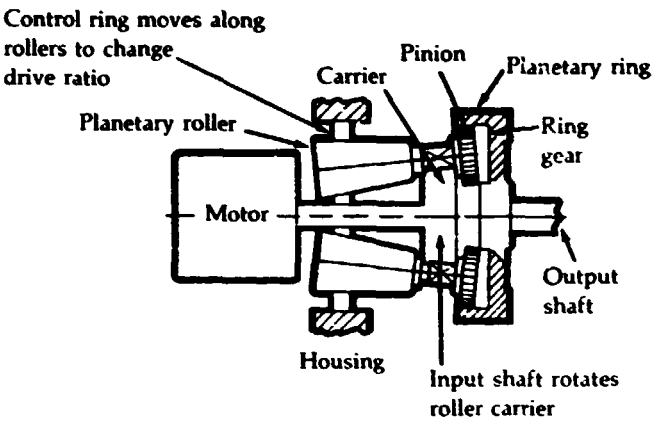

Toroidal Drive

Has had a great deal of attention over the years and has been the subject of more patents than any other type. Practical models are limited to light-duty instrument drives, but automotive and industrial variations are now under development. This drive has the potential for serving as automatic transmission in light automobiles

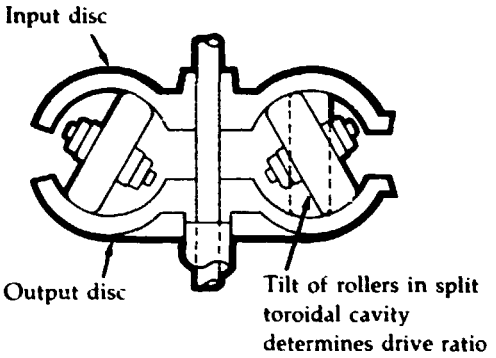

Tilt of spool-shaped roller determines drive ratio.

Figure 13

Cone Roller Toroidal Drive

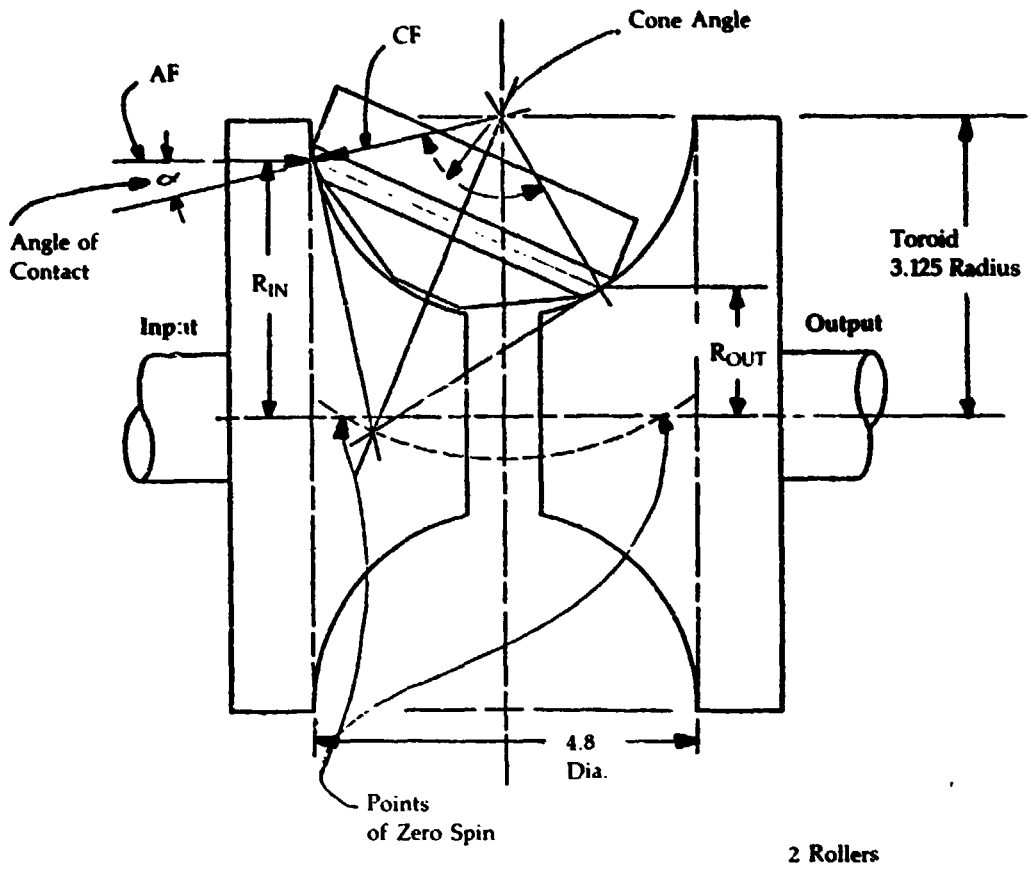

Figure 14

CVT Regenerative Transmission Overall Transmission Efficiency (For Single Shaft Automotive Gas Turbine)

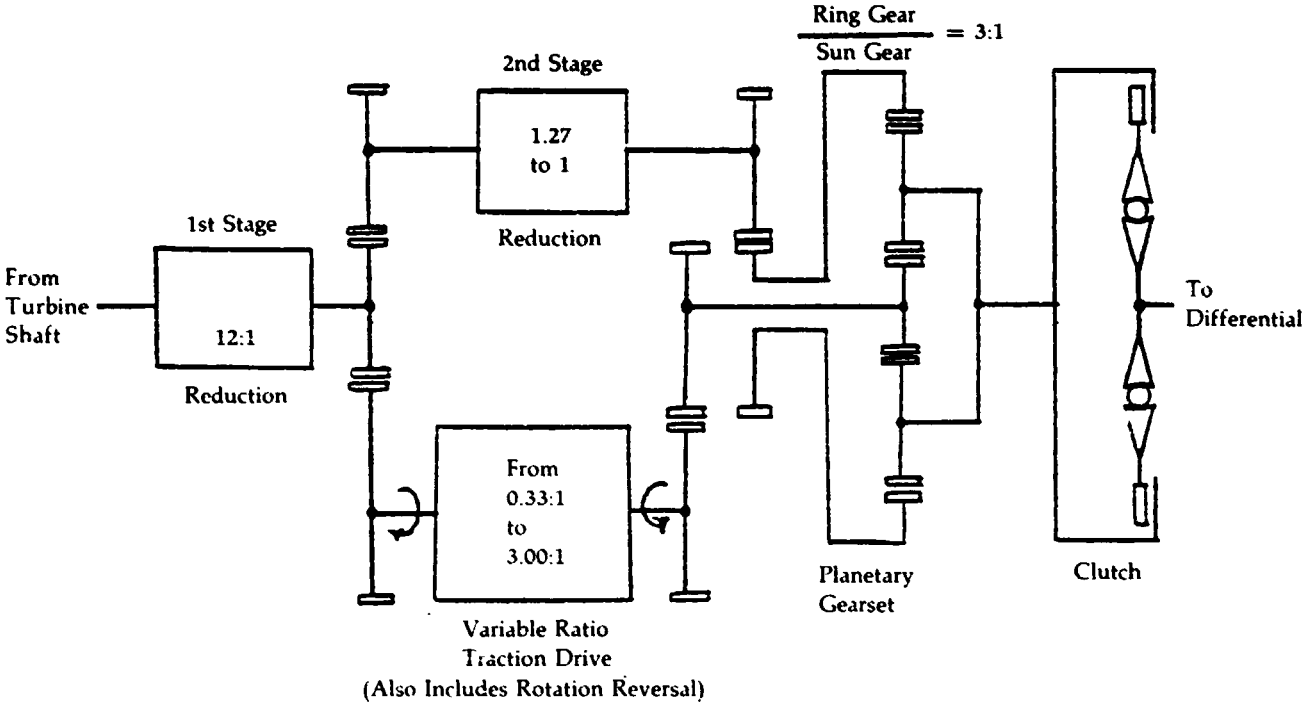

Equivalent Gear	Traction Drive Variable Ratio	Speeds (Planetary) Annulus	Sun	Output	Overall Efficiency*
1st	0.42 - 0.56 1	6561	19685-14805	0-1223	62%
2nd	0.56 - 0.75·1	6561	14805-11083	1223-2155	80%
3rd	0 75 - 1.31.1	6561	11083-6286	2155-3358	92%
4th	1 31 - 3.00·1	6561	6286-2729	3358-4249	97%
neutral	0.419:1	6561	19685	0	—
reverse	0.41 - 0.33.1	6561	19685-25252	0 -(-)1396	—

Note: Traction Drive is assumed to be 80% efficient.
(Turbine Speed 100,000 RPM)

*Additional Parasitic Losses: 1.5 HP at 50% Engine Speed
3.2 HP at 100% Engine Speed

Figure 15

CVT Regenerative Transmission Overall Transmission Efficiency

N_e Engine Speed
N_R Overall Speed Ratio
85% Traction Efficiency
W/O Bearing, Mesh Losses

1st Gear Set { ① N_e = 100% ; ② N_e = 50% }

2nd Gear Set { ② N_e = 100% ; ③ N_e = 50% }

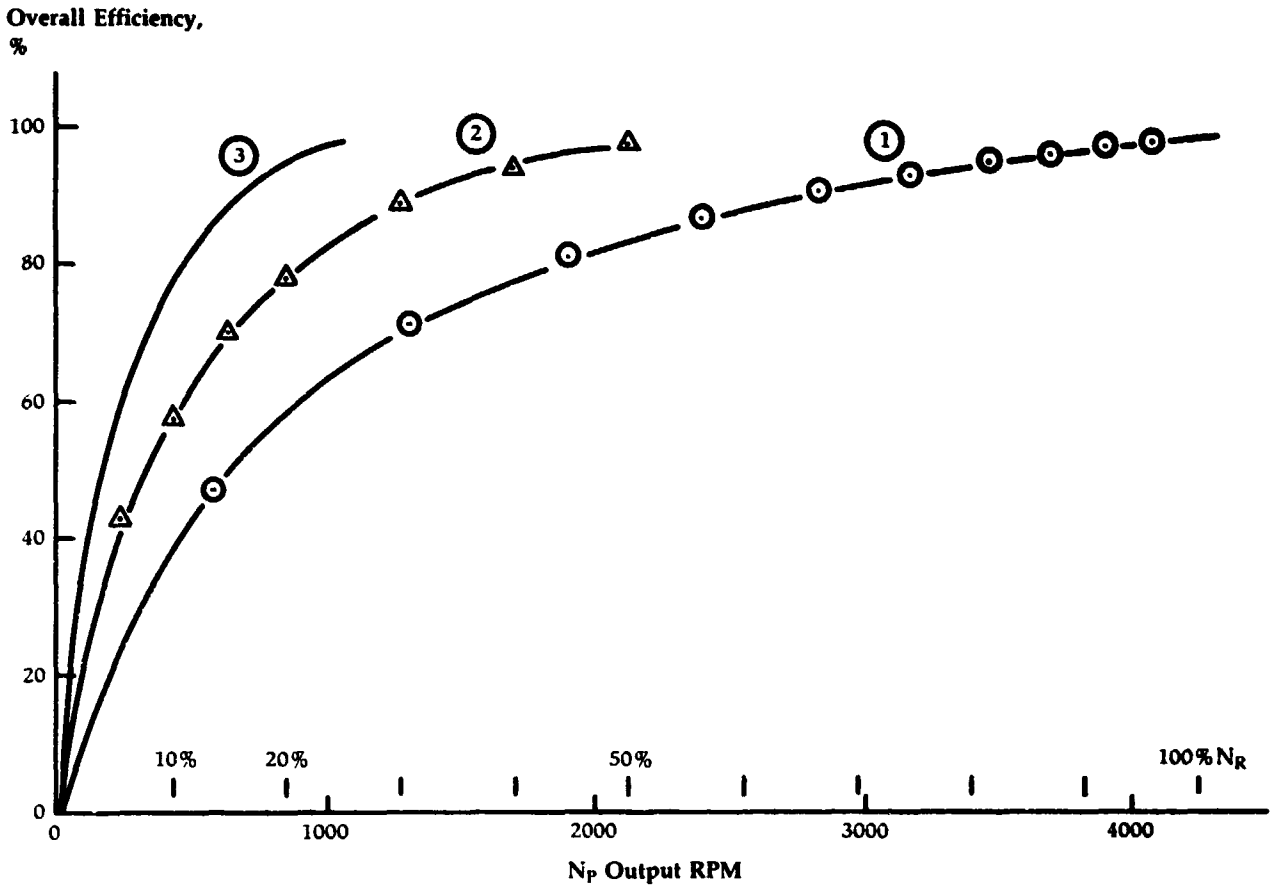

Figure 16

Hydrostatic Pump/Motor Module

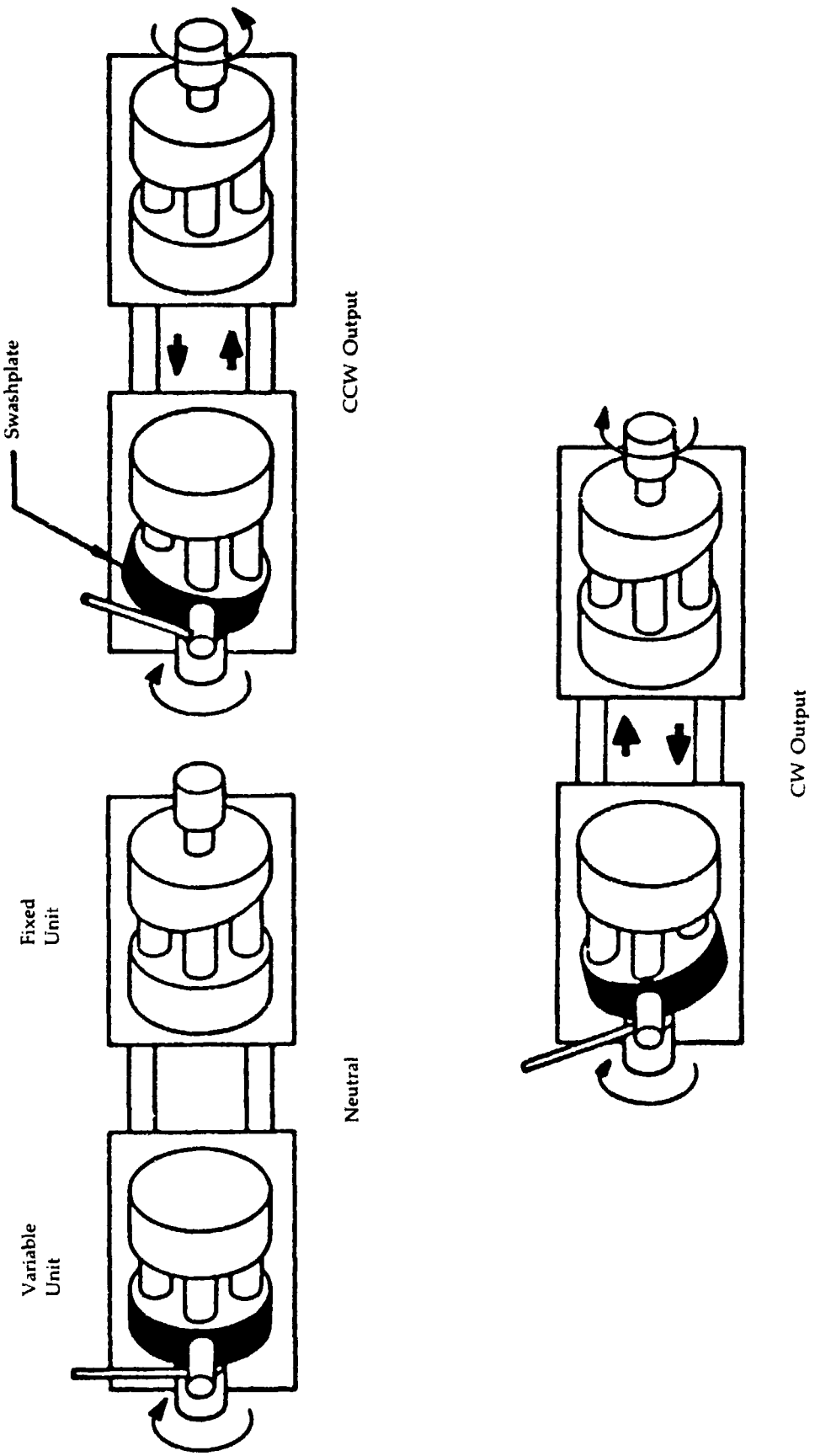

Figure 17

Hydromechanical Transmission Operation

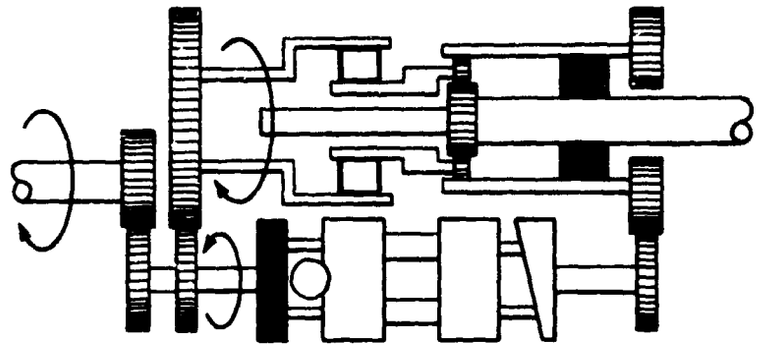

NEUTRAL

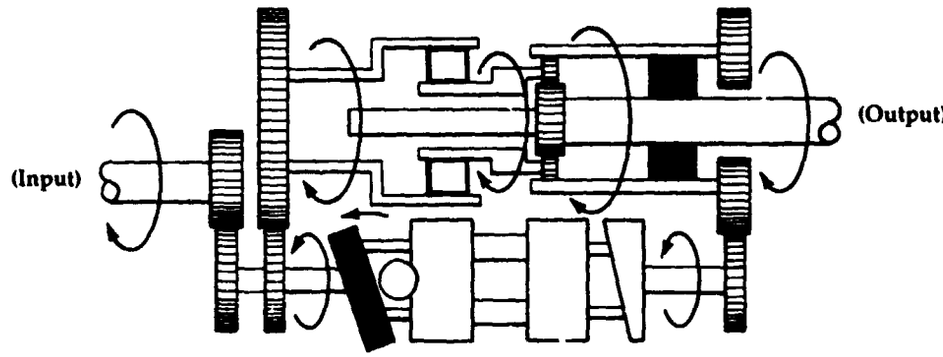

0 TO 20% VEHICLE SPEED

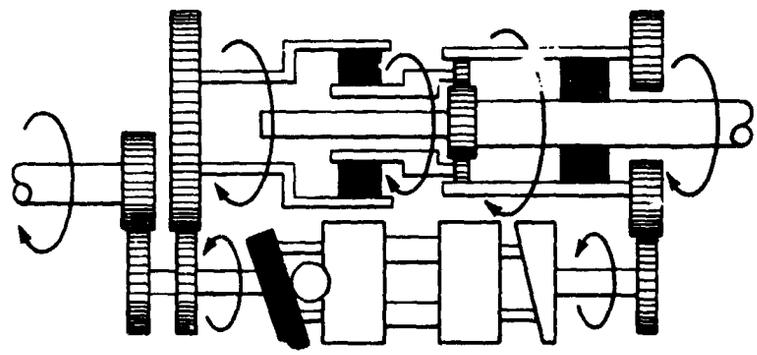

20% VEHICLE SPEED

Figure 18

Hydromechanical Transmission Operation

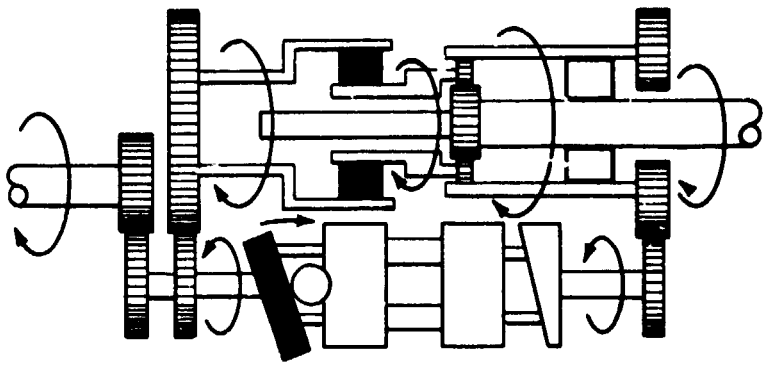

20% TO 60% VEHICLE SPEED

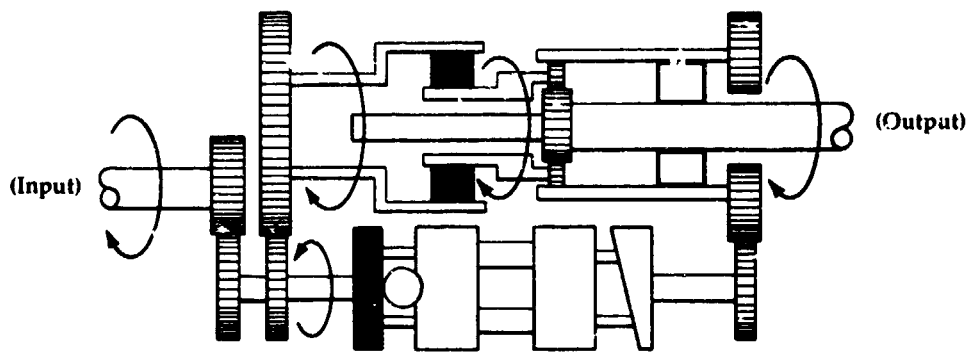

60% VEHICLE SPEED

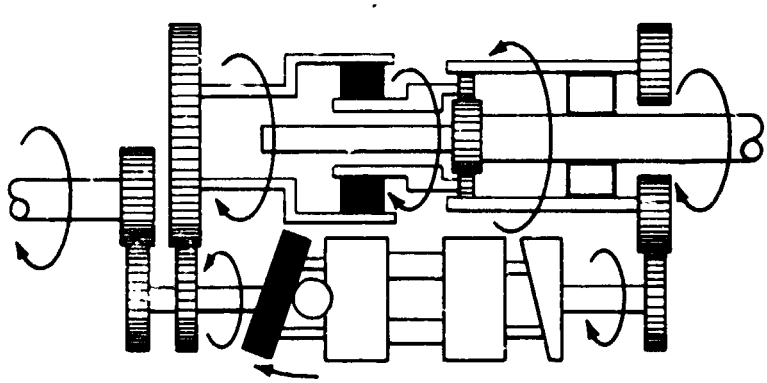

60% TO 100% VEHICLE SPEED

Figure 19

Multirange Hydromechanical Automobile Transmission

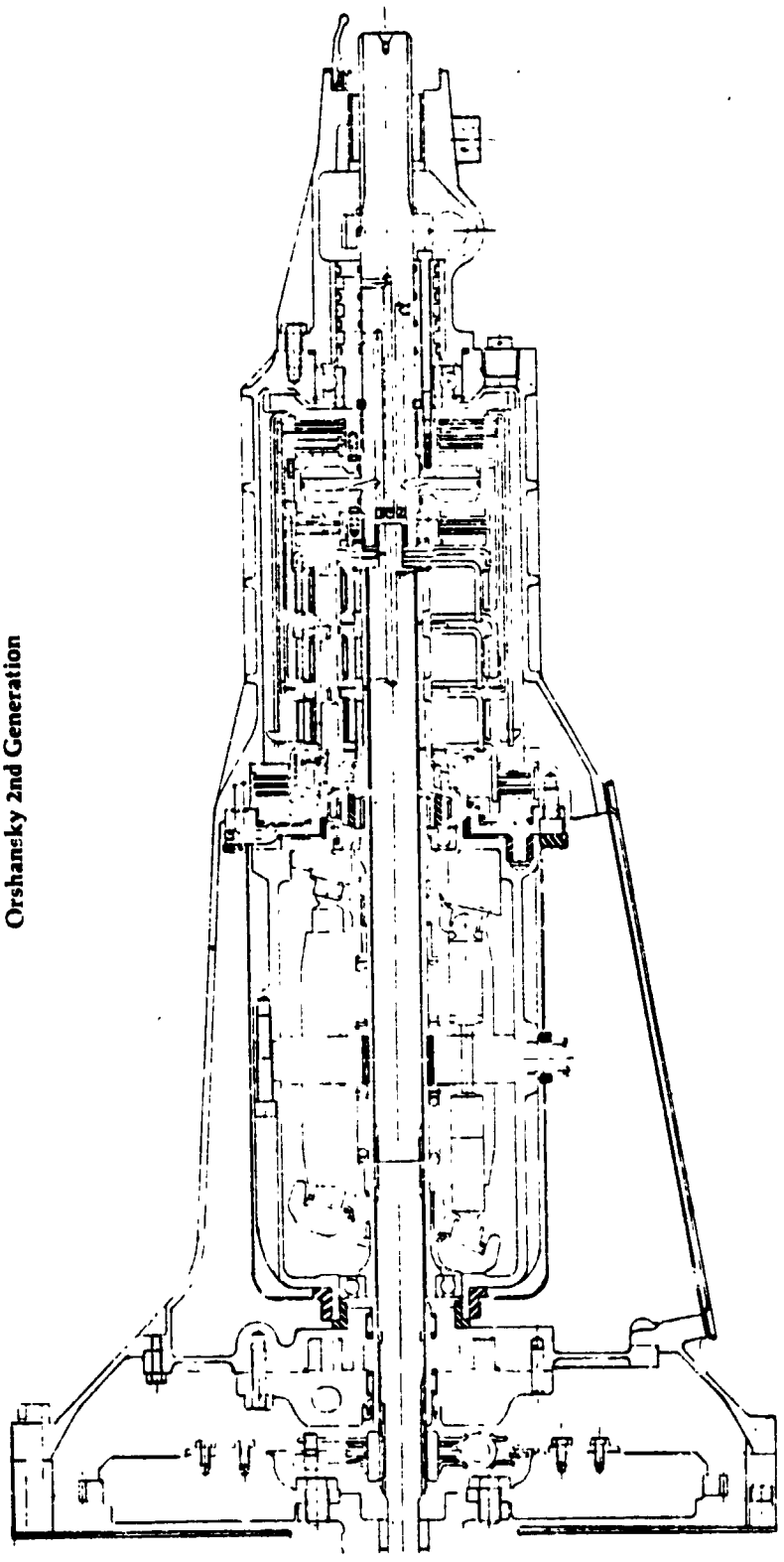

Orshansky 2nd Generation

SPECIFICATIONS

3 Ranges Forward
100 HP
∞:1 to 2.1 Overdrive
31.25 In. Overall Length
Weight 117 Lbs. Dry

Figure 20

Orshansky 2nd Generatio Three-Range Hydromechanical Transmission

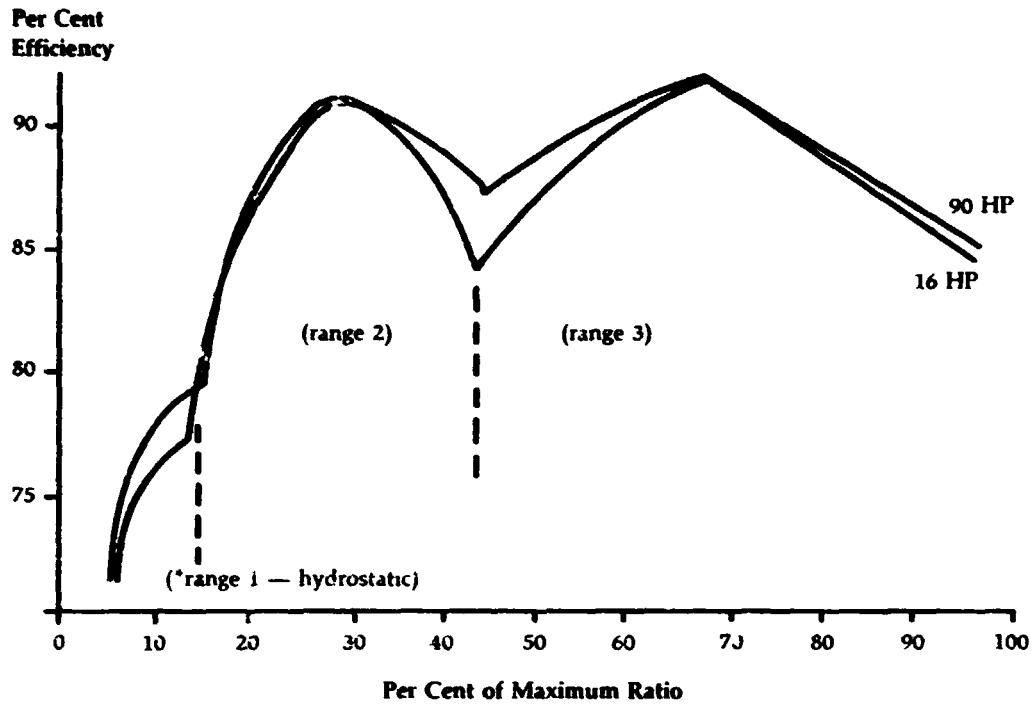

Figure 21

Orshansky Hydromechanical Transmission Efficiency at 35 HP

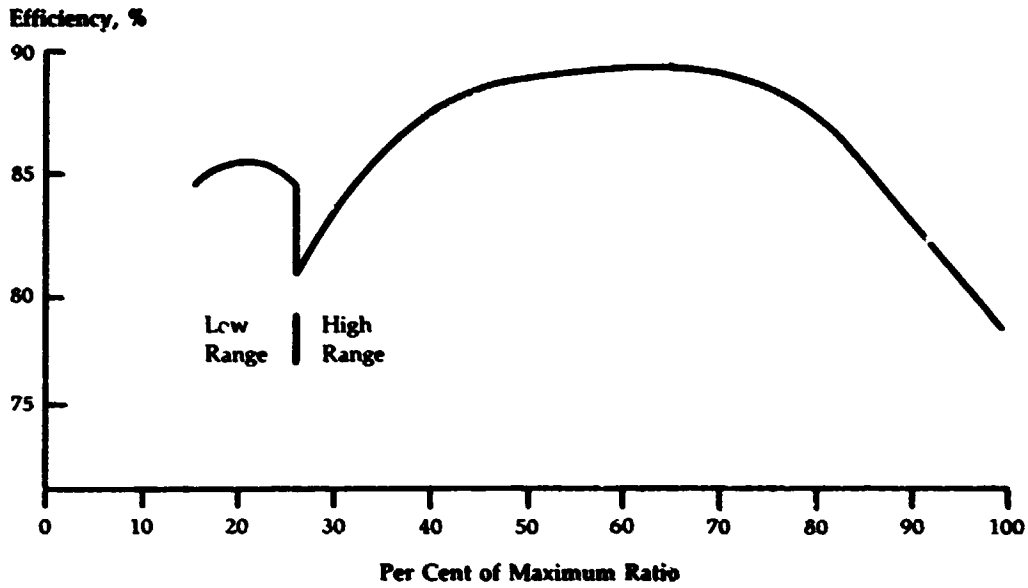

Figure 22

Orshansky Hydromechanical Transmission Efficiency at 5 HP

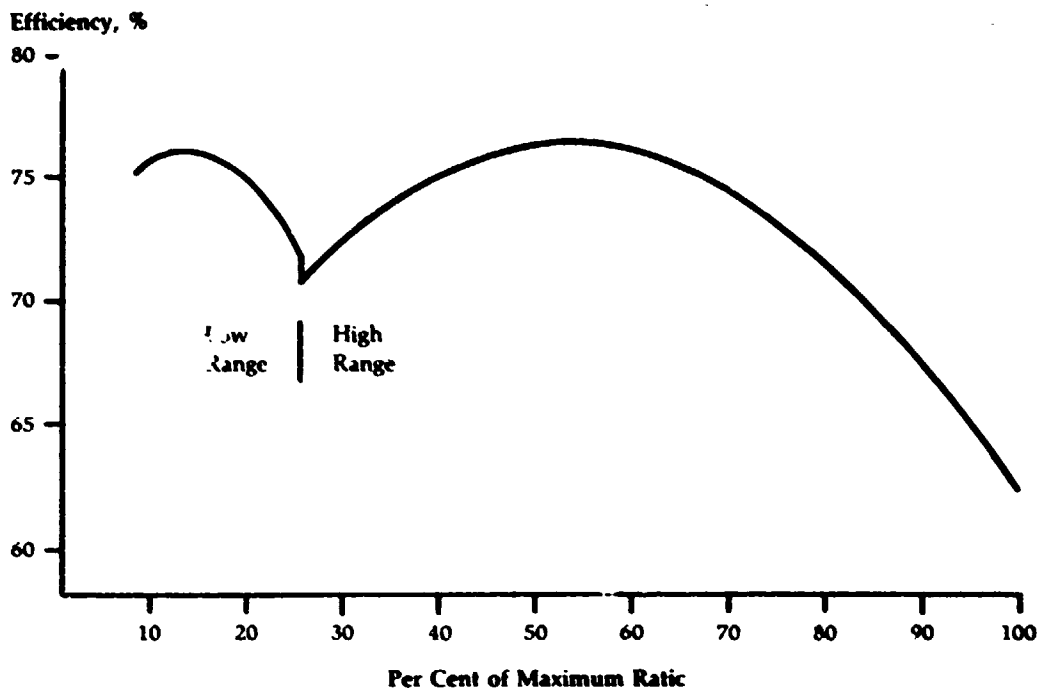

Figure 23

Orshansky Hydromechanical Transmission Efficiency at 10 HP

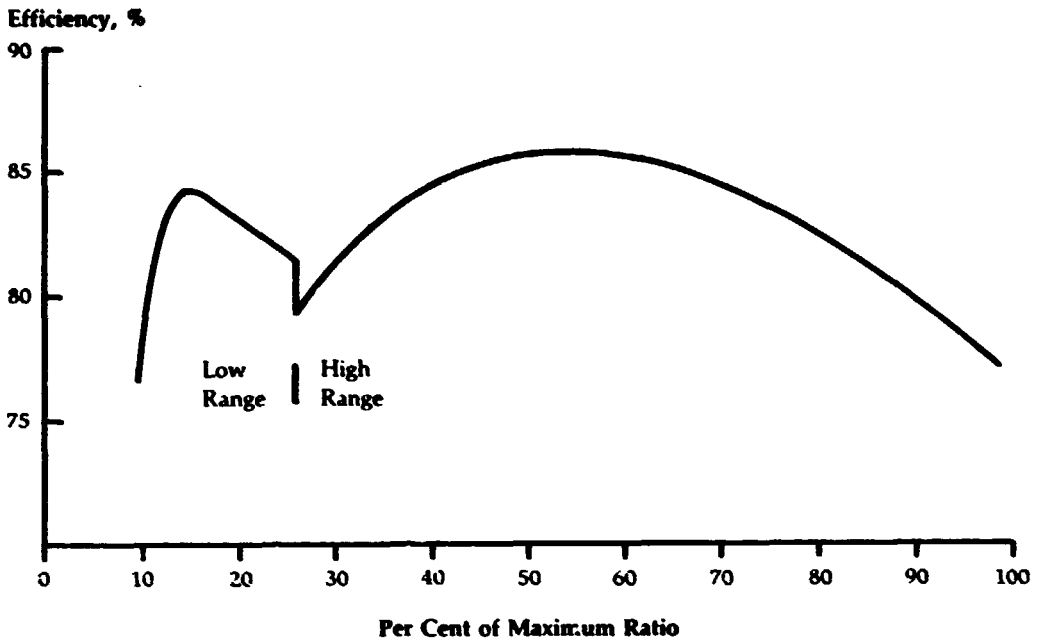

Figure 24

Sustrand "Responder" Hydromechanical Transmission Efficiency At Full Rated Power

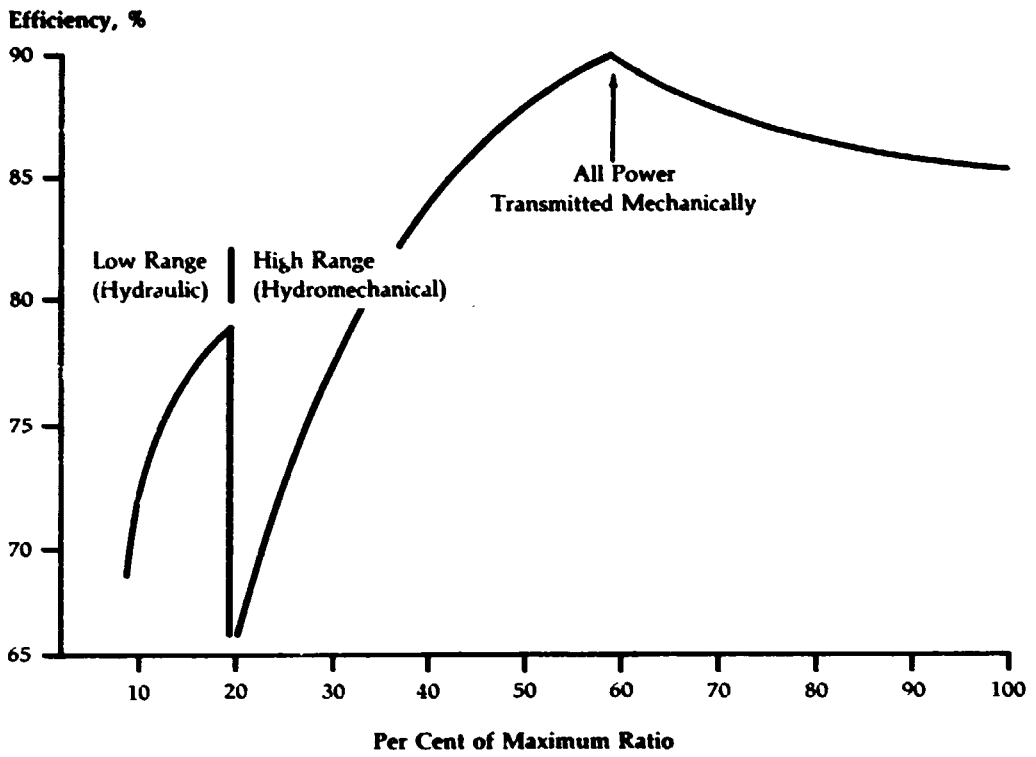

Figure 25

Variable Speed Belt Drive

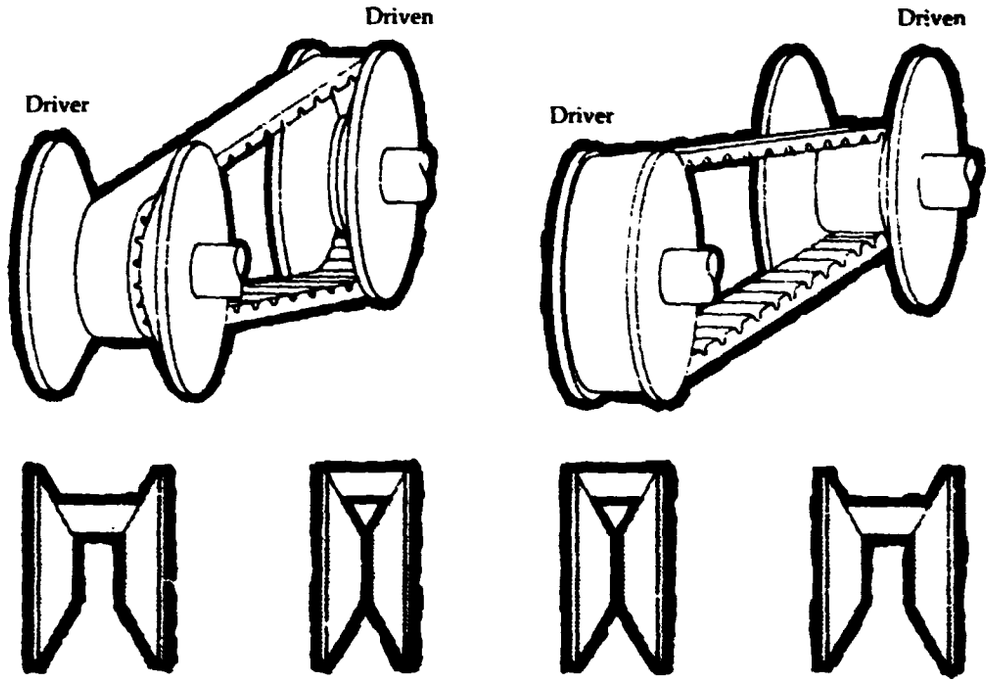

Speed Reduction **Speed Increase**

Figure 26

Variable Chain Drive CVT

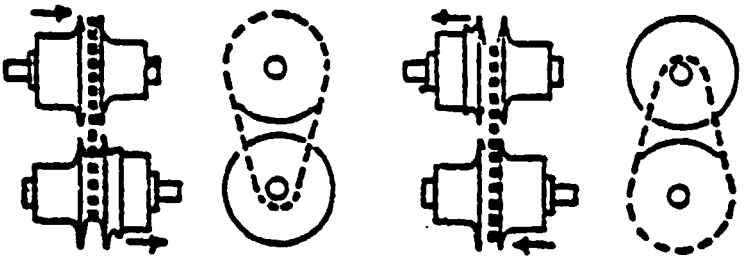

varying effective diameters changes speeds

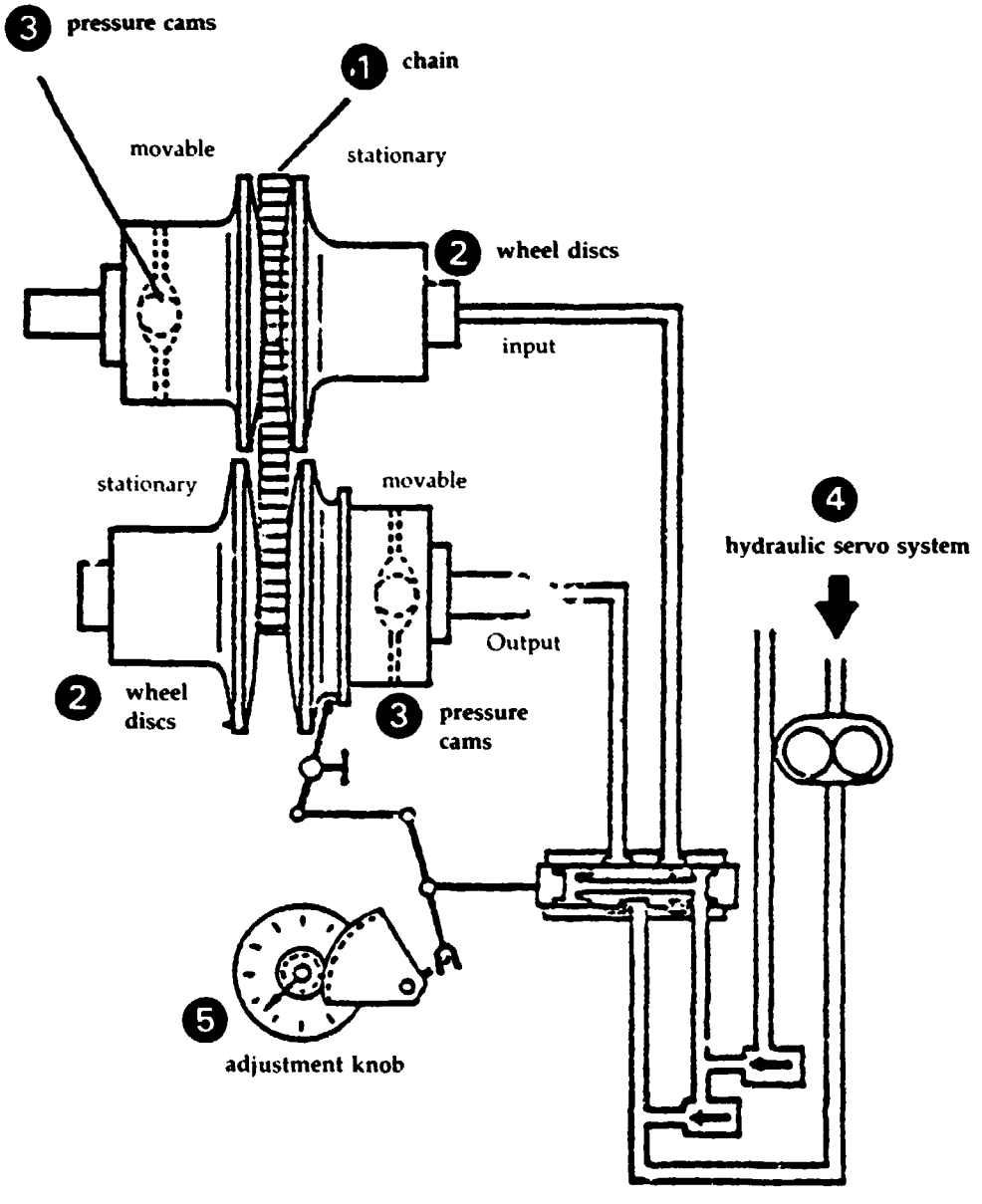

(from FMC Corp.)

Figure 27

Variable Speed Drive Chain Antrieb Werner Reimers A.G.

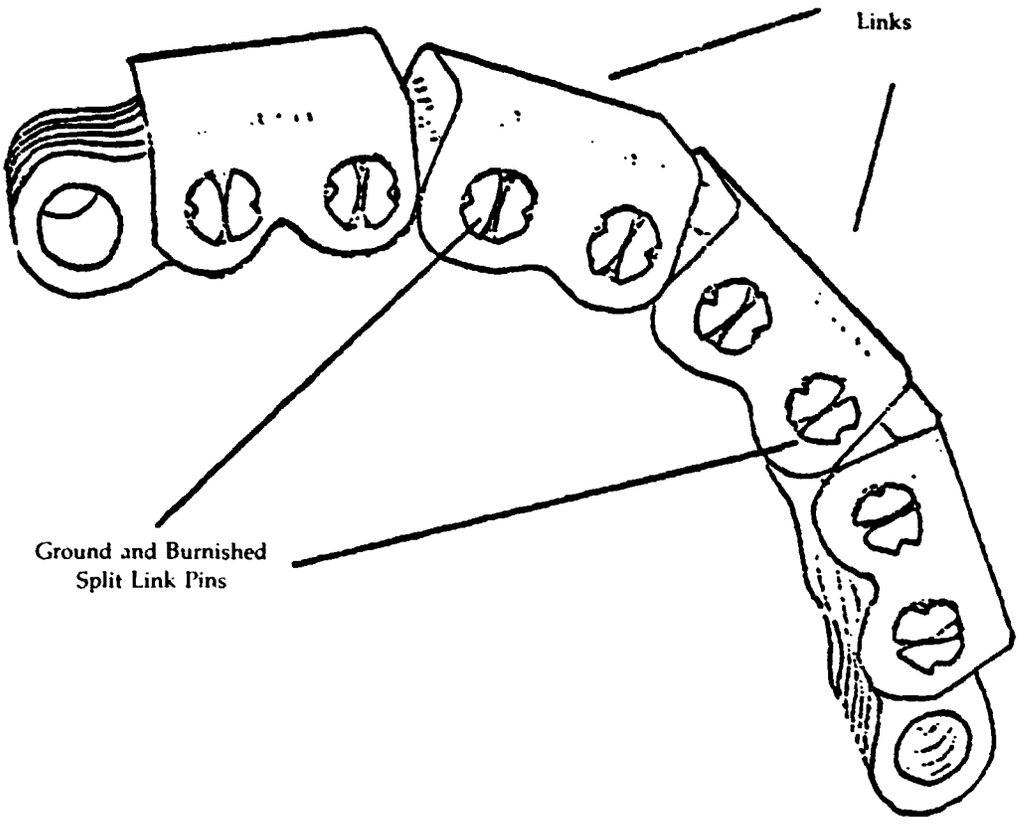

Figure 28

Continuously Variable Ratio Transmission Efficiency

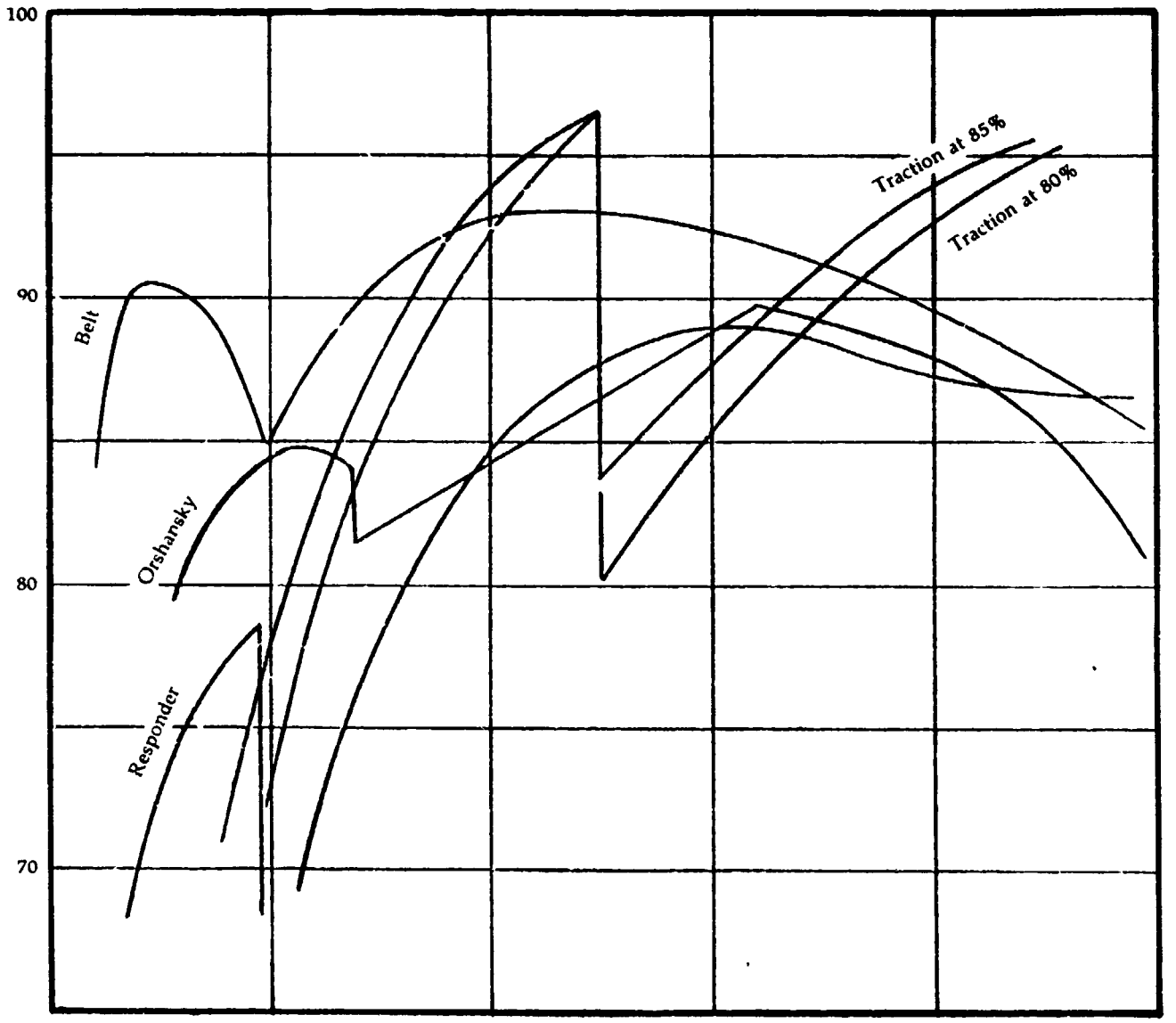

Figure 29

91 HP Single-Shaft Gas Turbine with 10 Speed Transmission

Gear No	1	2	3	4	5	6	7	8	9	10
Gear Ratio	301	263	173	124	95	79	61	52	126	35

Engine Speed Ratio vs. Vehicle Speed Curve

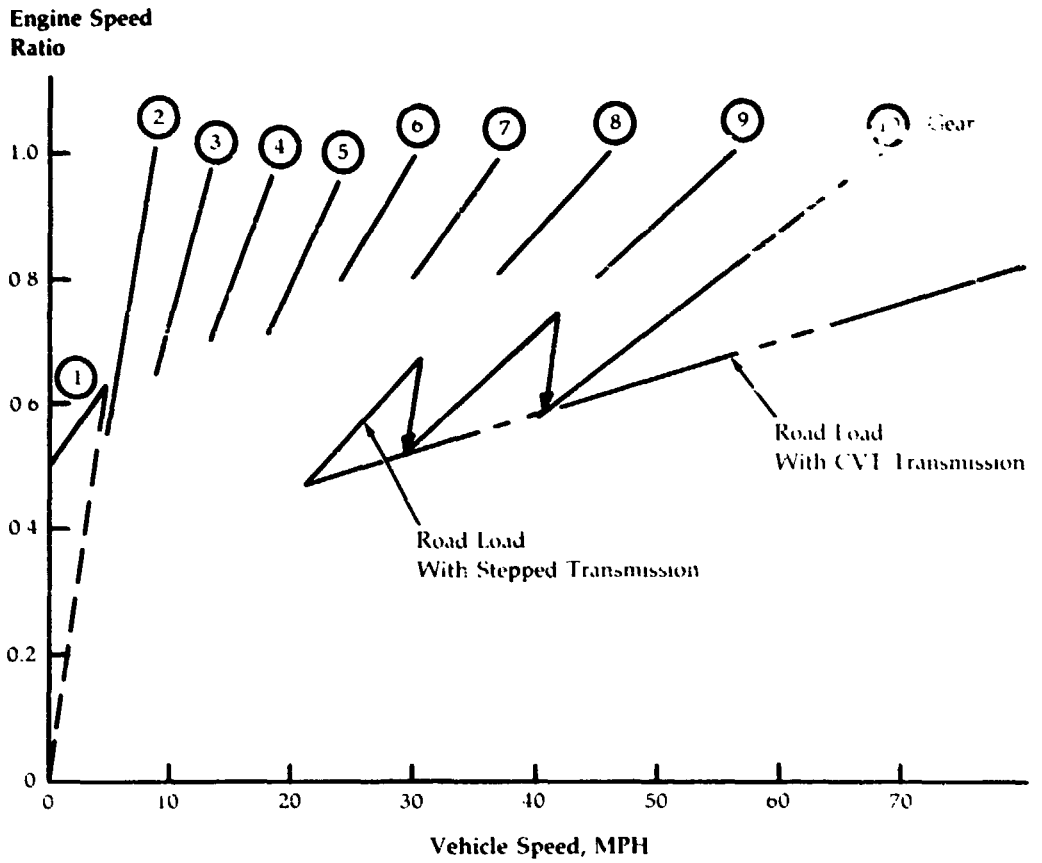

Figure 30

Two-Shaft Improved Gas Turbine

Fuel Economy Variation with Design Pressure Ratio

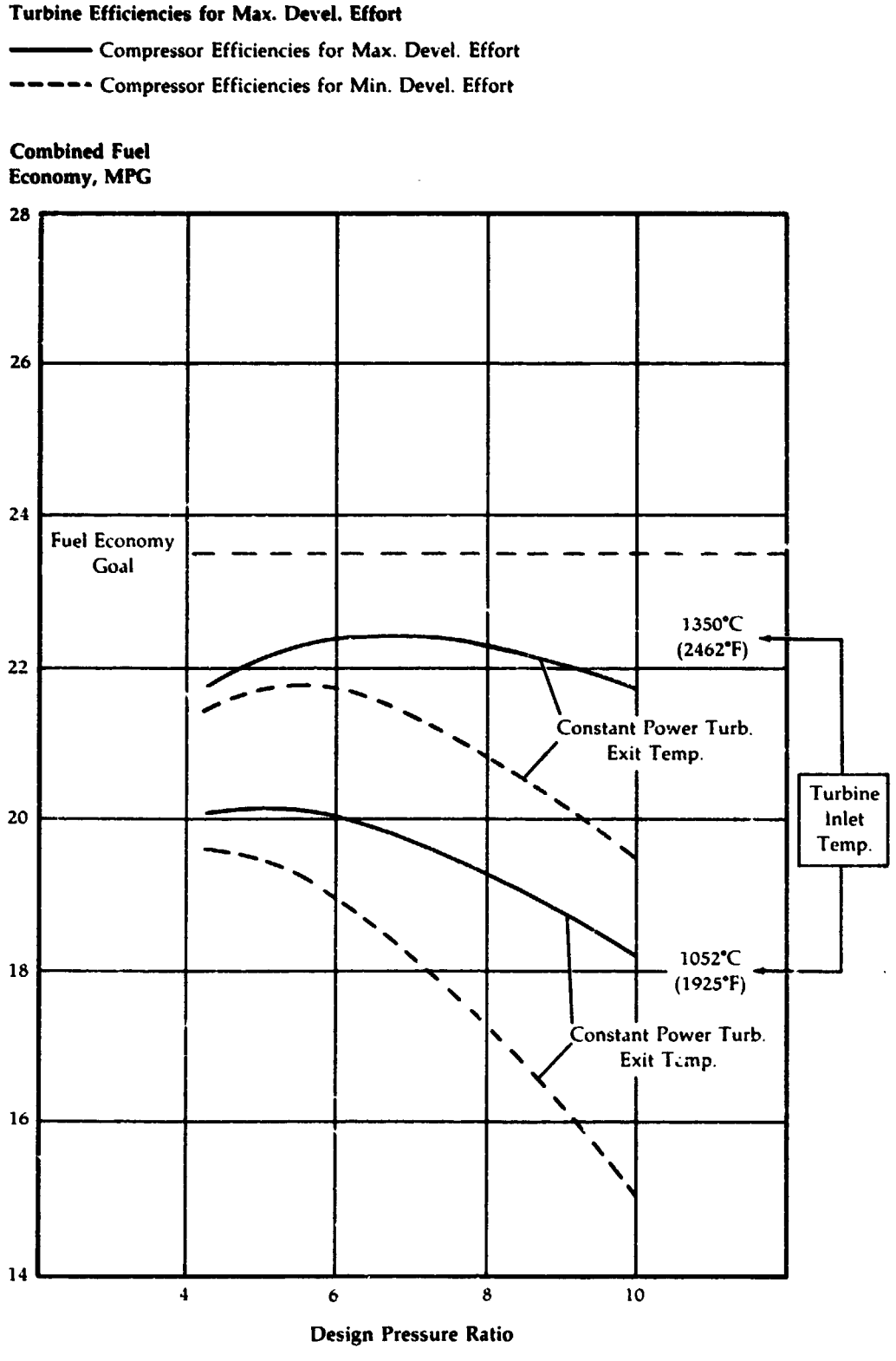

Figure 31

Composite Fuel Economy

91 HP Single-Shaft IGT

3500 Lb. Inertia Weight & CVT

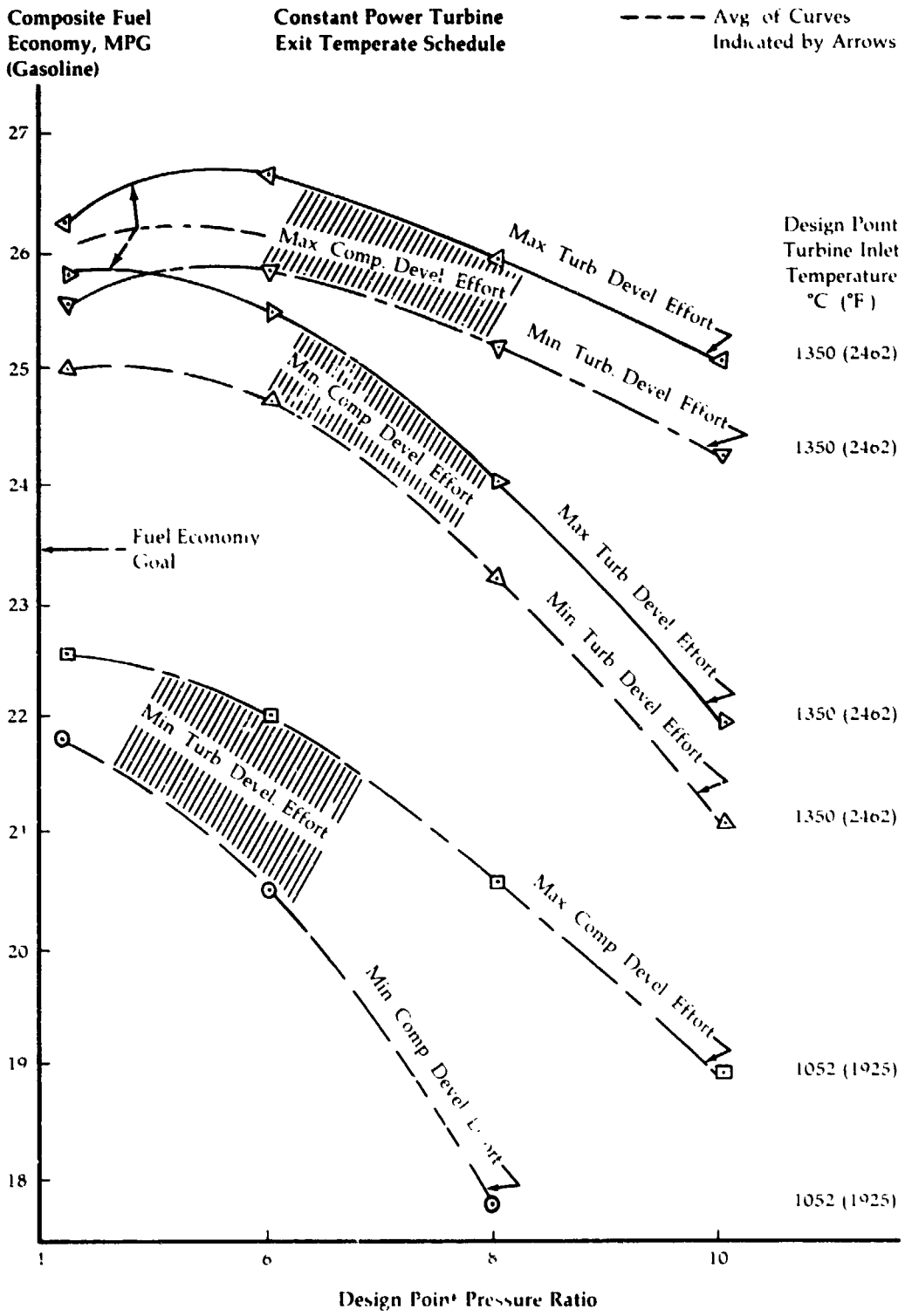

Figure 32

Two-Shaft Improved Gas Turbine

Fuel Economy Variation with Design Pressure Ratio

Turbine Efficiencies for Max. Devel. Effort

——— Compressor Efficiencies for Max. Devel. Effort

– – – – Compressor Efficiencies for Min Devel. Effort

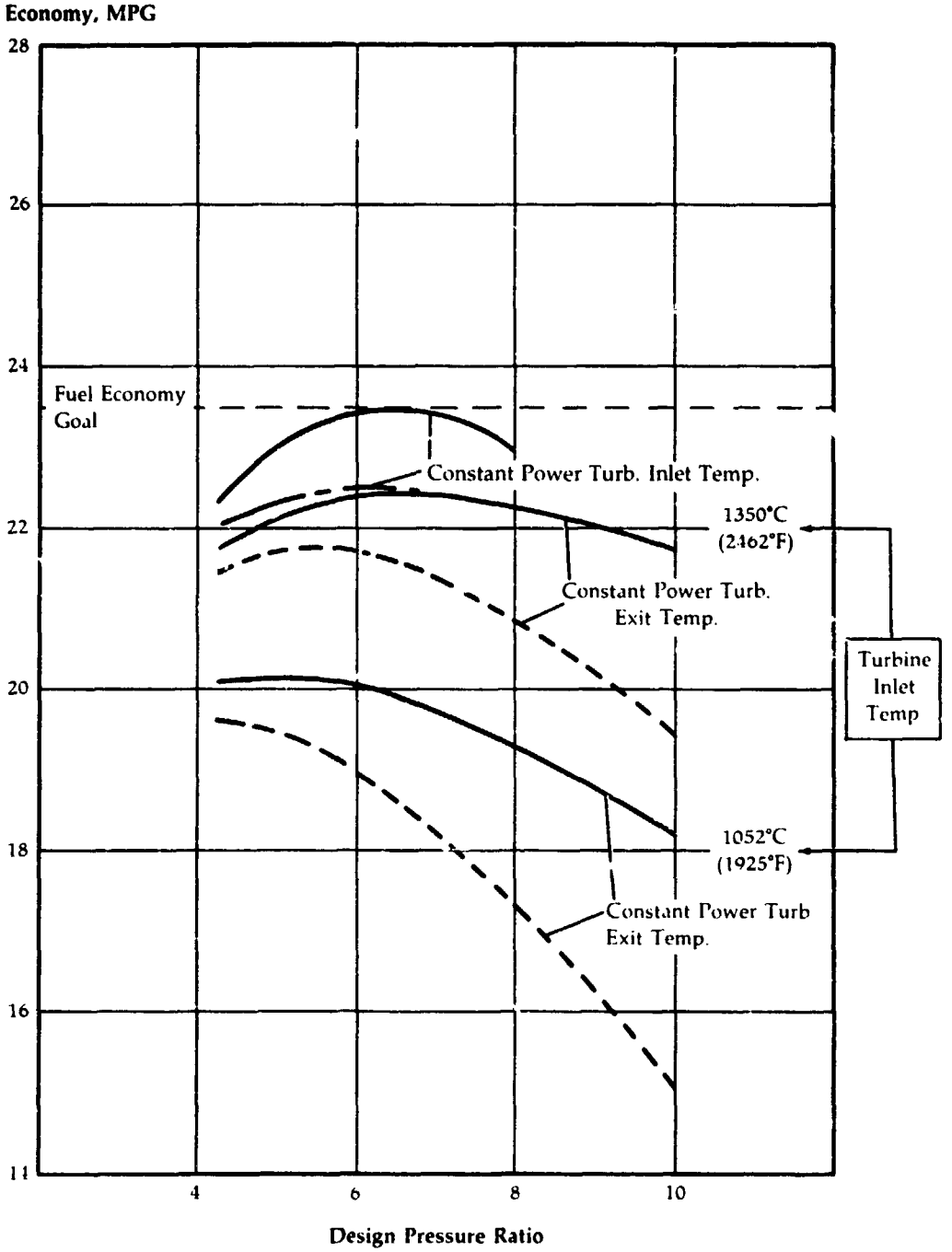

Figure 33

Preliminary Design of Turbine Sections for 2-Shaft Engines with Power Turbine Placed 1st and 2nd in Flowpath; Compressor Pressure Ratio Equal to 6:1

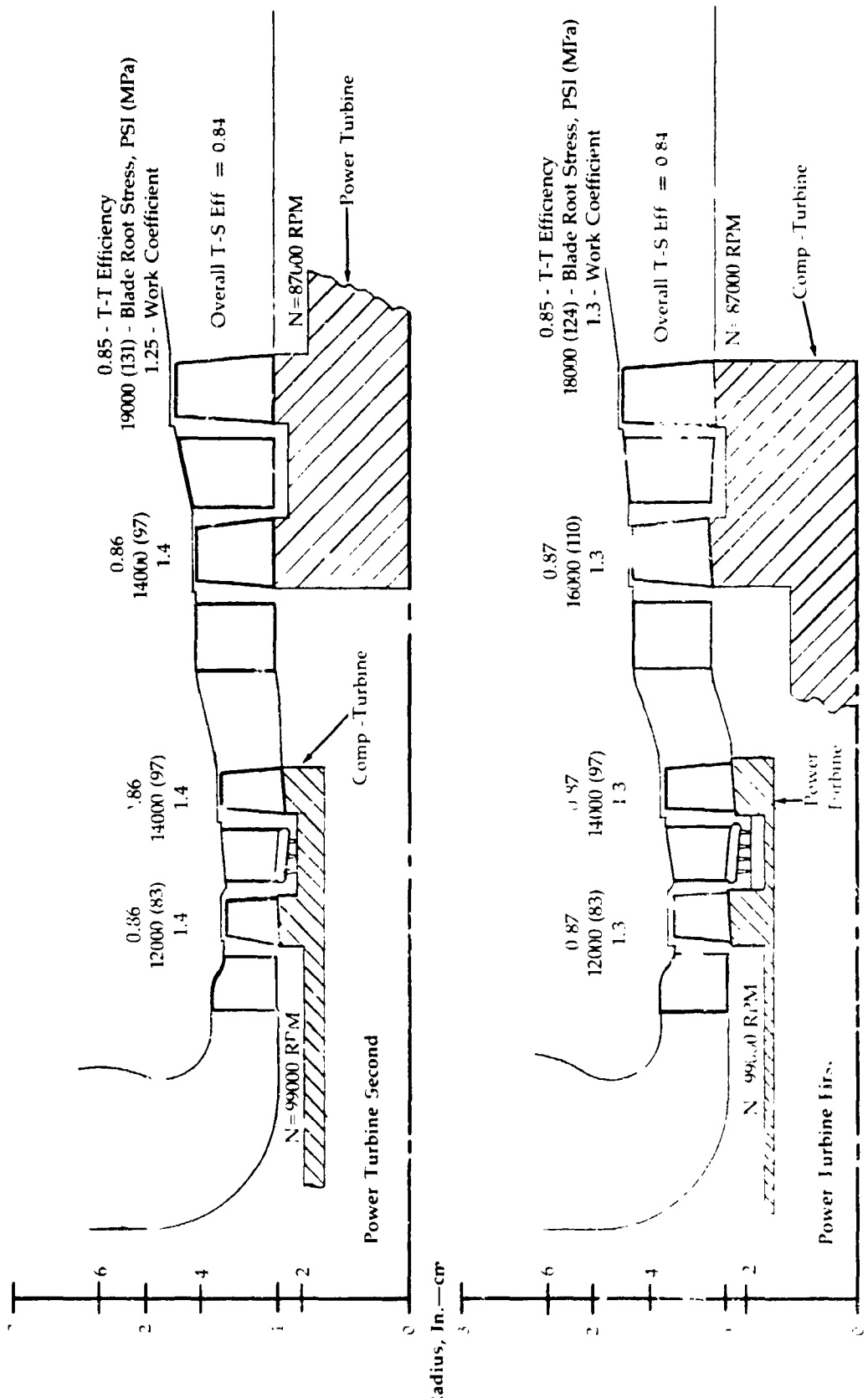

Figure 34

Preliminary Design of Turbine Section for a 2-Shaft Engine with Power Turbine in Front of Compressor-Turbine

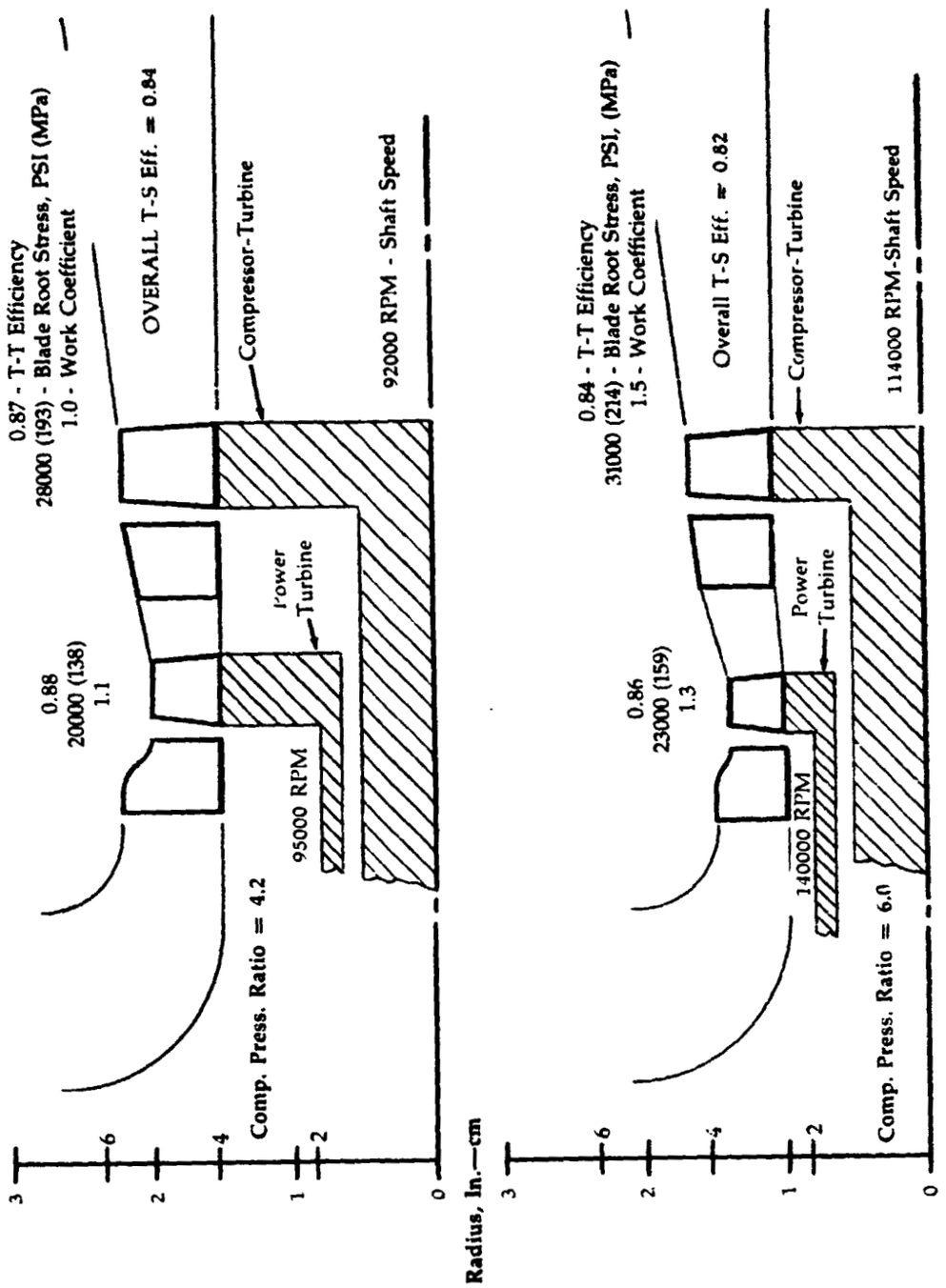

Figure 35

Preliminary Design of Turbine Sections for a Single-Shaft Engine; Compressor Pressure Ratio Equal to 4.2:1

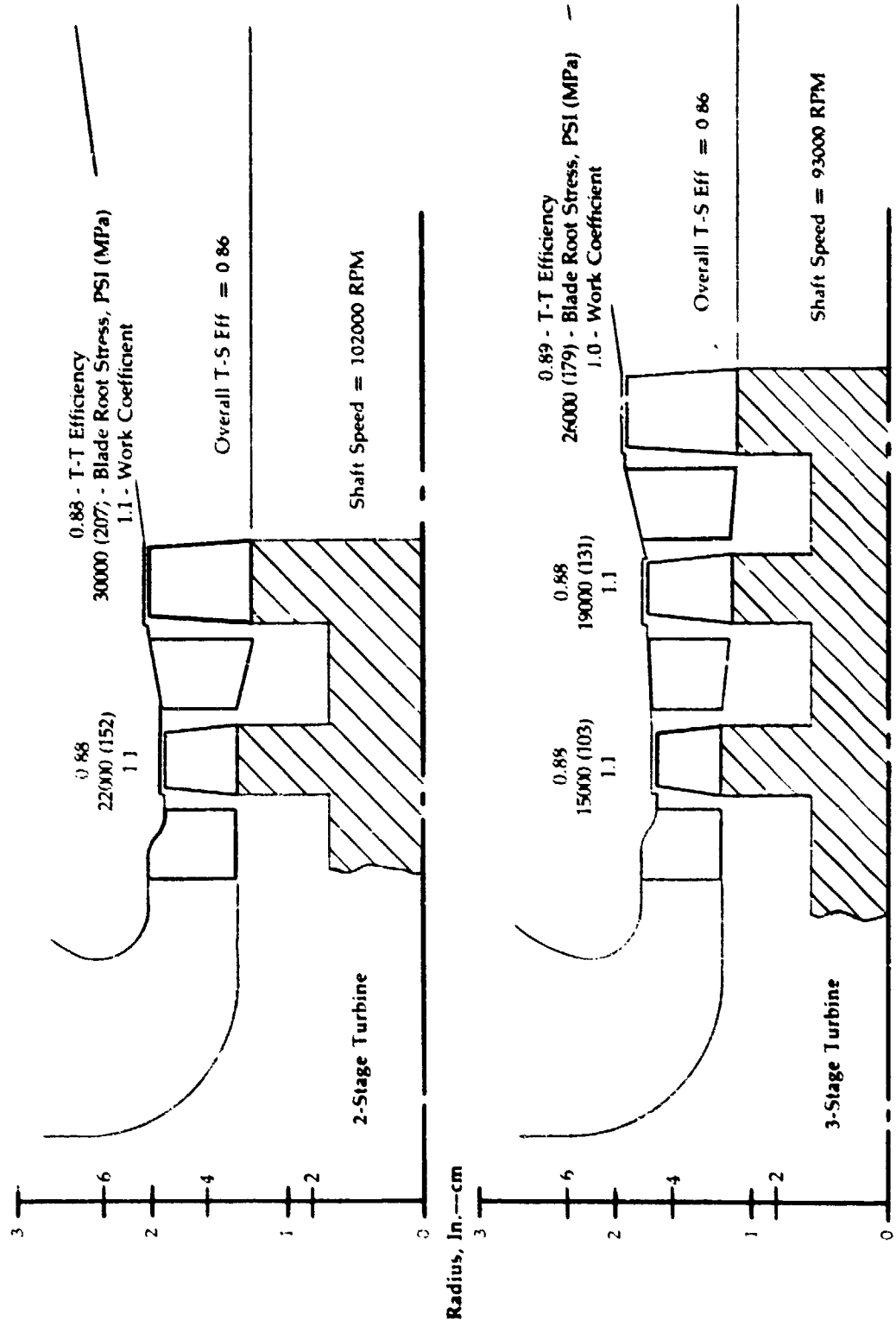

Figure 36

Preliminary Design of Compressor Section for 3-Shaft Engine with Twin-Spool Gas Generator; Compressor Pressure Ratio = 4.2:1

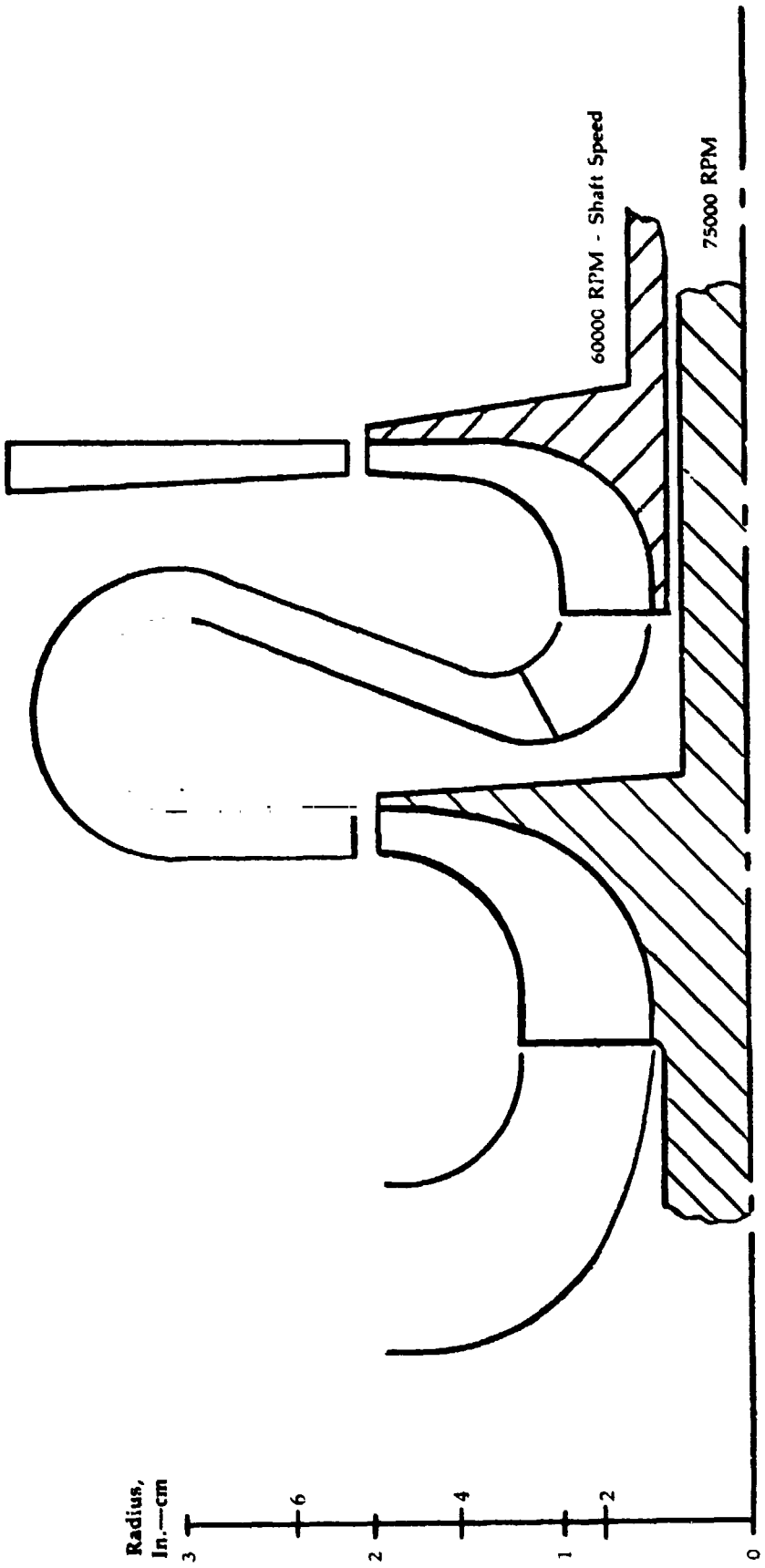

Figure 37

Preliminary Design of Turbine Section for 3-Shaft Engine with Twin-Spool Gas Generator; Compressor Pressure Ratio = 4.2:1

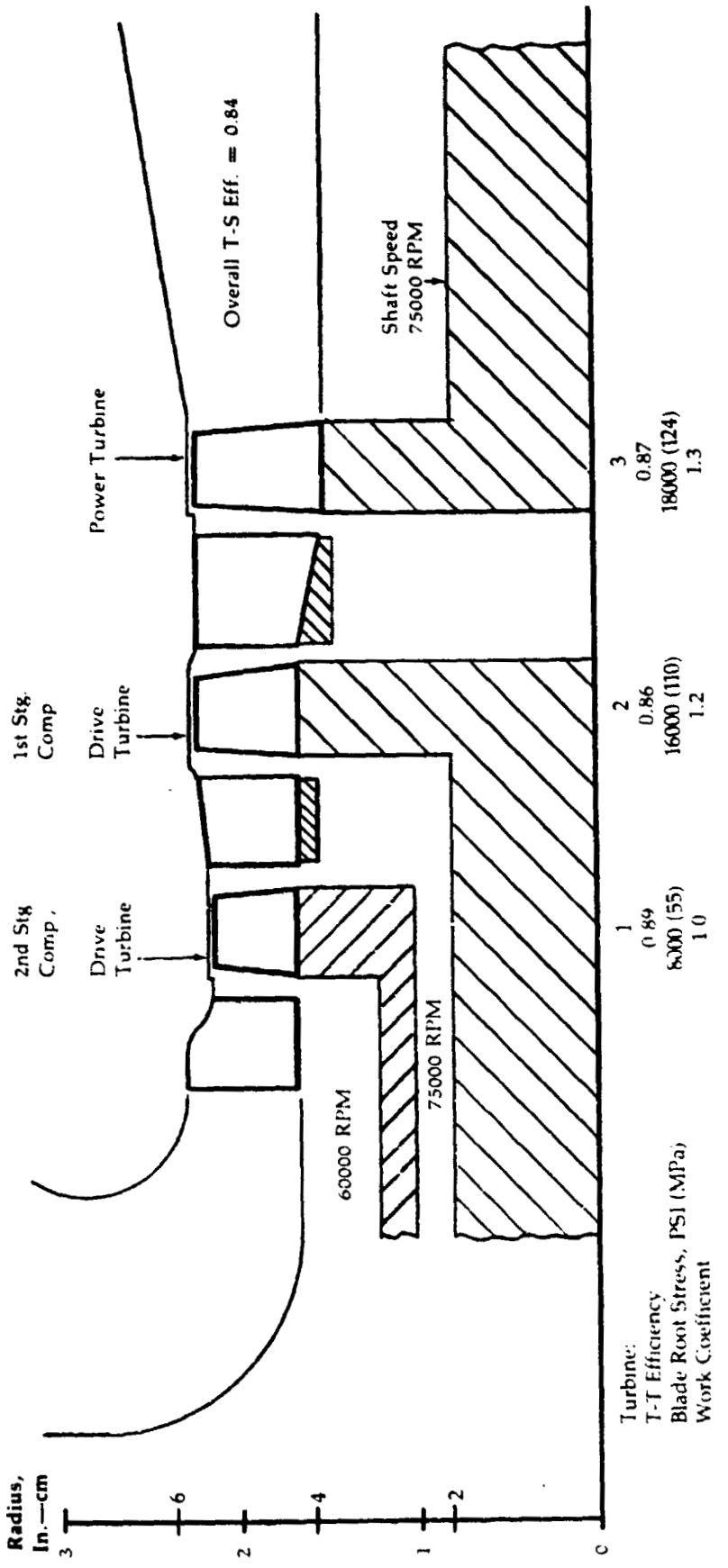

Figure 38

Two Shaft Turbine with Interconnection 1150°C. T.I.T.

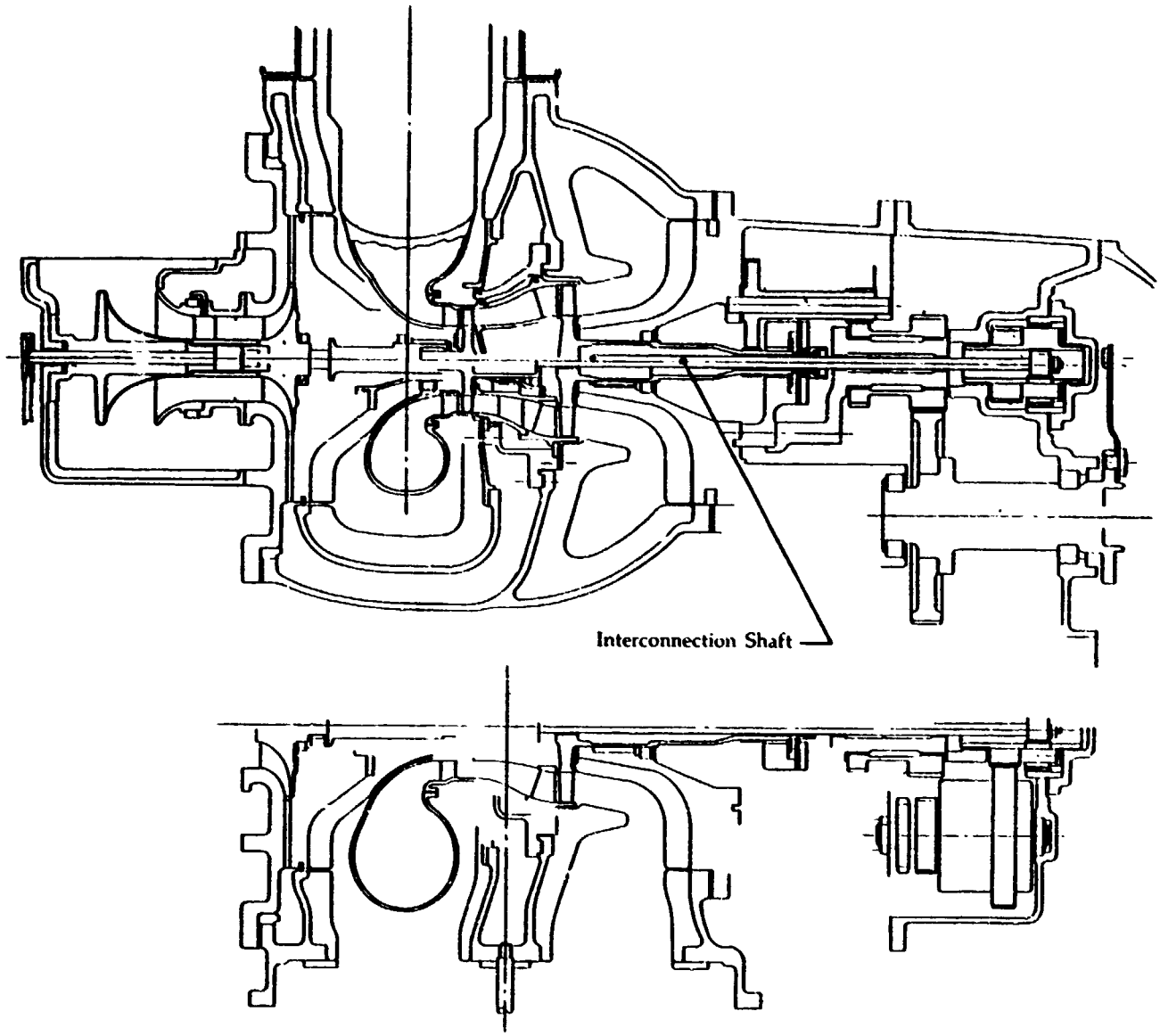

Figure 39

Single Shaft Engine

91 HP

1350°C. T.I.T.

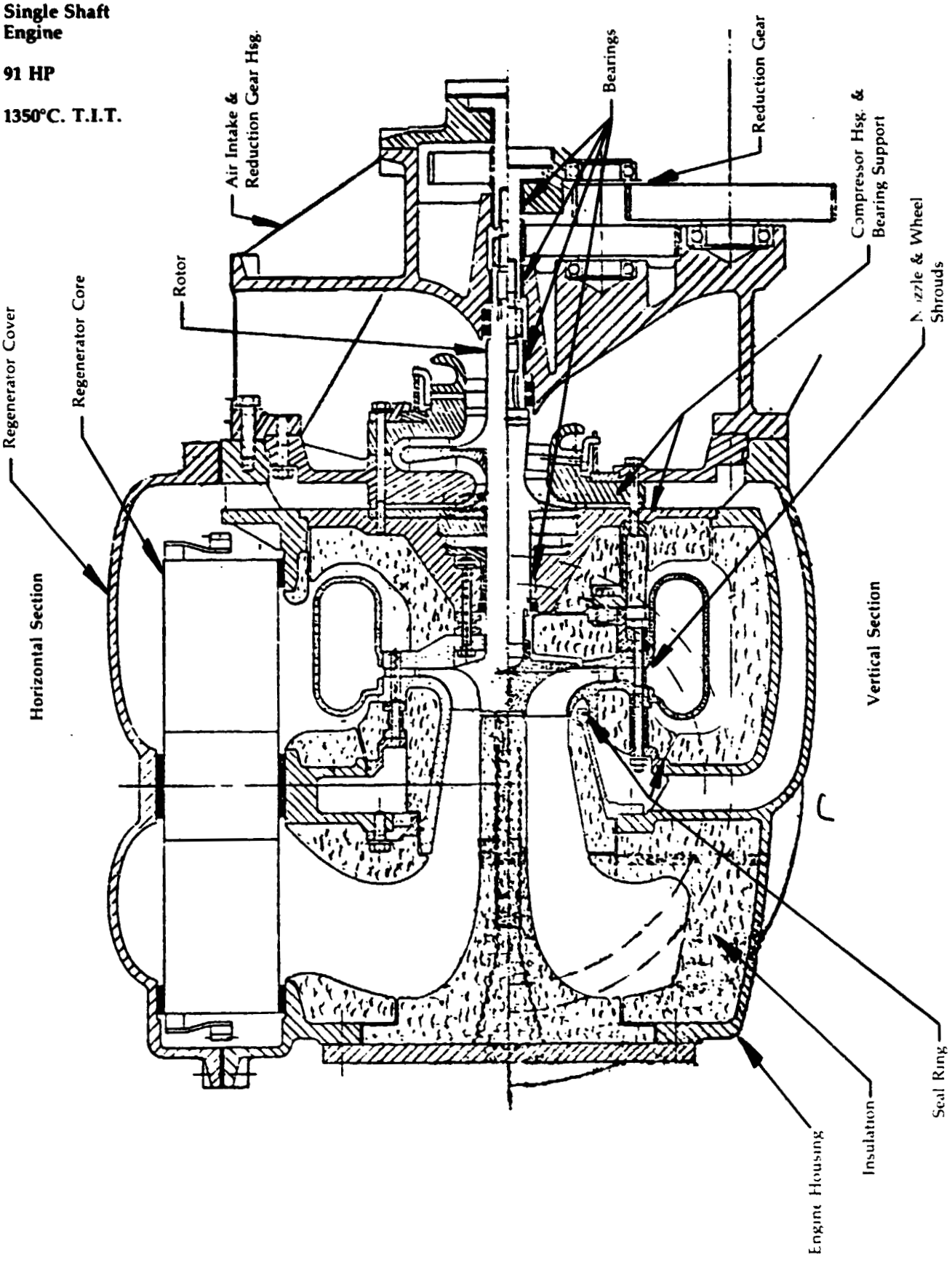

Figure 40

Single Shaft Engine with Radial Turbine

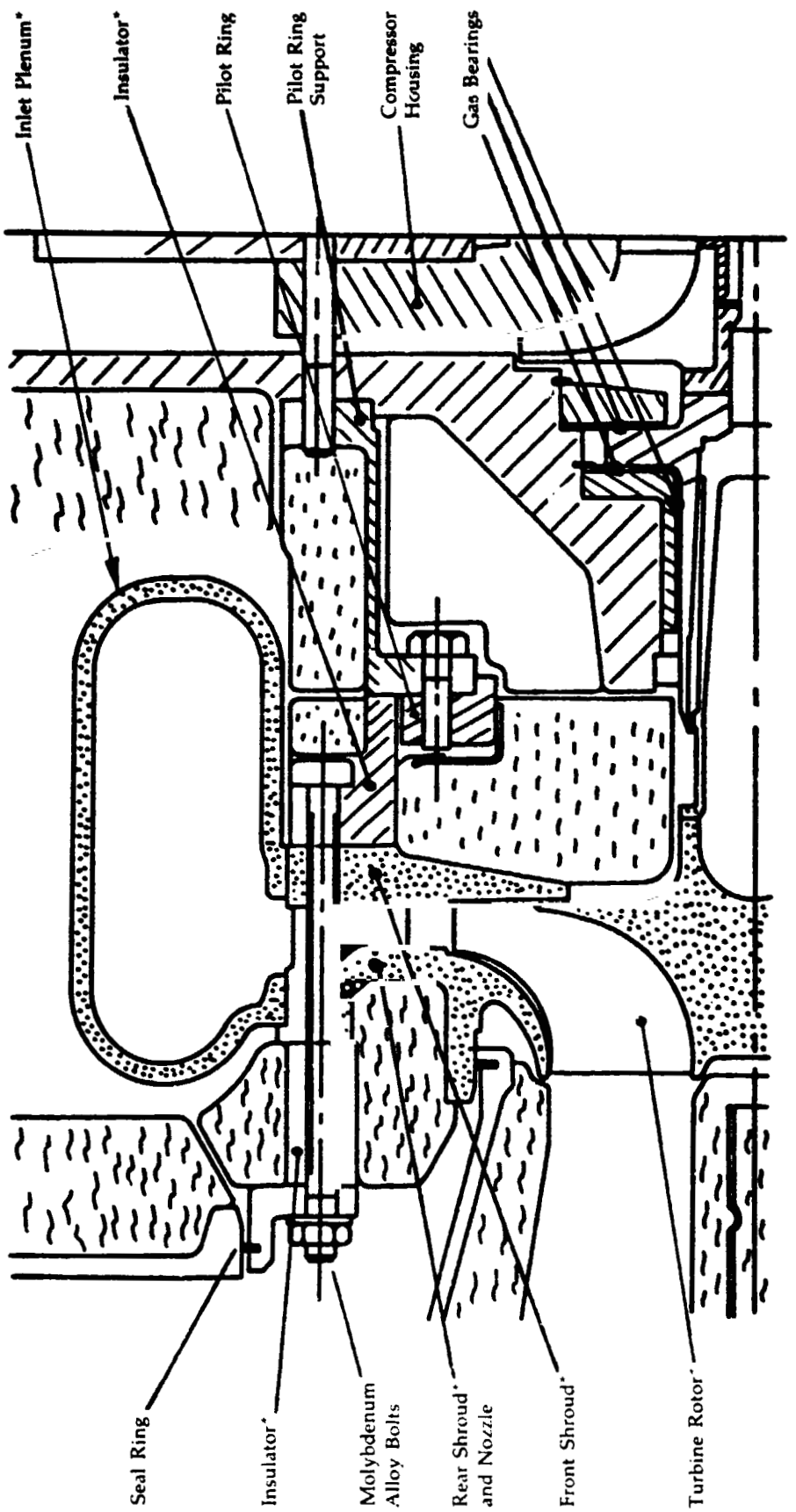

*Ceramic Components

Figure 41

Shroud Supports for Wheel Tip Clearance Control

Three-Shaft Free Power Turbine

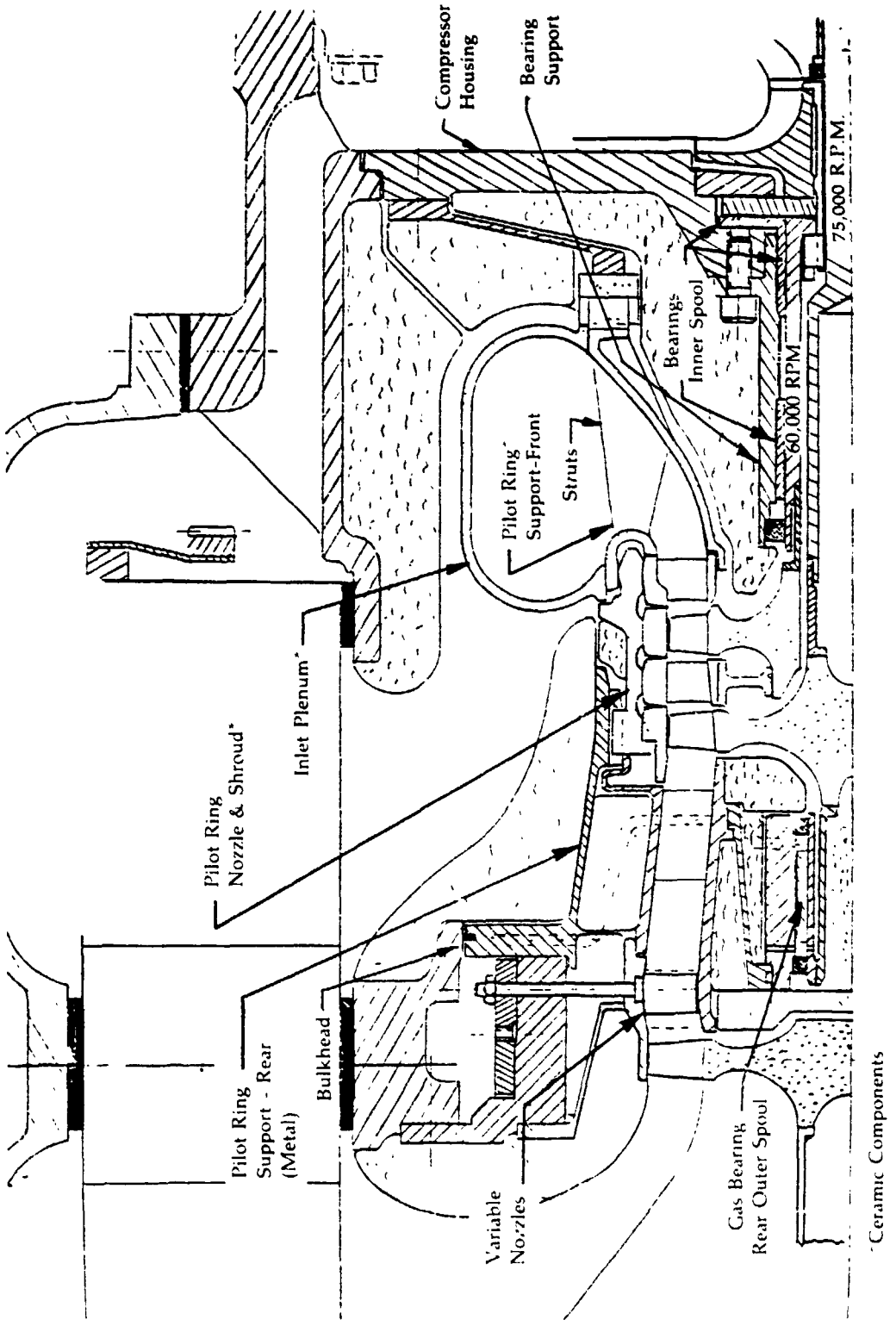

Figure 42

Single Shaft Engine with Variable Ratio Belt CVT

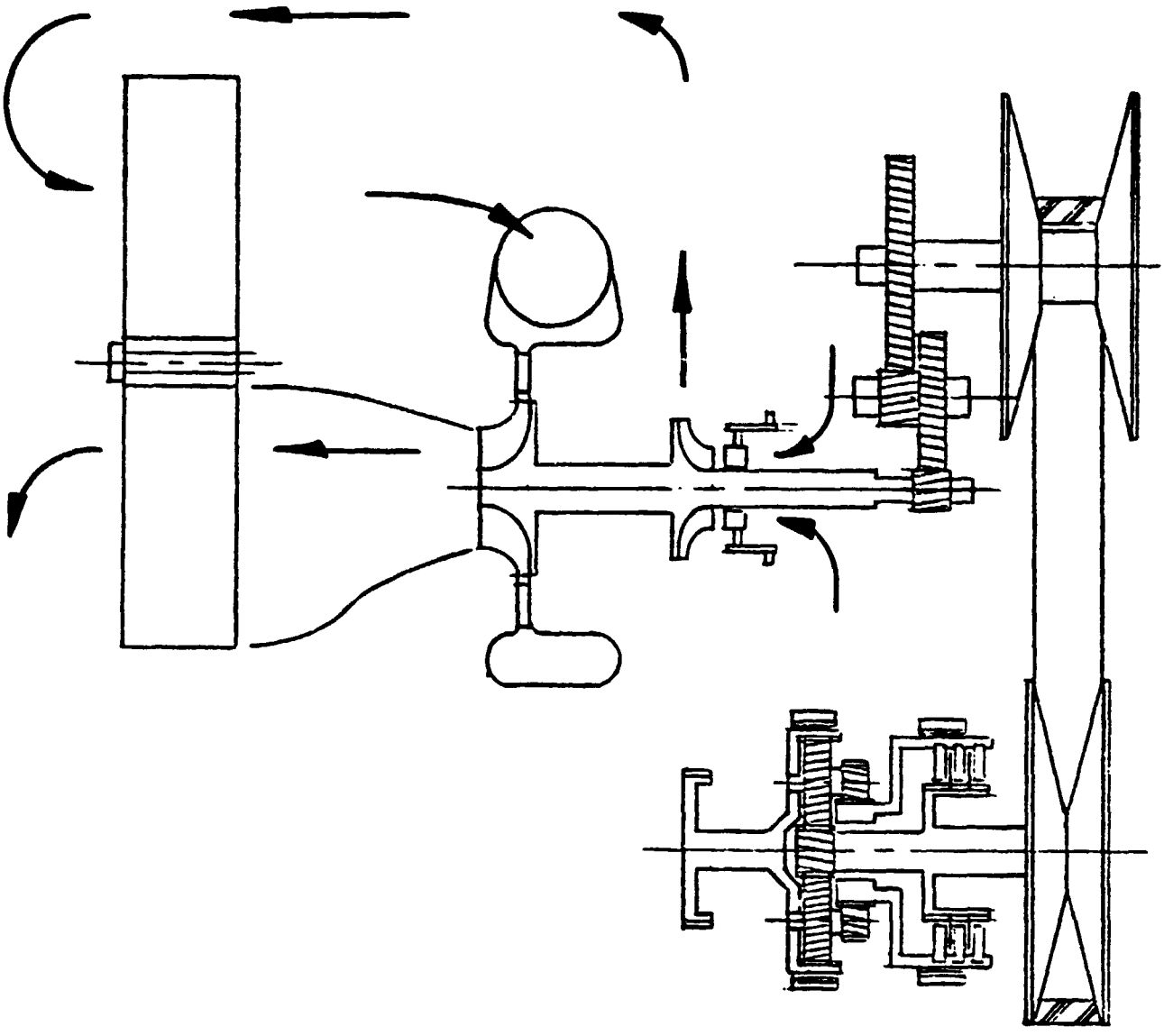

Figure 43

Schematic of Three-Shaft System with Single Regenerator*

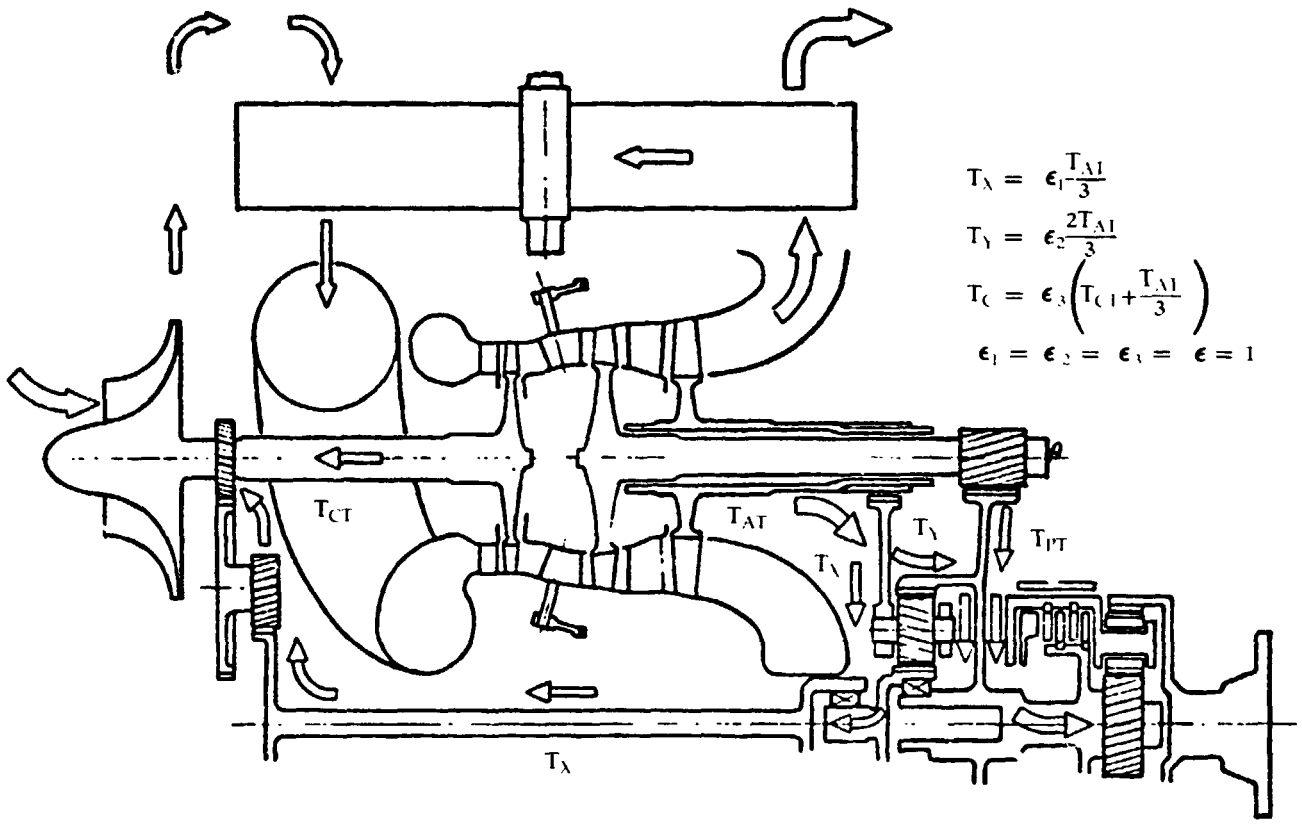

T_{CT} = Torque - Compressor Turbine
T_{AT} = Torque - Auxiliary Turbine = $T_X + T_Y$
T_{PT} = Torque - Power Turbine
ϵ = Gear Ratio

*Taken from Ref. ASME Paper No. 77-GT-94

Figure 44

Compressor Performance Estimate with Operating Line for Single-Shaft Engine

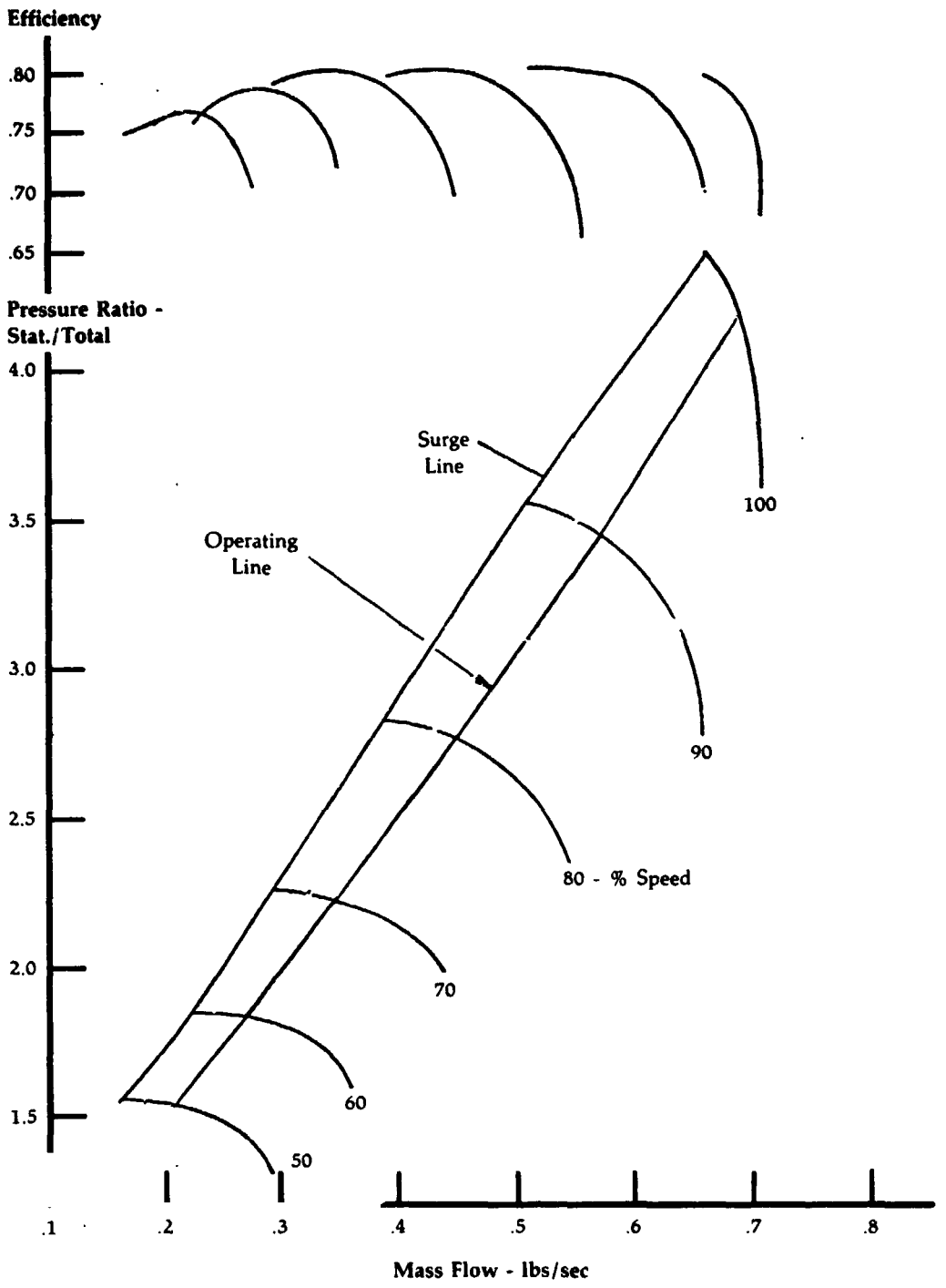

Figure 45

Single-Shaft Engine Operating Line Parameters

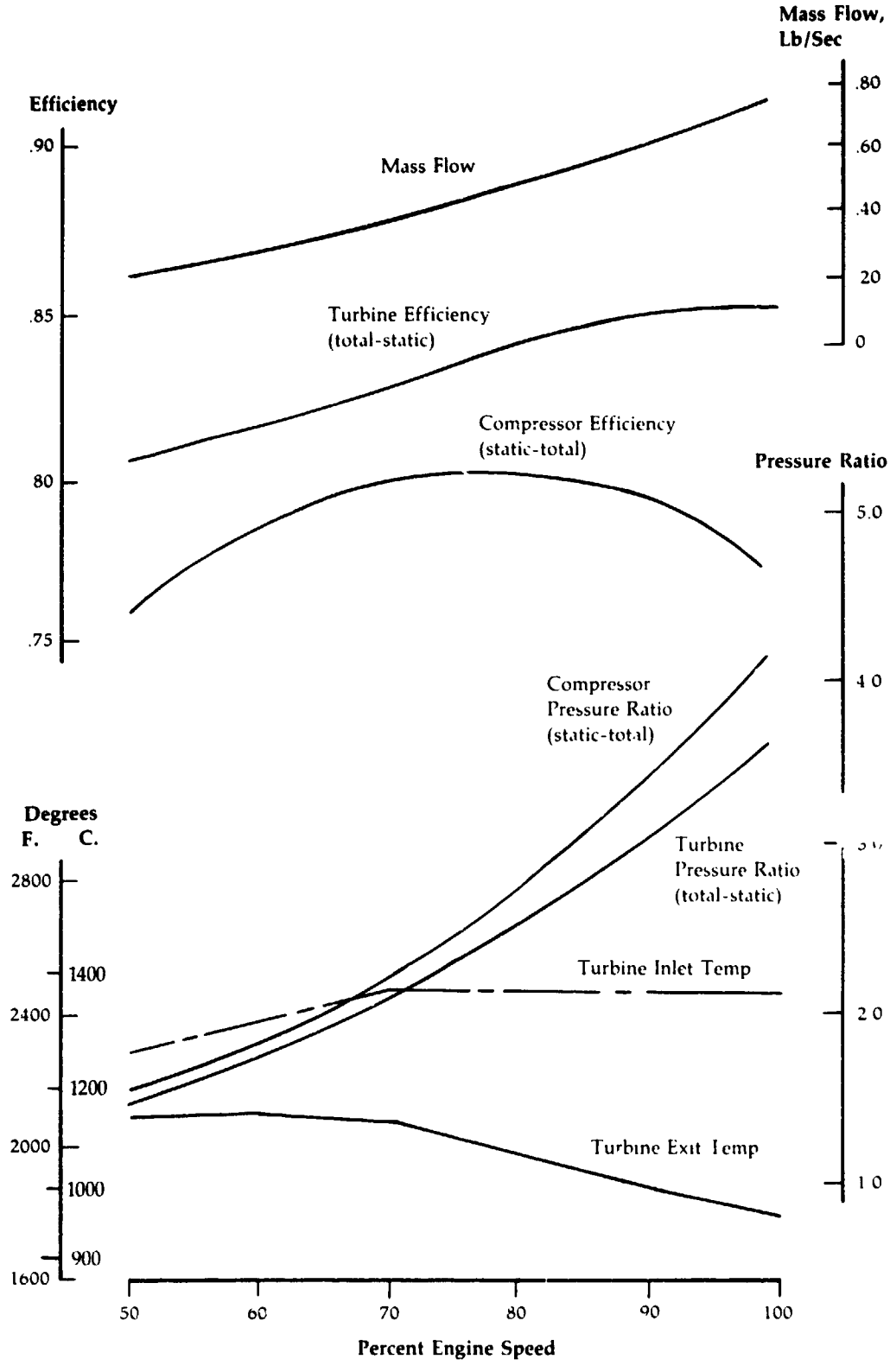

Figure 46

Single-Shaft Engine Performance Characteristics

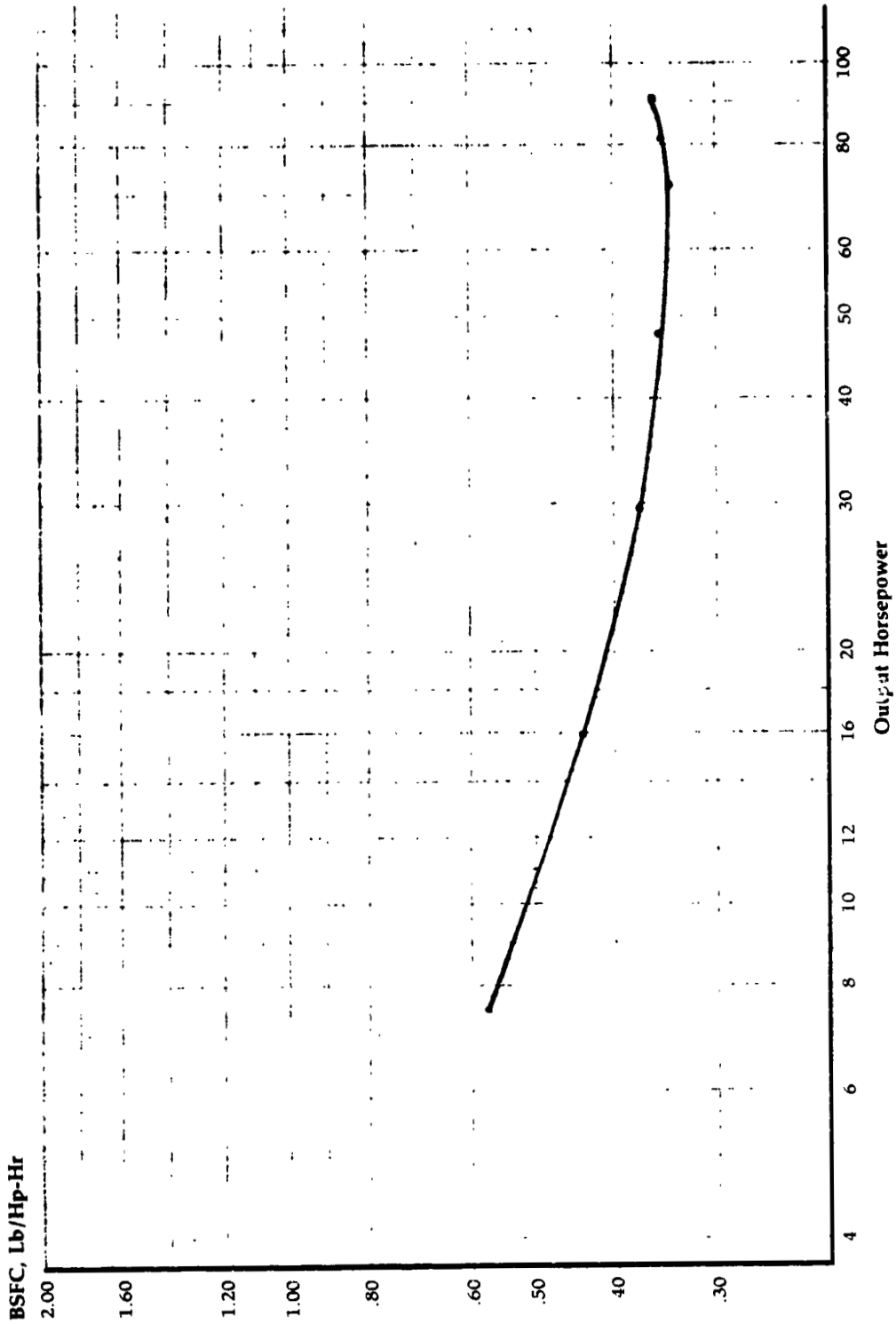

Figure 47

Variation of Transmission Efficiency with Constant Vehicle Speed

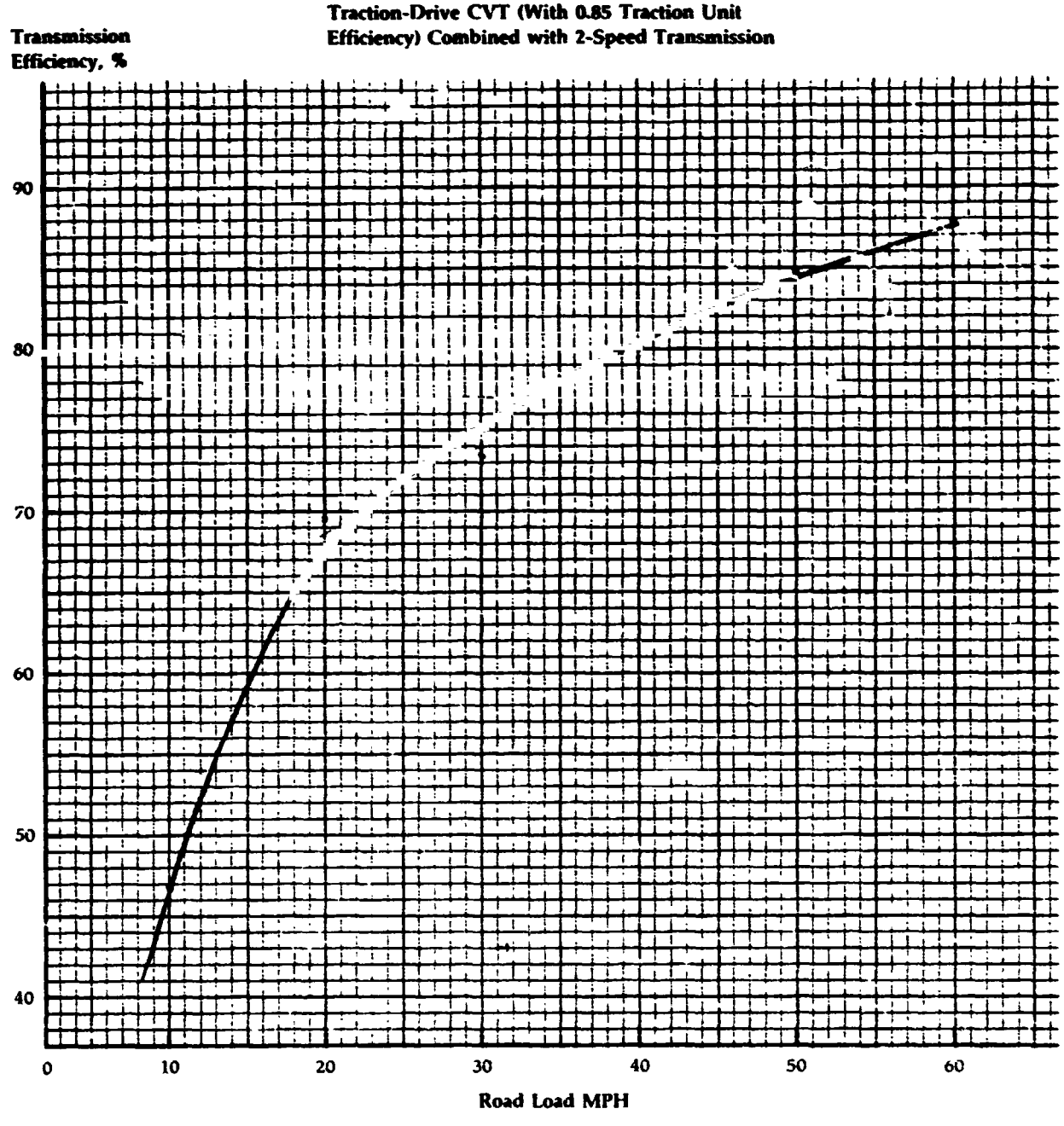

Figure 48

Variation of Combined Fuel Economy with Turbine Inlet Temperature, Type of Continuously Variable Transmission (CVT) and 5.3% Reduction in Power Requirement From Values in Federal Register

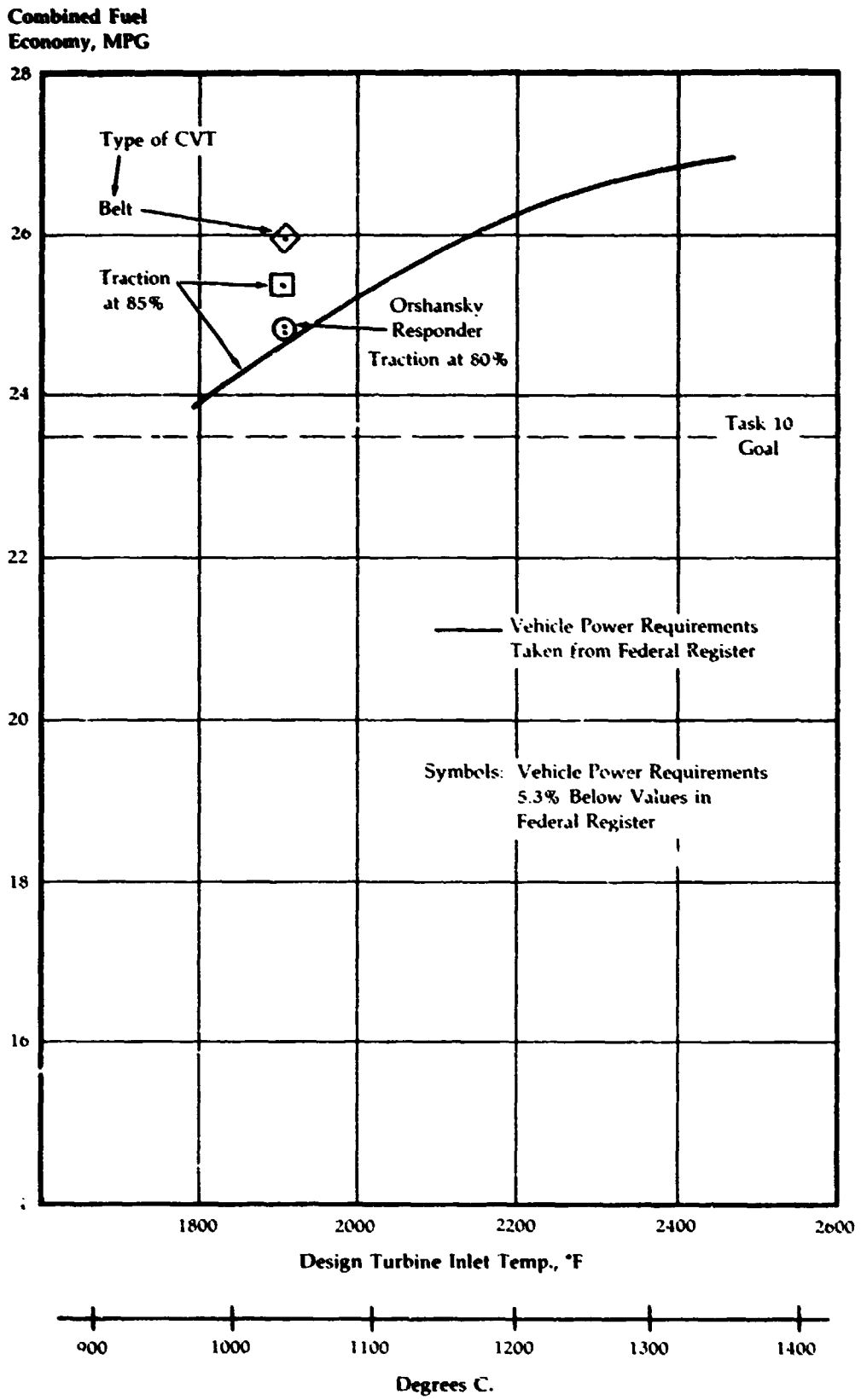

Figure 49

Single Shaft Engine 4.185 Pressure Ratio

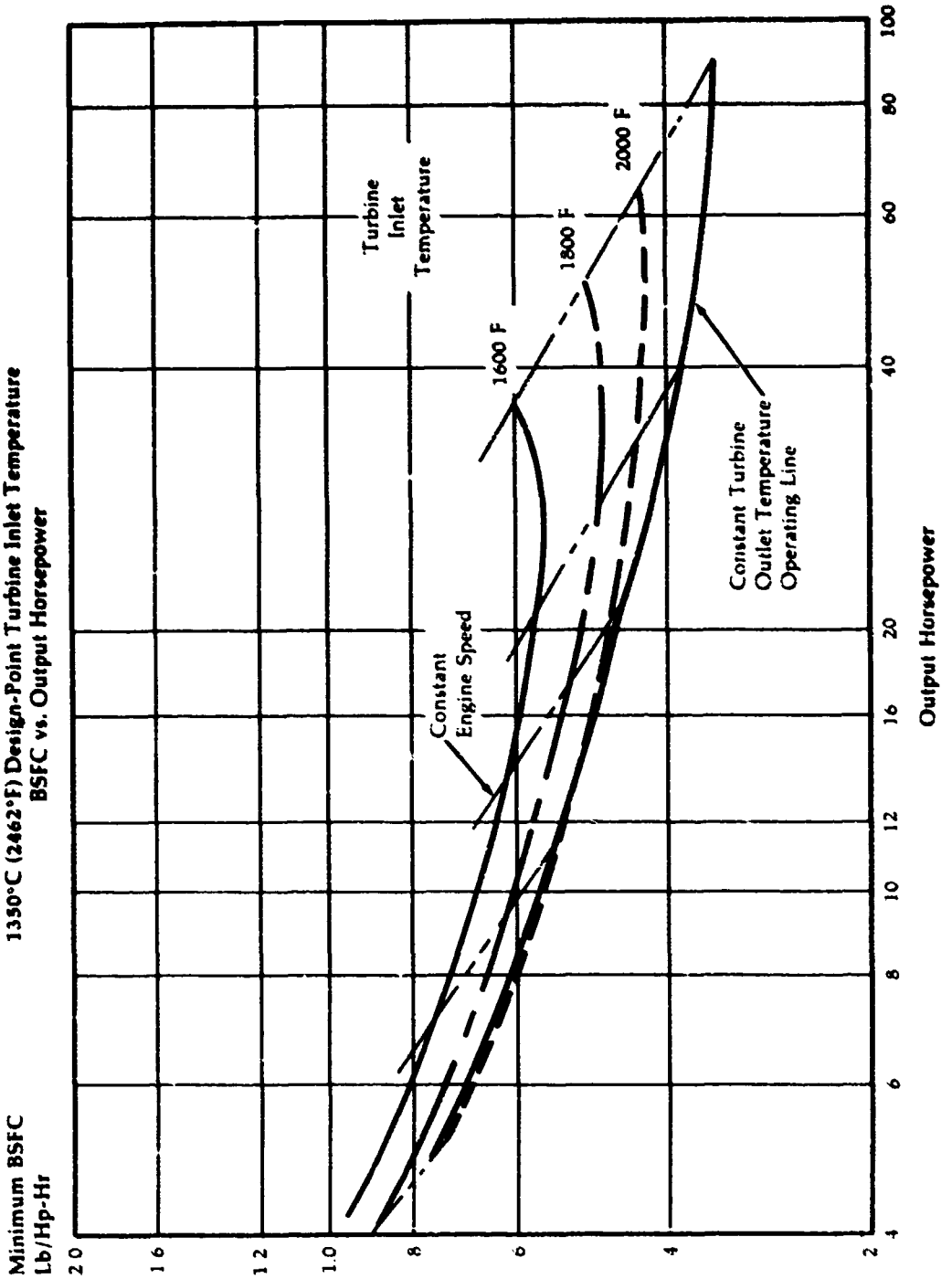

Figure 50

91 HP Single Shaft Gas Turbine Performance with 10-Speed Geared Transmission

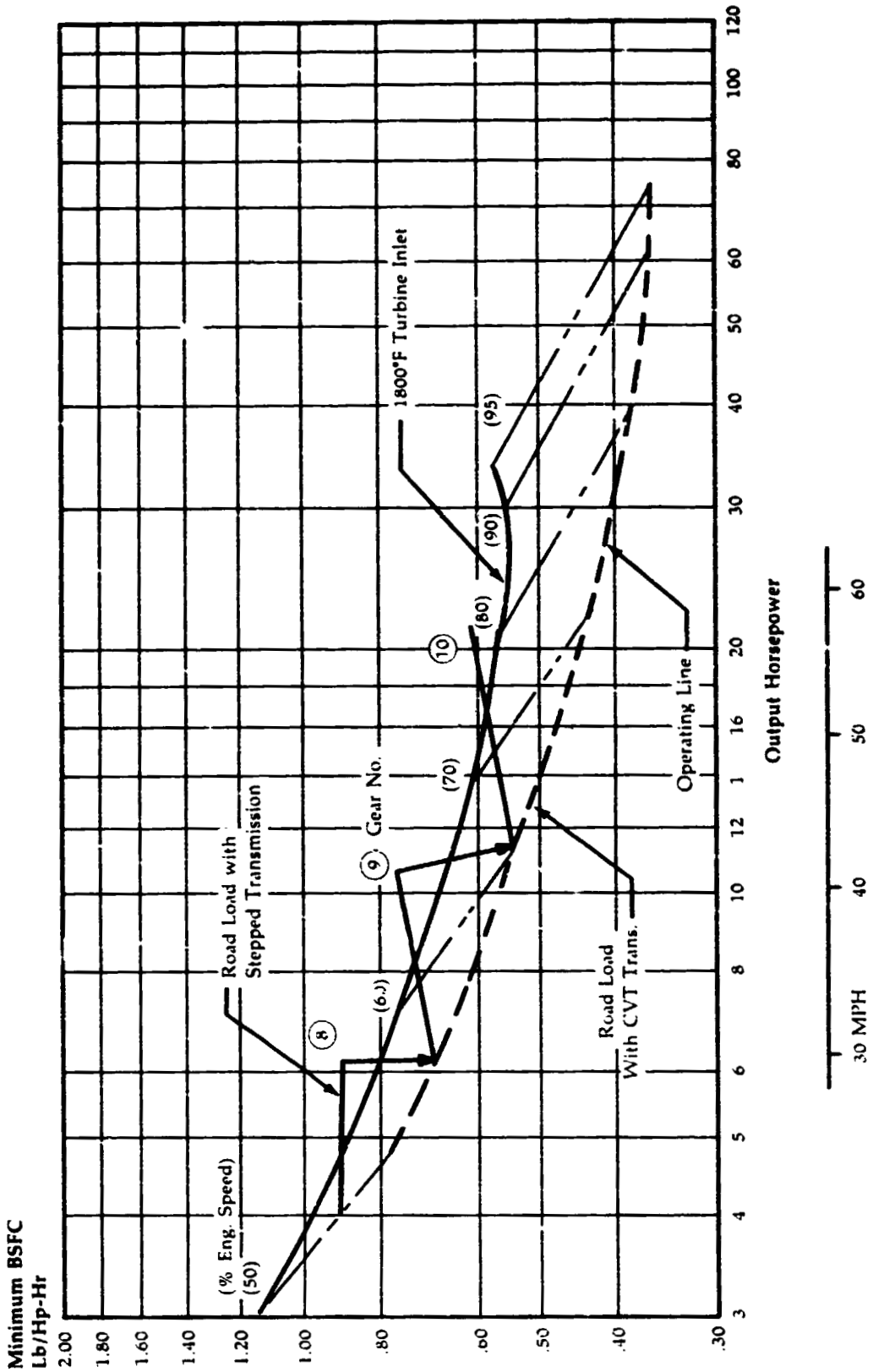

Figure 51

3500 IW 91 HP Single Shaft Gas Turbine Stepped vs. CVT Transmission Road Load

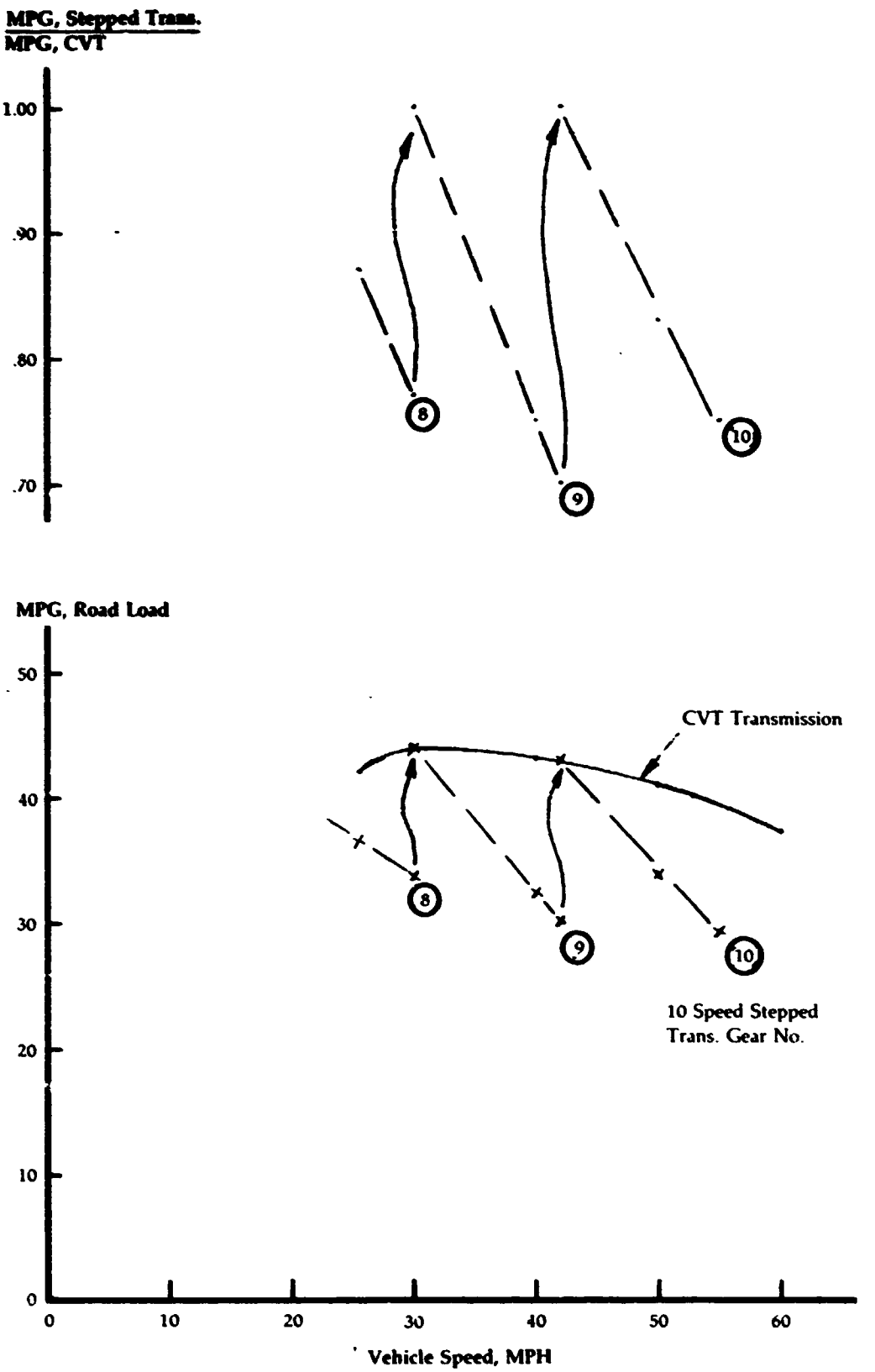

Figure 52

Two-Shaft Engine Operating Line Parameters

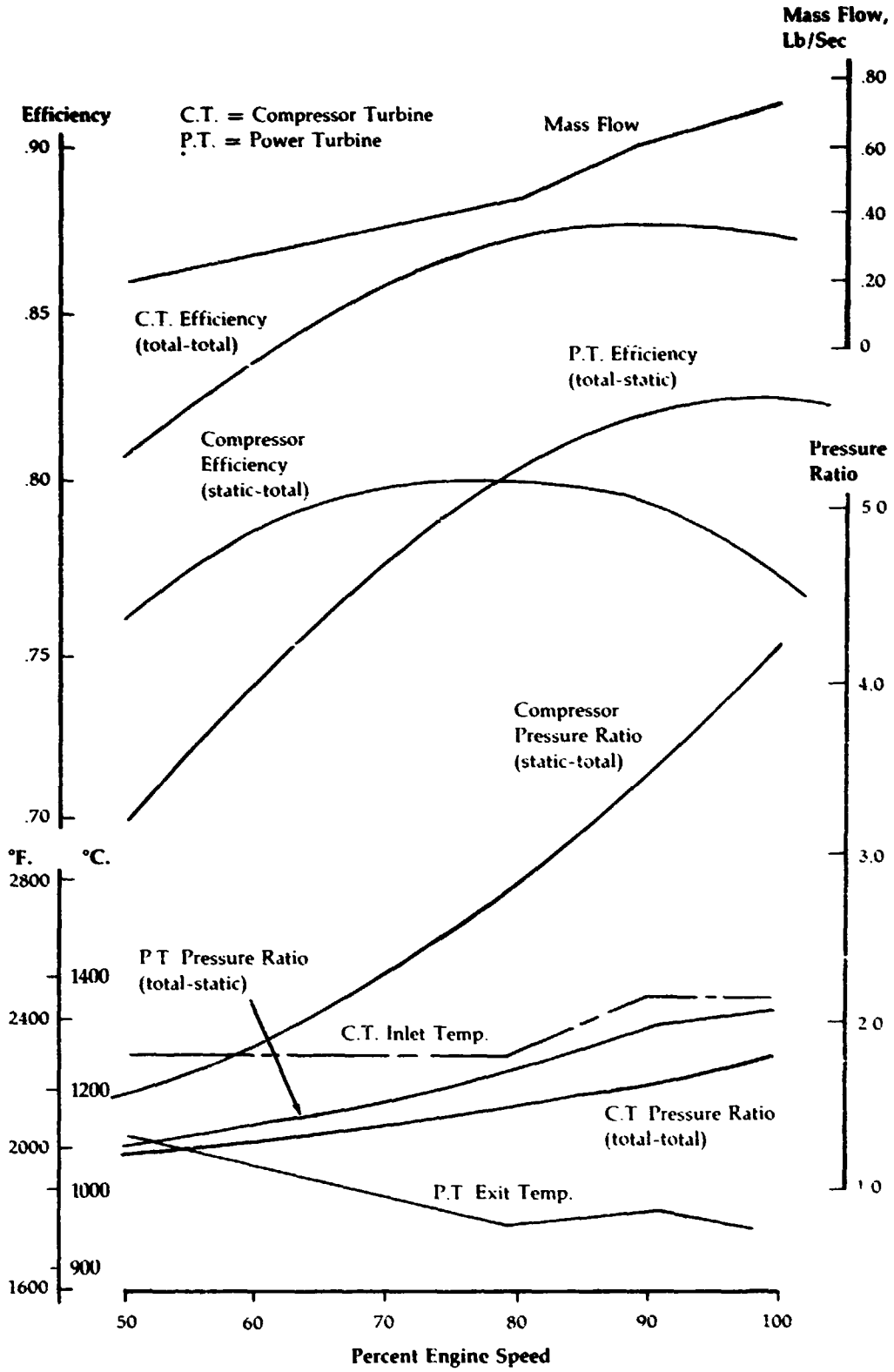

Figure 53

Two-Shaft Engine Performance Characteristics

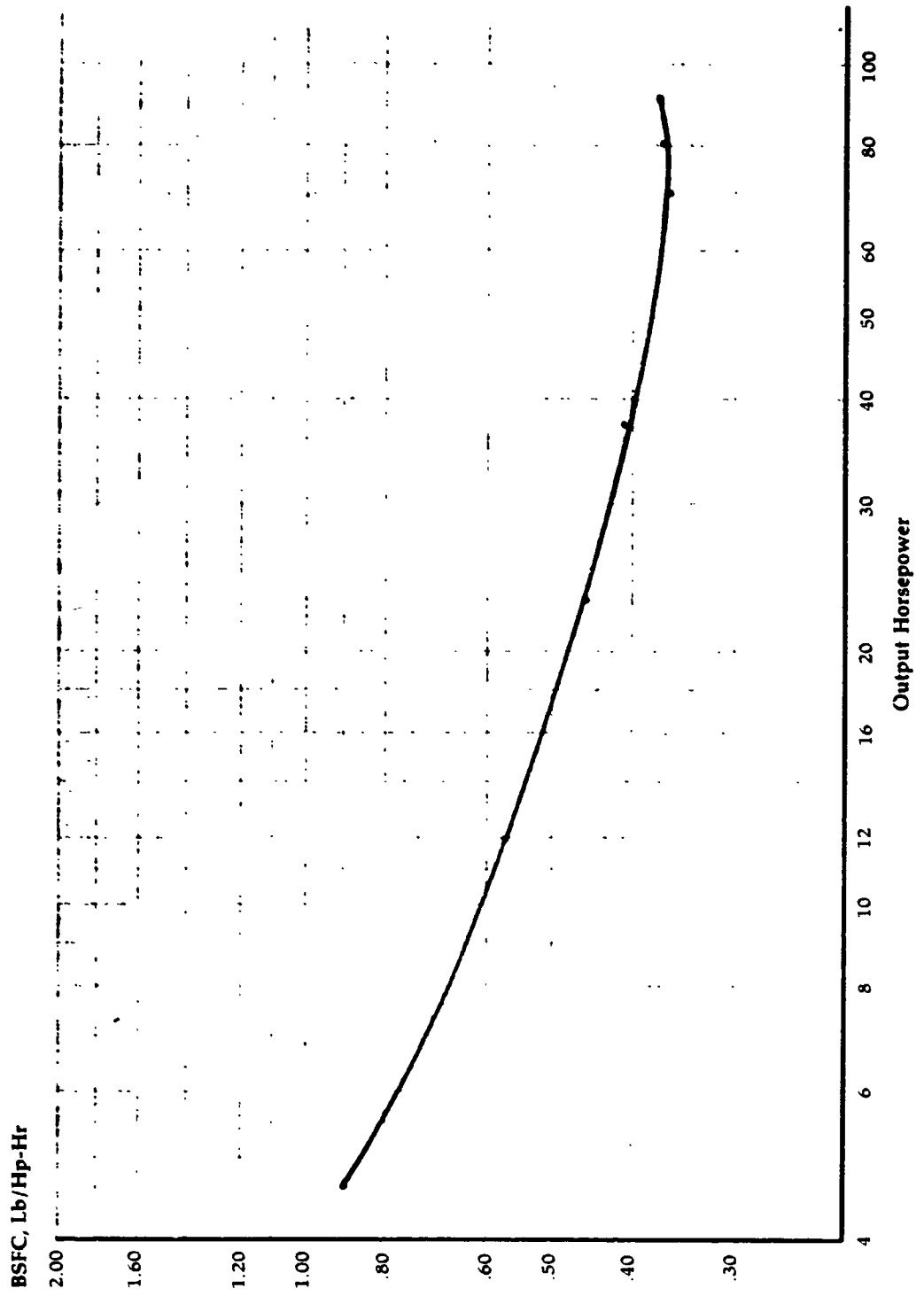

Figure 54

Variation of Transmission Efficiency with Constant Vehicle Speed

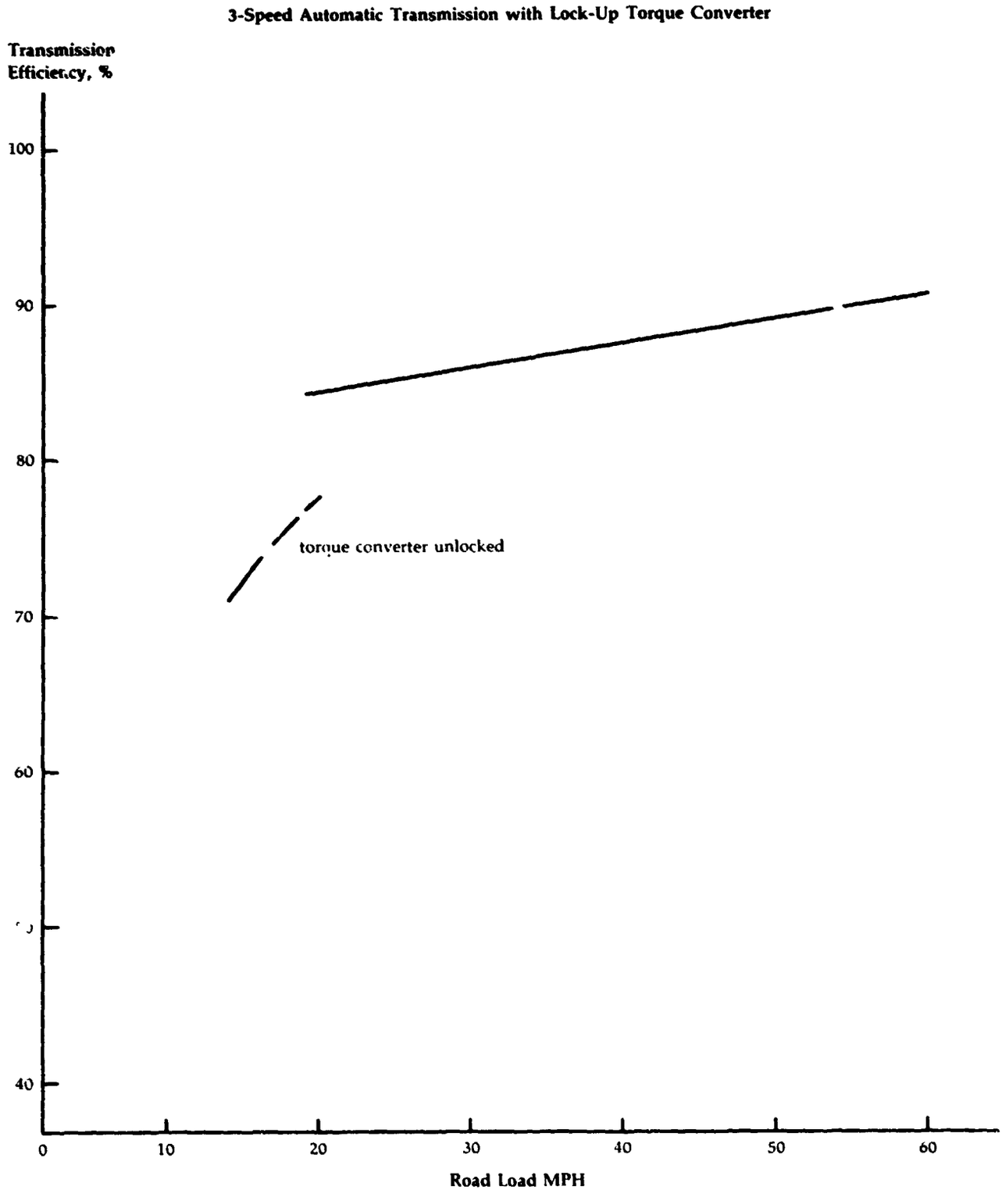

Figure 55

Component Matching Characteristics of Various Engine Configurations

Single Shaft

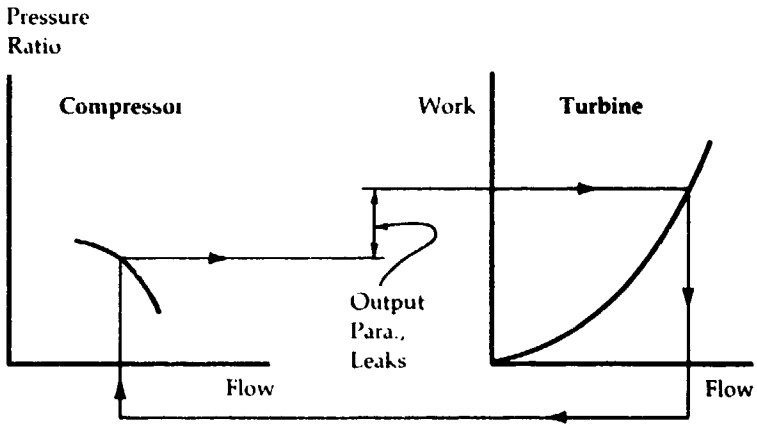

(A)

2-Shaft

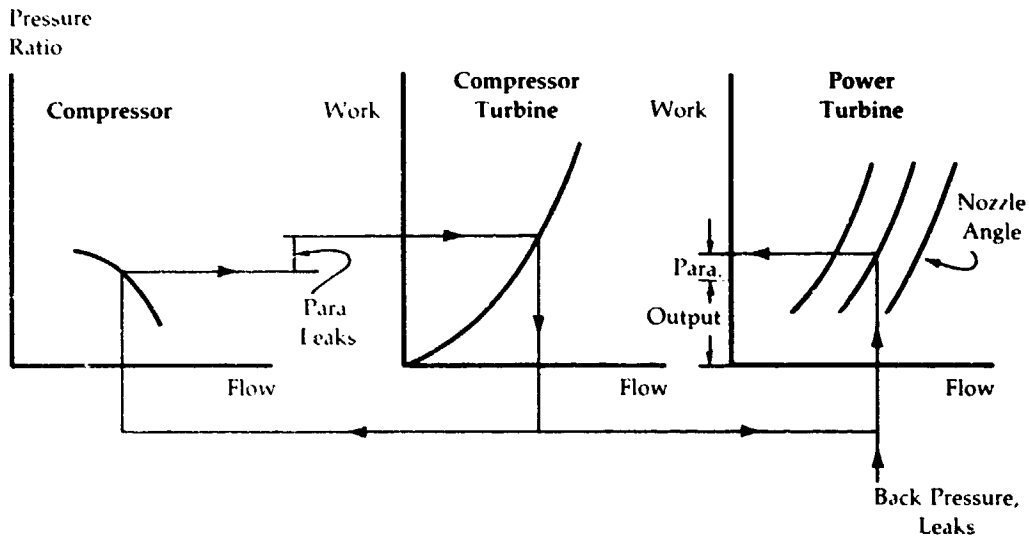

(B)

N.B.
Flow = Mass Flow
Arrows Indicate Calculation Path

Figure 56A & B

Component Matching (cont.)

3-Shaft, Auxiliary Turbine

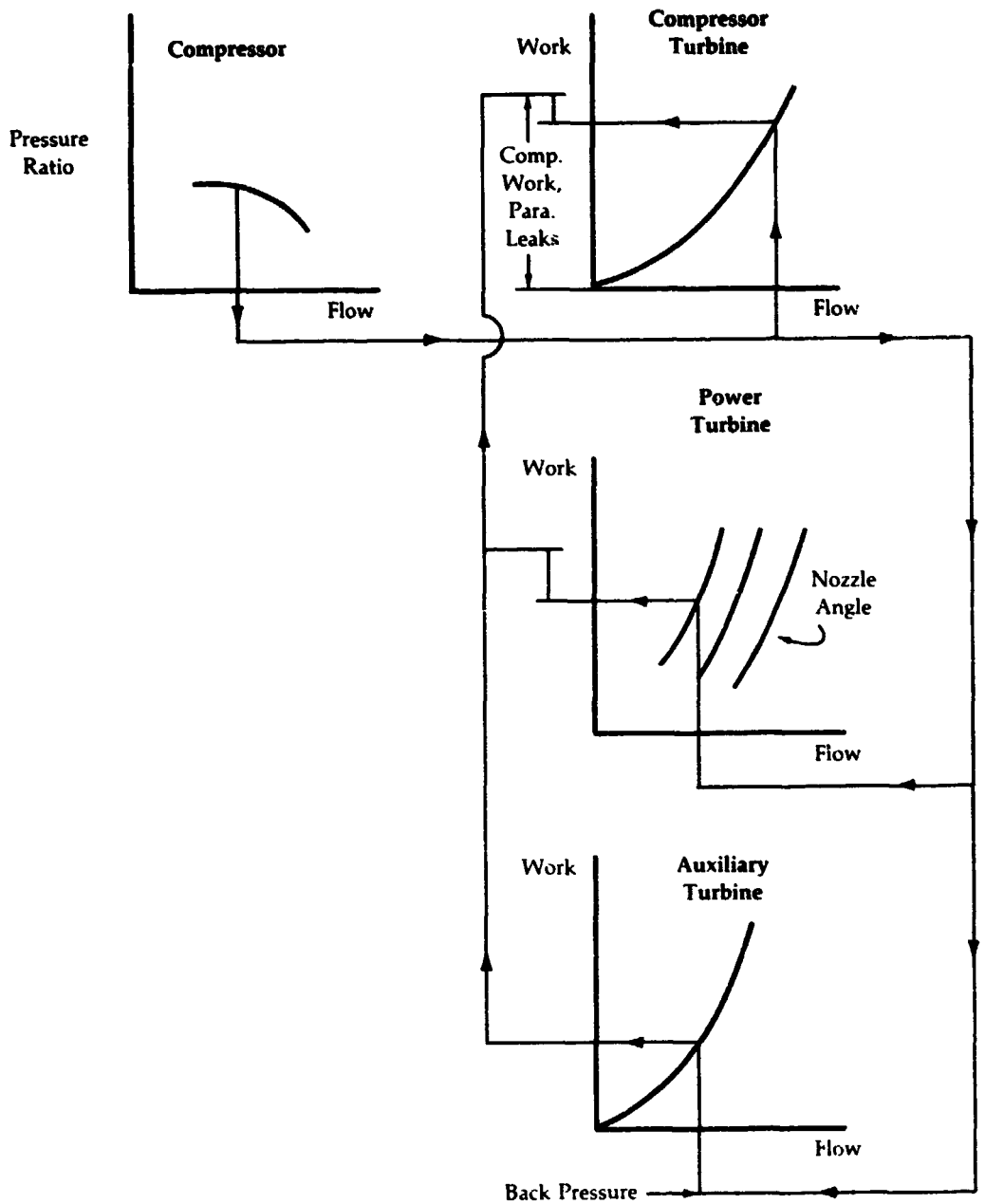

N.B.
Flow=Mass Flow
Arrows Indicate Calculation Path

Figure 56C

Design-Speed Torque and Power Characteristics, 2-Shaft vs. 3-Shaft

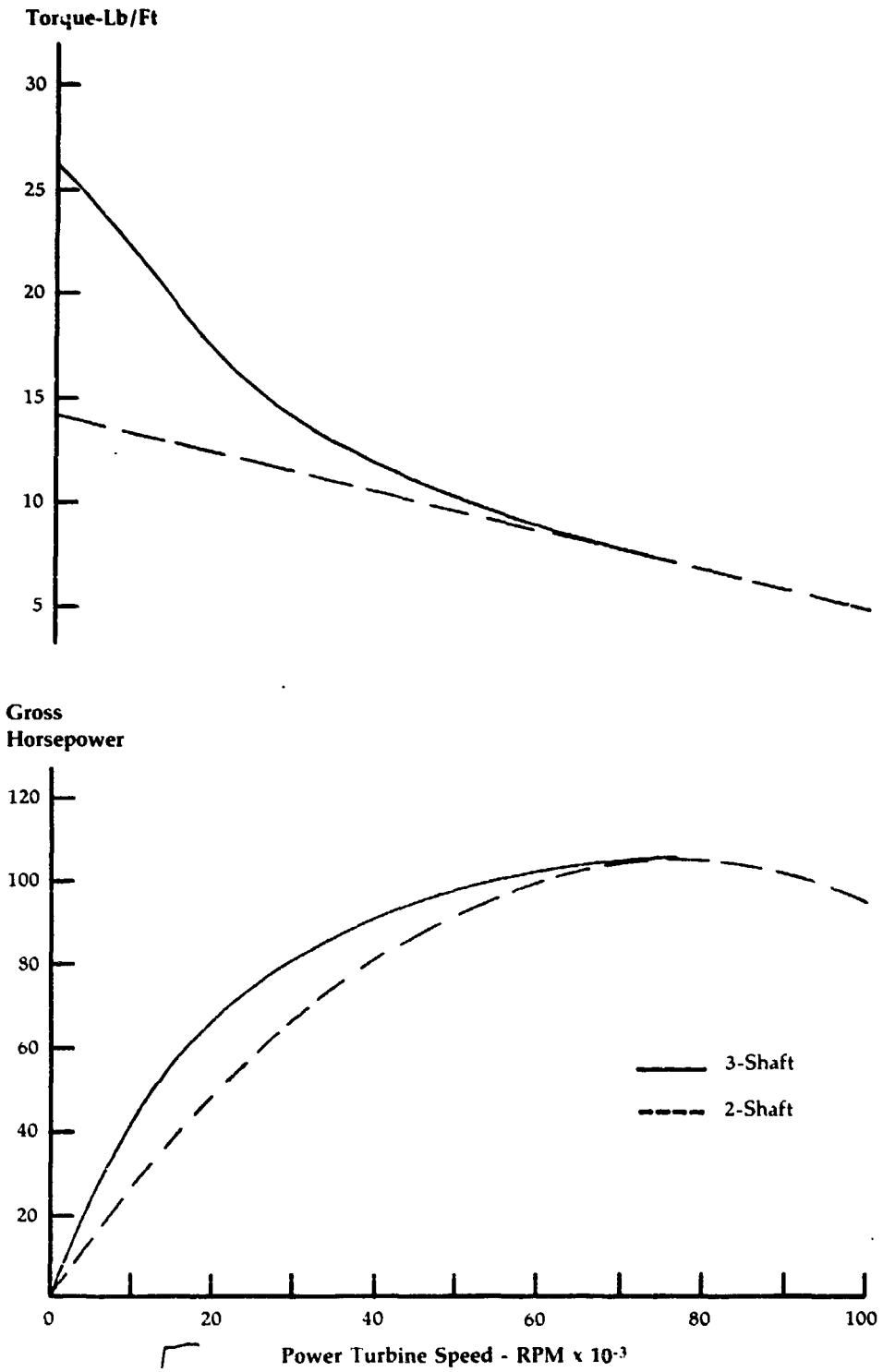

Figure 57

Torque and Efficiency of Power Turbine and Auxiliary Turbine for 3-Shaft Engine at Gas Generator Design Point

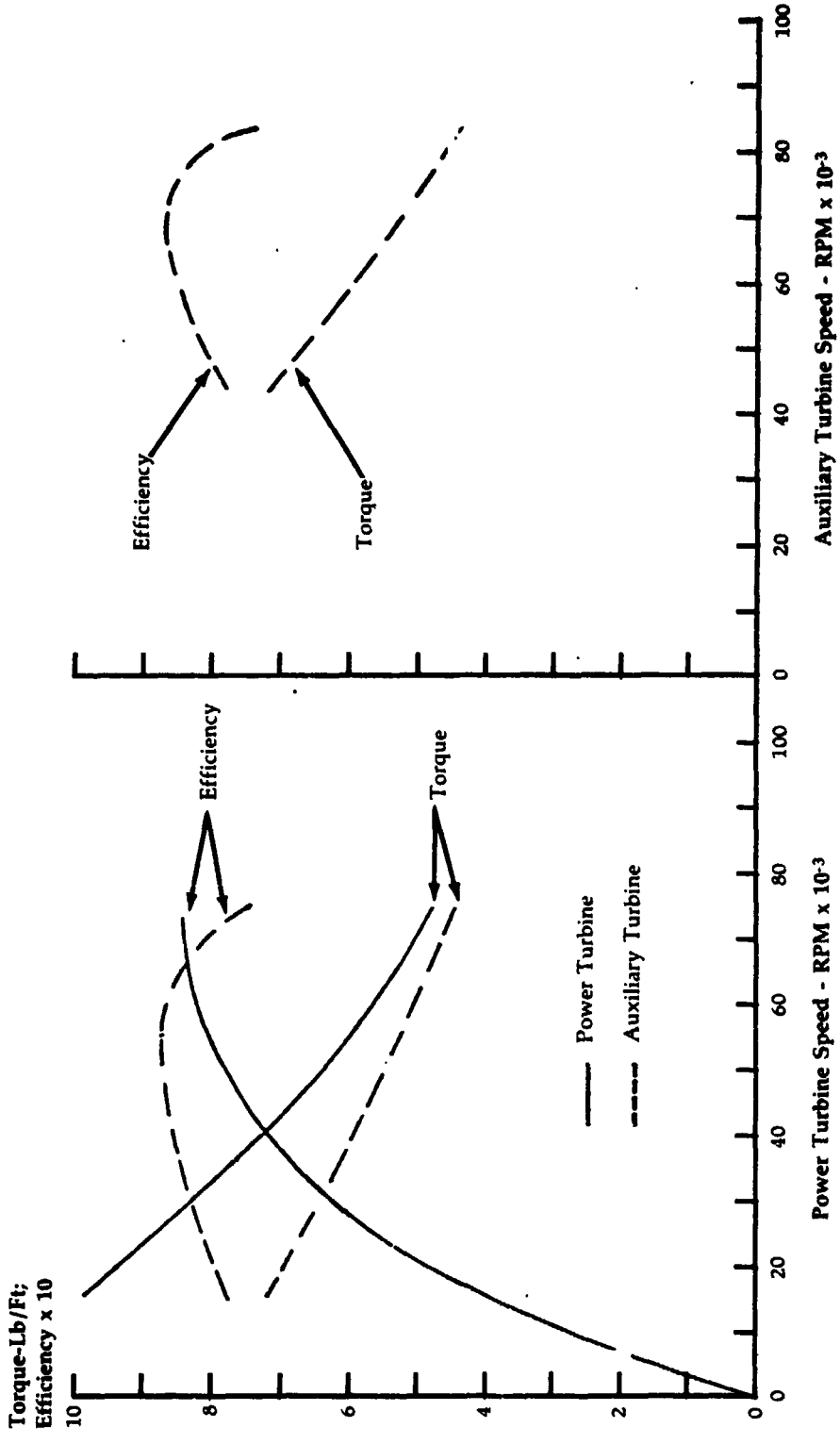

Figure 58

Torque and Efficiency Characteristics of Power Turbine and Auxiliary Turbine for 3-Shaft Engine at 50% Gas Generator Speed

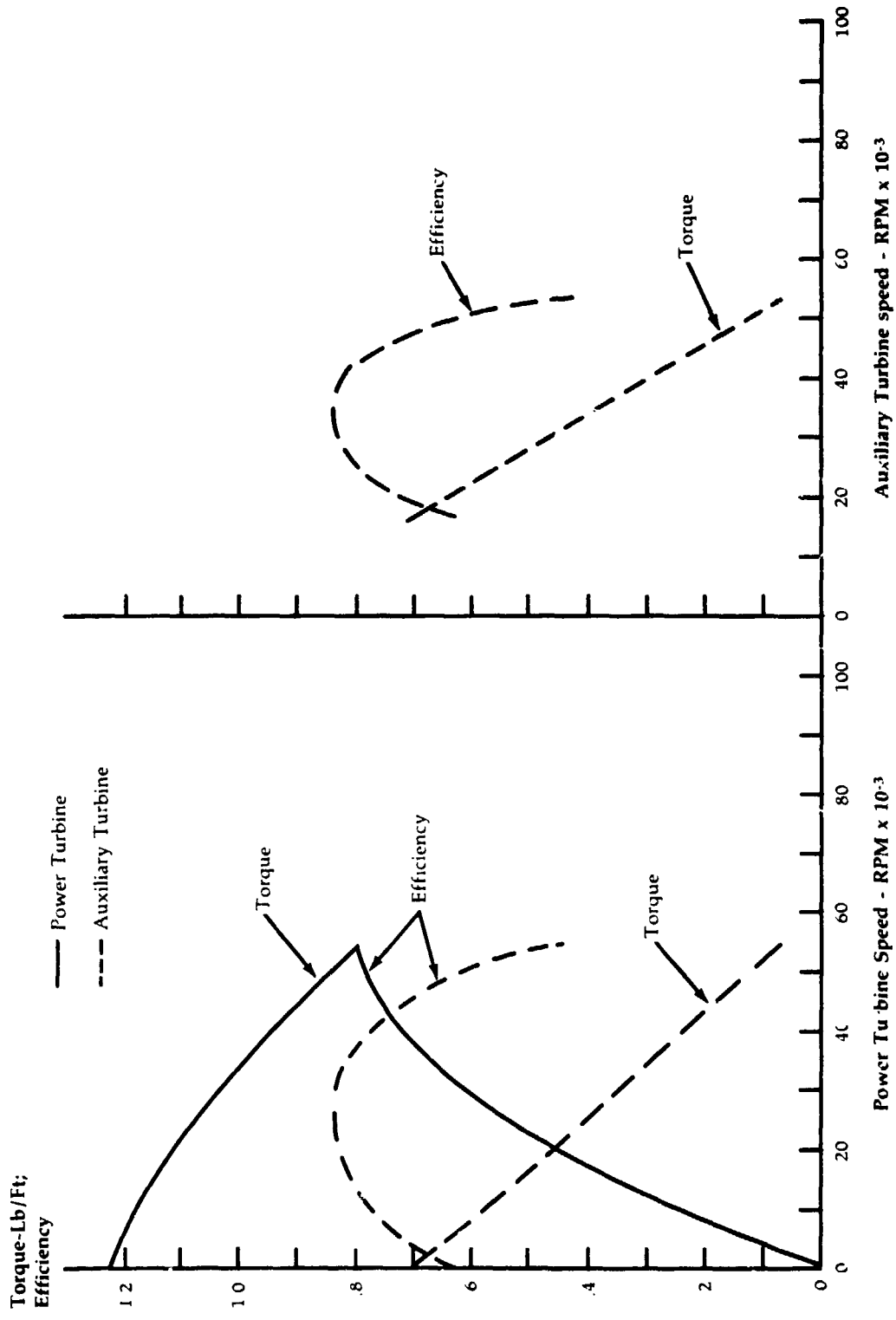

Figure 59

Variation of Engine Performance with Engine Configuration

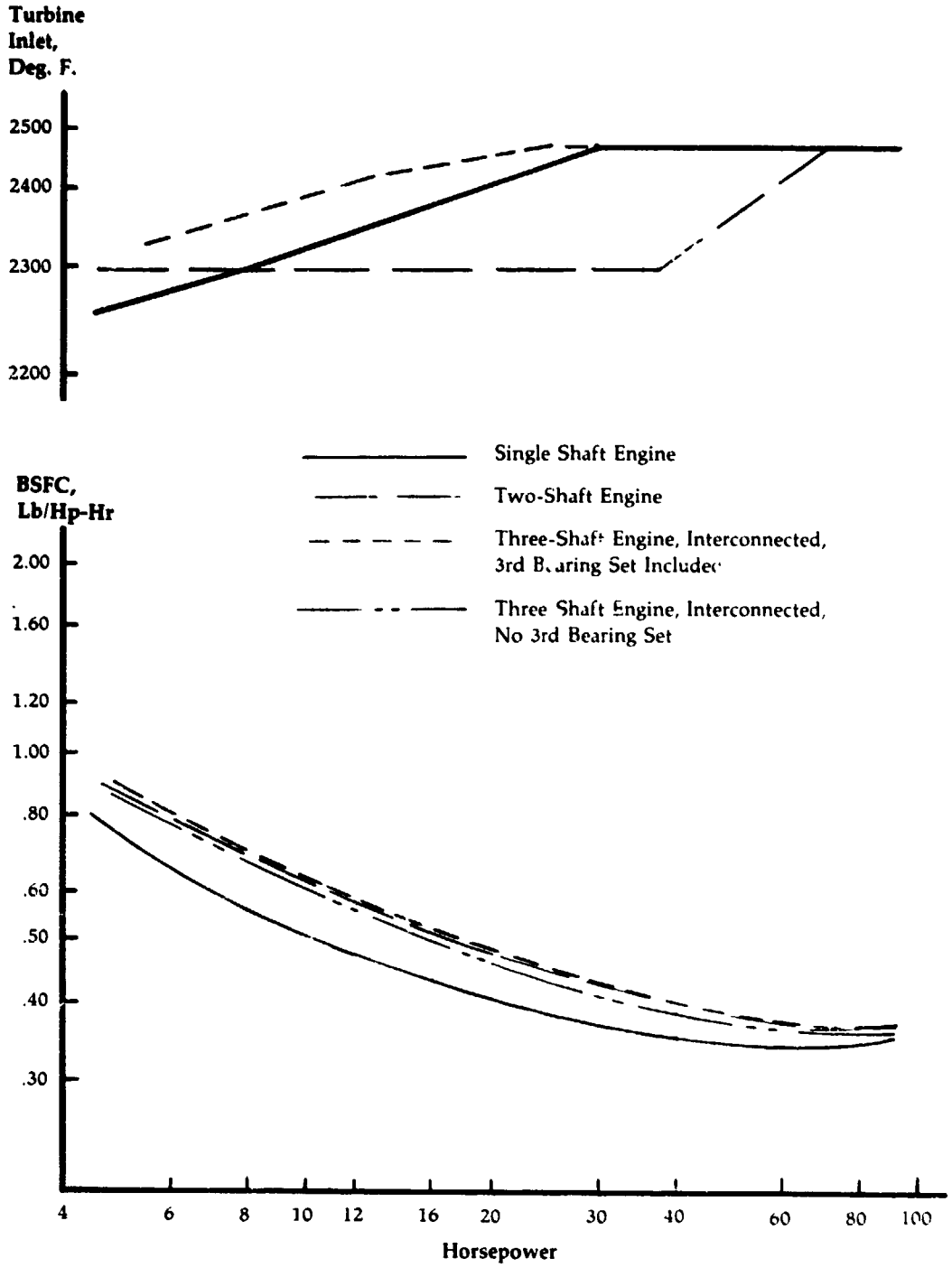

Figure 60

Component Matching Characteristics of Twin-Spool Gas Generator

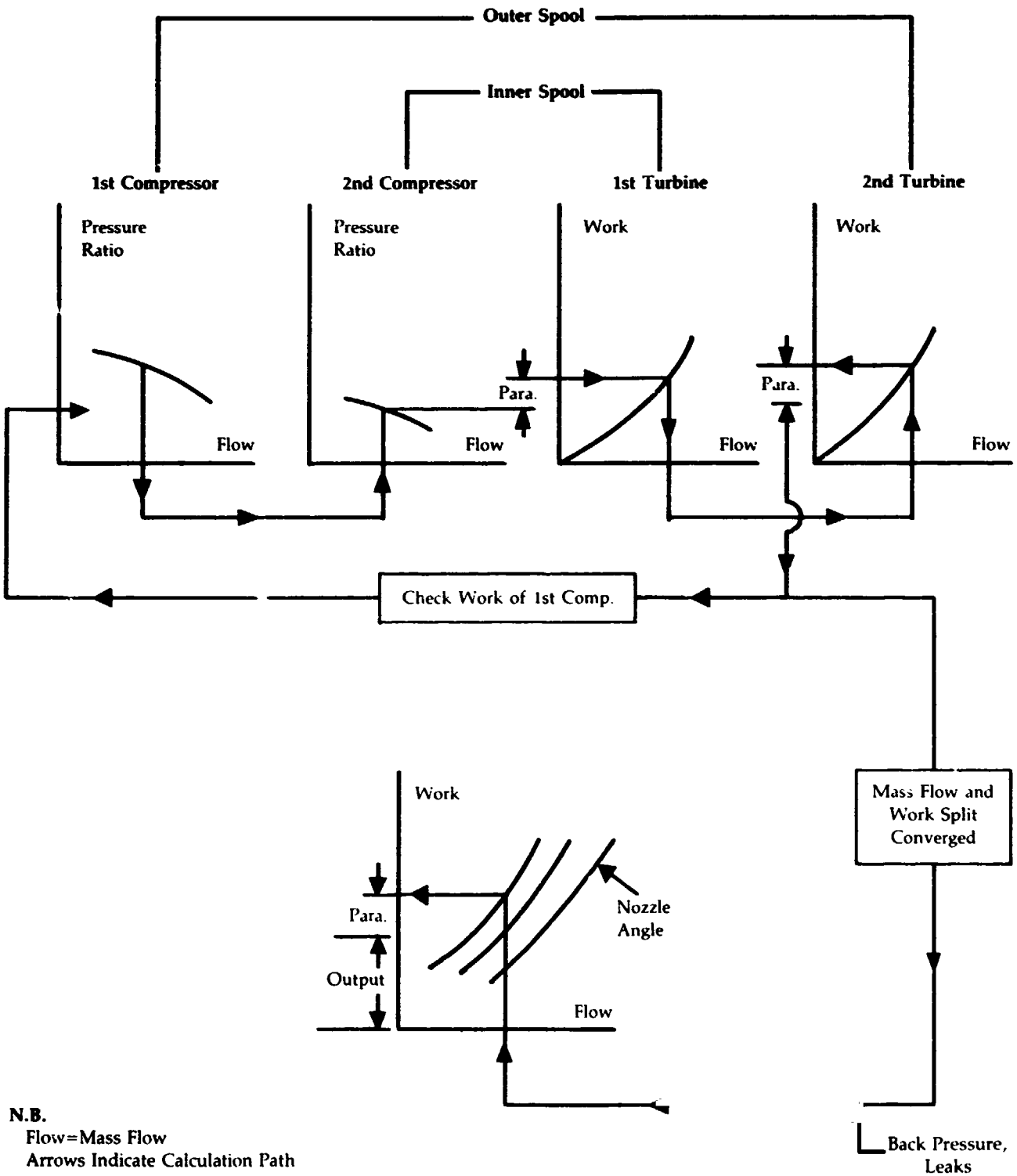

N.B.
Flow=Mass Flow
Arrows Indicate Calculation Path

Figure 61

Estimated Performance of 1st Stage Compressor for Twin-Spool Gas Generator

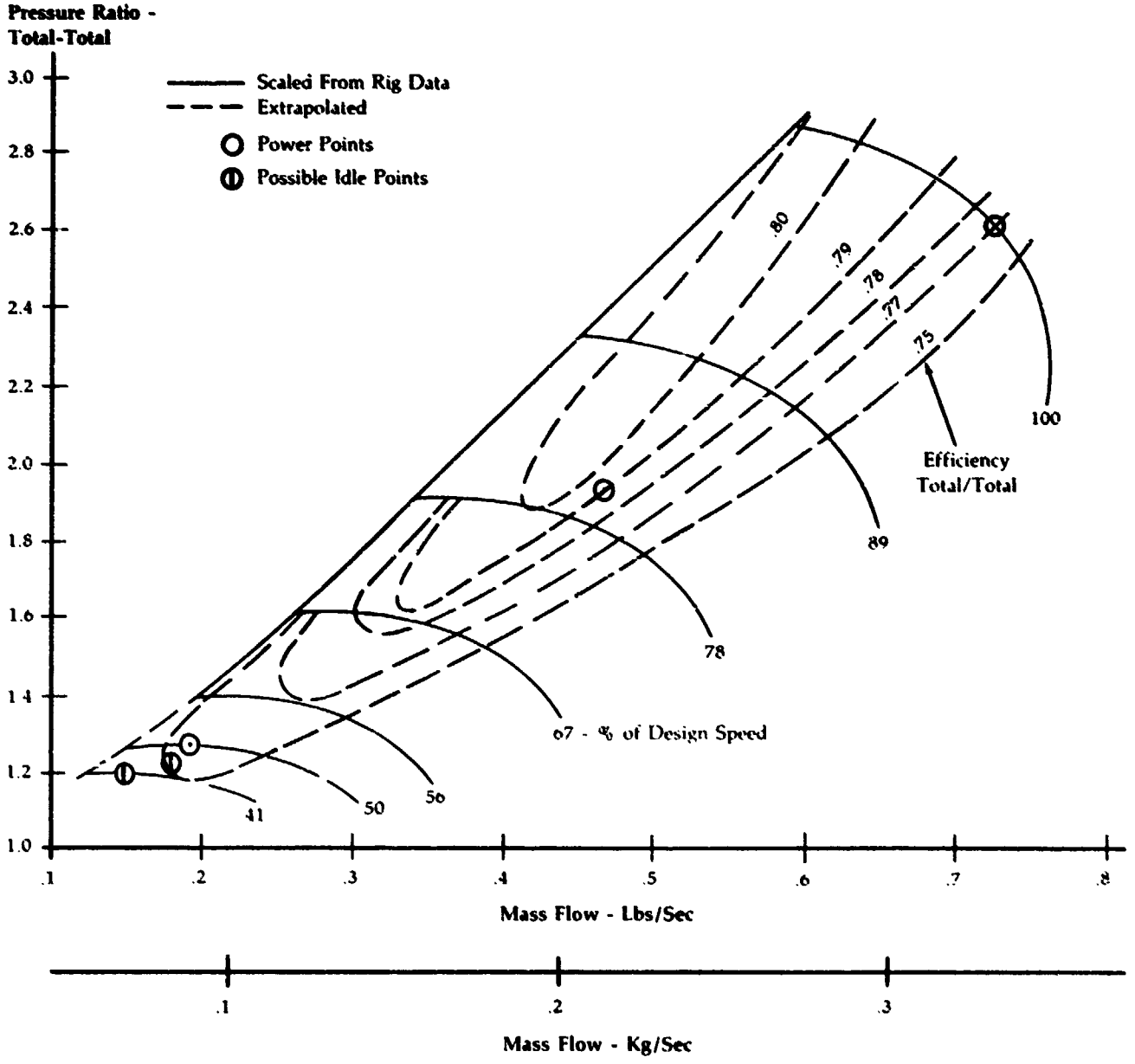

Figure 62A

Estimated Performance of 2nd Stage Compressor for Twin-Spool Gas Generator

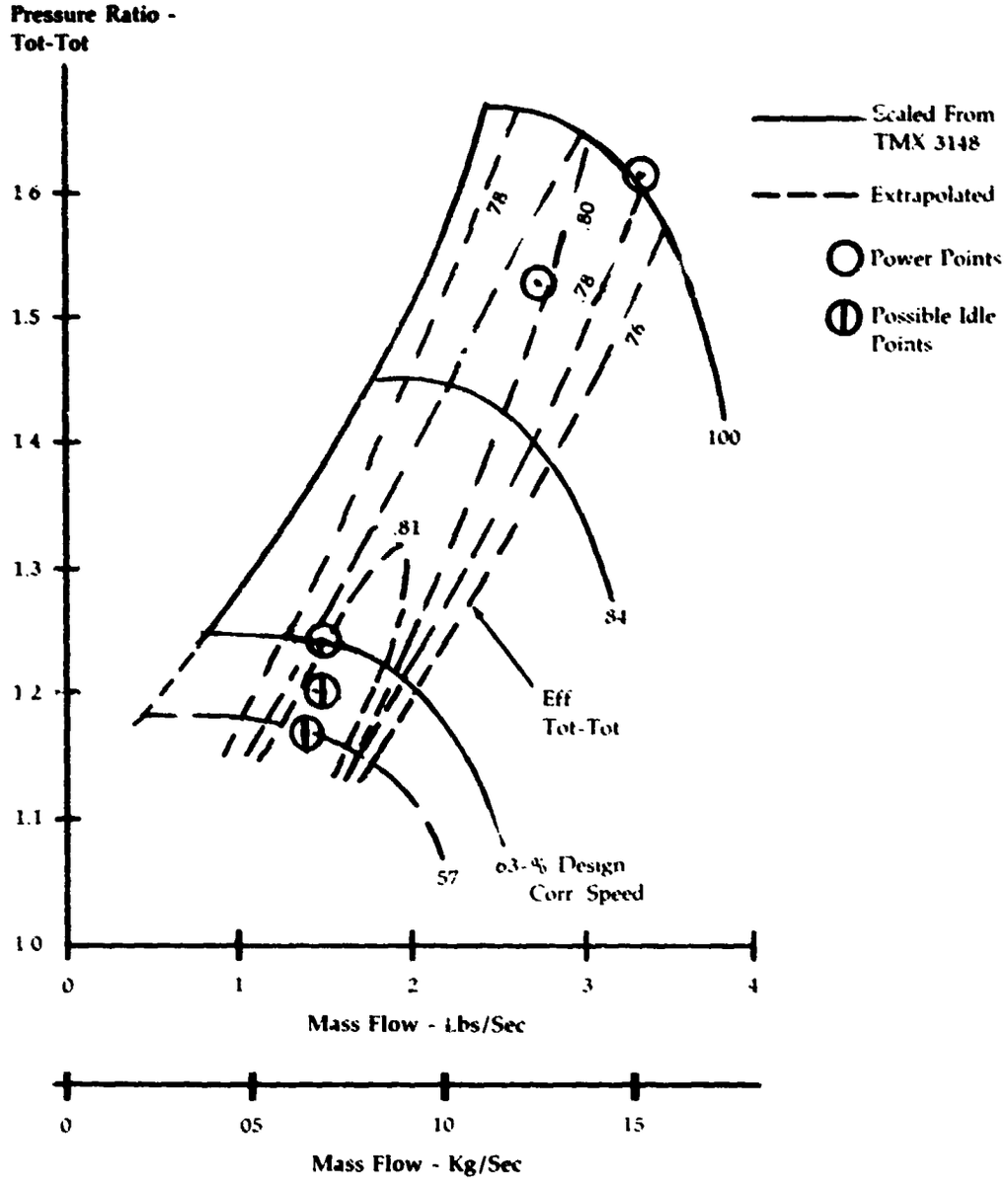

Figure 62B

Twin Spool, Free Power Turbine Variation of Mass Flow and Efficiency with Outer Spool Speed

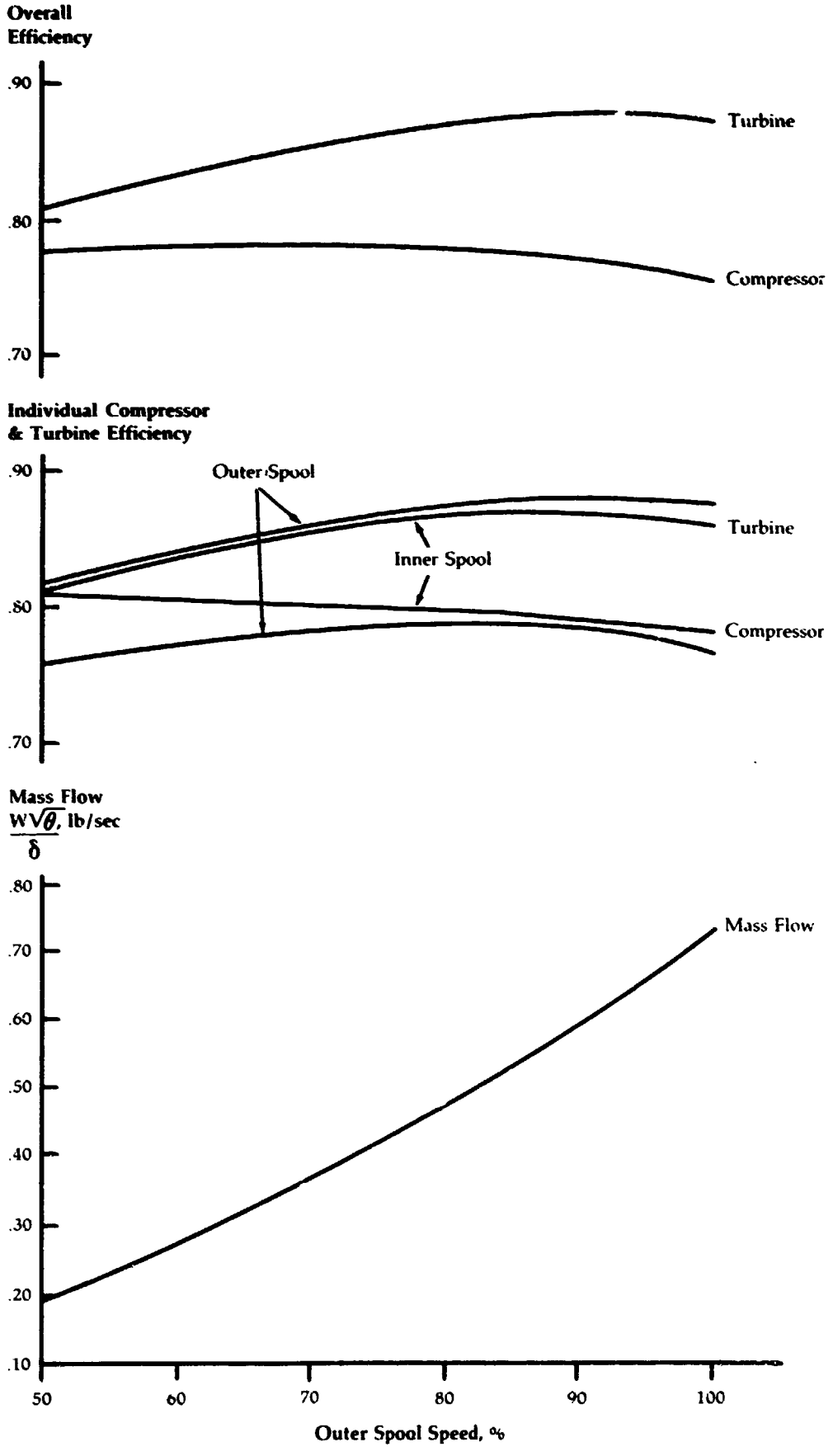

Figure 63

Twin-Spool, Free Power Turbine Variaton of Inner Spool Speed & Compressor Pressure Ratio with Outer Spool Speed

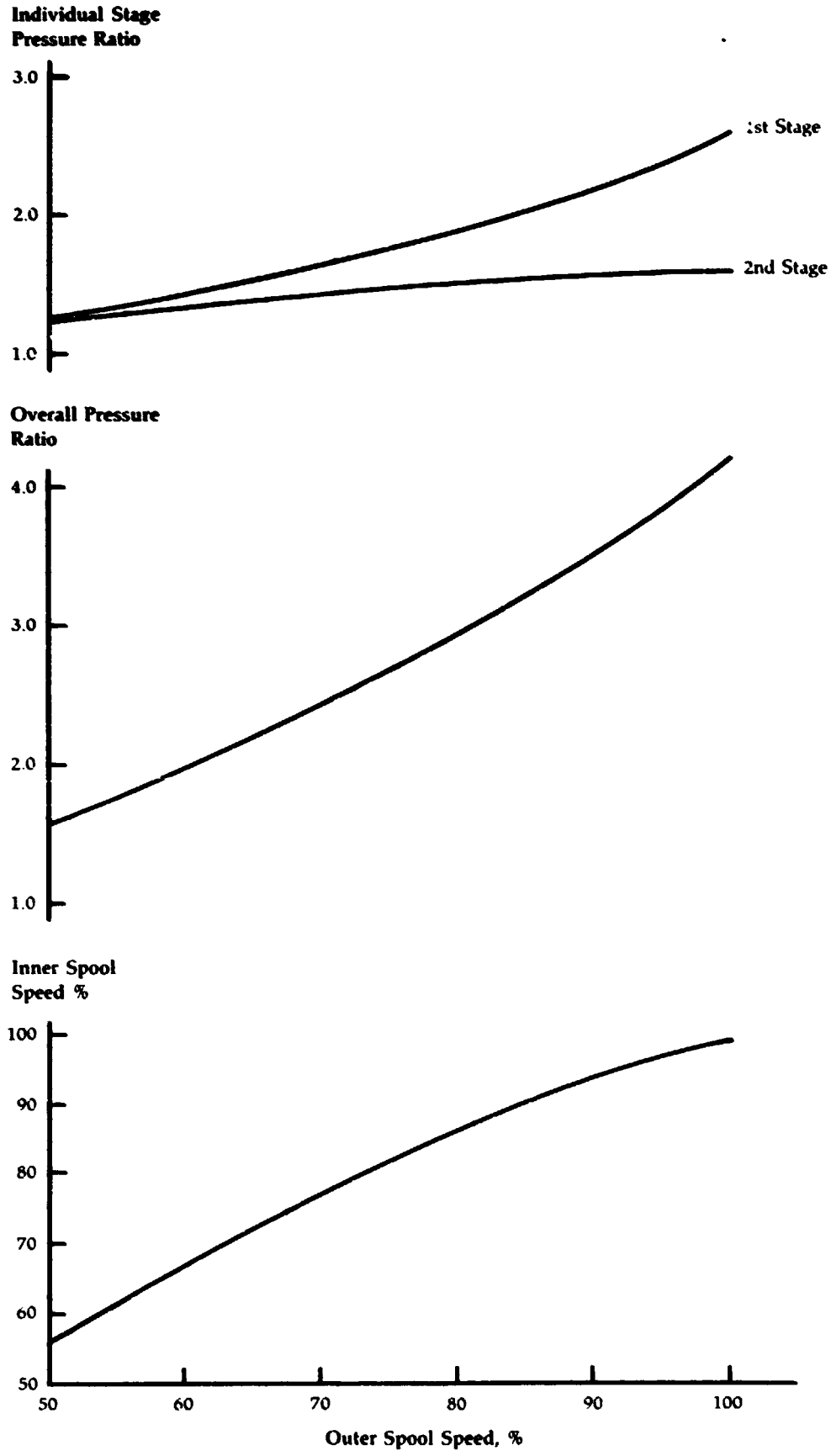

Figure 64

Twin Spool, Free Power Turbine 50% Speed & Idle Speed Power

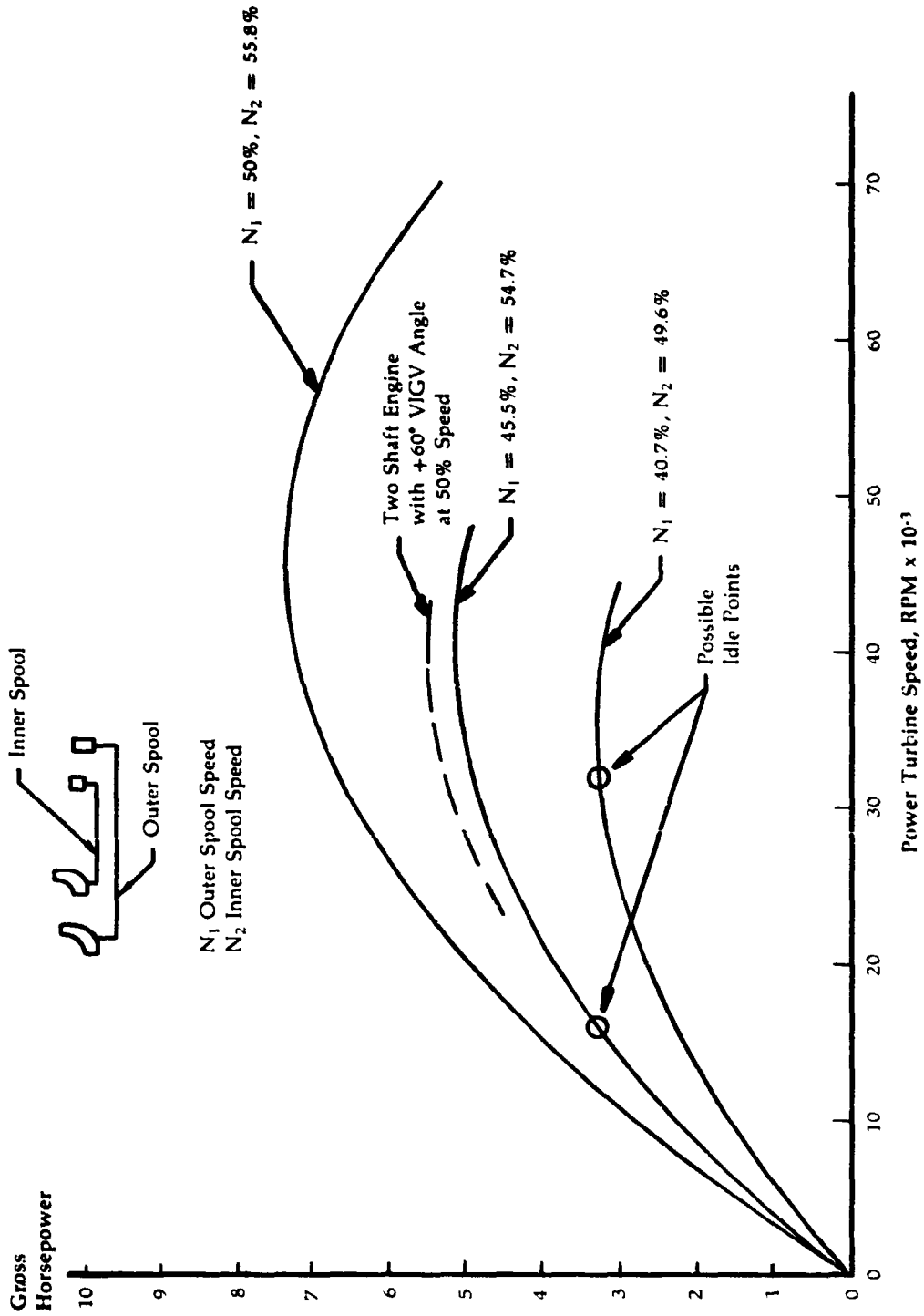

Figure 65

Comparison of Engine Performance Estimates for Single Spool and Twin-Spool Gas Generators for Free Power Turbine Engine Configuration

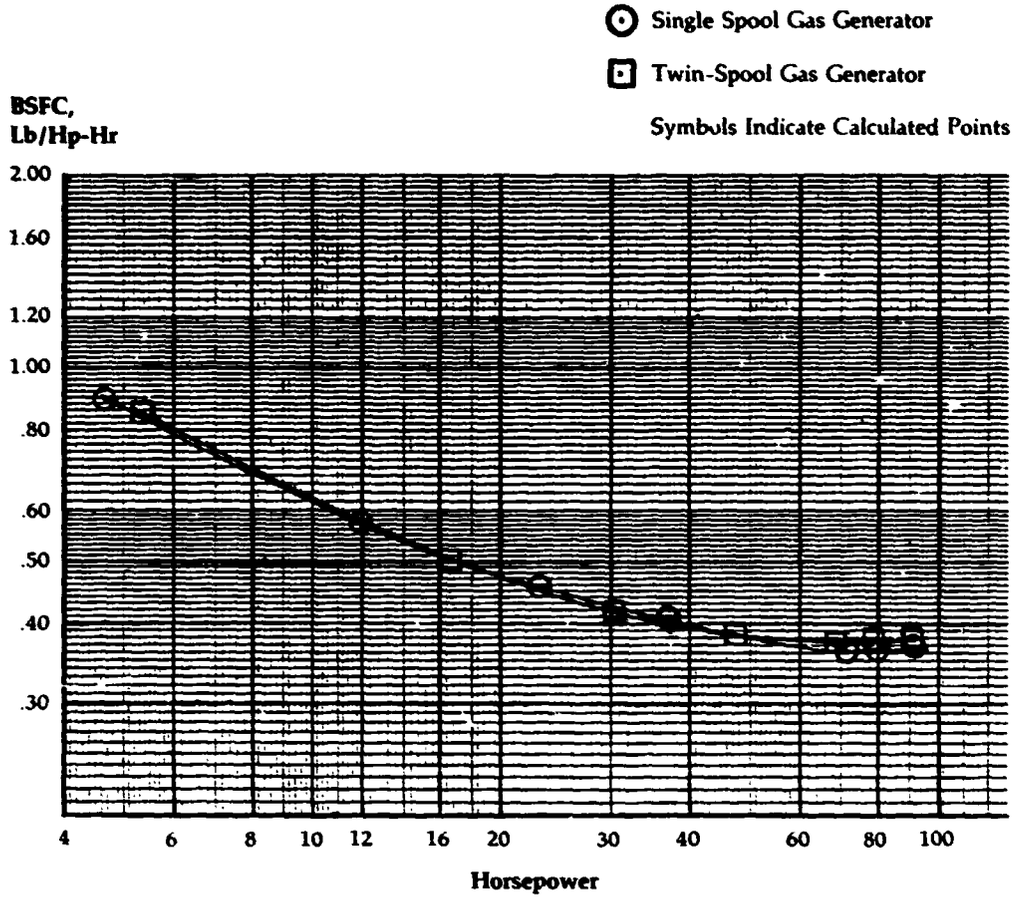

Figure 66

Turbine Wheel
Thermal Gradients

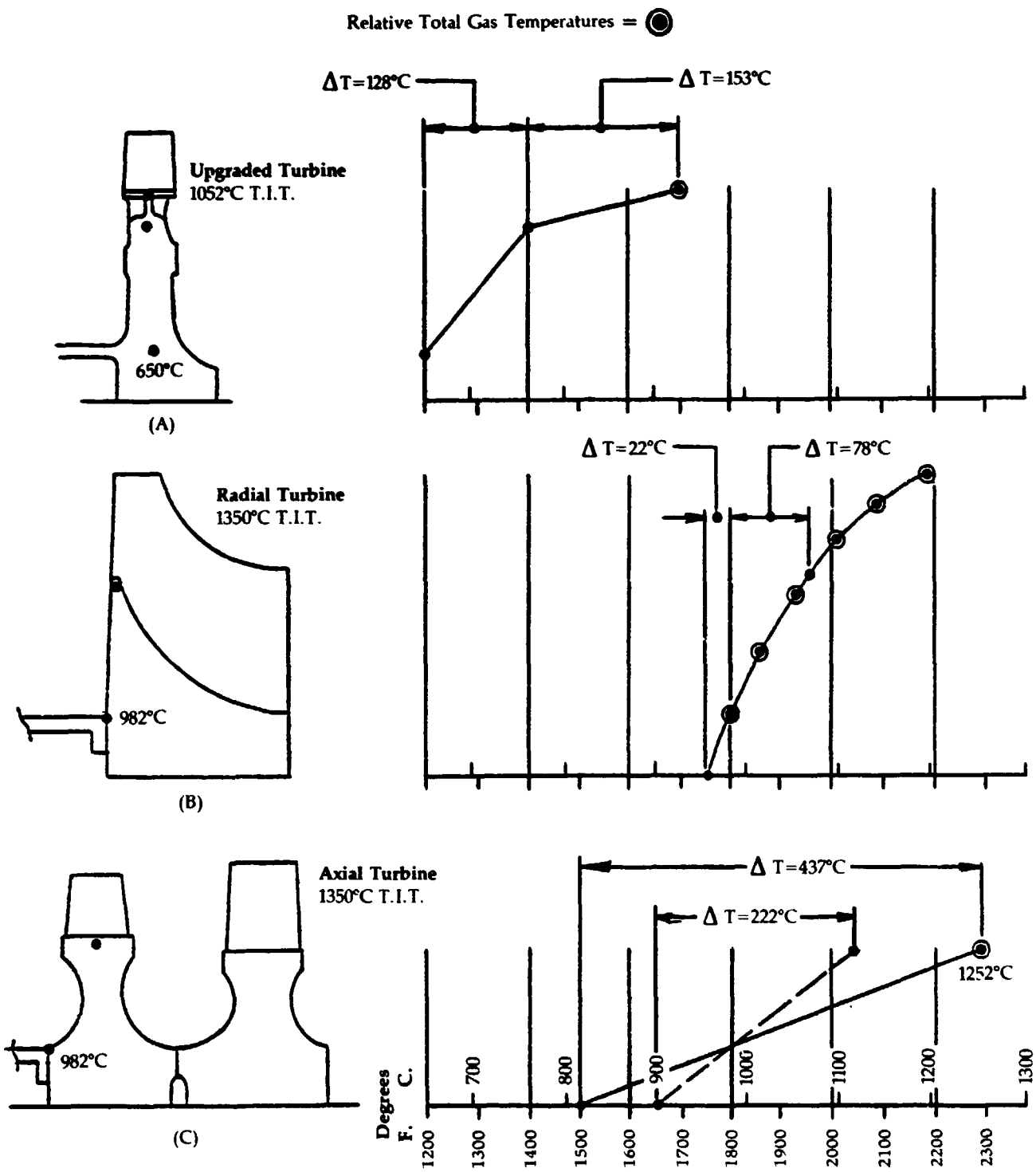

Figure 67

Turbine Wheel Stress - Alpha Silicon Carbide

Single Shaft - 4:1 Radial
103,000 RPM
1350°C T.I.T.

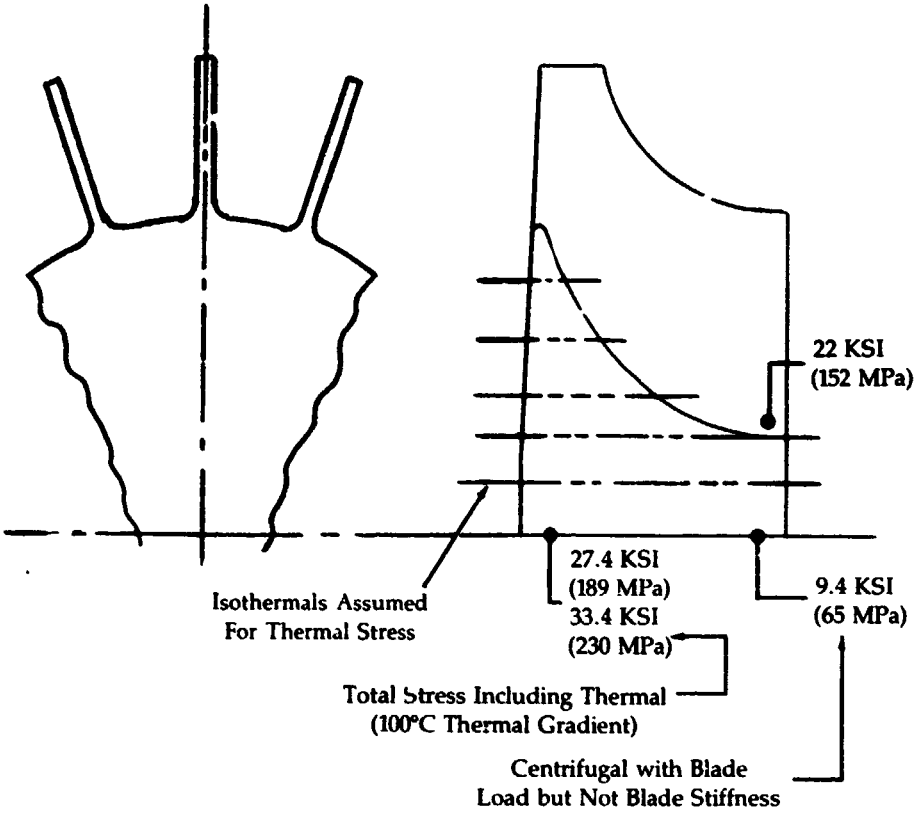

(A)

Single Shaft - 2 Stage Axial
101,000 RPM
1350°C T.I.T.

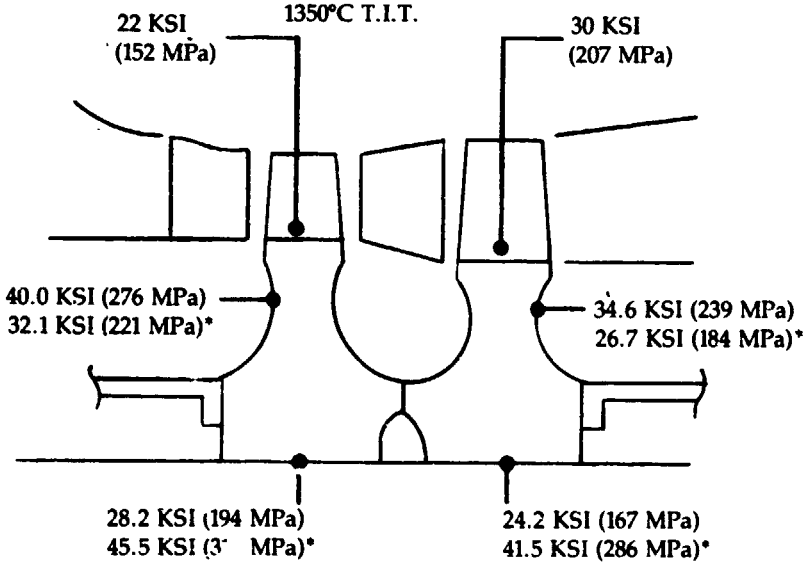

*Total Stress Including Thermal
(222°C Disc Gradient)

(B)

Figure 68

Turbine Wheel Stress
1150°C Metal
Program Engine

Single Shaft - 4:1 Radial
94,000 RPM
1150°C T.I.T.

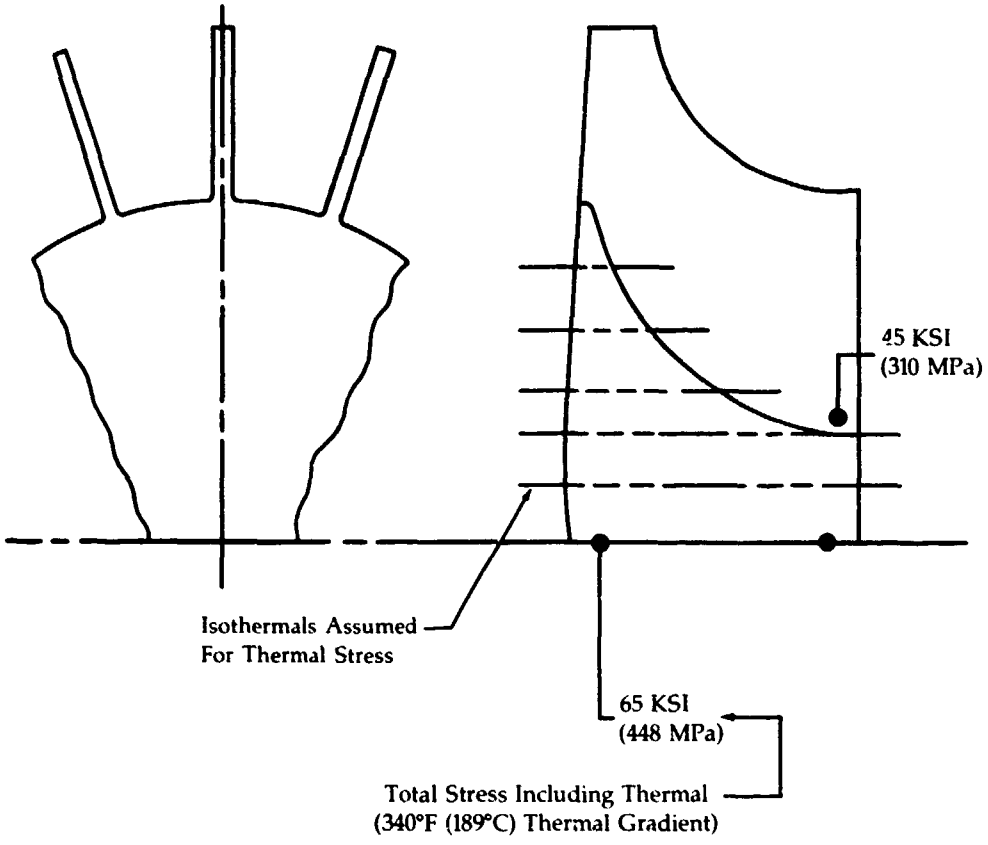

Figure 69

High Temperature Material Assumptions Turbine Wheel

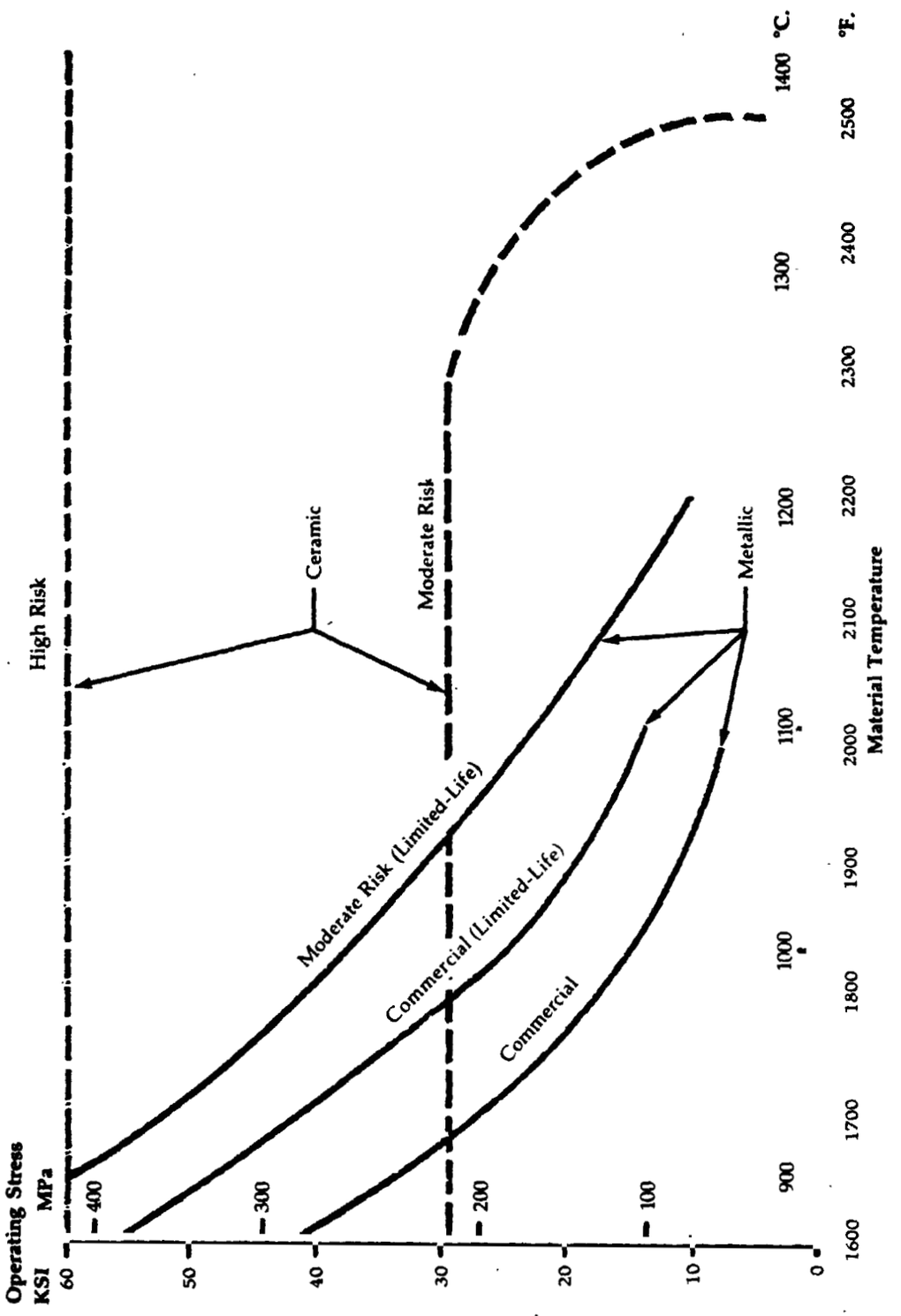

Figure 70

Cost Effective
Upgraded Engine

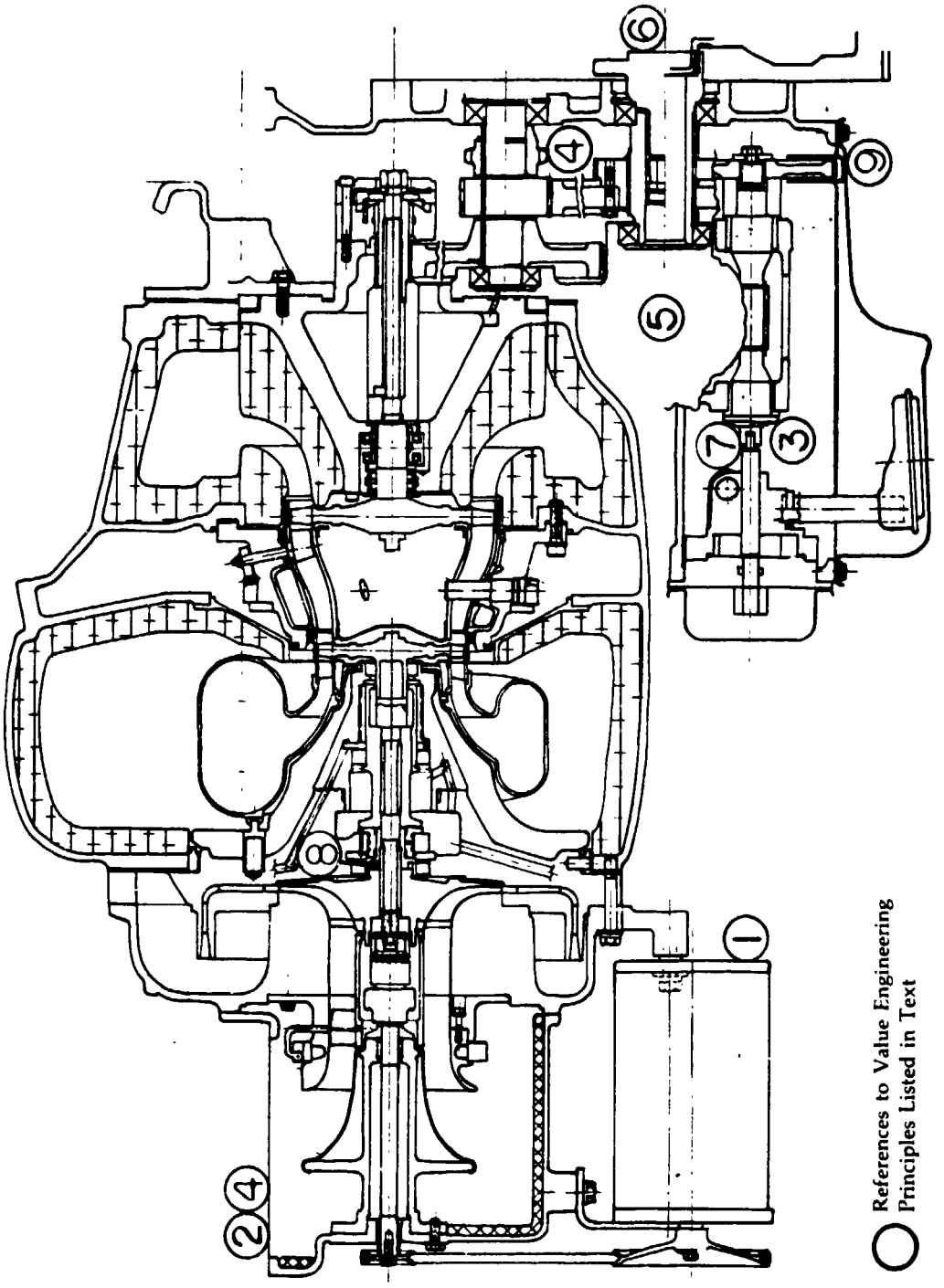

Figure 71

Selected Engine Preliminary Design

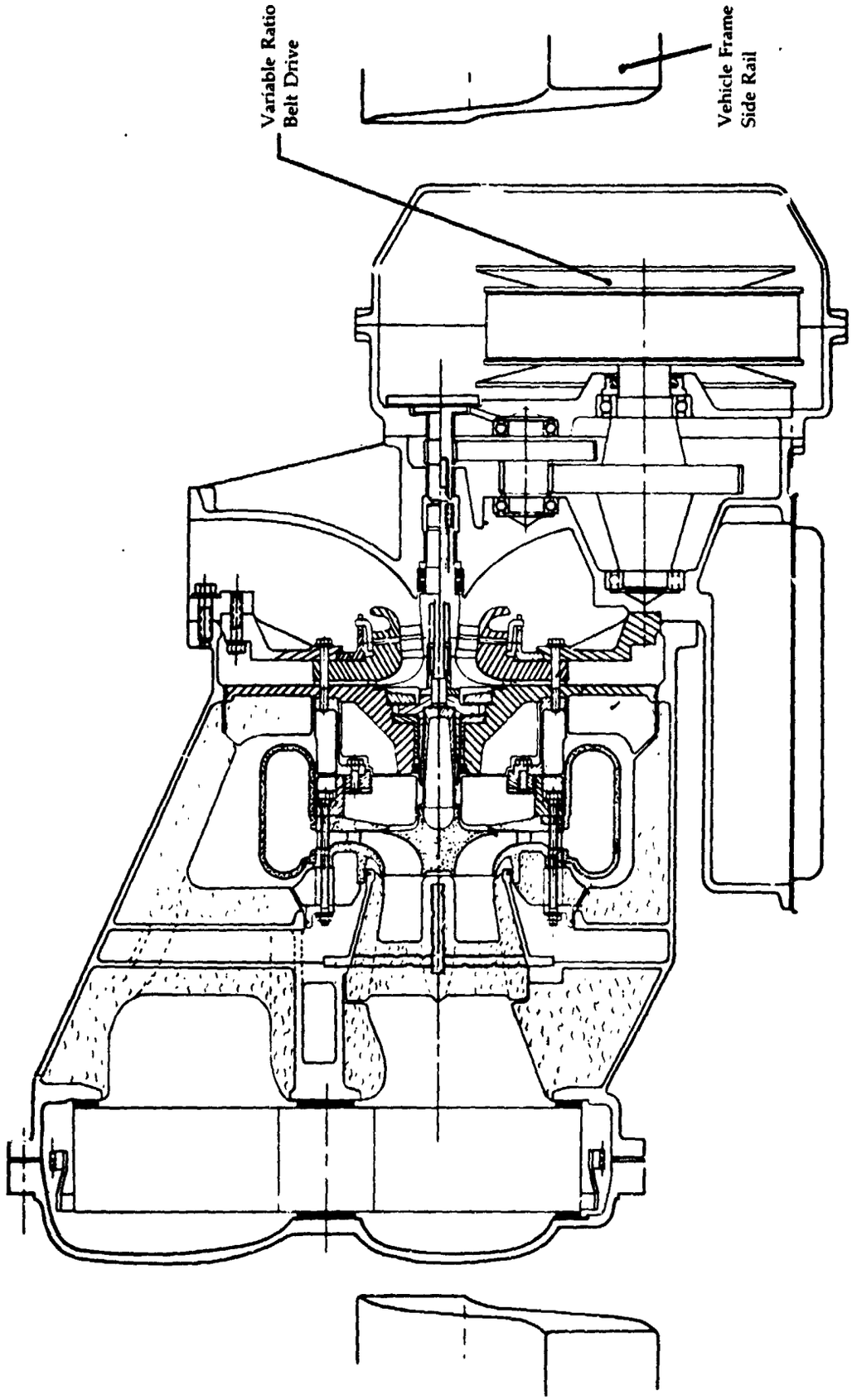

Figure 72

Single Shaft Engine

Front View in Vehicle Installation

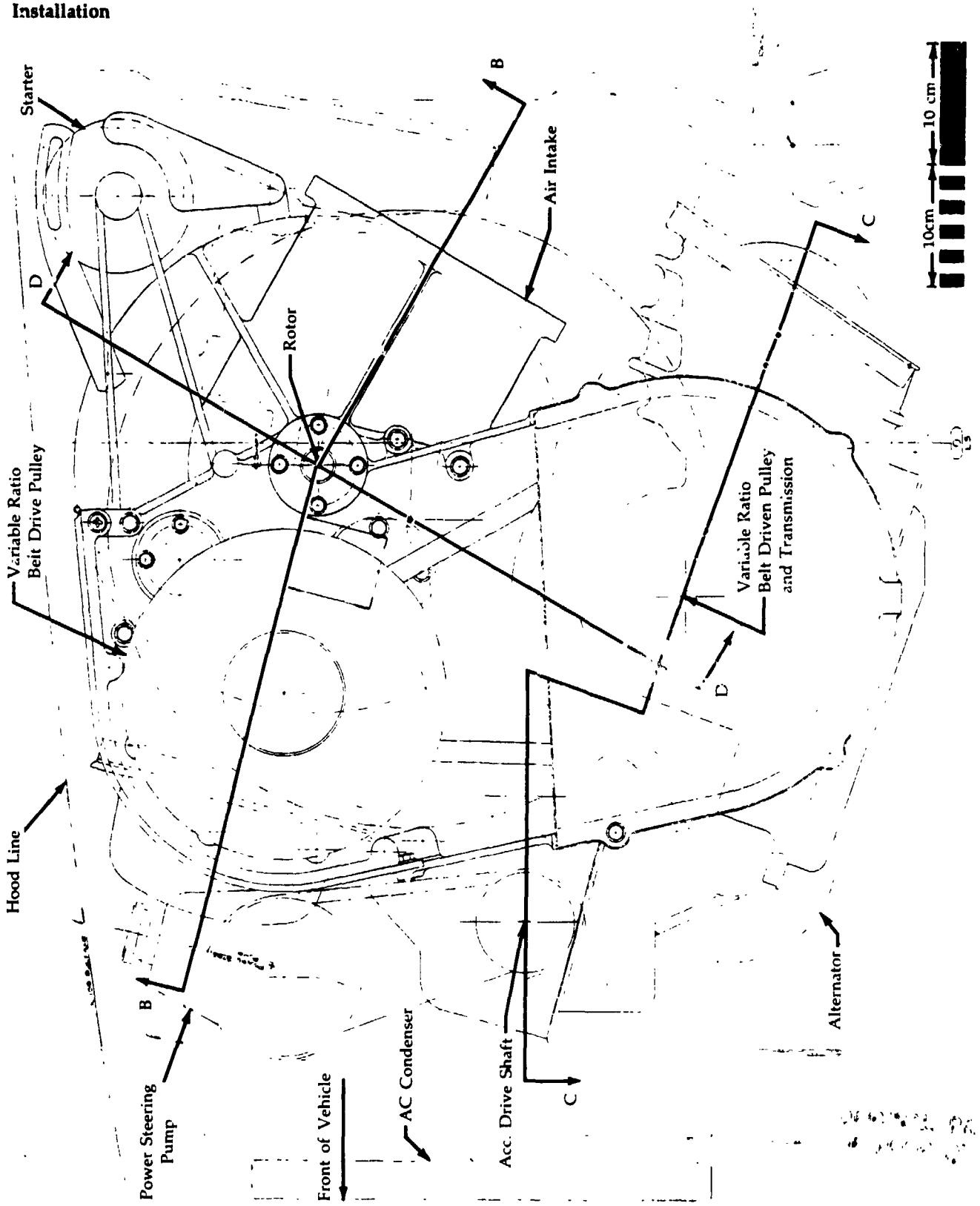

Figure 73A

Single Shaft Engine

Side View in Vehicle Installation

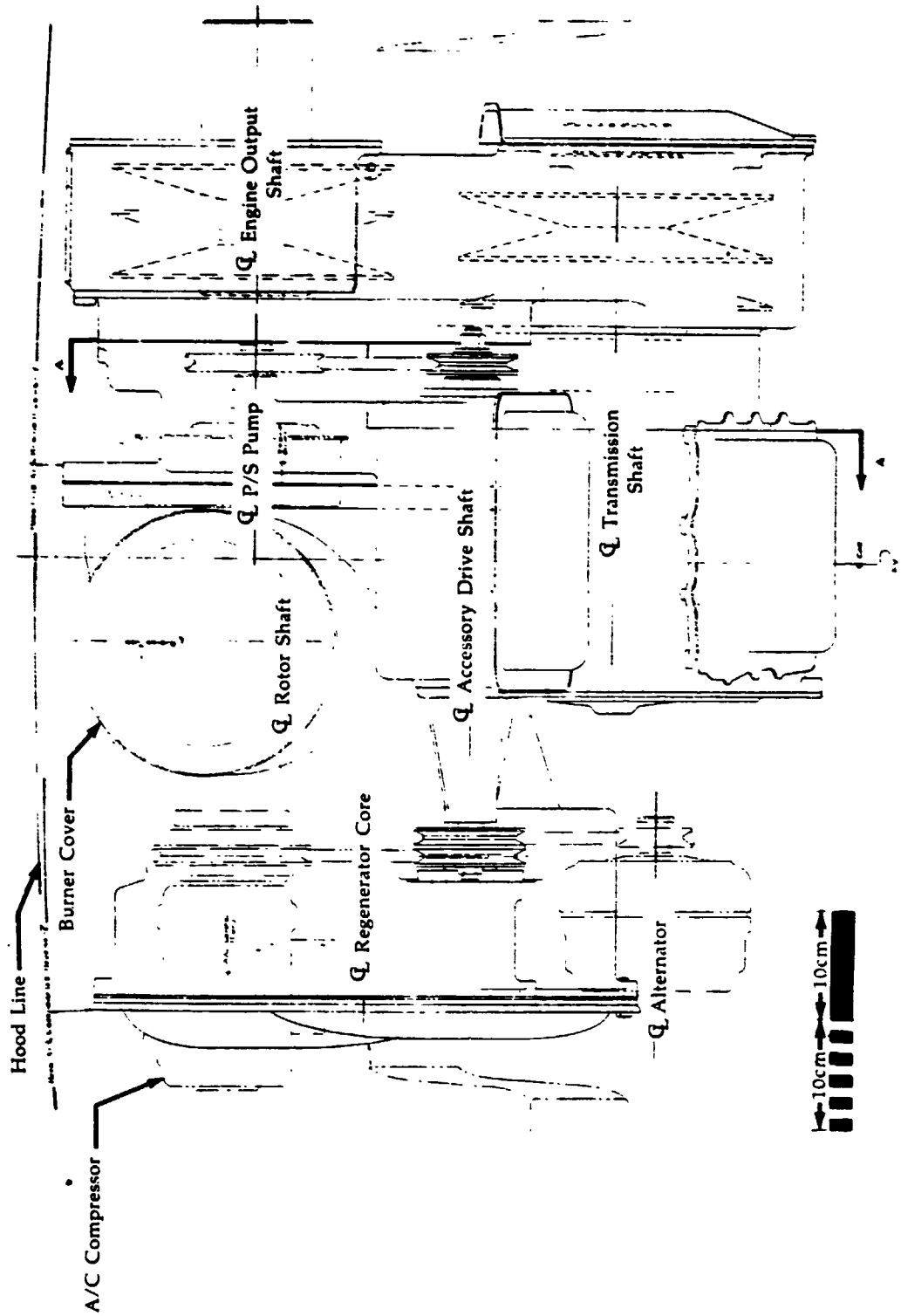

P/S = Power Steering
A/C = Air Conditioning
℄ = Centerline

Figure 73B

Single Shaft Engine
Cutaway View

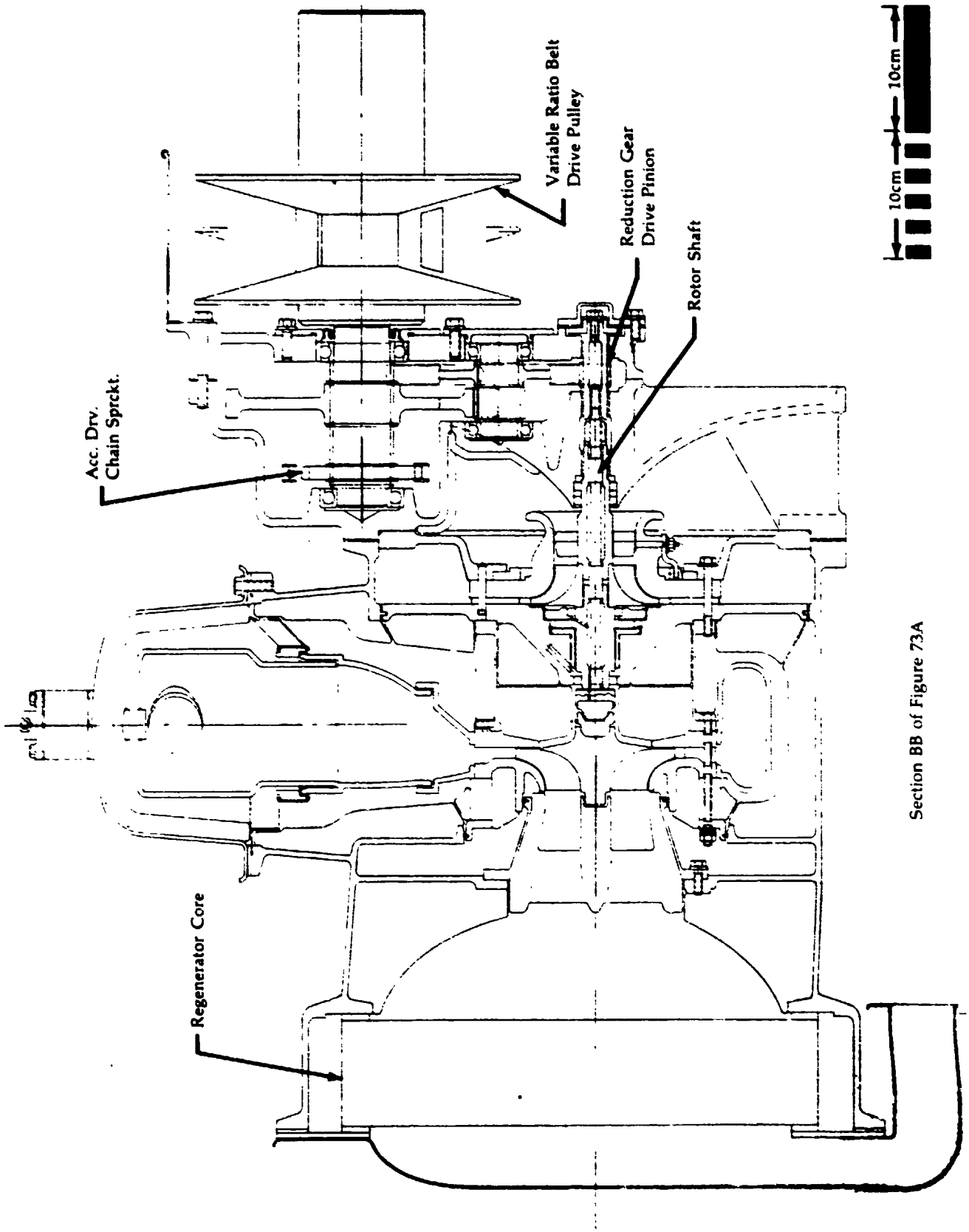

Figure 73C

Single Shaft Engine with Front-Mounted Variable Ratio Belt Drive Installed in Pickup (Side View)

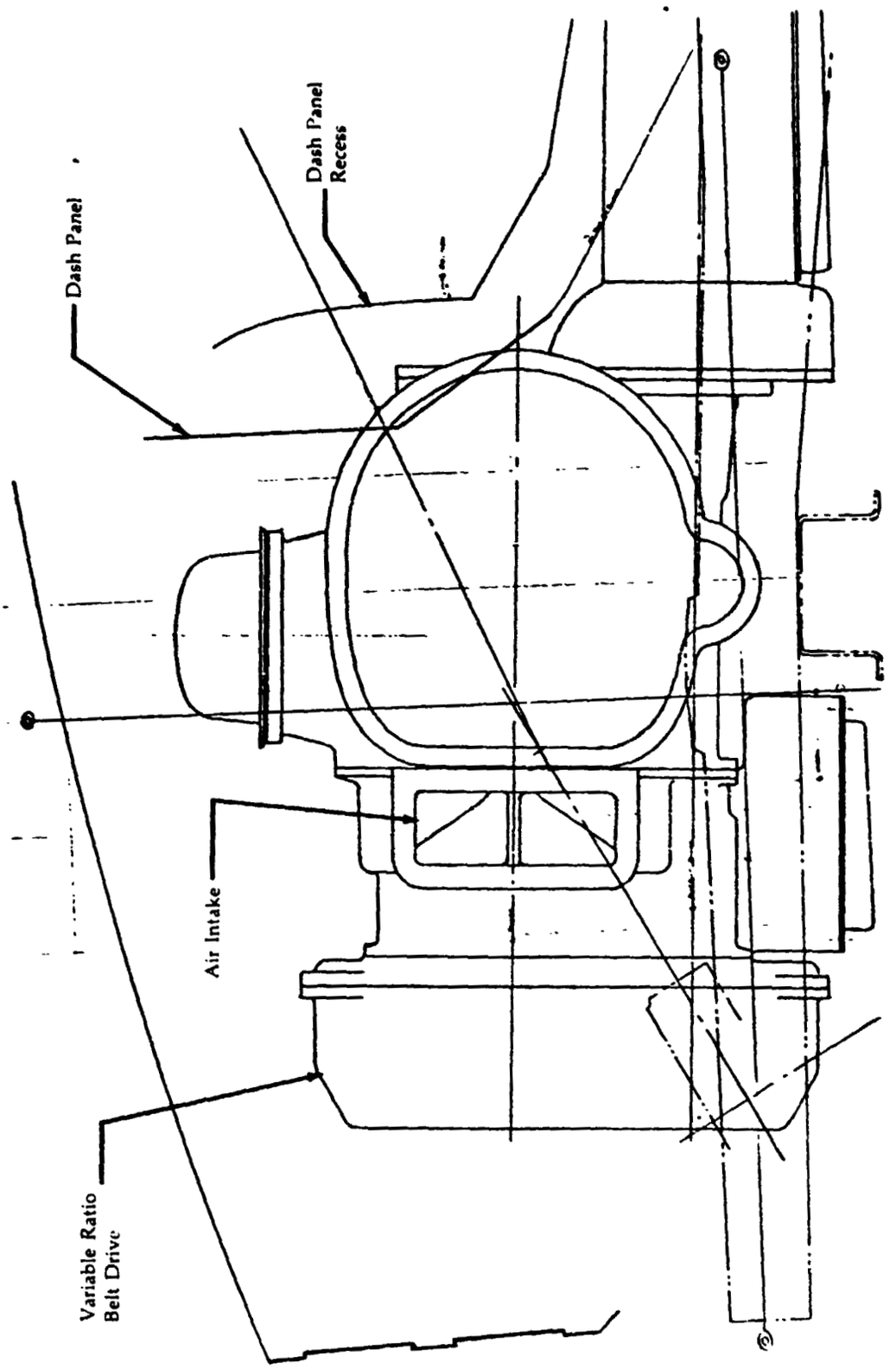

Figure 74A

Single Shaft Engine with Front-Mounted Variable Ratio Belt Drive Installed in Pickup (Front View)

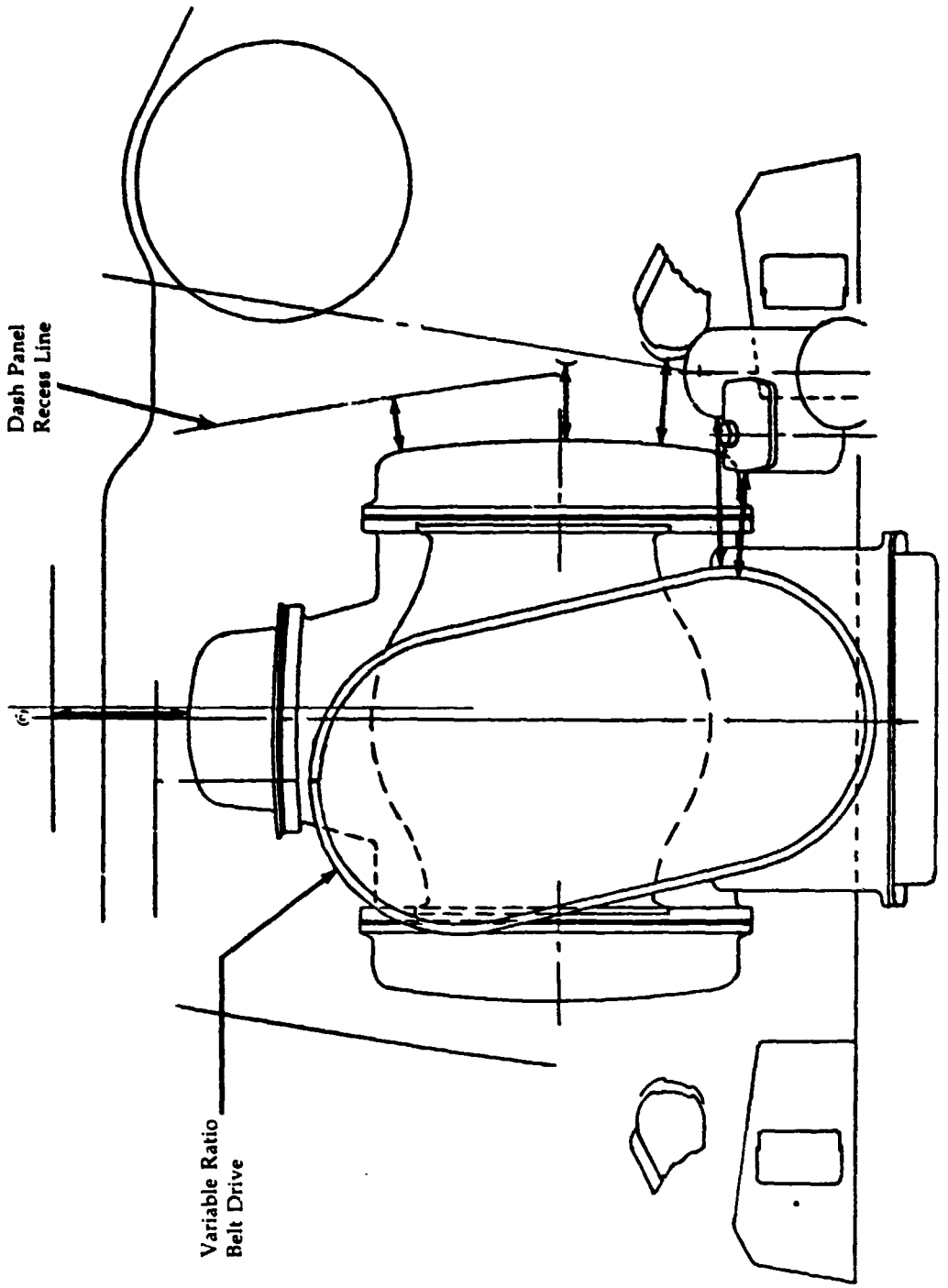

Figure 74B

Single Shaft Engine with Front-Mount Variable Ratio Belt Drive

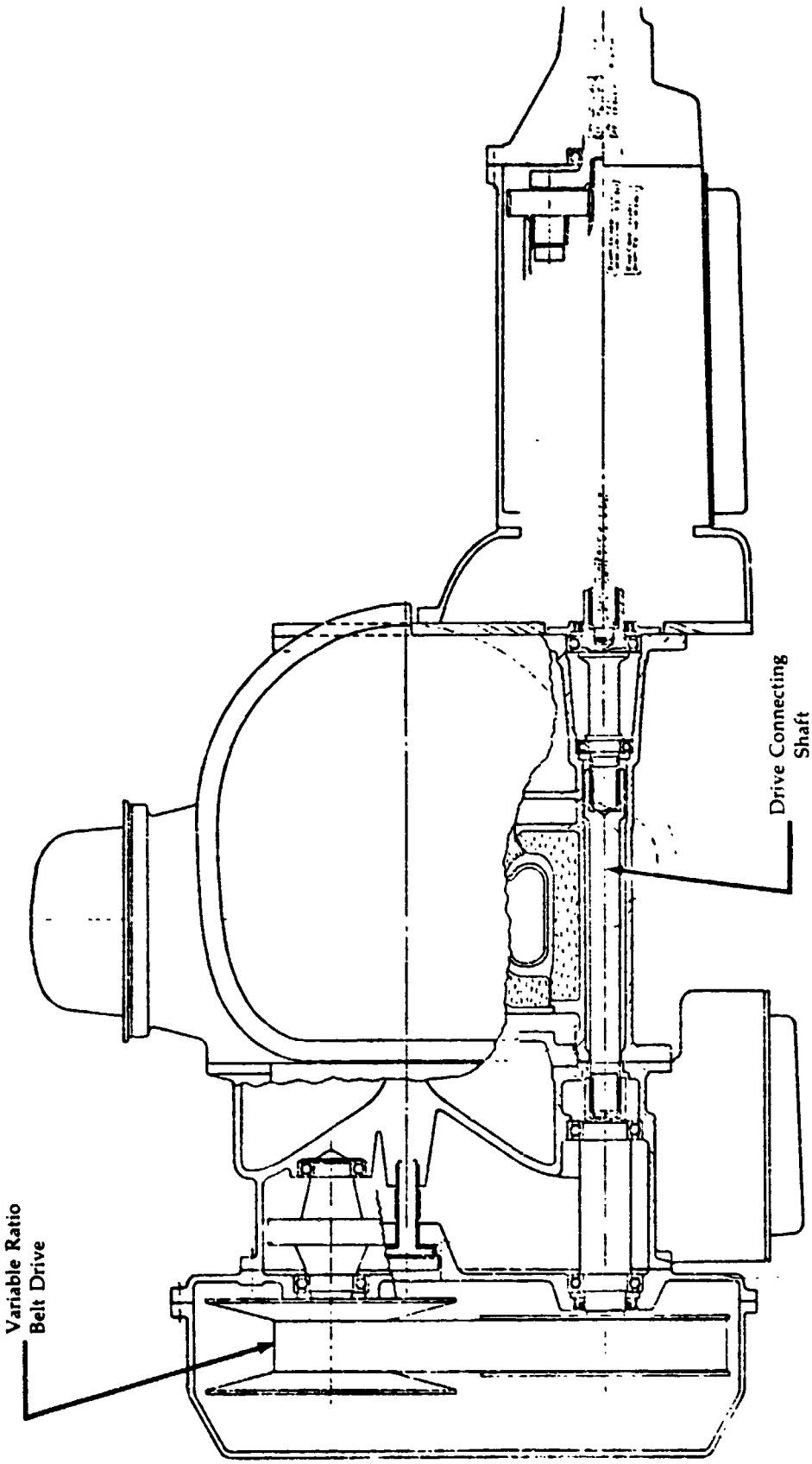

Figure 75

Vehicle Performance

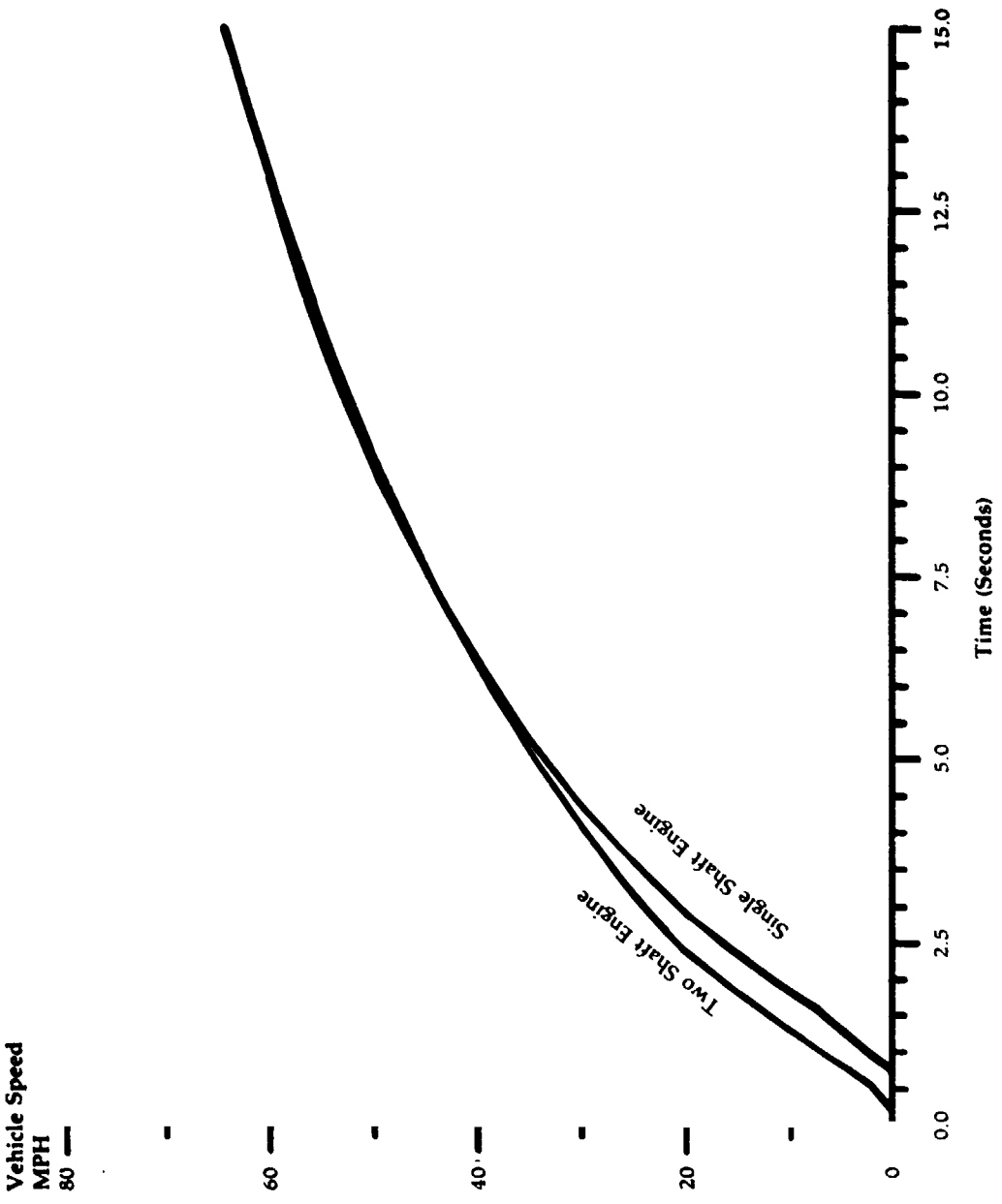

Figure 76

Vehicle Performance

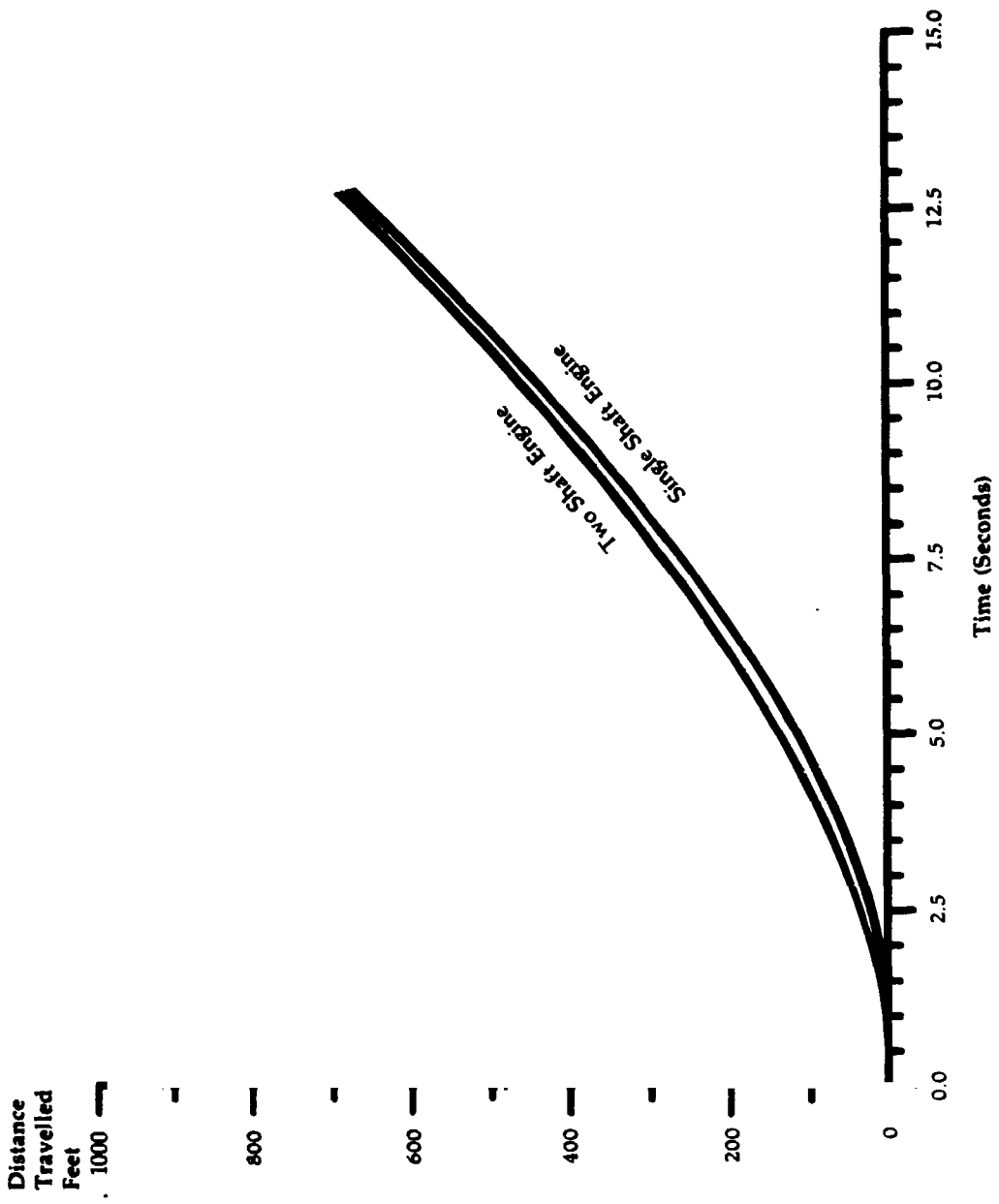

Figure 77

Performance Comparison of Various Power Plants

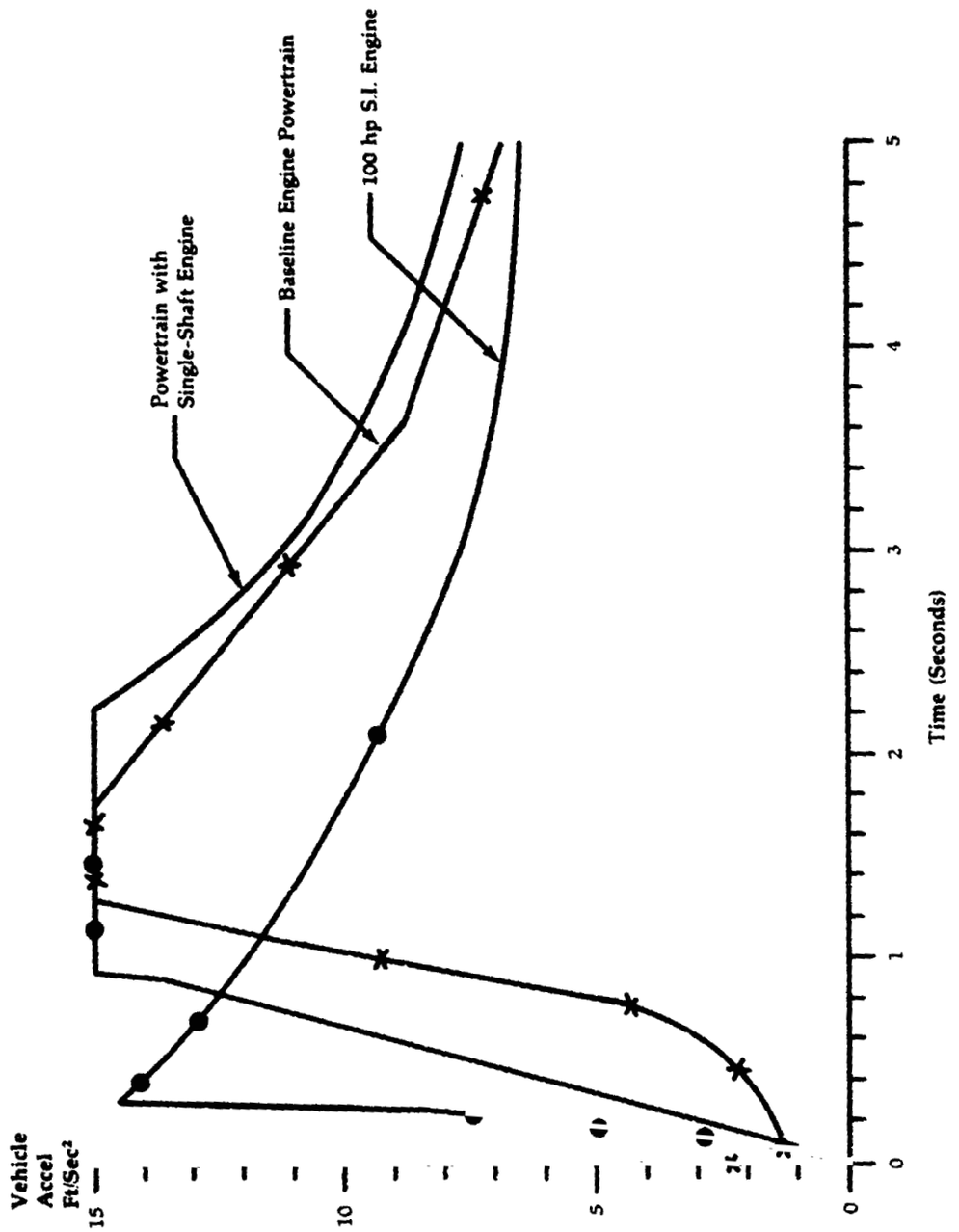

Figure 78

Vehicle Performance

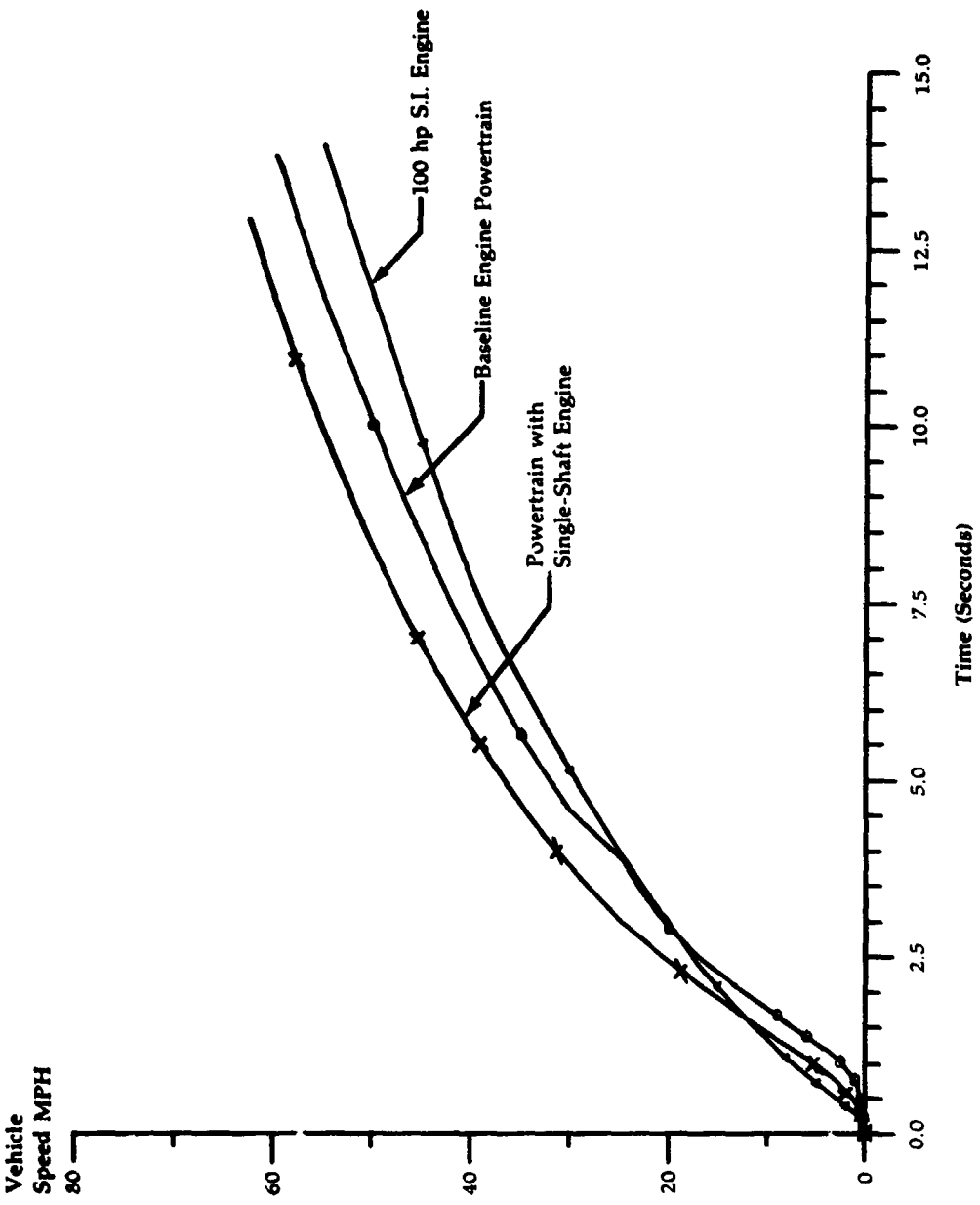

Figure 79

Performance Comparison of Various Power Plants

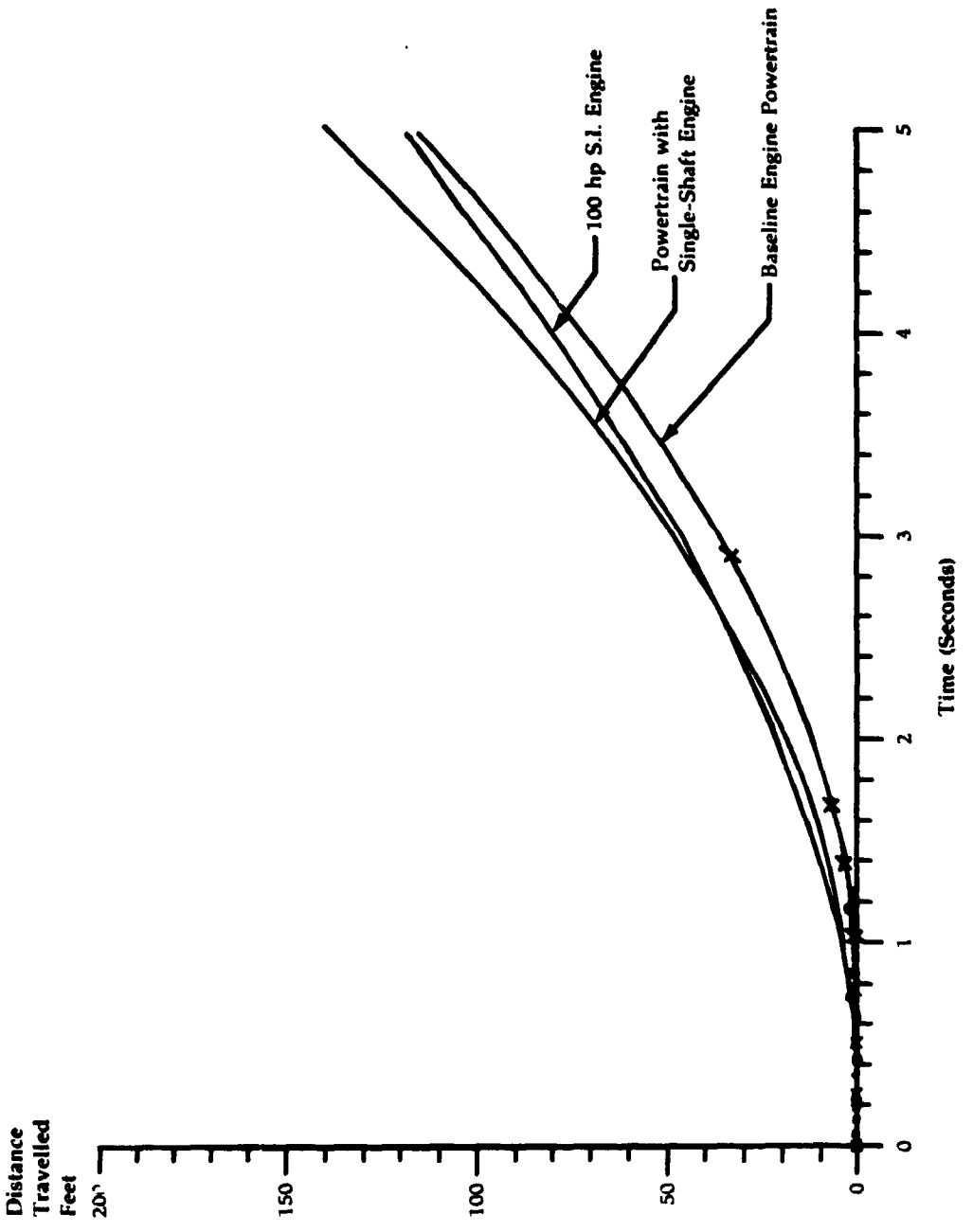

Figure 80

Single Shaft Gas Turbine 4.2 Pressure Ratio

Maximum Temperature Schedule

BSFC vs. Output Horsepower

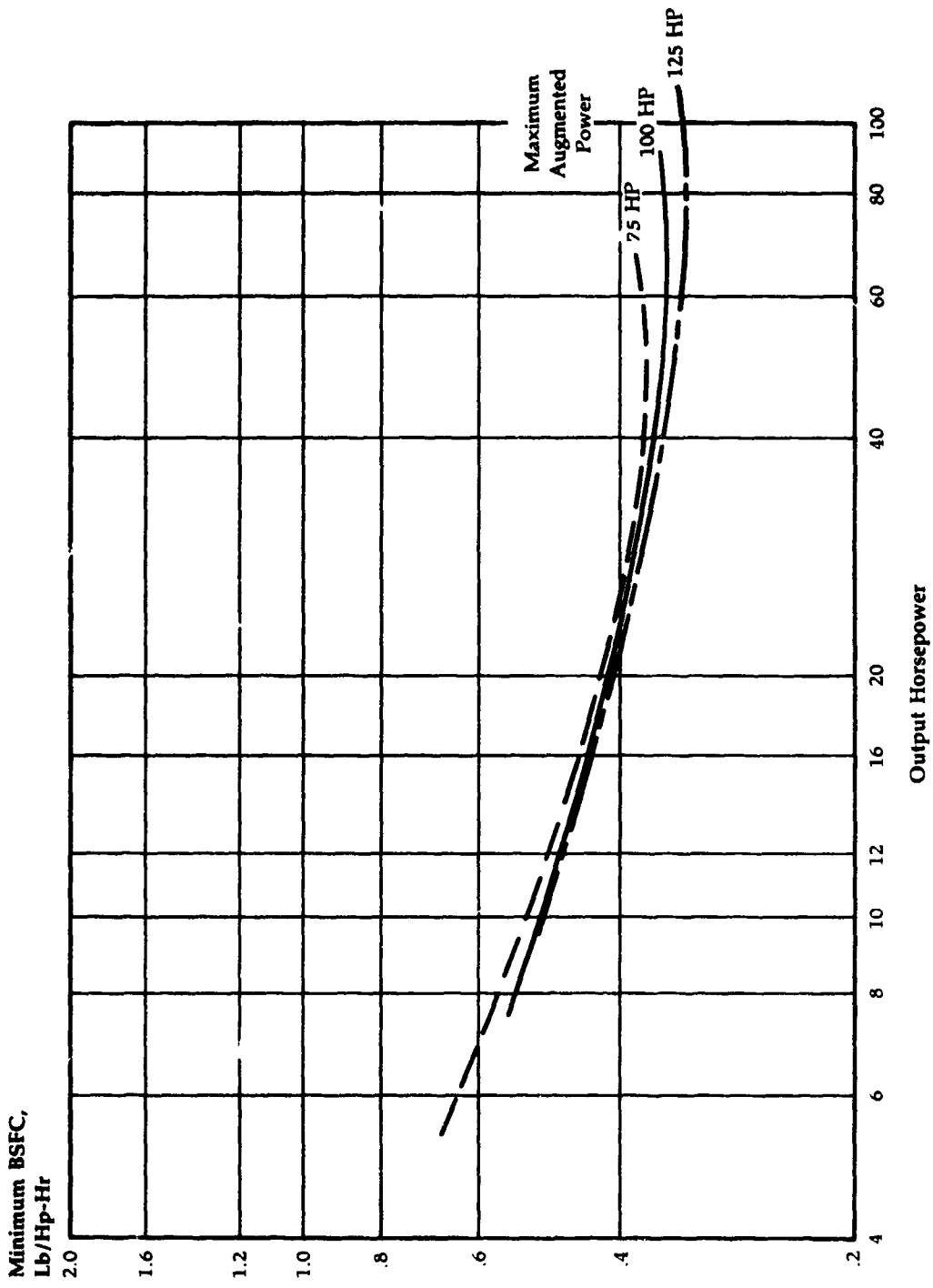

Figure 81

Fuel Economy Comparison

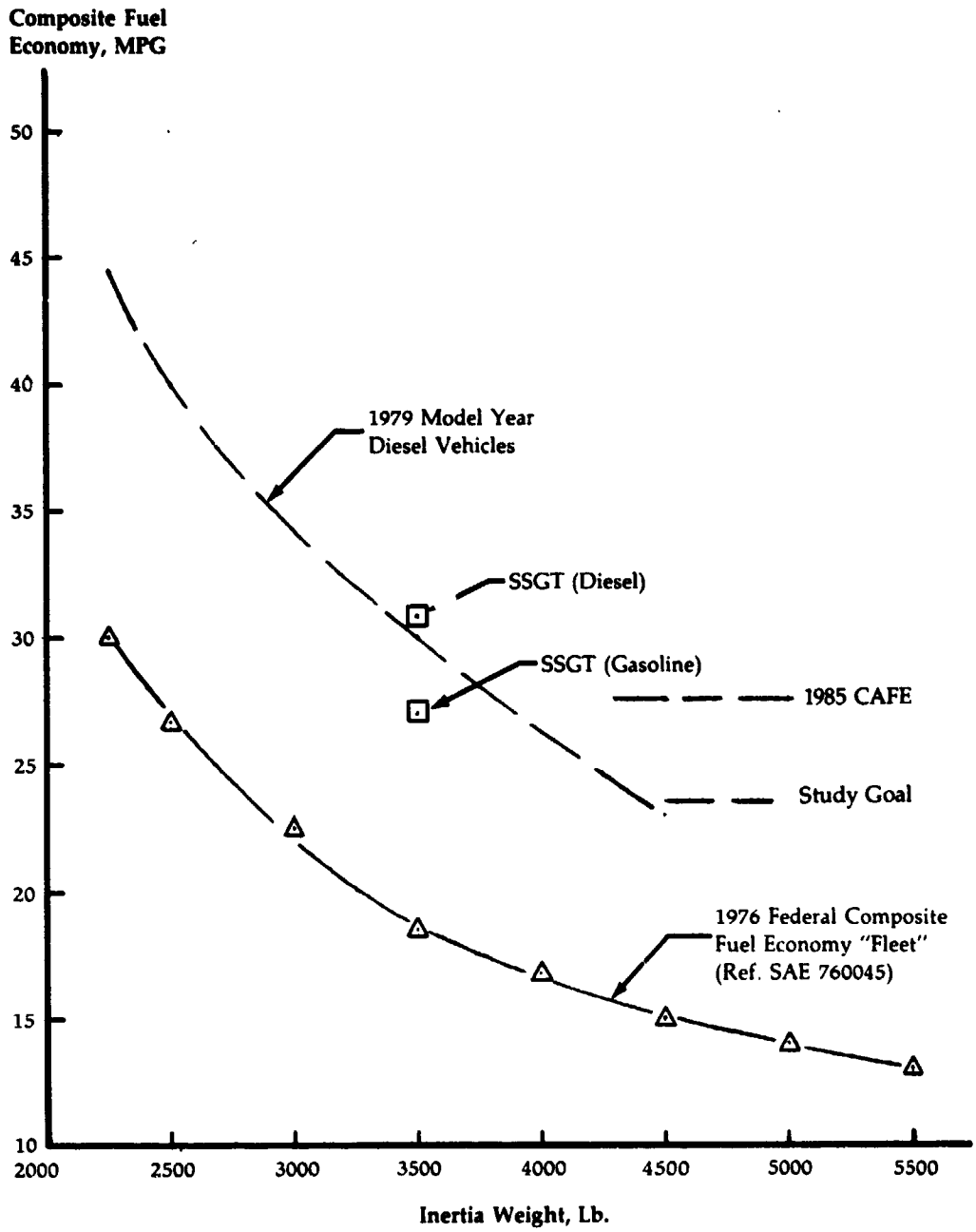

SSGT = Single-Shaft Gas Turbine

Figure 82

U.S. Car & Truck Market

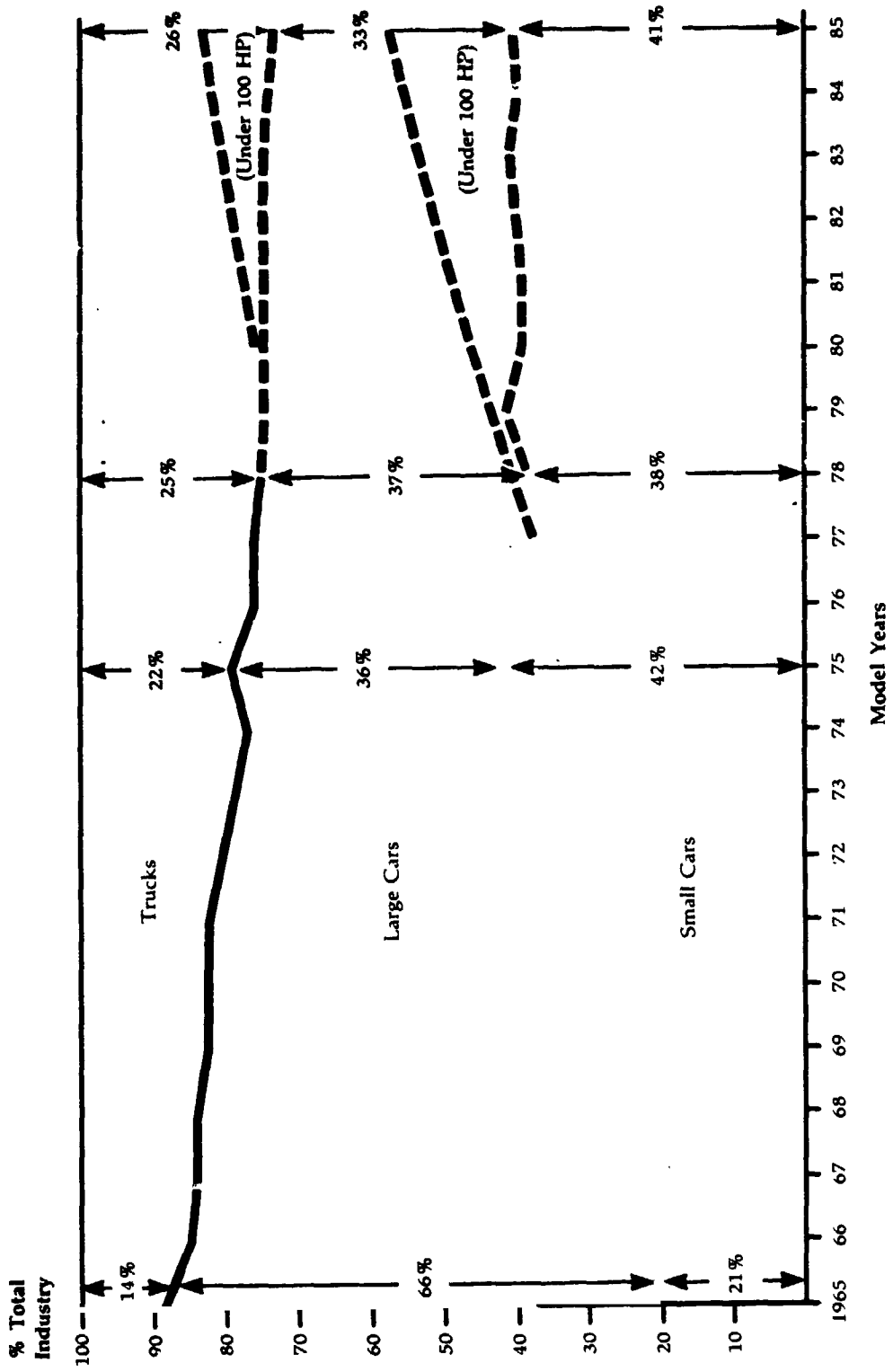

Figure 83

IGT Development Plan

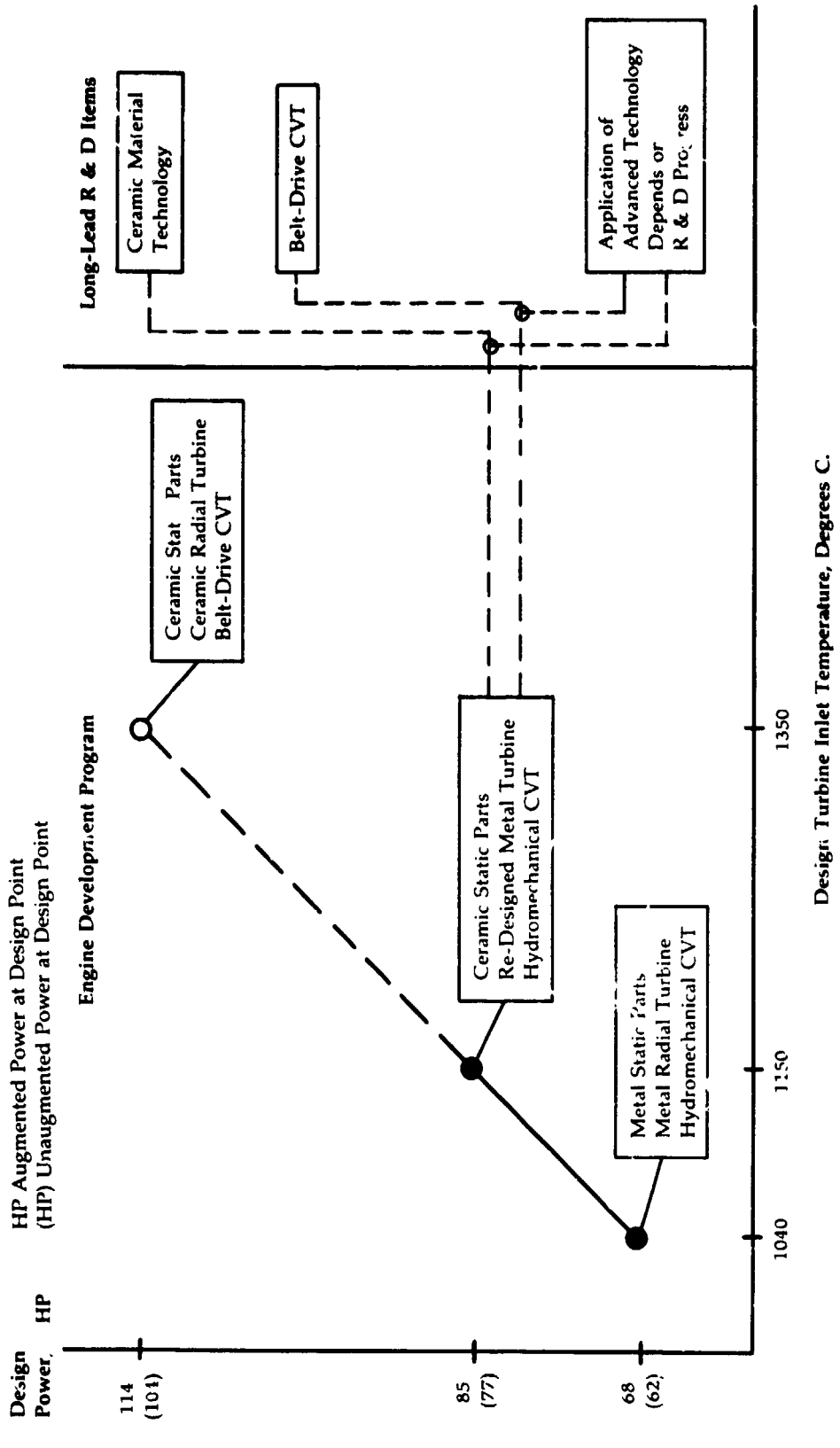

Figure 84

Figure 85

IAGT Program
2,100°F 85 HP
Single Shaft
Engine

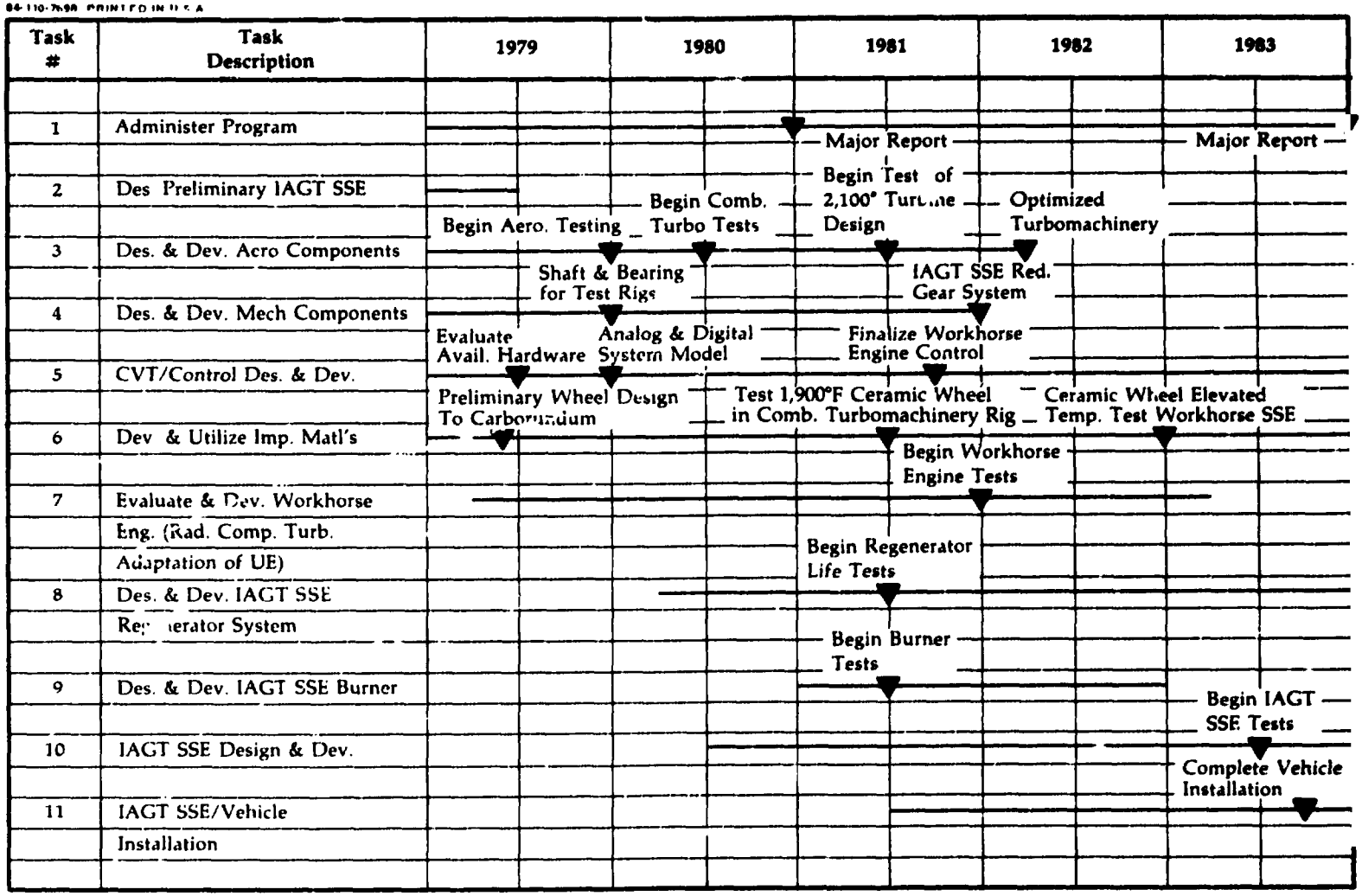

APPENDIX A

Vehicle and Duty-Cycle Characteristics

The vehicle fuel economies were determined by calculating the amount of fuel that would be consumed during each second while operating a vehicle according to the EPA Urban and Highway Dynamometer Driving Schedules, as described in Volumes 41 and 42 of the Federal Register.

The composite urban cycle fuel economy was calculated using the actual vehicle distance traveled, 7.45 miles, rather than the 7.5 miles specified for pre-1978 model-year vehicles, consistent with the more recent federal regulations. The fuel used during the first 505 seconds of the drive cycle, the transient phase, was weighted by a 43-percent factor for a cold-start condition and a 57-percent factor for a warm-start condition. An increment of fuel was added to the fuel usage calculated for warm-engine operation to represent the amount required to bring the engine to operating temperature. This transient-phase fuel flow was added to the stabilized-phase fuel flow, representing the remainder of the 1371-second drive cycle in calculating the composite urban cycle fuel economy.

The highway cycle fuel economy was calculated using the actual vehicle distance traveled and the warm engine fuel usage for the 765 second highway driving schedule. The engine deceleration fuel usage was assumed to be equal to the engine idle fuel usage for both drive cycles.

The combined federal drive cycle fuel economy was calculated by harmonically weighting the composite urban and highway cycle fuel economies on a 55-and and 45-percent basis, as follows:

$$\text{Combined fuel Economy, mpg} = \frac{1}{\frac{0.55}{\text{Urban fuel economy, mpg}} + \frac{0.45}{\text{Highway fuel economy, mpg}}}$$

The fuel properties used for the calculations were those specified by the EPA Certification Division for unleaded gasoline, — 6.167 pounds per gallon and 114,107 BTU per gallon lower heating value rather than the 133,000 BTU per gallon fuel specified for this design study. This provides a consistent basis for the intended thermal efficiency comparison.

The vehicle specification for the study is shown on Tables 1 and 2. This vehicle is in the 3500-pound inertia-weight class category, as specified in the Federal Register The specified dynamometer power absorption setting for the inertia-weight class (11.2 horsepower at 50-miles-per-hour road-load) was used for the calculations. The reduced road-load power requirements of alternate vehicles was not considered in determining powertrain thermal efficiency improvements.

The vehicle drive-shaft force required at road-load operation on the chassis dynamometer at the specified setting is given by the following formula developed at Chrysler Corporation,

$$F = 49.4625 + 0.05114 \times U + 0.00238 \times U^2 + 0.04682 \times U^{1.83}$$

F = Pounds force
U = Vehicle speed, miles per hour

The vehicle drivetrain used for the majority of the powertrain arrangements consisted of the following:

tires - FR78 × 14, 800 tire revolutions per mile (45 miles per hour)

rear axle ratio - 3.23:1

transmission - 3-speed automatic with transmission pump; 2.45, 1.45 and 1:1 forward gear ratios

torque converter - 10.75 in. diameter, with lock-up at first-to-second gear-shift point

The efficiency losses and rotating inertias associated with the above components as well as those of the vehicle power-steering pump were included in the vehicle fuel economy calculations The power steering pump power requirement was that for vehicle straight-ahead operation

APPENDIX B

Preliminary Parts List, Single-Shaft Engine

Chrysler Layout 951-2131 Dated 9-7-78

Part No.	Part Name	No. Req'd	Material
001	**Assembly, Engine Housing**	1	
002	Housing, Engine Machining	1	
003	Insulation, HSG Bulkhead-Front L.H.	1	Fibrous
004	Insulation, HSG Bulkhead-Front R.H.	1	Fibrous
005	Insulation, HSG Bulkhead-Front Upper	1	Fibrous
006	Insulation, HSG Bulkhead-Front Lower	1	Fibrous
007	Insulation, HSG Burner-Front	1	Fibrous
008	Insulation, HSG Burner-Rear	1	Fibrous
009	Insulation, HSG Burner-L.H.	1	Fibrous
010	Insulation, HSG Burner-R.H.	1	Fibrous
011	Insulation, HSG Bulkhead Rear L.H.	1	Fibrous
012	Insulation, HSG Bulkhead Rear R.H.	1	Fibrous
013	Insulation, HSG Bulkhead Rear Upper	1	Fibrous
014	Insulation, HSG Bulkhead Rear Lower	1	Fibrous
015	Insulation, HSG Regen. X-Arm-Upper	1	Fibrous
016	Insulation, HSG Regen. X-Arm Lower	1	Fibrous
017	Adhesive, Molded Insulation	AR	
018	Seamfiller, Molded Insulation	AR	
019	Coating, Abrasion Resistant	AR	
020	Seal, Regen. Pinion Shaft	1	Carbon
021	Spring, Regen. Pinion Shaft Seal Etc	1	Steel
022	Screw, Regen. Pinion Shaft Seal Ret	3	Steel
023	C'Washer, Regen. Pinion Shaft Seal Ret	3	
024	Dowel, Regen. Pinion Shaft Seal Supt.	1	Steel
025	Assembly, Fuel Dump Valve See Fig 1*	1	
026	Body, Fuel Dump Valve	1	302SS
028	Spring Fuel Dump Valve	1	316SS
029	Ball Fuel Dump Valve	1	304SS
030	Sleeve, Fuel Dump Valve	1	304SS
031	Washer, Fuel Dump Valve	1	Copper
032	Assembly Heater Conn. Elbow See Fig. 2	1	
033	Elbow, Heater Connector	1	304SS
034	Flange, Heater Connector Elbow	1	304SS
035	Gasket, Heater Connector Elbow	1	Asbestos
036	Bolt, Heater Connector	4	Steel
037	C'Washer, Heater Connector	4	Steel
038	Sensor, T-8 Temperature See Fig. 3	1	STD
039	Gasket, T-8 Temp. Probe	1	Asbestos
040	Bolt, T-8 Temp. Probe	2	Steel
041	C'Washer, T-8 Temp. Probe	2	Steel
042	Filter, T-8 Temp. Sensor Air Not Used	1	STD
043	Plug, T8 Temp. Probe Air Hole	1	Steel
044	Stud, Regenerator Cover	4	Steel
045	Screw, Regen Seal Locating	4	Steel
046	Pin, Regen. Seal Indexing	1	Steel
047	Bolt, Lifting Lug Hole	3	Steel
048	C'Washer, Lifting Lug Hole	3	Steel
049	Assy, Engine Front Support Brket-LH See Fig. 4	1	
050	Bracket, Engine Front Support-LH	1	Steel
051	Assembly, Insulator Bushing	1	**
052	Assembly, Engine Front Support Brkt. RH	1	
053	Bracket, Engine Front Support-RH	1	Steel
054	Assembly Insulator Bushing	1	**
055	Bolt, Eng. Front Supt Brkt. Assy	4	Steel
056	Coned Washer Eng. Front Supt. Brkt.	8	Steel

*See Appendix **Molded Rubber and Steel

APPENDIX B

Preliminary Parts List, Single-Shaft Engine

Chrysler Layout 951-2131 Dated 9-7-78 (continued)

Part No.	Part Name	No. Req'd	Material
057	Nut, Eng. Front Supt. Brkt.	4	Steel
058	**Assembly, Gas Generator**	1	
059	Assy. Comp. Bearing Housing	1	
060	Housing, Compressor Bearing	1	NOD CI
061	Seal, Comp. Brg. Housing	1	Carbon
062	Insulation, Compr. Brg. Hsg.	1	Fibrous
063	Ring, Compr. Brg. Hsg. Seal	1	Steel
064	Support Turbine Shroud	1	HAST X
065	Bolt, Shroud Suppt. to Seal Supt.	3	Super Alloy
066	Shroud Turbine Front	1	SiC
067	Insulation-Front Shroud	1	Fibrous
068	Assembly, Bearing See Fig. 5	1	
069	Cartridge - Gas, Gen. Rotor Brg.	1	Steel
070	Bearing - Gas Gen. Rotor (Air Foil)	1	See Fig. 5
071	O Ring, Brg. to Brg. Hsg	1	PTFE
072	Ring, Brg. Retaining	1	Steel
073	Shaft, Rotor Rear	1	Steel
074	Assy. Seal Housing	1	
075	Housing - Rotor Seal	1	Steel
076	Seal Rotor	1	STD
077	'O'-Ring Seal Hsg. to Compr. Brg. Hsg.	1	PTFE
078	Ring Seal Hsg. Retaining	1	Steel
079	Assy, Turbine Wheel	1	
080	Wheel Turbine (Ceramic)	1	SiC
081	Ring Turbine Wheel	1	Cermet
082	Shaft Turbine Wheel	1	Steel
083	Shroud Turbine Rear	1	SiC
084	Spacer Seal Support	1	Mullite
085	Support Bulkhead Seal	1	NOD CI
086	Ring Bulkhead Seal	1	NiResist
087	Nut Shr Supt. to Seal Supt Bolt	3	Superalloy
088	C-Washer Shr. Supt to Seal Supt Bolt	6	Superalloy
089	Insulation - Rear Shroud	1	Fibrous
090	Insulation - Seal Supt. Spacer	1	Fibrous
091	Insulation - Shroud Support	1	Fibrous
092	Plenum Burner	1	SiC
093	Insulation Compr. Brg. Housing	1	Fibrous
094	Assy, Compr. Impeller	1	
095	Impeller - Compr.	1	Aluminum
096	Shaft - Rotor Front	1	Steel
097	Washer Rotor Front Shaft	1	Steel
098	Nut Rotor Front Shaft	1	Steel
099	Cover Compressor	1	NOD CI
100	Ring V.I.G.V. Control	1	Steel
101	Vane Variable Inlet Guide	13	Steel
102	Arm Variable Inlet Guide Vane	13	Steel
103	Nut Variable Inlet Guide Vane	13	Steel
104	Washer Variable Inlet Guide Vane	13	Steel
105	Cover Collector	1	NOD CI
106	Pin G.G. Cover to Brg. Hsg	2	Steel
107	Bolt G.G. Cover to Shr. Supt.	12	Steel
108	C-Washer G.G. Cover to Sur. Supt.	12	Steel
109	'O'-Ring G.G. Cover to Red. Gr. Hsg	1	Viton
110	Bolt G.G. Cover to Red. Gr. Hsg	10	Steel
111	C-Washer G.G. Cover to Red. Gr. Hsg.	10	Steel

APPENDIX B

Preliminary Parts List, Single-Shaft Engine

Chrysler Layout 951-2131 Dated 9-7-78 (continued)

Part No.	Part Name	No. Req'd	Material
112	**Assembly, Reduction Gear and Sump**	1	
113	Assy, Red. Gear Hsg. and Cover	1	
114	Housing Reduction Gear	1	Aluminum
115	Bearing Rotor Shaft Front	1	STD
116	Bearing Pin. Rear	1	STD
117	Seal Rotor Shaft Front	2	
118	Cover Red. Gear Housing	1	Aluminum
119	Bearing Pinion Front	1	STD
120	Pin Cover to Hsg. Dowel	2	Steel
121	Plug Oil Press. Line	6	Steel
122	Plug Air Press. Line	2	Steel
123	Pin Red. Gr. Hsg. to Accy. Dr. Supt.	2	Steel
124	Assembly, Accessory Drive Support	1	
125	Supt. Accessory Drive	1	Aluminum
126	Brg. Accessory Drive Shaft	1	STD
127	Brg. Oil Pump Dr. Shaft Front	1	STD
128	Brg. Oil Pump Dr. Shaft Rear	1	Oilite
129	Shaft Oil Pump Drive	1	Steel
130	Plate Ring Gear Supt.	1	Steel
131	Roller Supt. Plate Bearing		Steel
132	Spacer Ring Gear Supt. Plate	1	Steel
133	Ring Spacer Retaining	1	Steel
134	Sprocket Oil Pump Drive Sh.	1	Steel
135	Washer Sprocket Thrust	1	Steel
136	Gear Planetary Dr. Ring	1	Steel
137	Ring Gear Retaining	1	Steel
138	Washer Planetary Gr. Set Thrust	2	Steel
139	Assembly, Planetary Gear Set	1	
140			
141	Spider Planetary Gear Set	1	Steel
142	Plate Planetary Gear Set	1	Steel
143	Gear Planetary	3	Steel
144	Washer Plaentary Gear Thrust	12	
145	Pin Planetary Gear	3	Steel
146	Hub Planetary Gear	1	Steel
147	Assembly, Pl. Gear Retaining Plate	1	
148	Plate Pl. Gear Retaining Plate	1	Steel
149	Bearing Planetary Gear Hub	1	STD
150	Bolt, Bolt-Ret. Pl. to Accy. Supt.	4	Steel
151	C. Washer Bolt-Ret. Pl. to Accy. Supt.	4	Steel
152	Plate Oil Pump Rotor Back	1	Steel
153	Key Oil Pump Drive Shaft	1	Steel
154	Assembly, Oil Pump Body	1	
155	Body Oil Pump	1	Cast Iron
156	Plunger-Press. Relief Valve	1	Steel
157	Spring Press. Relief Valve	1	Steel
158	Cap Press. Rel. Valve Spring	1	Steel
159	Pin Press. Rel. Valve Capcotter	1	Steel
160	Rotor Oil Pump-Inner	1	Steel
161	Rotor Oil Pump-Outer	1	Steel
162	'O'-Ring Oil Pump Body to Supt.	1	Steel
163	'O'-Ring Oil Pump Body to Supt.-Press	1	Viton
164	'O'-Ring Oil Pump Body to Supt-Suction	1	Viton
165	'O'-Ring Oil Pump Body to Supt-Drain	1	Viton
166	Screw Oil Pump Body to Acc. Dr. Supt.	5	Steel
167	C-Washer Oil Pump Body to Acc. Dr. Supt.	5	Steel

APPENDIX B

Preliminary Parts List, Single-Shaft Engi ·

Chrysler Layout 951-2131 Dated 9-7-78 (continued)

Part No.	Part Name	No. Req'd	Material
168	Bolt Accy. Dr. Supt. to Red. Gr. Hsg.	7	Steel
169	C-Washer Accy. Dr. Supt. to Red. Gr. Hsg.	7	Steel
170	Assembly, Oil Filter	1	STD
171	Adapter Oil Filter	1	Steel
172	Assembly, Oil Strainer - Complete	1	STD
173	Assembly, Oil Strainer - Partial	1	
174	Assembly, Oil Strainer Screen	1	
175	Shield Oil Strainer	1	S..el
176	Gasket Oil Strainer to Oil Pump	1	Vellumoid
177	Bolt Oil Strainer to Oil Pump	2	Steel
178	C'Washer Oil Strainer to Oil Pump	2	Steel
179	Trough Sprocket Oil See Fig. 6	1	Steel
180	Bolt Oil Trough	2	Steel
181	C'Washer Oil Trough	2	Steel
182	Assembly Oil Pan - Complete	1	
183	Assembly Oil Pan - Partial	1	
184	Pan Oil	1	Steel
185	Boss Oil Pan Drain Plug	1	Steel
186	Gasket Oil Pan Drain Plug	1	Nylon
187	Plug Oil Pan Drain	1	Steel
188	Gasket Oil Pan	1	Vellumoid
189	Bolt Oil Pan	15	Steel
190	C'Washer Oil Pan	15	Steel
191	Plug Lab T'Couple Hose	1	Steel
192	Assembly Oil Filler Tube - Welded See Fig. 7	1	Steel
193	O-Ring Oil Filler Tube	1	Viton
194	Bolt Oil Filler Tube	2	Steel
195	C'Washer Oil Filler Tube	2	Steel
196	Assembly Oil Filler Tube Cap	1	STD
197	Assembly Oil Level Dip Stick Tube	1	STD
198	O-Ring Oil Level Indicator Tube	1	Steel
199	Bolt Oil Level Ind. Tube	1	Steel
200	C'Washer Oil Level Ind. Tube	1	Steel
201	Dip Stick Oil Level	1	Steel
202	Shaft Accessory Drive	1	Steel
203	Sprocket Accessory Drive	1	PM Steel
204	Sprocket Oil Pump Drive	1	PM Steel
205	Gear Planetary Set Drive	1	Steel
206	Ring Drive Gear Retaining	1	Steel
207	Ring Oil Pump Dr. Sprocket Ret.	1	Steel
208	Chain Oil Pump Drive	1	Steel
209	Assy, Accy Dr. Sh. Retainer Plate	1	
210	Plate Accy. Dr. Shaft Retainer	1	Alumi ·um
211	Bearing Accy. Drive Shaft	1	STD
212	Seal Accy Drive Shaft Oil	1	Viton
213	Shim Accy Dr Sh. Ret Plate	AR	Steel
214	Bolt Ret. Plate to Red. Gr. Hsg	4	Steel
215	C-Washer Ret Plate to Red. Gr. Hsg.	4	Steel
216	Key Accy Drive Shaft	1	Steel
217	Pulley P/Strg Pump Drive	1	Steel
218	Washer P/Strg Pump Drive Pulley	1	Steel
219	Nut P/Strg. Pump Drive Pulley	1	Steel
220	Assy, Ancillary Dr. Shaft Hsg.	1	
221	Housing Ancillary Dr. Shaft Hsg.	1	Aluminum
222	Bearing Ancillary Dr. Shaft	1	STD
223	Seal Ancillary Dr. Shaft Oil	1	STD

APPENDIX B

Preliminary Parts List, Single-Shaft Engine

Chrysler Layout 951-2131 Dated 9-7-78 (continued)

Part No.	Part Name	No. Req'd	Material
224	Shaft Ancillary Drive	1	Steel
225	Bearing Ancillary Drive Sh. Ball	1	STD
226	Ring Bearing Retaining	1	STD
227	Ring Bearing Retaining	1	STD
228	Connector Ancil. Dr. Sh. to Accy. Dr. Sh.	1	Steel
229	Bolt Shaft Hsg. to Red. Gr. Hsg.	4	Steel
230	C-Washer Shaft Hsg. to Red. Gr. Hsg.	4	Steel
231	Key Ancillary Drive Shaft	1	Steel
232	Pulley A/C Compr. and Alternator Dr.	1	Steel
233	Washer A/C Compr. and Alternator Dr.	1	Steel
234	Nut A/C Comp and Alternator Dr.	1	Steel
235	Gasket Red. Gr. Hsg. to Engine Hsg.	1	
236	Bolt Red. Gr. Hsg. to Engine Hsg.	16	Steel
237	C-Washer Red. Gr. Hsg. Engine Hsg.	16	Steel
238	Pinion Gas Gen. Rotor	1	Steel
239	Assy, Intermediate Sh. Gear and Brg.	1	
240	Shaft Pinion Gear and Intermediate	1	Steel
241	Key Intermediate Shaft Gear	1	Steel
242	Gear Intermediate Shaft	1	Steel
243	Bearing Intermediate Shaft	2	
244	Assembly, Output Shaft	1	
245	Shaft Output	1	Steel
246	Gear Output Shaft	1	Steel
247	Sprocket-Output Shaft	1	Steel
248	Ring Sprocket and Gear Retaining	4	Steel
249	Bearing Output Shaft Front	1	STD
250	Bearing Output Shaft Rear	1	STD
251	Chain Accessory Drive	1	STD
252	Bolt Cover to Red. Gr. Hsg.	12	Steel
253	C-Washer Cover to Red. Gr. Hsg.	12	Steel
254	Rotor Pinion Thrust	1	Steel
255	Washer Pinion Thrust Rotor	1	Steel
256	Screw Pinion Thrust Rotor	1	Steel
257	Cover Pinion Thrust Rotor	1	Aluminum
258	Bolt Pinion Thrust Rotor Cover	4	Steel
259	C-Washer Pinion Thrust Rotor Cover	4	Steel
260	Plate Intermediate Shaft Ret.	1	Aluminum
261	'O' Ring Intermediate Shaft Ret. Pl.	1	Aluminum
262	Screw Retainer Plate to Cover	4	Steel
263	C-Washer Retainer Plate to Cover	4	Steel
264	Assy, Output Sh. Ret. Plate	1	
265	Plate Output Shaft Retainer	1	Aluminum
266	Seal Output Shaft Oil	1	Viton
267	'O'-Ring Ret. Plate to Cover	1	Viton
268	Screw Ret. Plate to Cover	4	Steel
269	C-Washer Ret. Plate to Cover	4	Steel
270	Assembly, V.I.G.V. Acutator-See Fig. 8	1	
271	Bracket Starter Motor Mounting	1	Steel
272	Bolt Starter Brkt. to Eng. Hsg.	2	Steel
273	C'Washer Starter Brkt. to Eng. Hsg.	2	Steel
274	Assembly Starter Motor	1	
275	Pivot Starter to Bracket	2	Steel
276	Bolt Pivot to Bracket	2	Steel
277	C'Washer Pivot to Bracket	2	Steel
278	Strap Starter Motor Adjusting	1	Steel
279	Bolt Strap to Engine Hsg.	1	Steel

APPENDIX B

Preliminary Parts List, Single-Shaft Engine

Chrysler Layout 951-2131 Dated 9-7-78 (continued)

Part No.	Part Name	No. Req'd	Material
280	C'Washer Strap to Engine Hsg.	1	Steel
281	Bolt Strap to Starter Motor	1	Steel
282	C'Washer Strap to Starter Motor	1	Steel
283	Pulley Starting Motor Similar to PT No. 217	1	Steel
284	Key Starting Motor Pulley	1	Steel
285	C'Washer Starting Motor Pulley	1	Steel
286	Bolt Starting Motor Pulley	1	Steel
287	Vee-belt Starter Drive	1	STD
288	**Assembly, Burner - Complete**	1	
289	Assembly Burner Cover-Insulation	1	
290	Cover Burner	1	Steel
291	Insulation Burner Cover	1	Fibrous
292	Insulation Burner Cover - Pre-mixer	1	Fibrous
293	Adhesive Molded Insulation	AR	
294	Seam Filler Molded Insulation	AR	
295	Coating Abrasion Resistant	AR	
296	Tube Burner	1	SiC
297	Assembly Torch Chamber - Welded See Fig. 9	1	
298	Gasket Torch Chamber	2	Asbestos
299	Support Torch Nozzle See Fig. 10	1	304SS
300	Nozzle Torch (Stewart-Warner) See Fig. 11	1	304SS
301	Bolt Torch Nozzle and Chamber	2	Steel
302	C'Washer Torch Nozzle and Chamber	2	Steel
303	Assembly Pre-mixer Tube Insulation	1	
304	Assembly Pre-mixer - Welded See Fig. 12	1	
305	Tube Pre-mixer	1	HAST X
306	Tube Pre-mixer - Outer Swirl	1	304SS
307	Tube Pre-mixer - Inner Swirl	1	304SS
308	Support Pre-mixer Tube	1	304SS
309	Insulation Pre-mixer Tube Support	2	Fibrous
310	Injector Pre-mixer Fuel See Fig. 13	1	304SS
311	Gasket Pre-mixer Tube Assembly	2	Asbestos
312	Bolt Pre-mixer Tube Assembly	6	Steel
313	C'Washer Pre-mixer Tube Assembly	6	Steel
314	Plug Hex Head Pipe 1/8	1	Steel
315	Plug Hex Head Pipe 1/4	1	Steel
316	Assembly Igniter Plug (Champion RN-12Y)	1	
317	Spacer Igniter Plug	1	Steel
318	Gasket Burner Cover	1	STL-ASB
319	Bolt Burner Cover	14	Steel
320	C'Washer Burner Cover	14	Steel
321	Assembly Fuel Metering Valve See Fig. 14	1	
322	Assembly Fuel Metering Valve w/Press. Reg.	1	
323	Assembly Flow Transducer	1	
324	Assembly Pressure Switch	1	
325	Element In-Line Filter	1	STD
326	Insulator 2-Way Male Connector	1	Plastic
327	Terminal Male	2	Steel
328	Insulator 3-Way Male Connector	1	Plastic
329	Terminal Male	3	Steel
330	Bracket Fuel Metering Valve Assembly	1	Steel
331	Nut Fuel Metering Valve Bracket	2	Steel
332	Screw Fuel Metering Valve To Bracket	2	Steel
333	Valve Fuel Solenoid	1	STD
334	Valve Fuel Check	2	STD

APPENDIX B

Preliminary Parts List, Single-Shaft Engine

Chrysler Layout 951-2131 Dated 9-7-78 (continued)

Part No.	Part Name	No. Req'd	Material
335	Solenoid Bleed	1	STD
336	Control, Electronic - Unit (ECU) See Fig. 15		
337	Exciter Ignition (Bendix Type TVN)	1	
338	Cable Ignition Exciter to Igniter Plug	1	
339	**Assembly Regenerator - Complete**		
340	Assembly Regenerator Inner Seal "L"	1	
341	Seal Inner Crossarm Rubbing (Coated)	1	To Be Developed
342	Plate Inner Crossarm Rubbing Seal	1	Inconel X
343	Seal Regen. Inner Rear Rim - Rubbing	1	See No. 341, 342
344	Seal Regen. Inner Front Rim - Rubbing	1	See No. 341, 342
345	Retainer Rubbing Seal	2	304SS
346	Clip Regen. Seal Retaining	5	304SS
347	Screw Regen Seal Retaining	5	304SS
348	Lock Washer Regen. Seal Retaining Screw	5	304SS
349	Assembly Regenerator Core - Complete	1	
350	Core Regenerator	1	Al Silicate
351	Assembly Regen. Gear and Rim	1	
352	Rim Regen Core Gear	1	Steel
353	Gear Regen. Core	1	Cast Iron
354	Pin Regen. Core Gear	8	Steel
355	Ring Regen. Core Safety	1	Steel
356	Bearing Regenerator Core	1	Graphite
357	Shaft Regenerator Center	1	Steel
358	Key Regen. Center Shaft	1	Steel
359	Sleeve Regen. Core Brng. - Eccentric	1	Steel
360	Ring Regen. Core Hold Down Wash Ret.	1	Steel
361	Washer Regen. Core Hold Down	1	Steel
362	Assembly Regenerator Outer Seal	1	
363	Seal Outer Rubbing	1	See No 341, 342
364	Retainer Rubbing Seal	2	304SS
365	Clip Regen. Seal Retaining	2	304SS
366	Screw Regen. Seal Retaining	2	304SS
367	Lockwasher Regen. Seal Retaining Screw	2	304SS
368	Assy , Regen. Drive Shaft Housing	1	
369	Housing Regen. Drive Shaft Housing	1	Aluminum
370	Bearing Regen Drive Shaft	1	STD
371	Seal Regen. Drive Shaft Oil	1	Viton
372	Shaft Regenerator Drive	1	Steel
373	Bearing Regenerator Drive Shaft	1	STD
374	Ring Bearing Retaining	1	STD
375	Ring Bearing Retaining	1	STD
376	Bolt Shaft Hsg. to Eng. Hsg.	4	Steel
377	C'Washer Shaft Hsg. to Eng. Hsg.	4	Steel
378	Key Regen. Drive Shaft	1	Steel
379	Pinion Regenerator Drive	1	Steel
380	Screw Regenerator Drive Pinion	1	Steel
381	Washer Regenerator Drive Pinion	1	Steel
382	Tube Shaft Hsg to Eng. Seal	1	Aluminum
383	'O' Ring Sealing		Viton
384	Connector Regen. Drive Shaft	1	Steel
385	Assembly. Regenerator Cover	1	
386	Cover Regenerator - Machining	1	Steel
387	Screw Regen. Seal Locating	4	Steel
388	Pin Regen. Seal Indexing	1	Steel
389	Insert Mo x 1.0 Tap Lock	5	304SS
390	Plug Heater Controls Air Supply	1	Steel

APPENDIX B

Preliminary Parts List, Single-Shaft Engine

Chrysler Layout 951-2131 Dated 9-7-78 (continued)

Part No.	Part Name	No. Req'd	Material
391	Bushing Regen. Center Shaft	1	Steel
392	A Washer Regen. Center Shaft	1	Steel
393	Nut Regen. Center Shaft	1	Steel
394	Lock Plate Regen. Center Shaft Nut	1	Steel
395	Bolt Center Shaft Nut Lock Plate	1	Steel
396	Coned Washer Center Shaft Nut Lock Plate	1	Steel
397	Shim Regenerator Cover - (0.2)	AR	Steel
398	Shim Regenerator Cover - (0.4)	AR	Steel
399	Shim Regenerator Cover - (0.8)	AR	Steel
400	Shim Regenerator Cover - (1.0)	AR	Steel
401	Shim Regenerator Cover - (1.5)	AR	Steel
402	Gasket Regenerator Cover - (0.4)	AR	Asbestos
403	Gasket Regenerator Cover - (0.8)	AR	Asbestos
404	Bolt Regenerator Cover - Short	28	Steel
405	Bolt Regenerator Cover - Long	2	Steel
406	Nut Regenerator Cover	4	Steel
407	Washer Regenerator Cover	34	Steel
408	Coned Washer Regenerator Cover	34	Steel
409	Assembly, Air/Oil Separator See Fig. 16	1	
410	Bolt, Air/Oil Separator Assy.	2	Steel
411	C'Washer/Air/Oil Separator Assy.	2	Steel
412	Elbow/Air Vent See Fig. 17	1	Steel
413	O-Ring, Air Vent Elbow	1	Viton
414	Gasket, Air Vent Elbow	1	Asbestos
415	Bolt, Air Vent Elbow	2	Steel
416	C'Washer, Air Vent Elbow	2	Steel
417	Assembly, Separator Drain Tube See Fig. 18	1	Steel
418	Nut, Air/Oil Separator Oil Drain Tube	1	Steel
419	Bolt, Air/Oil Separator Oil Dr. Tube Assy.	1	Steel
420	C'Washer, Air/Oil Separator Oil Dr Tube Assy.	1	Steel
421	Connector, Air/Oil Sep. Oil Dr. Tube Assy.	1	Steel
422	Assembly, Power Steering Pump - Complete	1	
423	Assembly, Power Steering Pump - Partial	1	
424	Reservoir, P/S Pump - Modified	1	Steel
425	Assembly, P/S Pump Reservoir Cap	1	Steel
426	Bracket, P/S Pump - Rear See Fig. 19	1	Steel
427	Bolt, P/S Pump to Brkt. Pivot - Rear	1	Steel
428	C'Washer, P/S Pump to Brkt. Pivot - Rear	1	Steel
429	Washer, P/S Pump to Brkt. Adj. Spacer	1	Steel
430	Bolt, P/S Pump to Brkt. Adjusting	1	Steel
431	C'Washer, P/S Pump to Brkt. Adjusting	1	Steel
432	Bracket, P/S Pump - Front	1	Steel
433	Nut, P.S Pump to Brkt. Pivot - Front	1	Steel
434	C'Washer, P/S Pump to Brkt. Pivot - Front	1	Steel
435	Pulley, P/S Pump	1	Steel
436	Bolt, Rear Bracket to Engine Hsg.	2	Steel
437	C'Washer, Rear Bracket to Engine Hsg.	2	Steel
438	Bolt, Front Bracket to Gear Hsg.	2	Steel
439	C'Washer, Front Bracket to Gear Hsg.	2	Steel
440	V-Belt, P/S Pump Drive	1	STD
441	Assembly, Alternator and Pulley	1	
442	Assembly, Alternator (12 volt-65 amp)	1	STD
443	Pulley, Alternator	1	Steel
444	Bracket, Alternator Mounting	1	Steel
445	Bolt, Alternator Mounting	3	Steel

APPENDIX B

Preliminary Parts List, Single-Shaft Engine

Chrysler Layout 951-2131 Dated 9-7-78 (continued)

Part No.	Part Name	No. Req'd	Material
446	Bolt, Alternator Mounting Pivot	1	Steel
447	Coned Washer, Alternator Mounting Pivot	1	Steel
448	Washer, Alternator Mounting Pivot	2	Steel
449	Nut, Alternator Mounting Pivot	1	Steel
450	Spacer, Alternator Pivot Bracket	1	Steel
451	Strap, Alternator Adjusting	1	Steel
452	Bolt, Alt. Adj. Strap to Hsg.	1	Steel
453	Coned Washer, Alt. Adj. Strap to Hsg.	1	Steel
454	Bolt, Alt. Adj. Strap to Alt.	1	Steel
455	Coned Washer, Alt. Adj. Strap to Alt.	1	Steel
456	V-Belt, Alternator Drive	1	STD
457	Assembly, Transmission - Complete	1	

APPENDIX B

Sketch of
Low Cost Dump
Valve Section

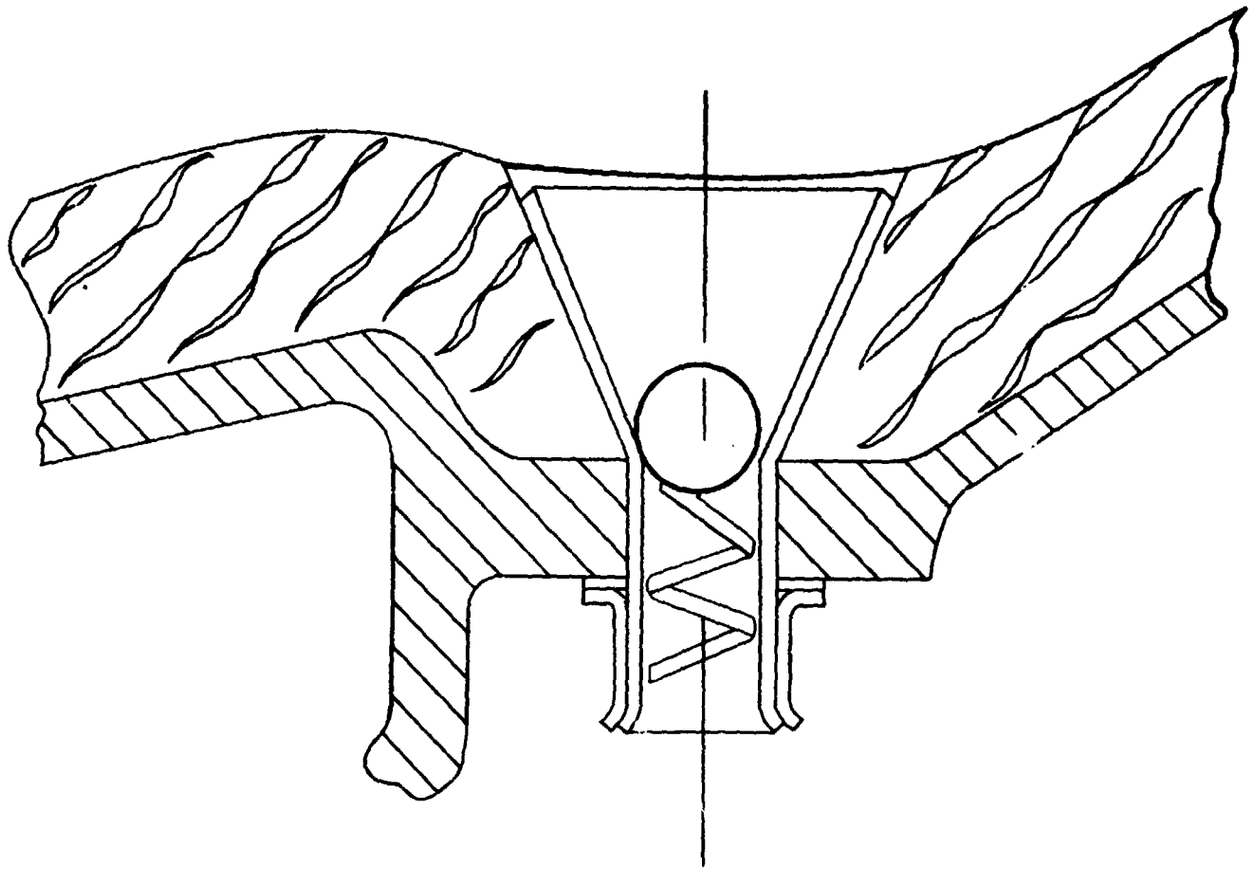

Figure 1B

APPENDIX B

Pt. No. 032
Assembly Heater
Connector Elbow

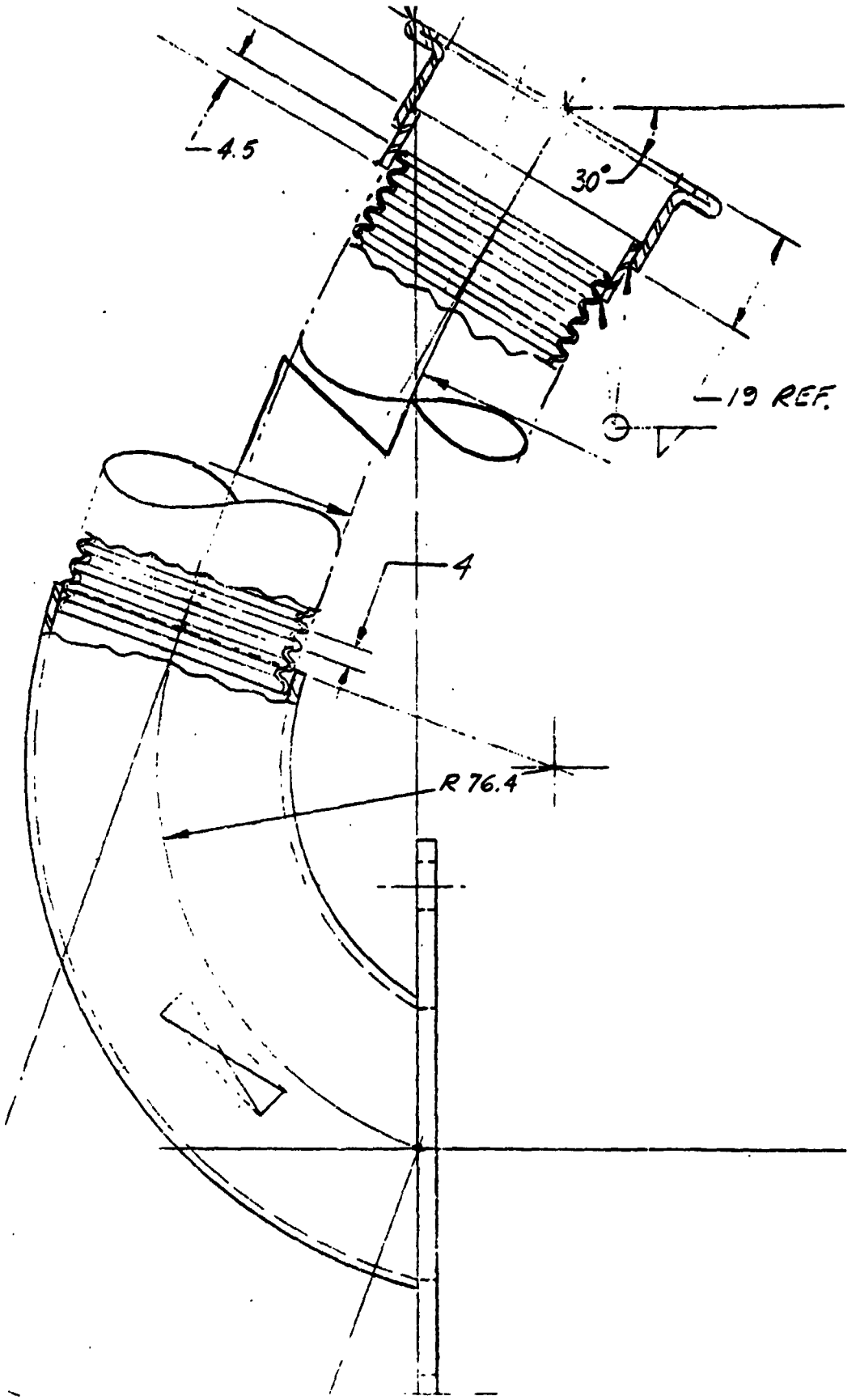

Figure 2B

APPENDIX B

Pt. No. 038
Sensor, T8
Temperature

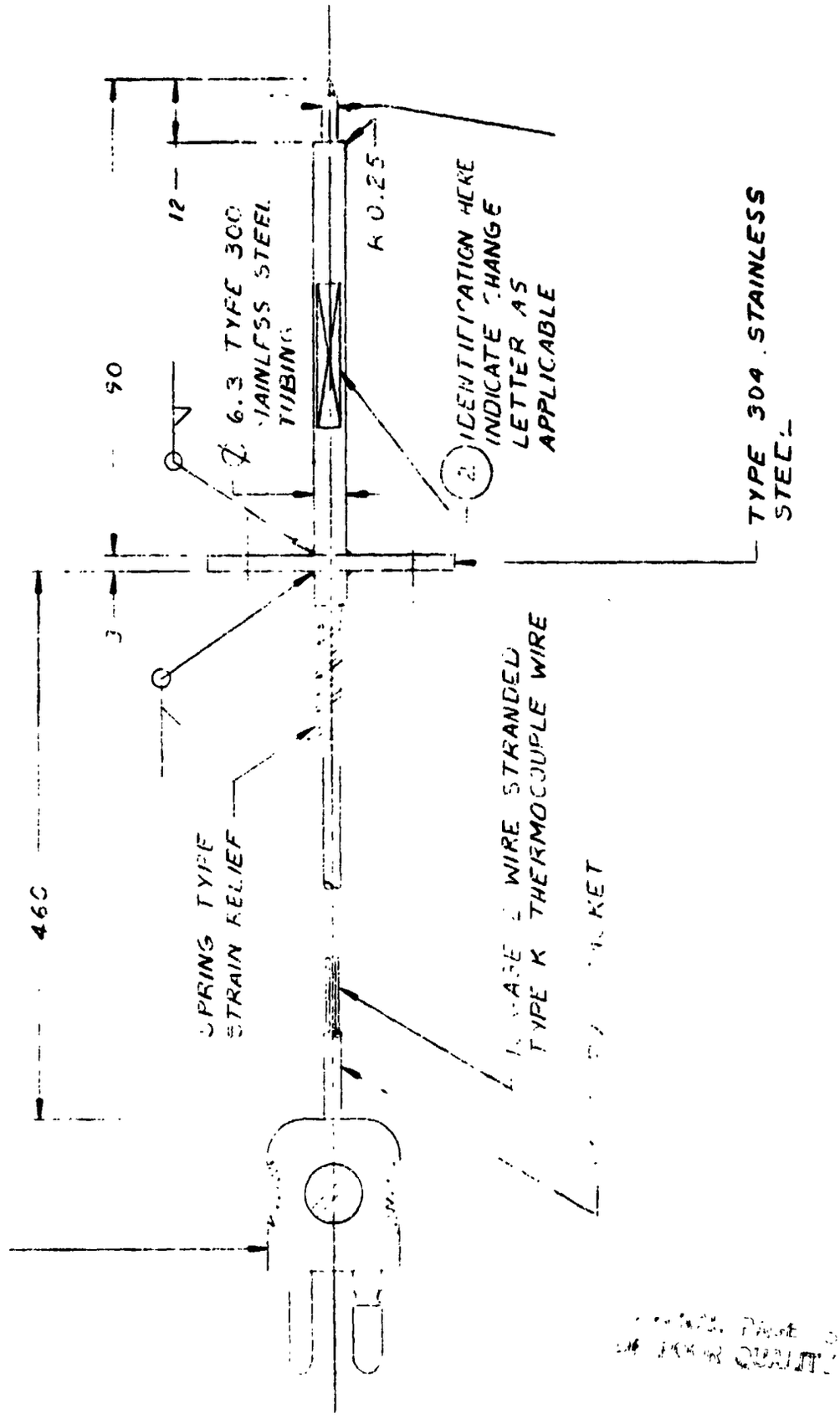

Figure 3B

APPENDIX B

Pt. No. 049
Assembly Engine
Front Support
Brkt.

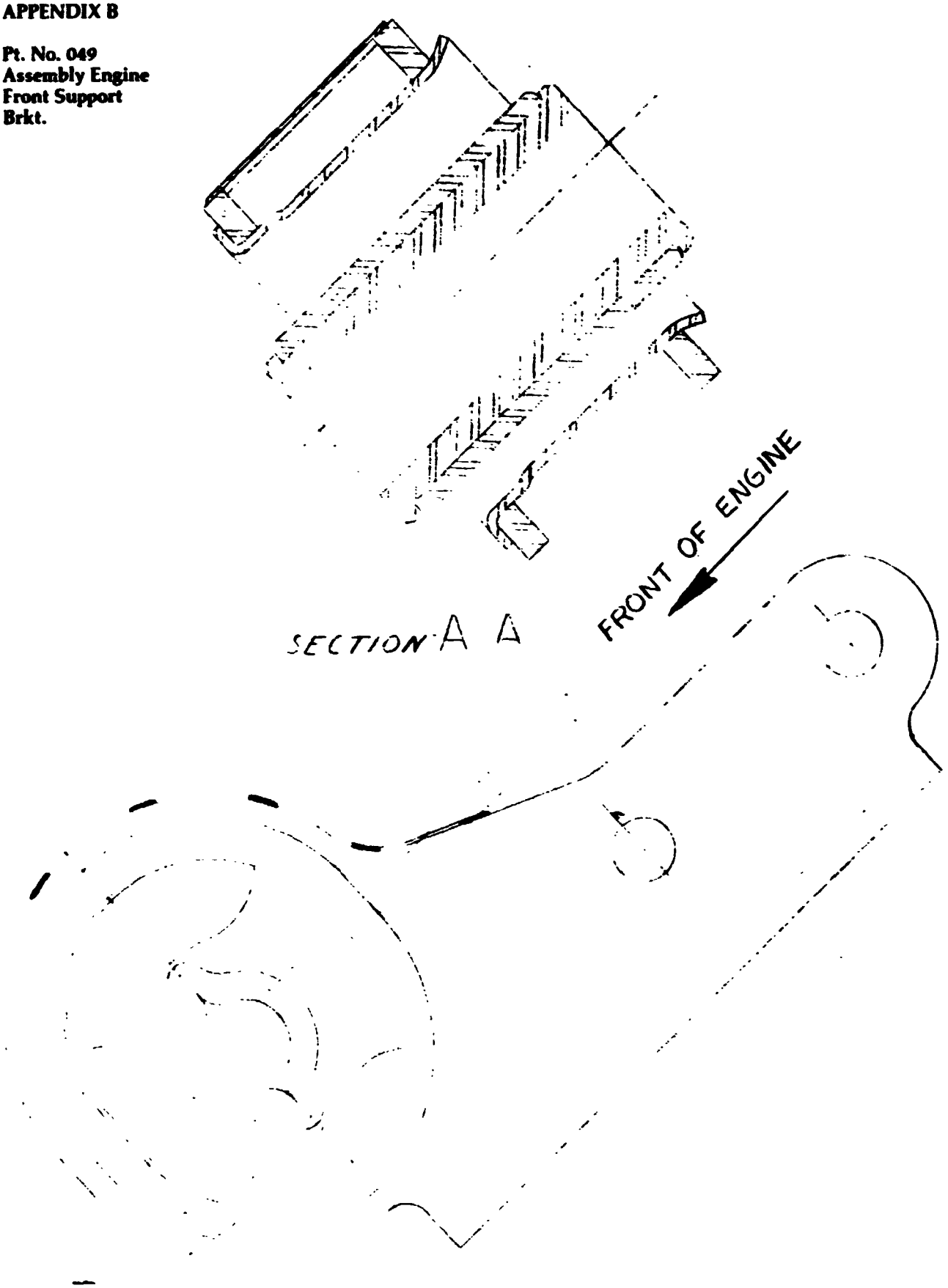

Figure 4B

APPENDIX B

Pt. No. 068
Assembly, Bearing

M.T.I. Hydrexil Compliant Foil Bearing

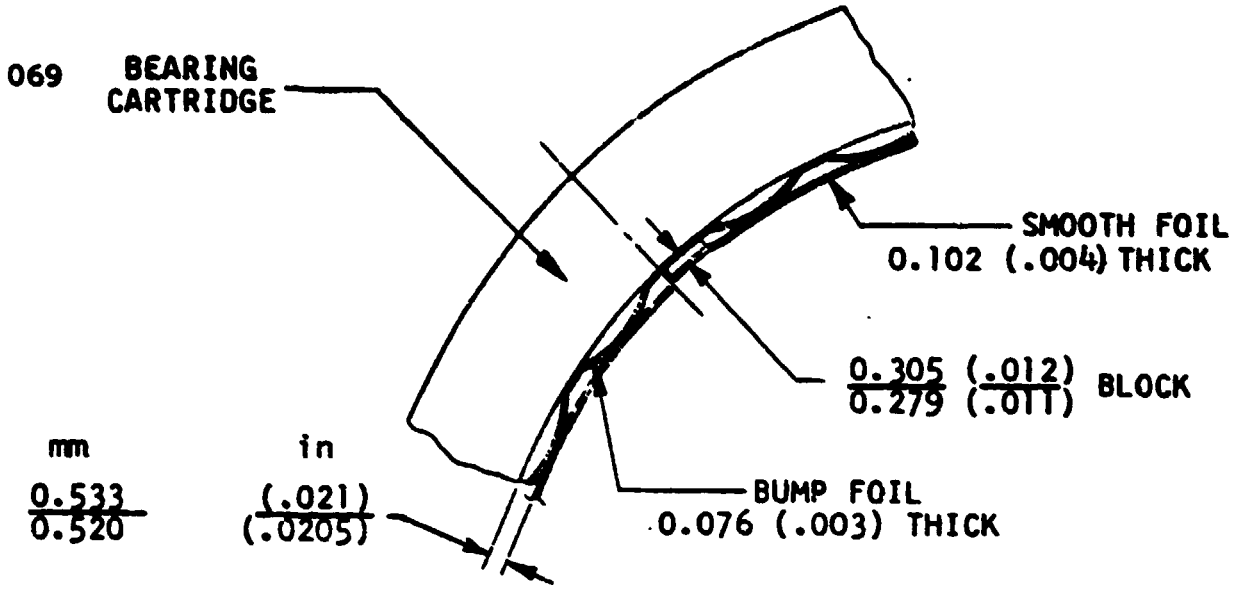

VIEW IN CIRCLE

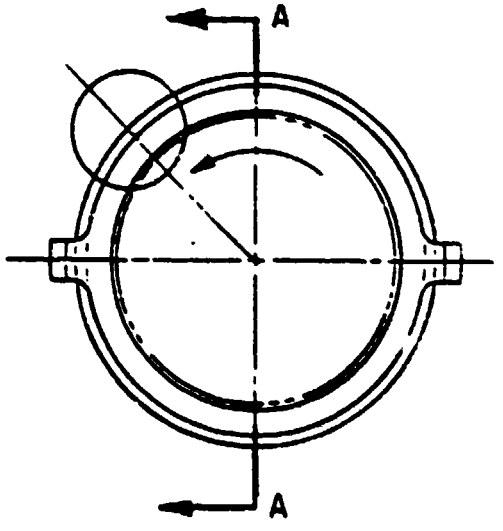

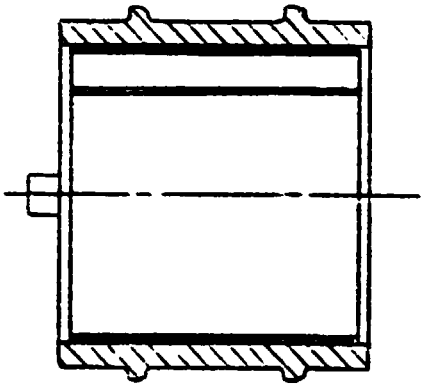

SECTION A-A

Materials

Shaft	17-4 PH
Coating	Chrome Carbide
Foils	Inconel X750
Dry Film	H-1284

Figure 5B

APPENDIX B

Pt. No. 179
Trough
Sprocket Oil

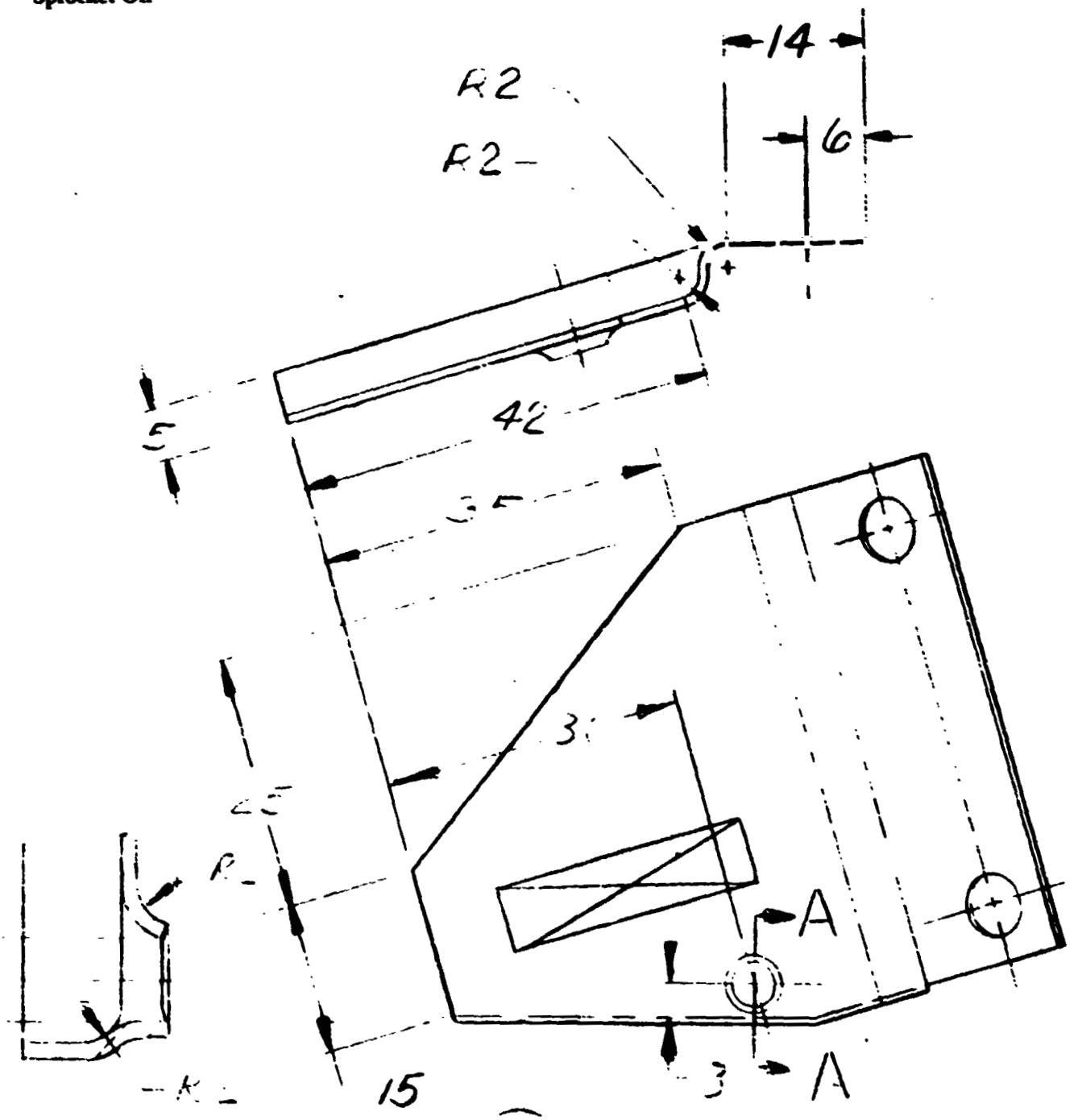

Figure 6B

APPENDIX B

Pt. No. 192
Assembly Oil
Filler Tube

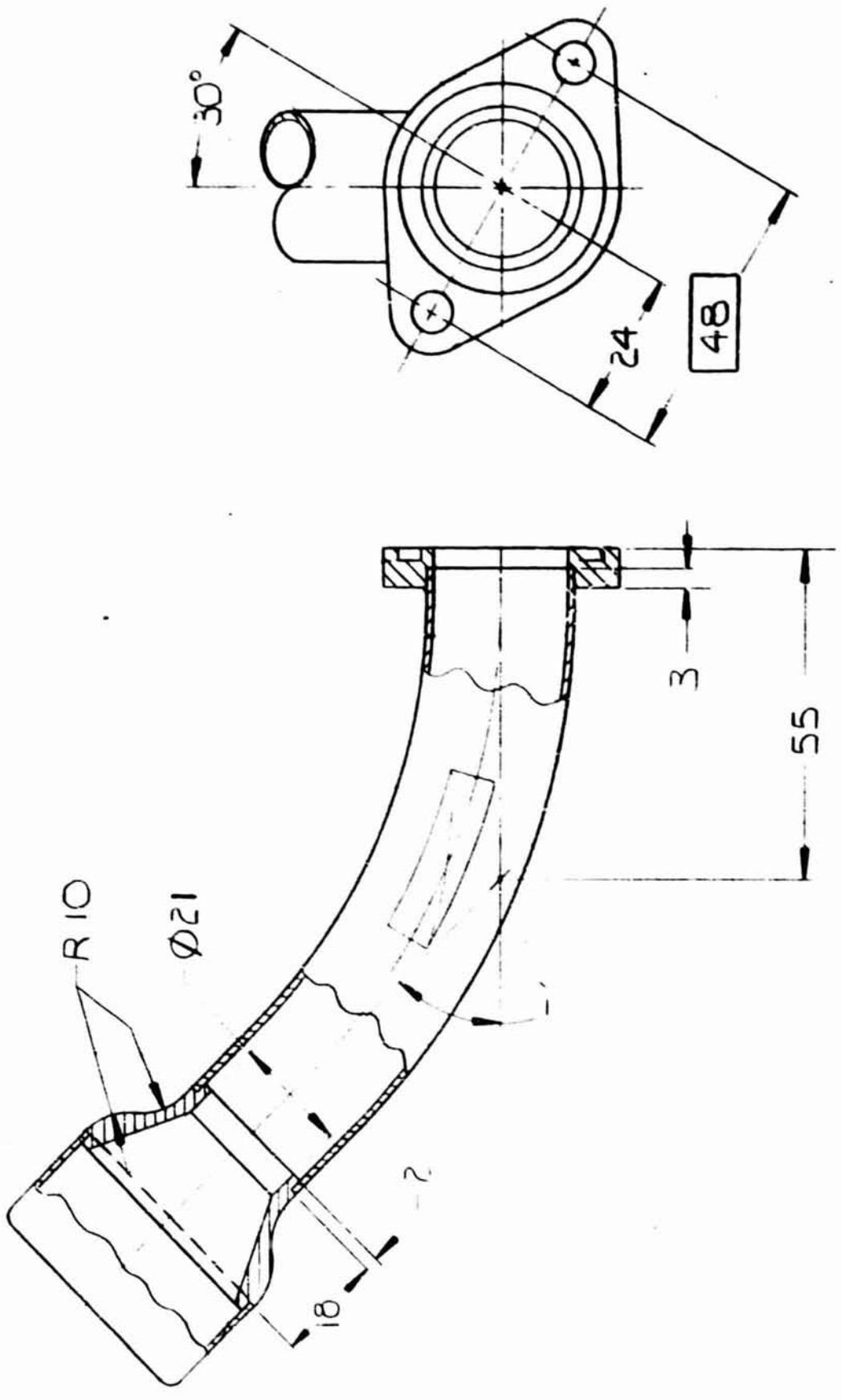

Figure 7B

APPENDIX B

Pt. No. 192
Assembly Oil
Filler Tube

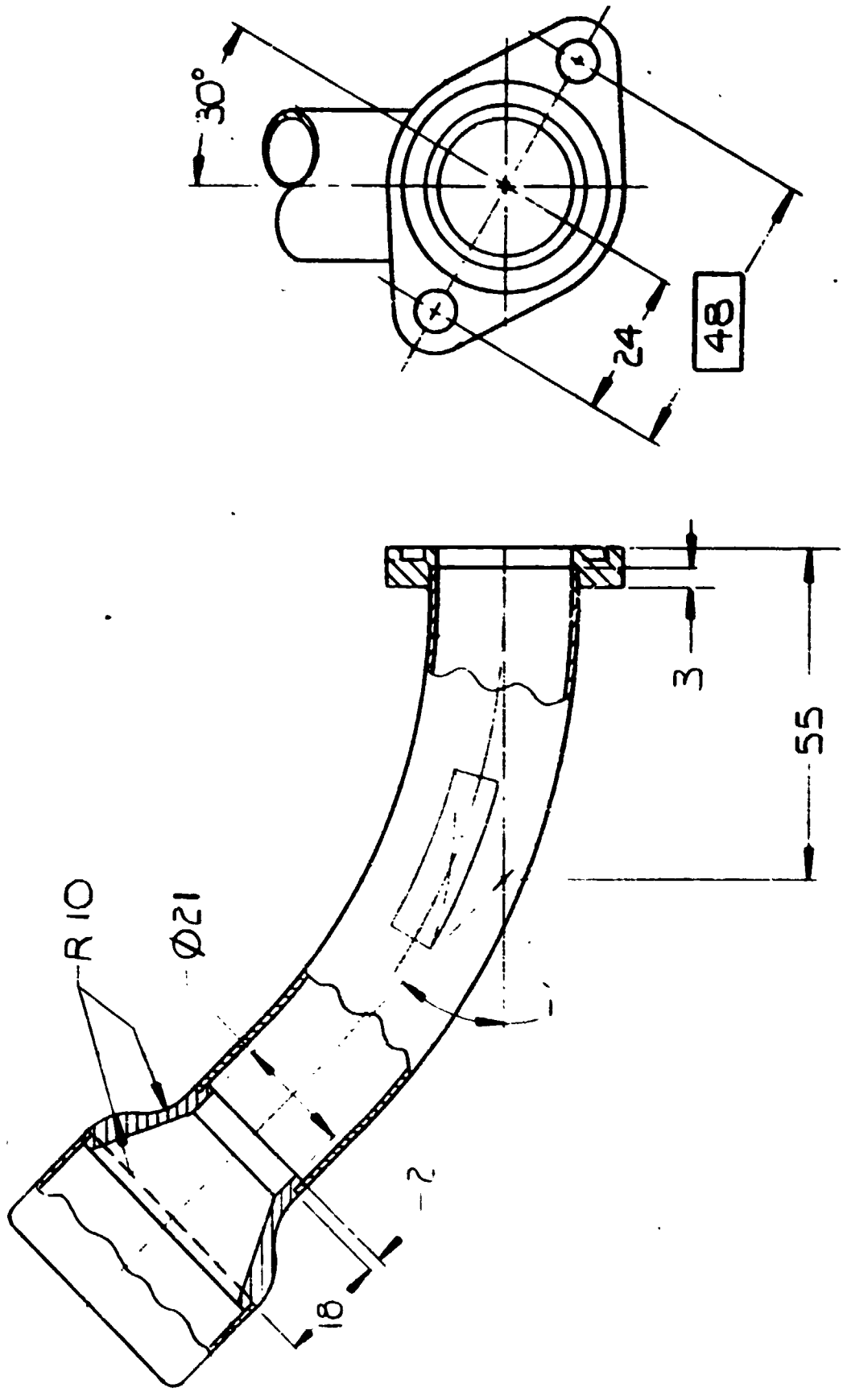

Figure 7B

APPENDIX B

Pt. No. 270
Assembly V.I.G.V.
Actuator

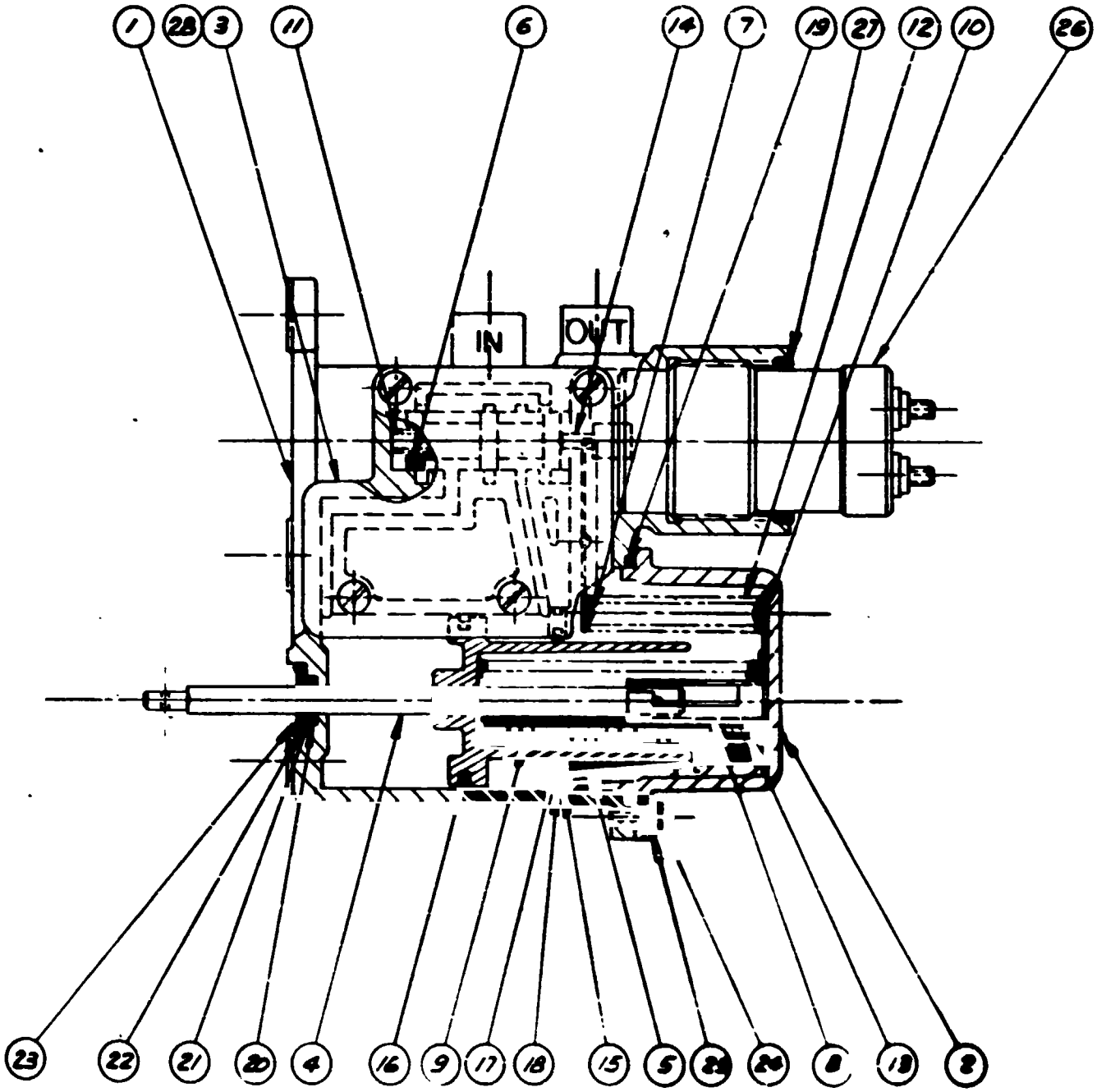

Figure 8B

APPENDIX B

Pt. No. 270
Assembly V.I.G.V.
Actuator

4096174	28	1	———	GASKET	
DOW CORNING SILASTIC 733 RTV OR EQUIV	27	—	———	SEALANT	
3814718	26	1	400673	FORCE MOTOR	
116118	25	7	400140-81	LOCK WASHER	
152711	24	7	400154-134	SCREW	#8-32 x .38 LG.
3814719	23	1	———	RETAINING RING	TRUARC #5005-56
3814724	22	1	———	WASHER	5/16 O.D. x 9/32 I.D. x 1/16 THK.
3814722	21	1	400606-3	RING	
3814723	20	1	400546-26	O-RING	
3814659	19	1	———	O-RING	PRECISIONS O-RING TABLE I # 031
3813875	18	1	———	O-RING	PRECISIONS O-RING TABLE I # 029
3814720	17	1	———	PISTON-RING	1.000 SHAFT DIA JOHN CRANE "CHEMLOY"
3814721	16	1	———	PISTON-RING	1.500 BORE DIA JOHN CRANE "CHEMLOY"
3814717	15	1	482136	SEAL-RING	
3814716	14	1	482137	ADAPTER-MOTOR	
3814715	13	1	482143	SPRING	
3814714	12	1	482142	SPRING	
3814713	11	1	482139	SPRING	
3814712	10	1	482134	GUIDE-SPRING	
3814711	9	1	482133	RETAINER-SPRING	
3814710	8	1	482138	GUIDE-SHAFT	
3814709	7	1	482135	LEVER-ARM	
3814708	6	1	482129	SPOOL-VALVE	
3814707	5	1	482132	RETAINER-SEAL	
3814704	4	1	482128	PISTON-SHAFT ASSY.	
3814703	3	1	482125	PLATE	
3814702	2	1	482124	COVER	
3814701	1	1	482123	BASE	
[illegible] PART NO.	ITEM	REQ	PART NO.	DESCRIPTION	REMARKS (REF.) NO

Figure 8B

APPENDIX B

Pt. No. 297
Assembly Torch
Chamber-Welded

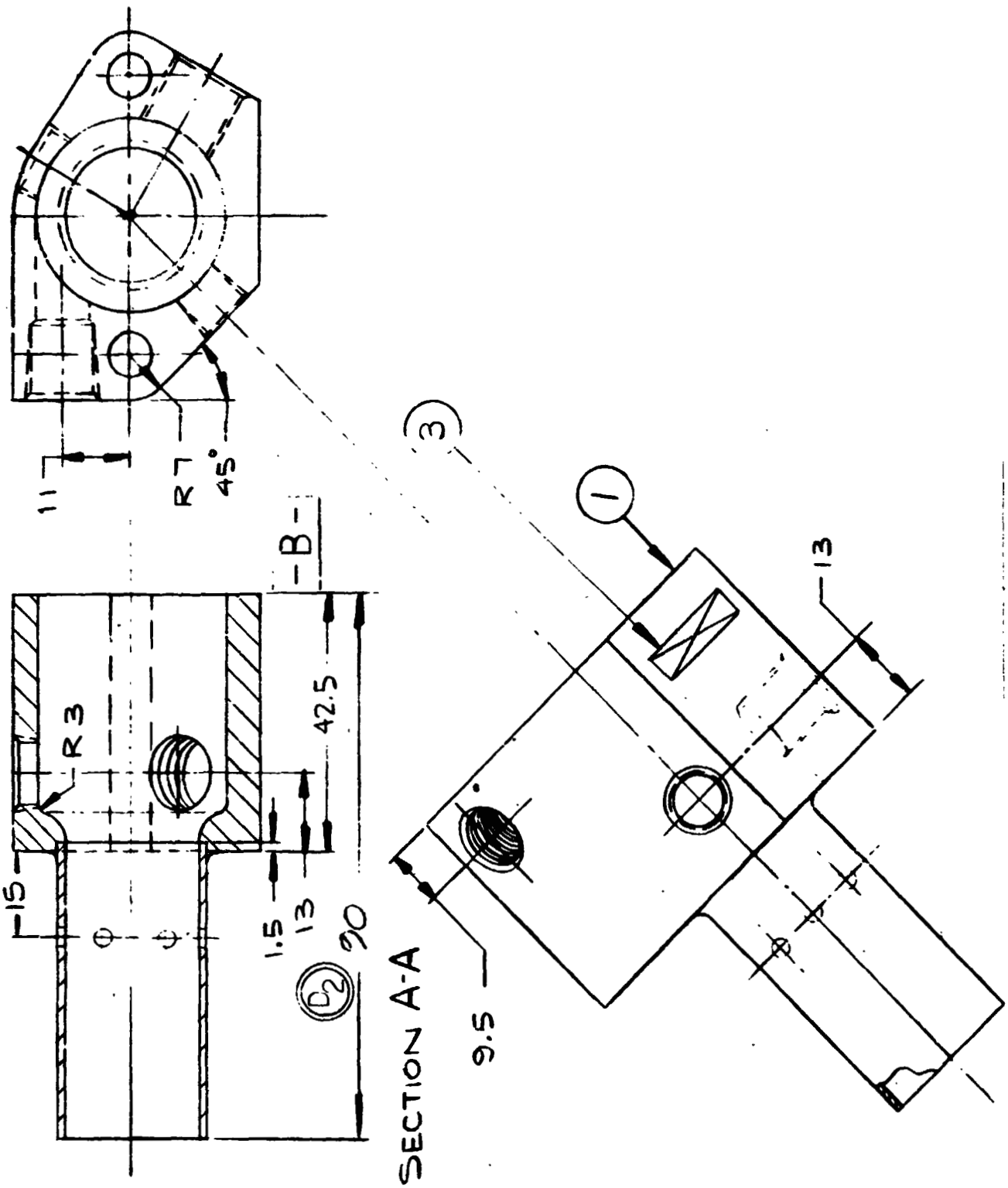

Figure 9B

APPENDIX B

Pt. No. 299
Support Torch
Nozzle

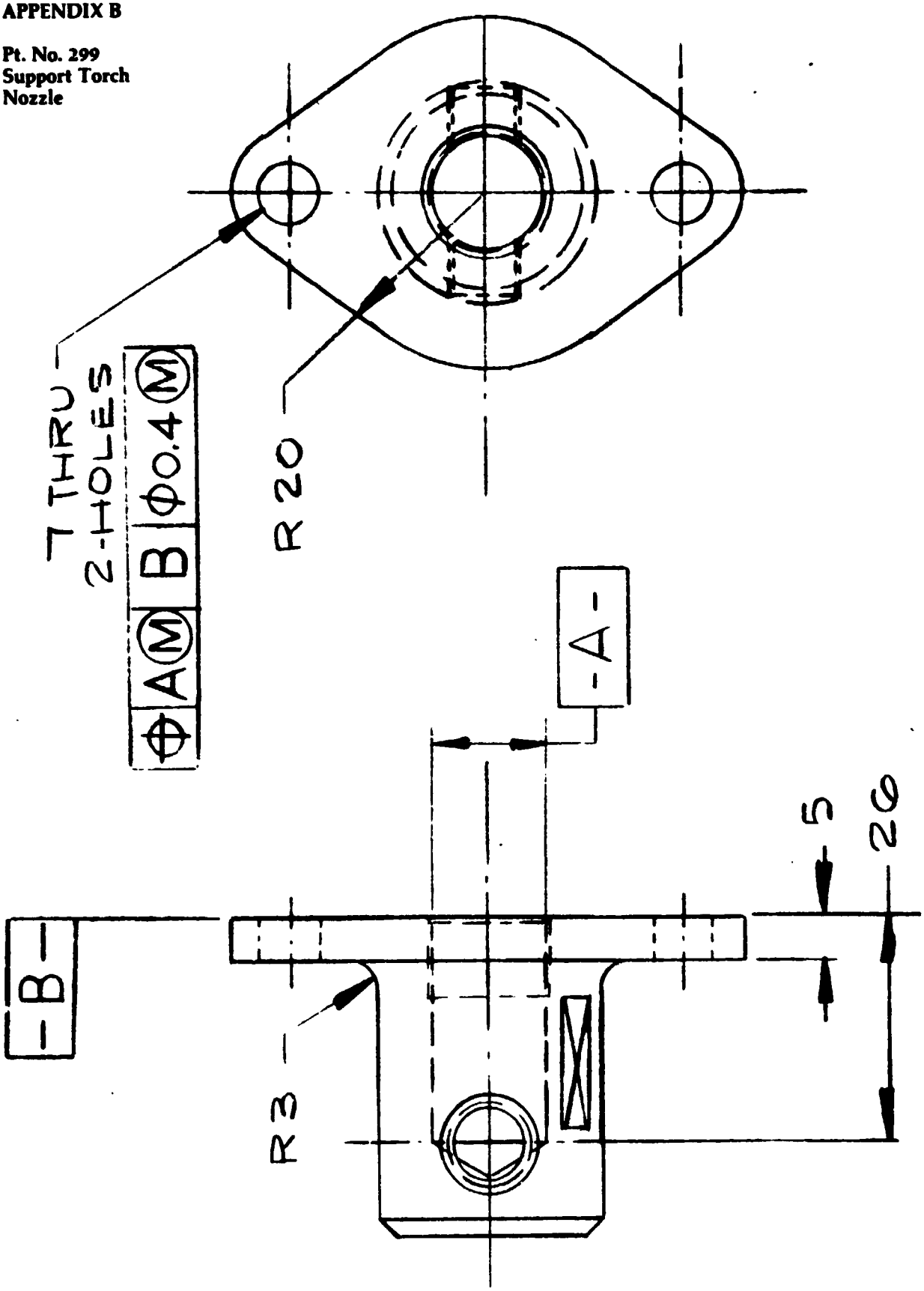

Figure 10B

APPENDIX B

Pt. No. 300
Nozzle Torch

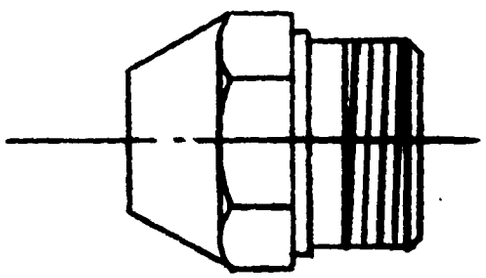

Figure 11B

APPENDIX B

Pt. No. 304
Assembly Premixer
Welded

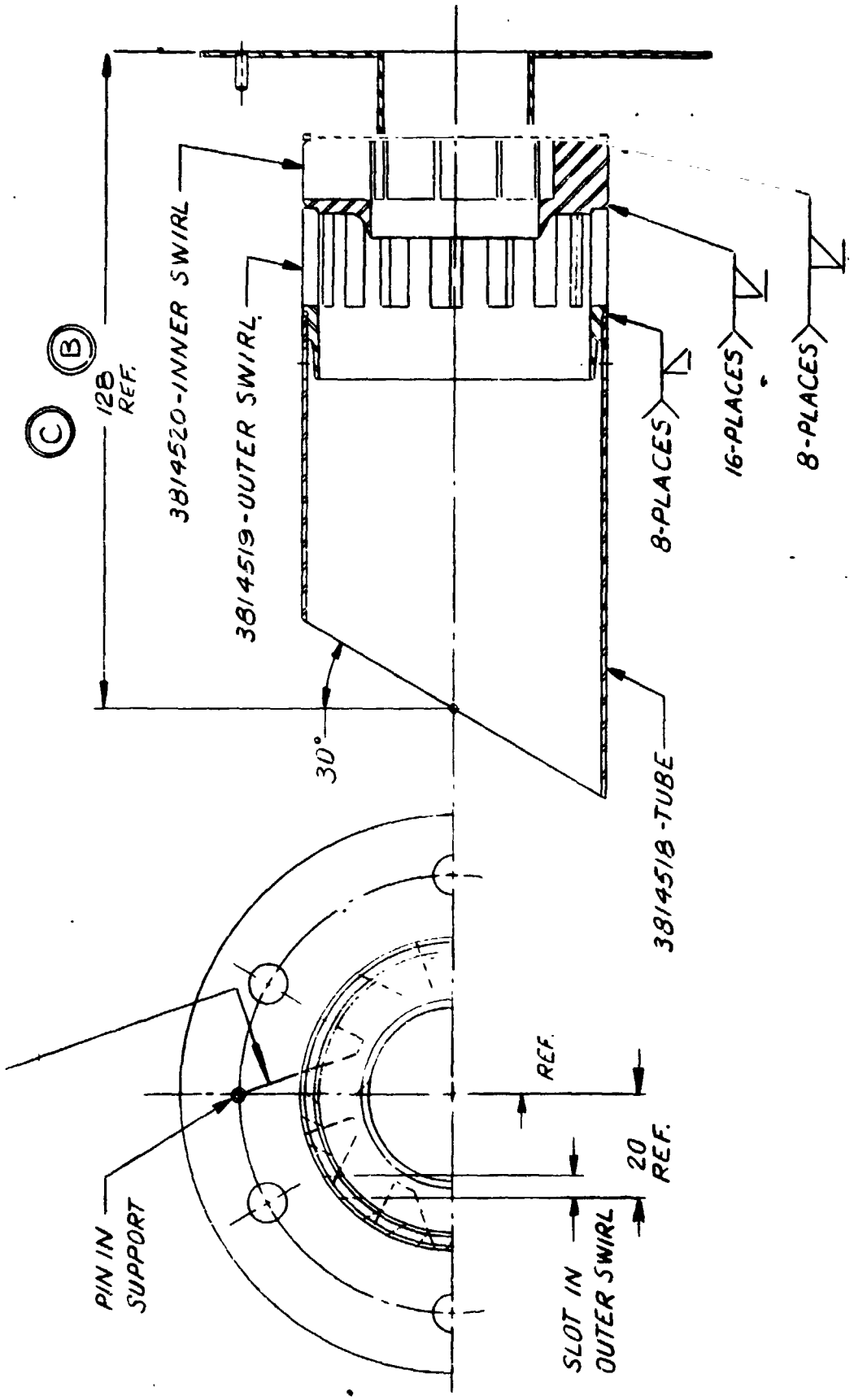

Figure 12B

APPENDIX B

Pt. No. 310
Injector Premixer

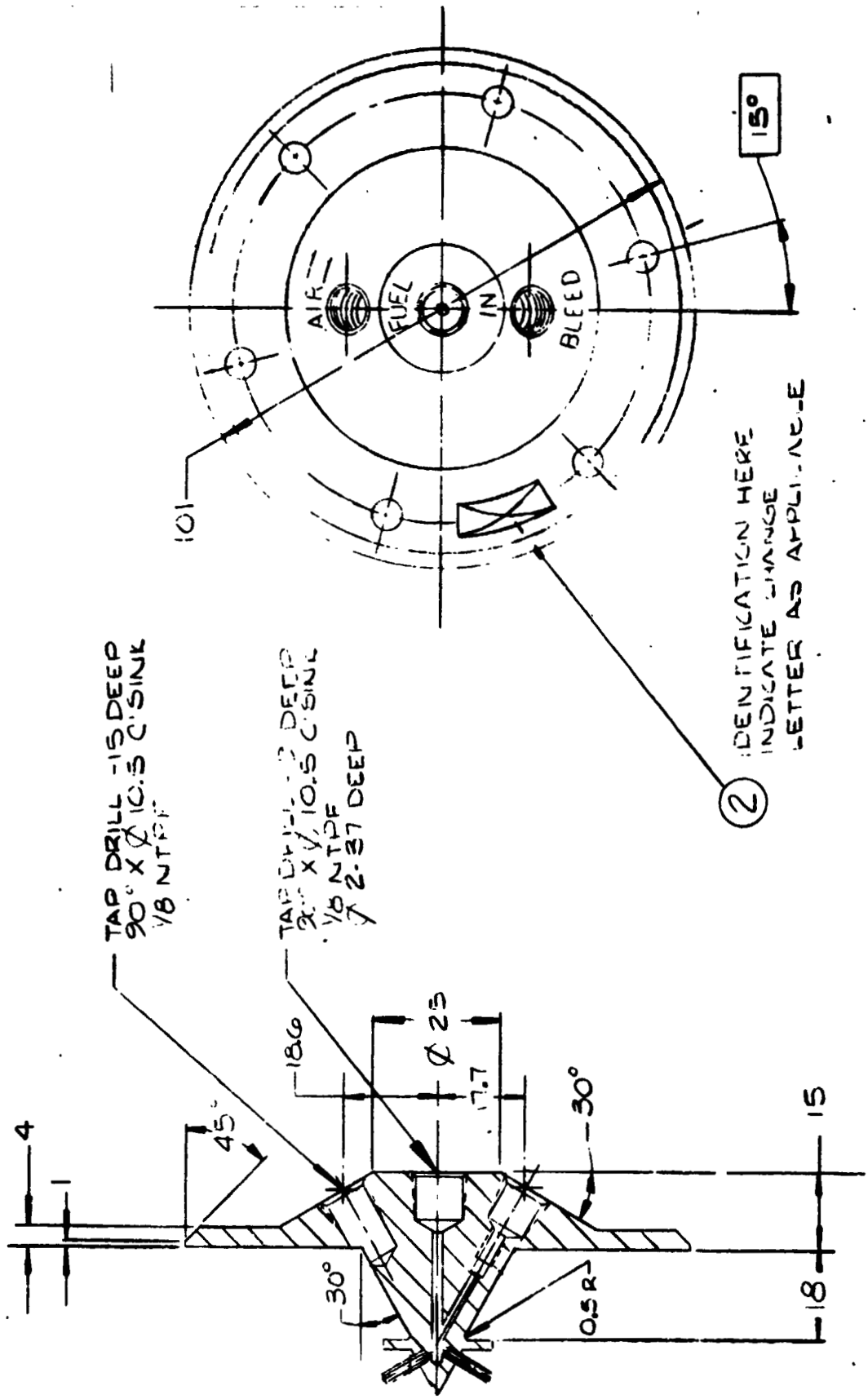

Figure 13B

APPENDIX B

Pt. No. 321
Assembly Fuel
Metering Valve

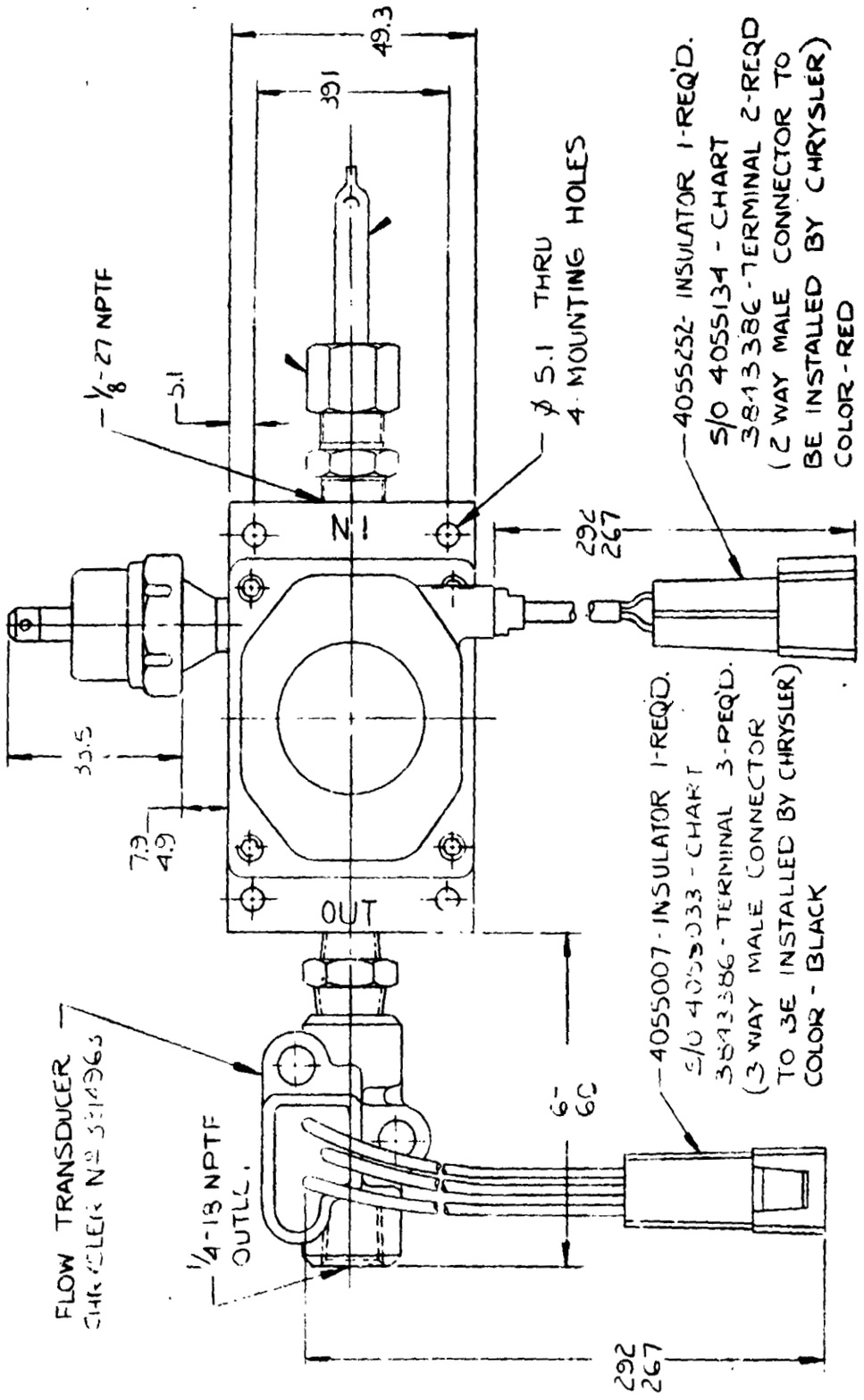

Figure 14B

APPENDIX B

Pt. No. 336 Control, Electronic-Unit (ECU)

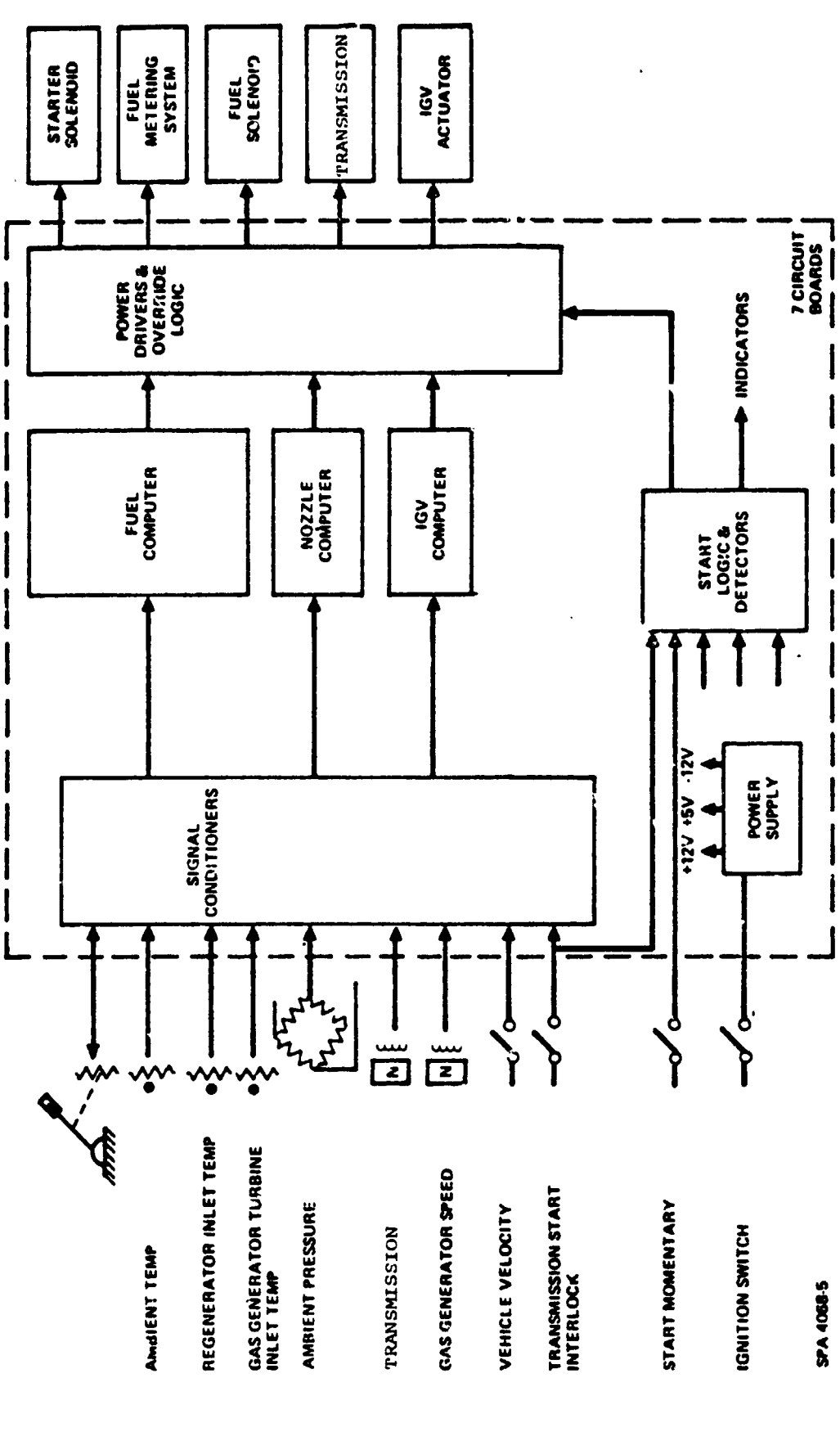

Figure 15B

APPENDIX B

Pt. No. 409
Assembly Air/Oil
Separator

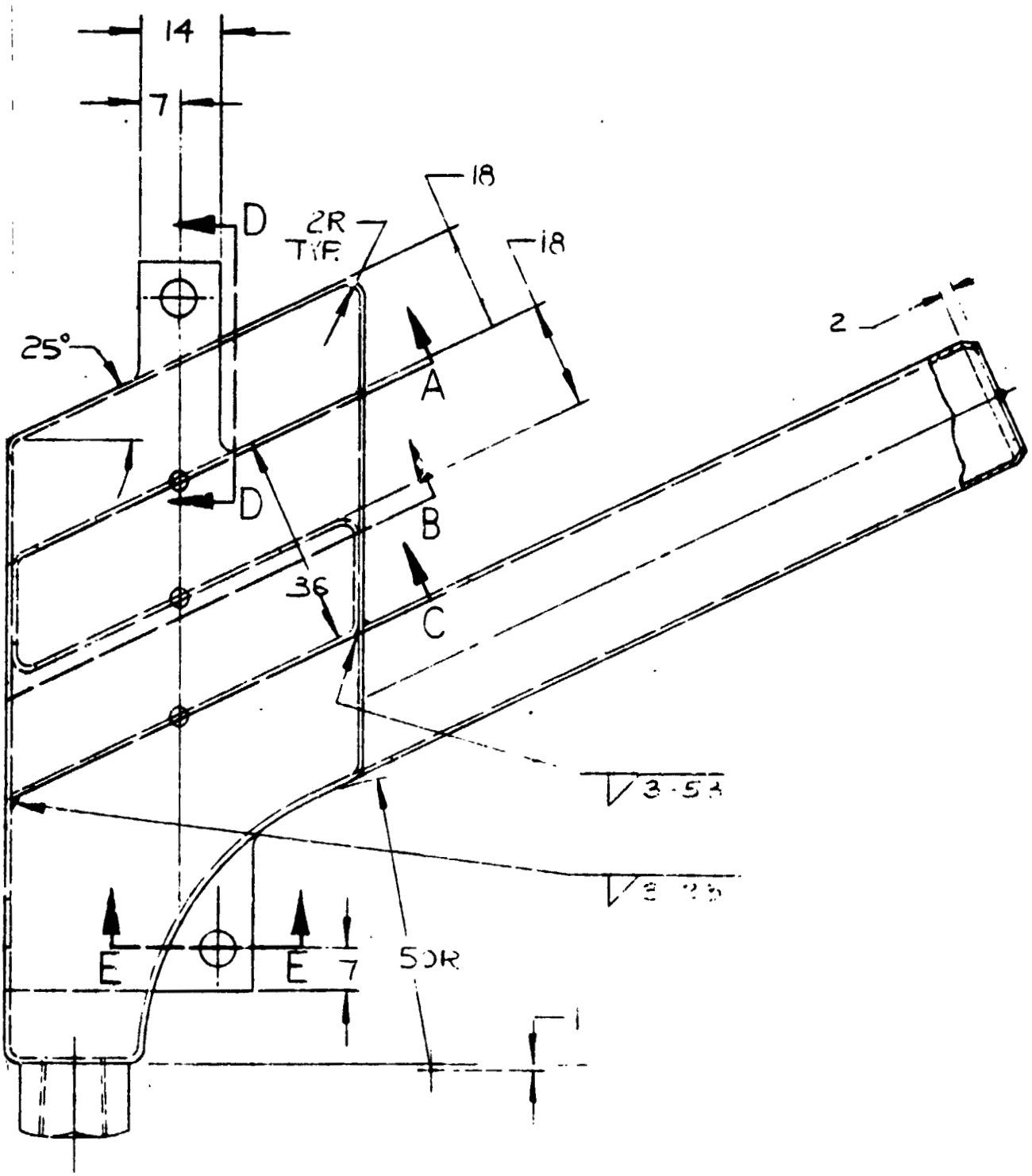

Figure 16B

APPENDIX B

Pt. No. 412
Elbow Air Vent

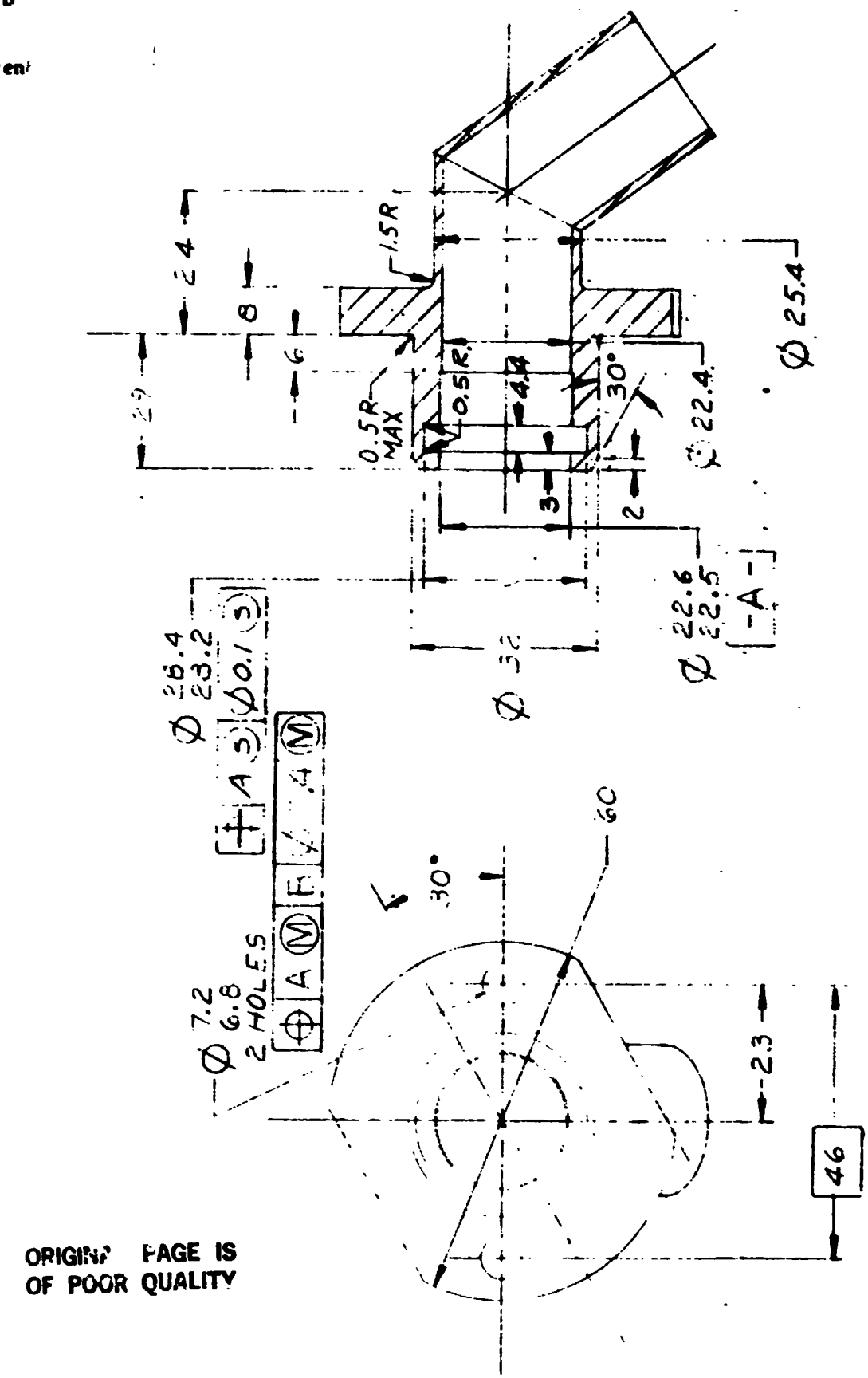

ORIGINAL PAGE IS
OF POOR QUALITY

Figure 17B

APPENDIX B

Pt. No. 417
Assembly
Separator Oil
Drain

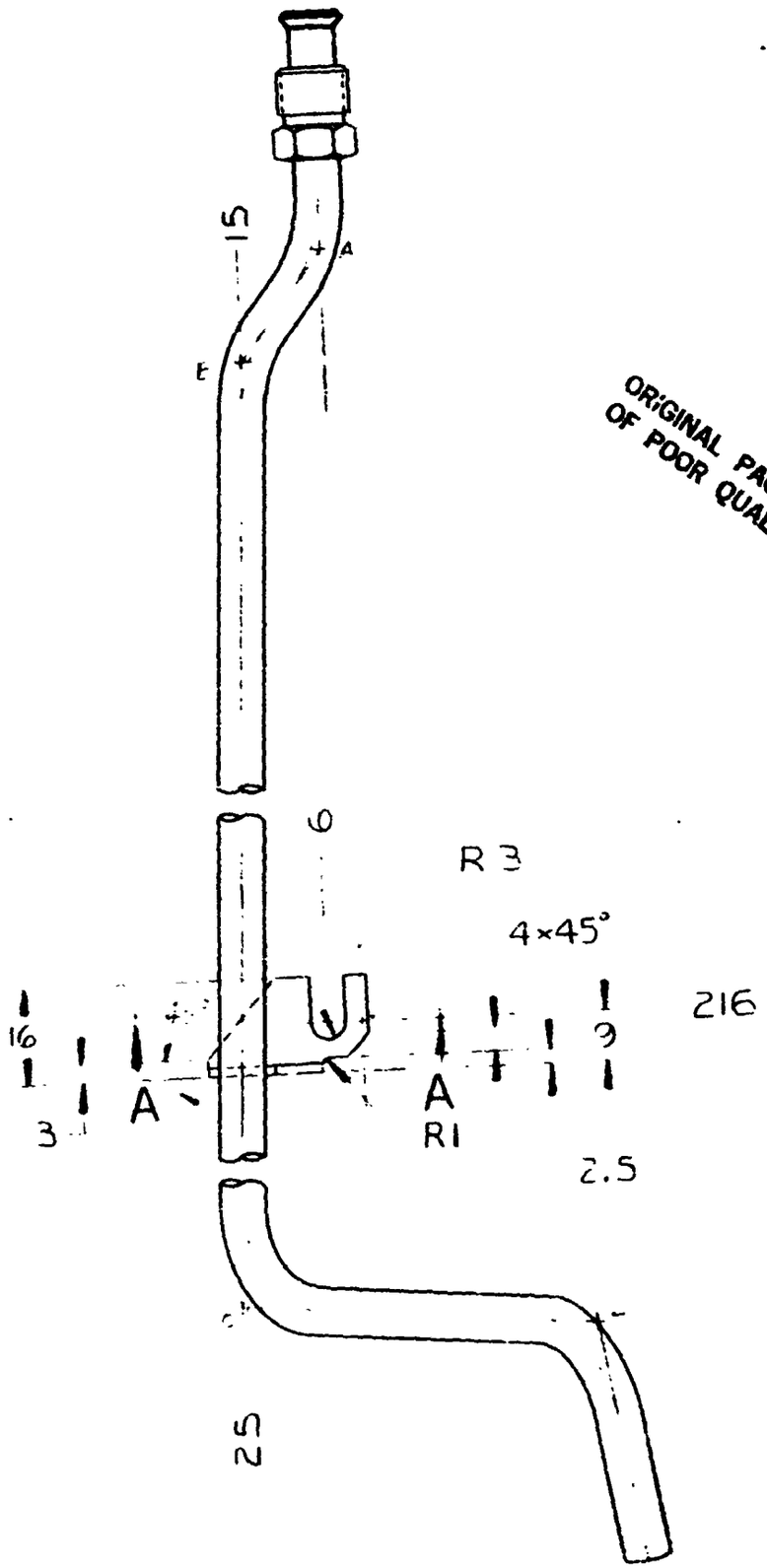

Figure 18B

APPENDIX B

Pt. No. 426
Bracket P/S Pump
Rear

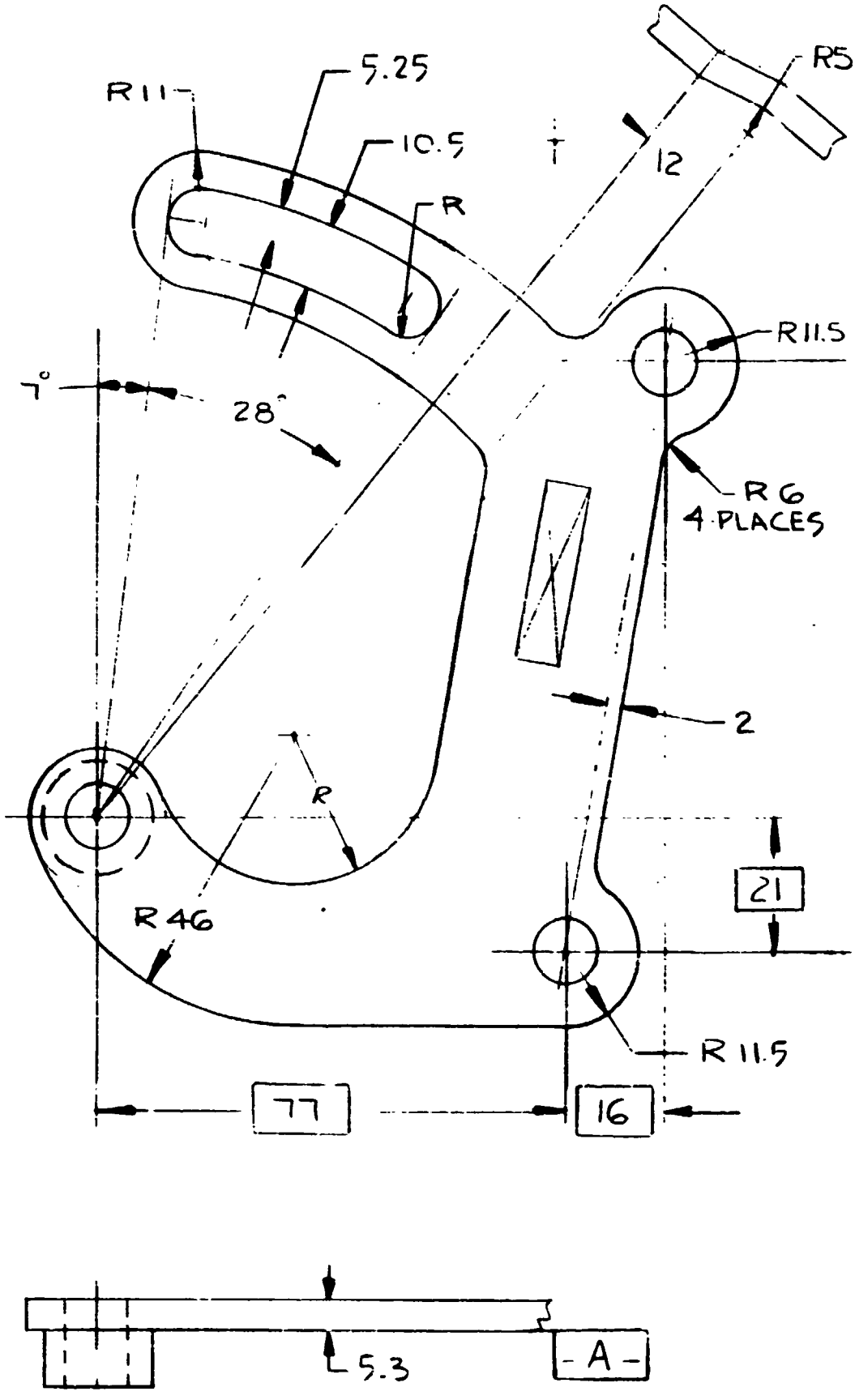

Figure 19B

Chrysler Layout 951-2131
Single-Shaft Gas Turbine Prelim. Layout 2100°F 85 H.P.
Engine Features are Ballooned to Correspond with
Part Numbers on the Preliminary Parts List

APPENDIX C

Details of Program Plan

APPENDIX C

IAGT Program

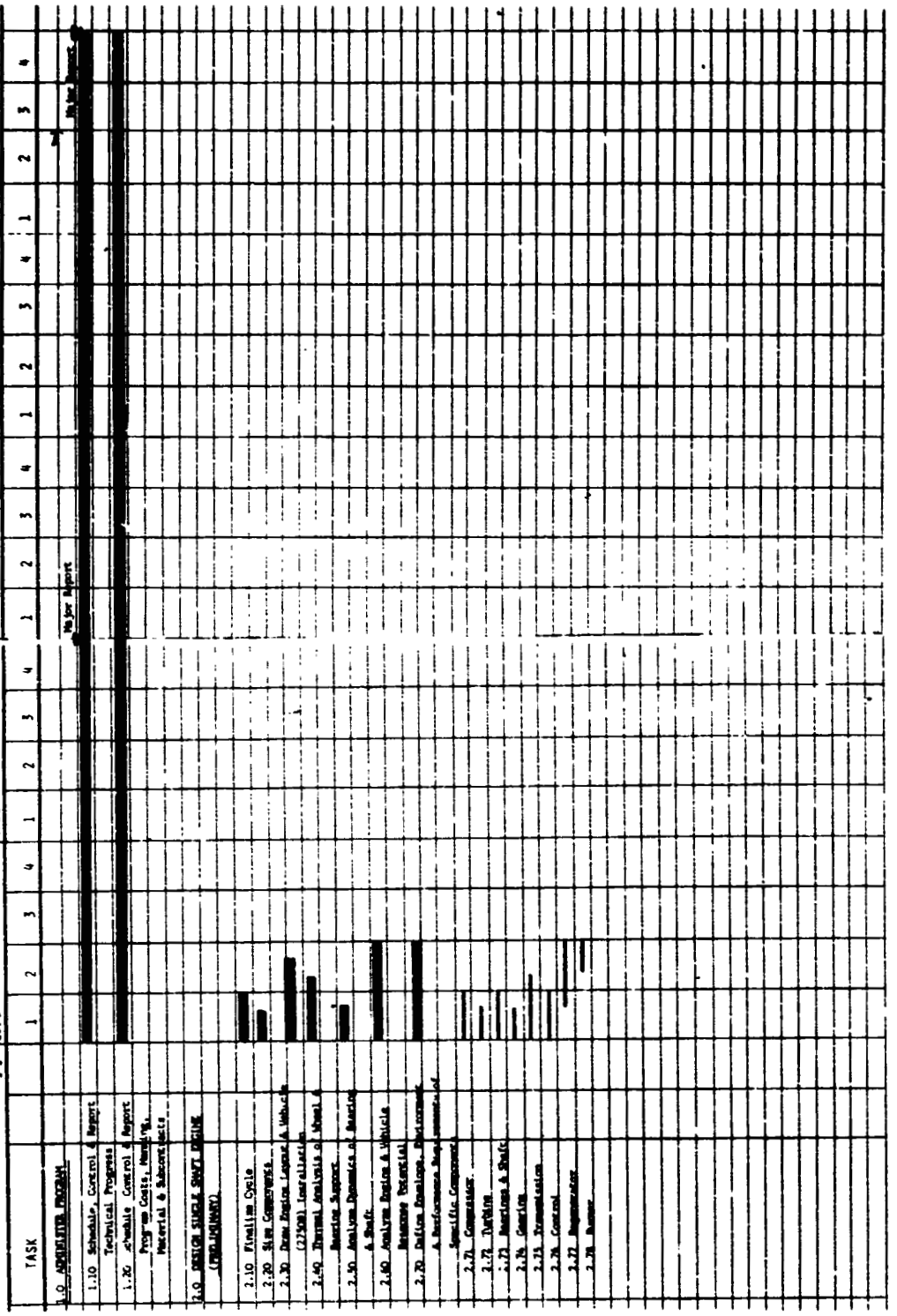

Figure 1C

APPENDIX C

IAGT Program

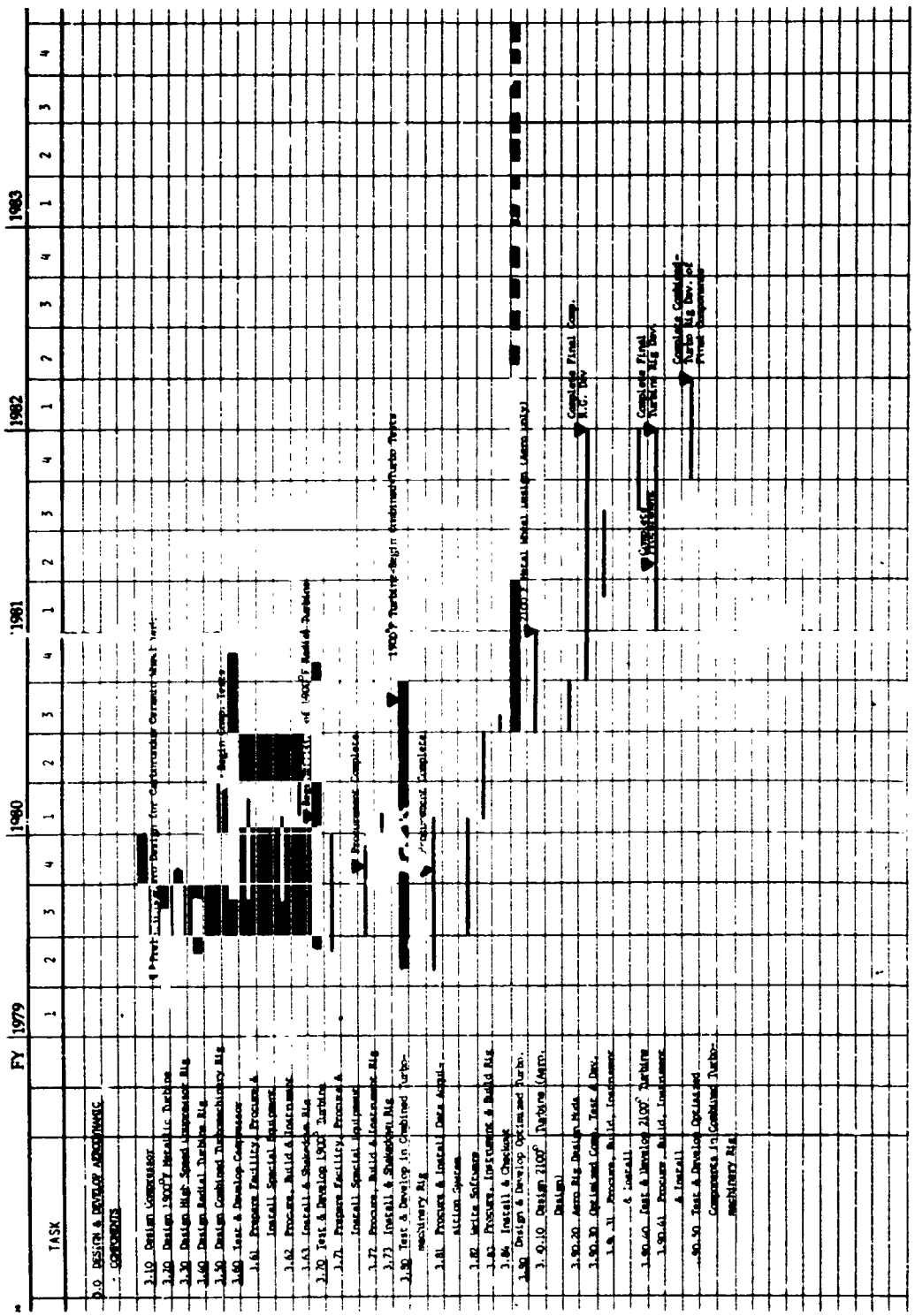

Figure 2C

APPENDIX C

IAGT Program

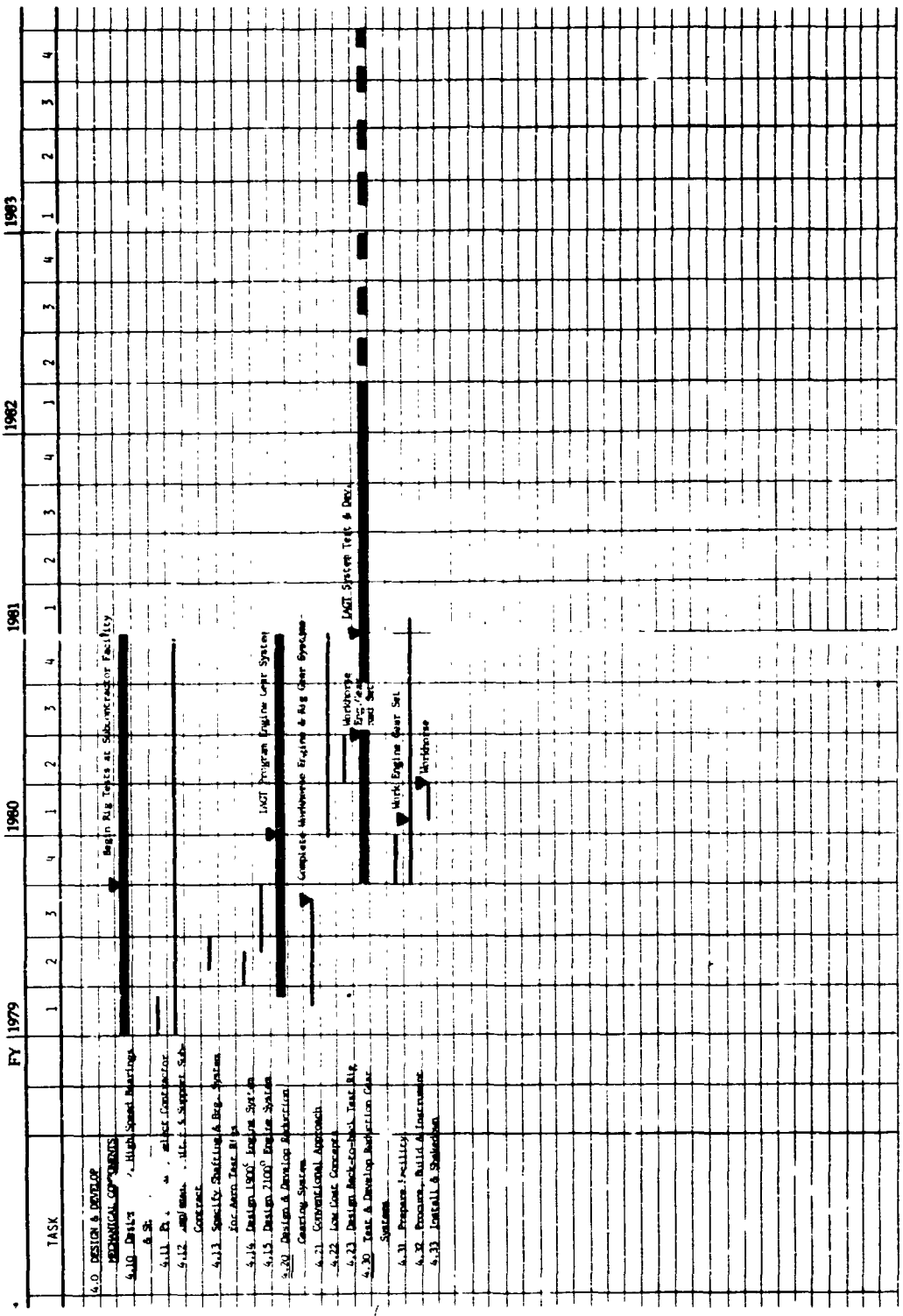

Figure 3C

APPENDIX C

IAGT Program

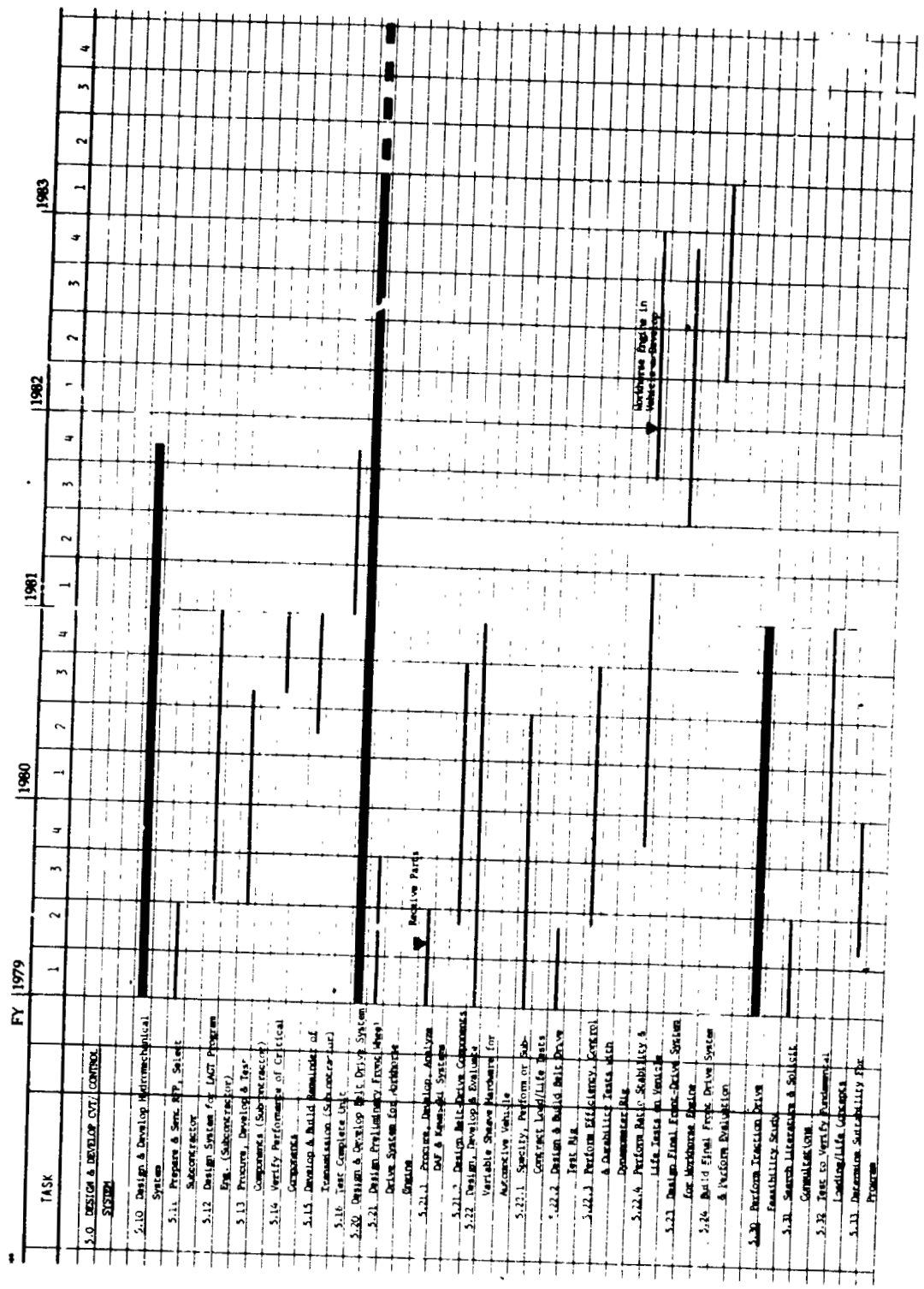

Figure 4C

APPENDIX C

IAGT Program

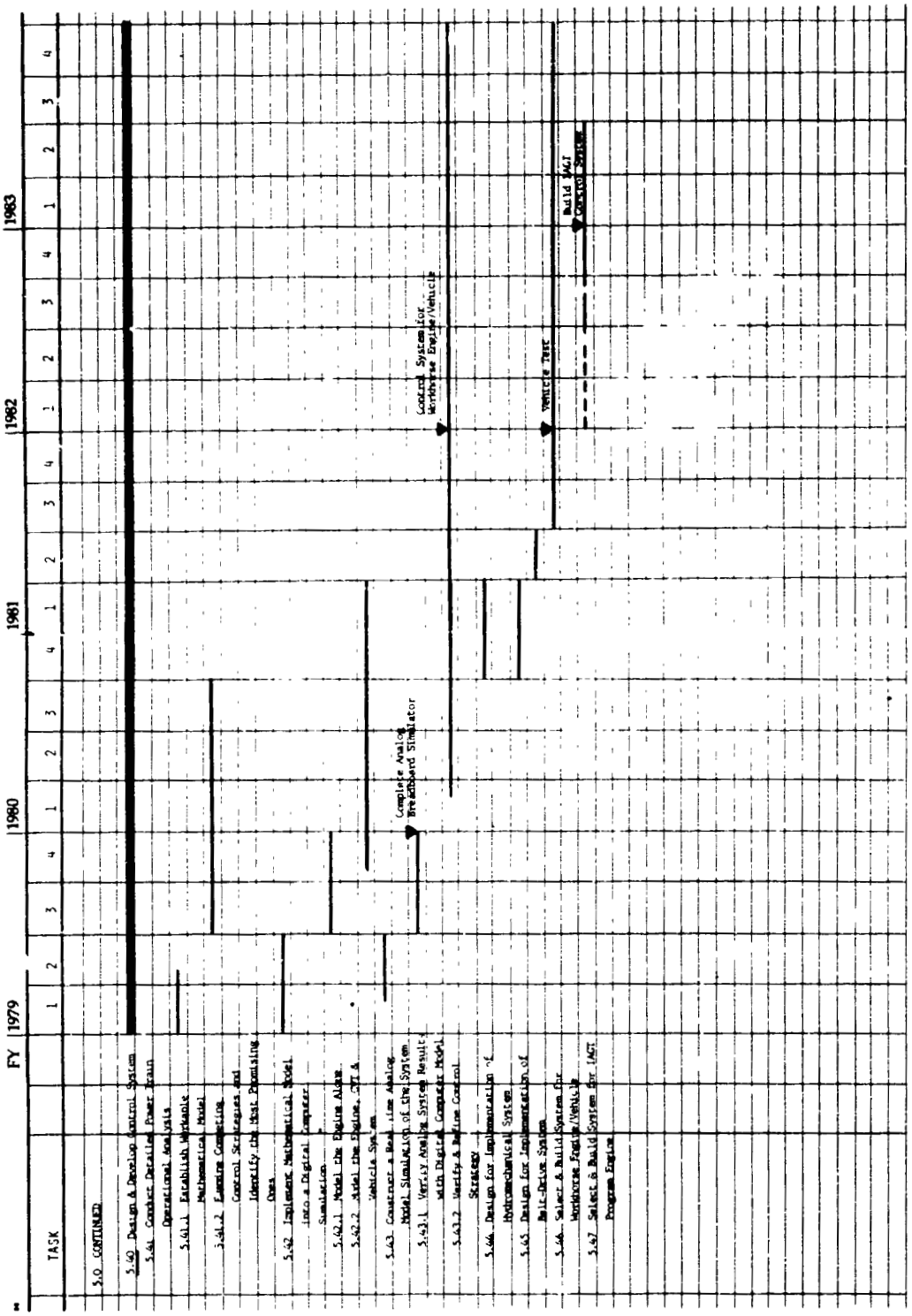

Figure 5C

APPENDIX C

IAGT Program

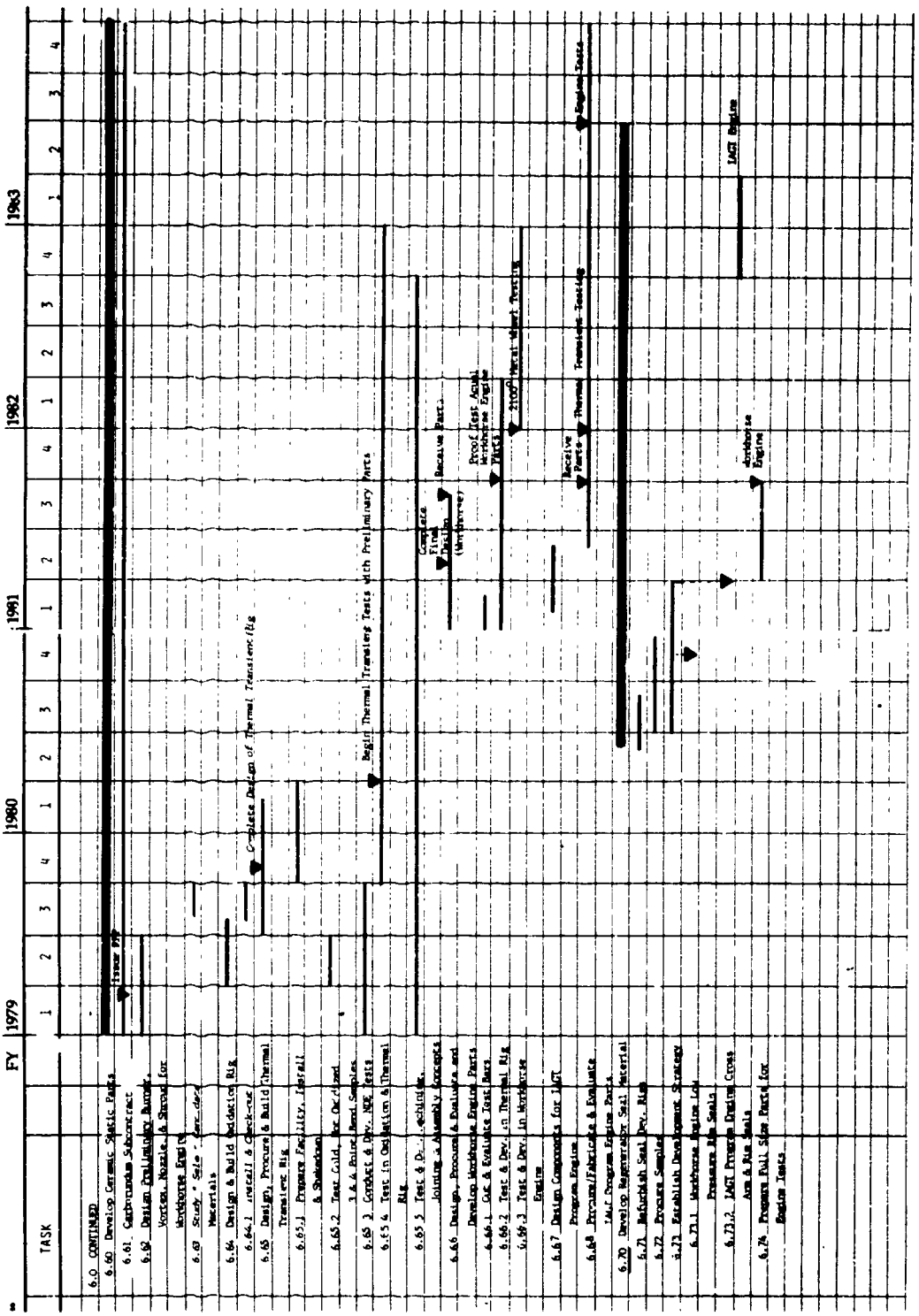

Figure 6C

APPENDIX C

IAGT Program

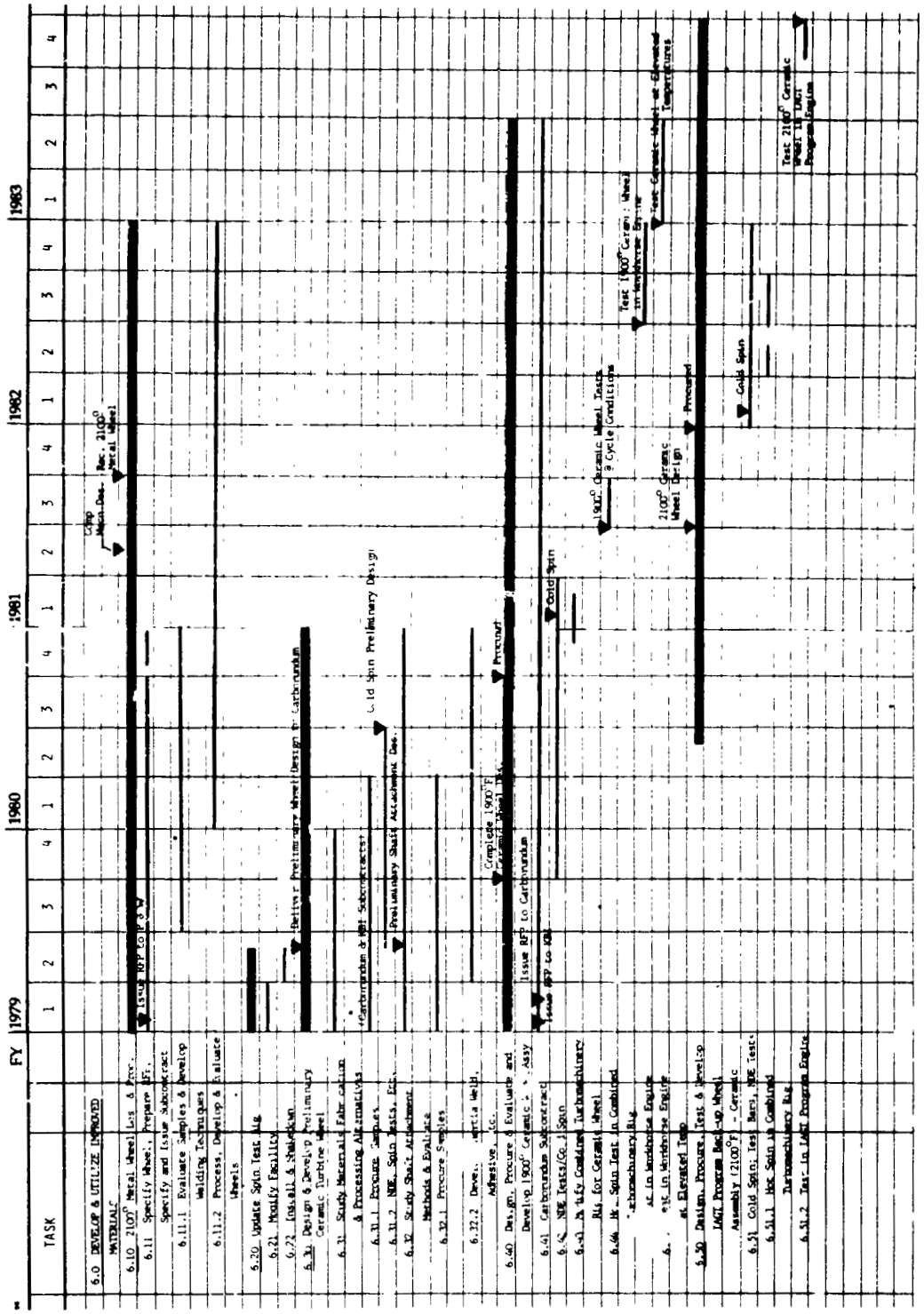

Figure 7C

APPENDIX C

IAGT Program

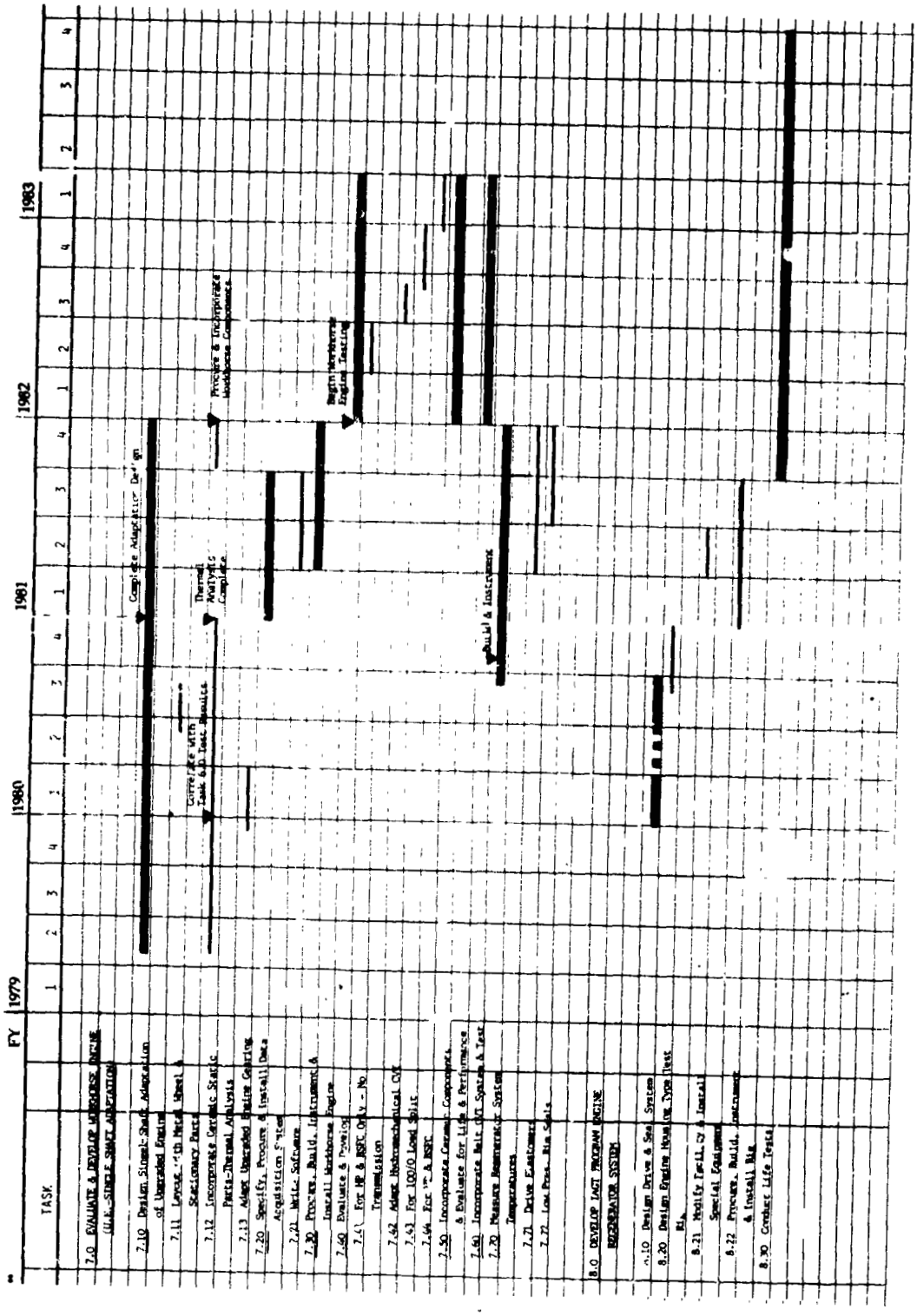

Figure 8C

APPENDIX C

IAGT Program

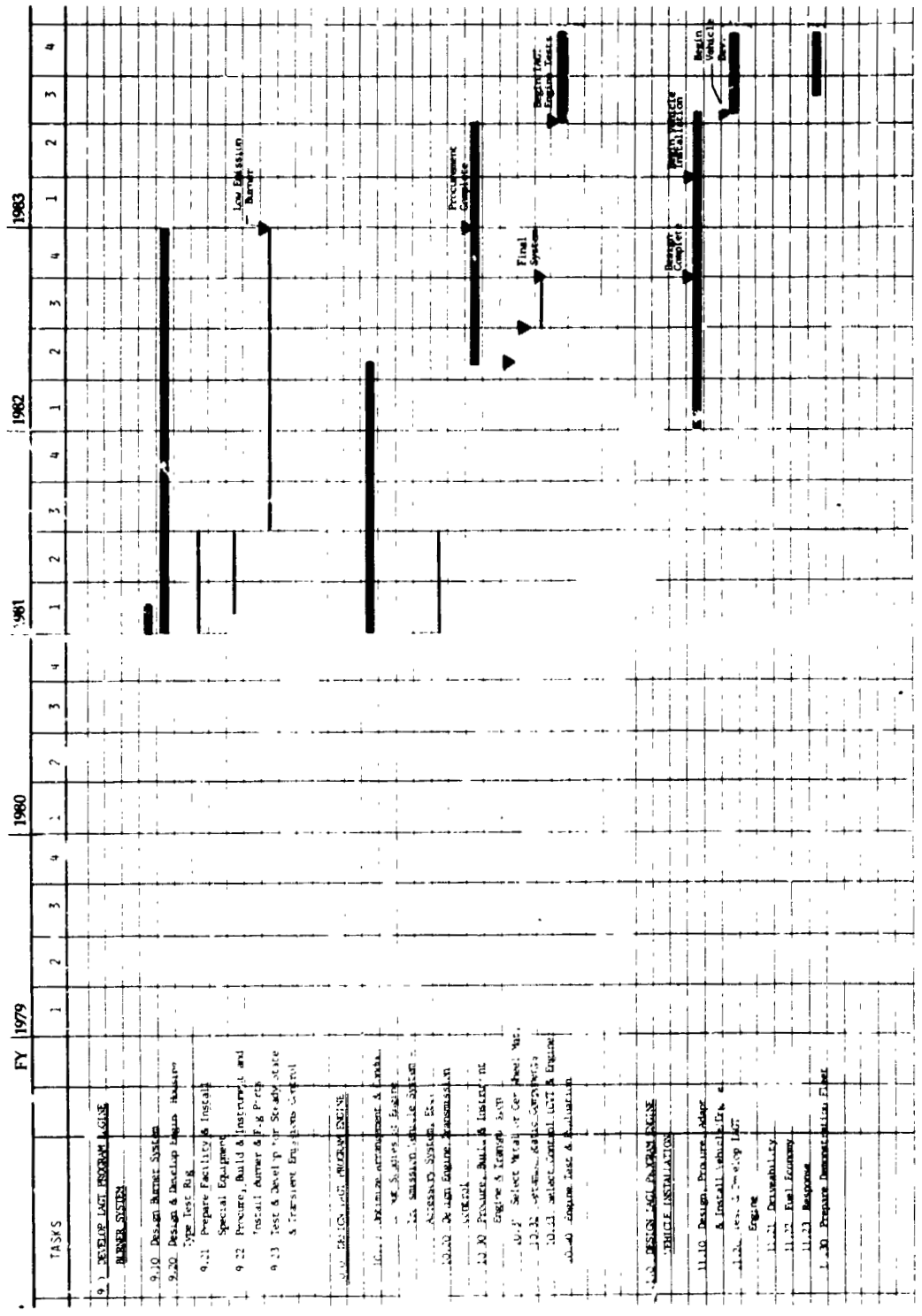

Figure 9C

APPENDIX C

Tasks 1 and 2 - Effort and Material Cost Estimates

Administer Program and Design Single Shaft Engine (Preliminary)

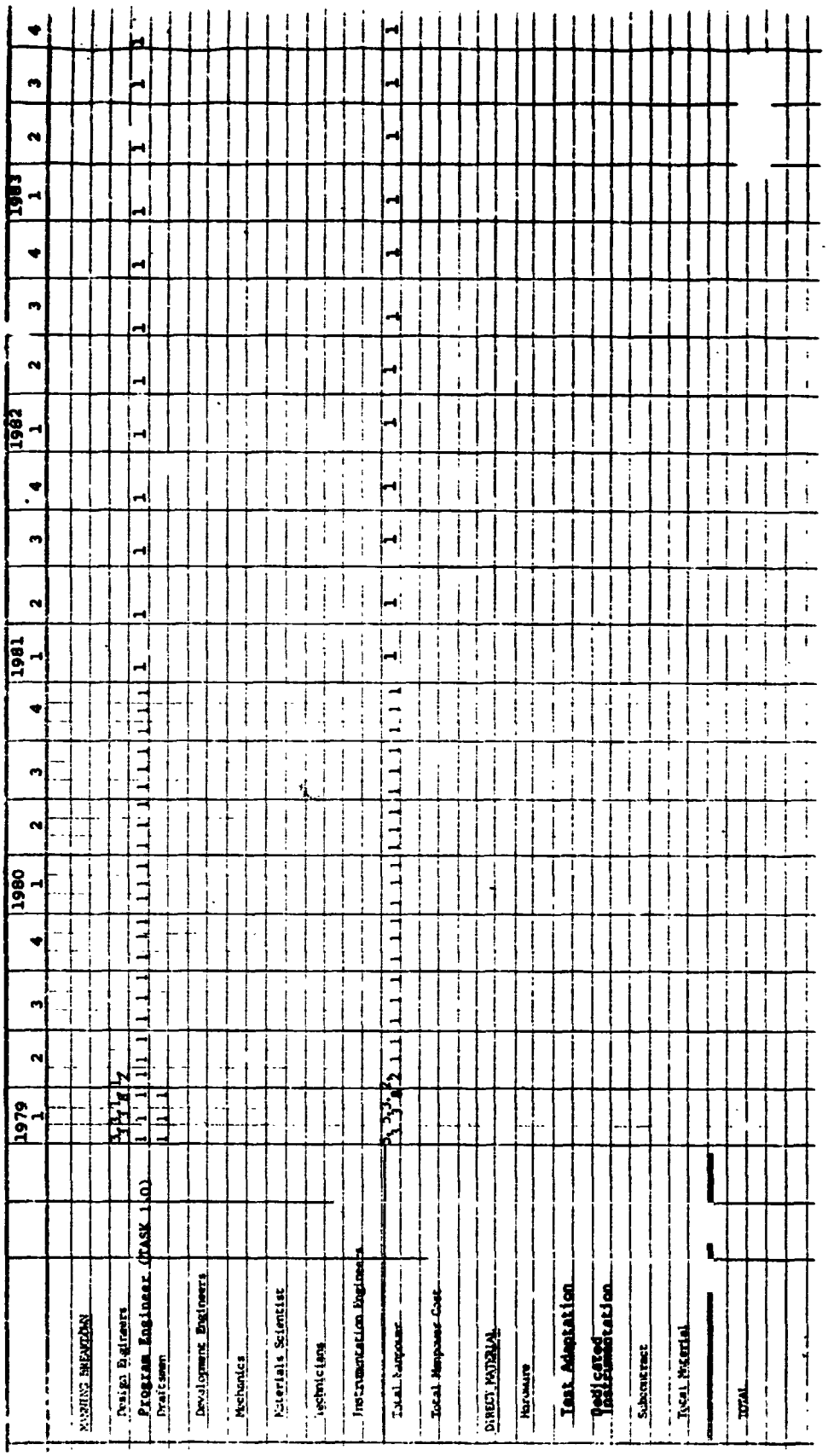

C-3

Figure 10C

APPENDIX C

Task 3 - Effort and Material Cost Estimates

Design and Develop Aerodynamic Components

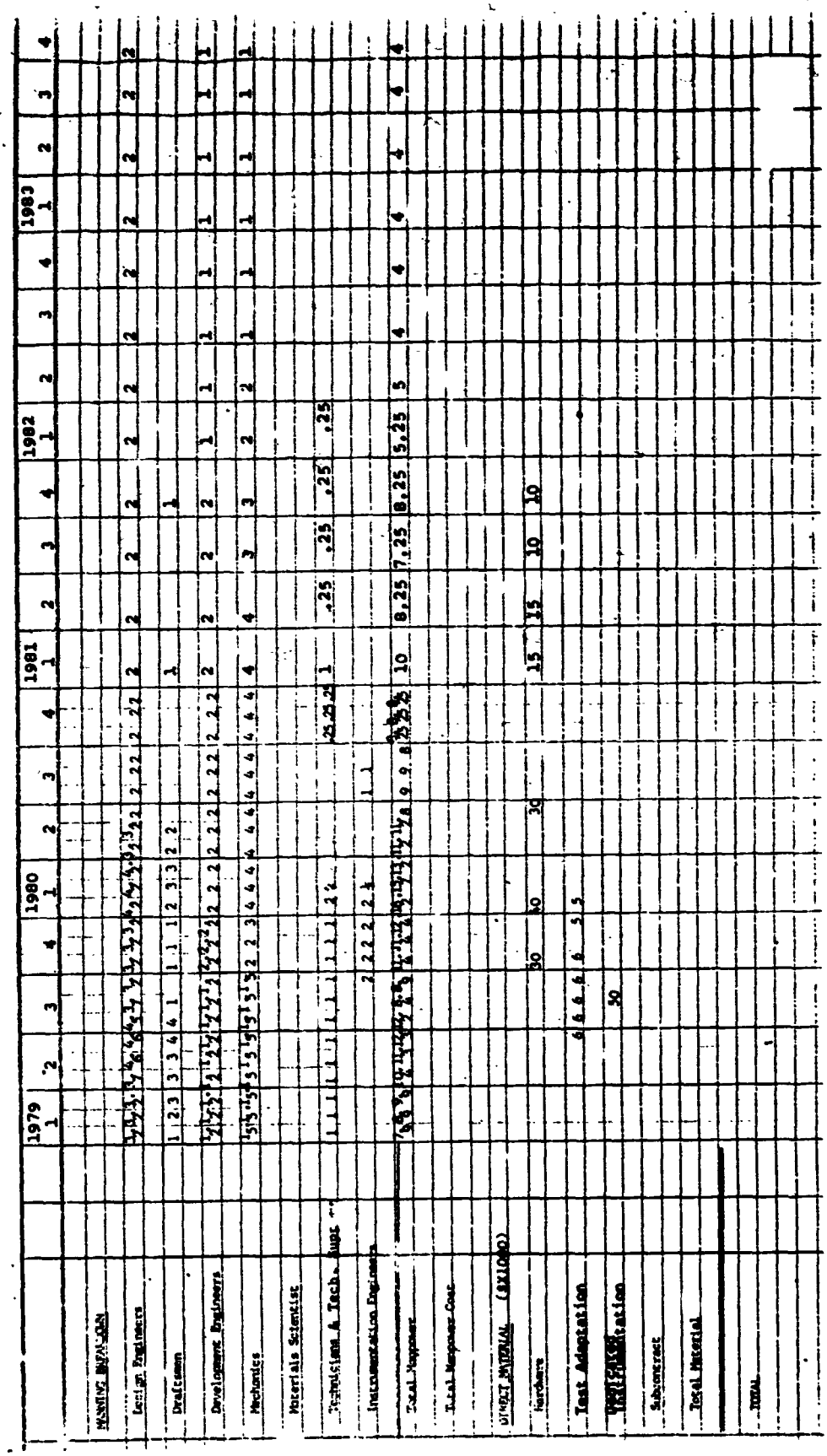

Figure 11C

APPENDIX C

Task 4 - Effort and Material Cost Estimates

Design and Develop Mechanical Components

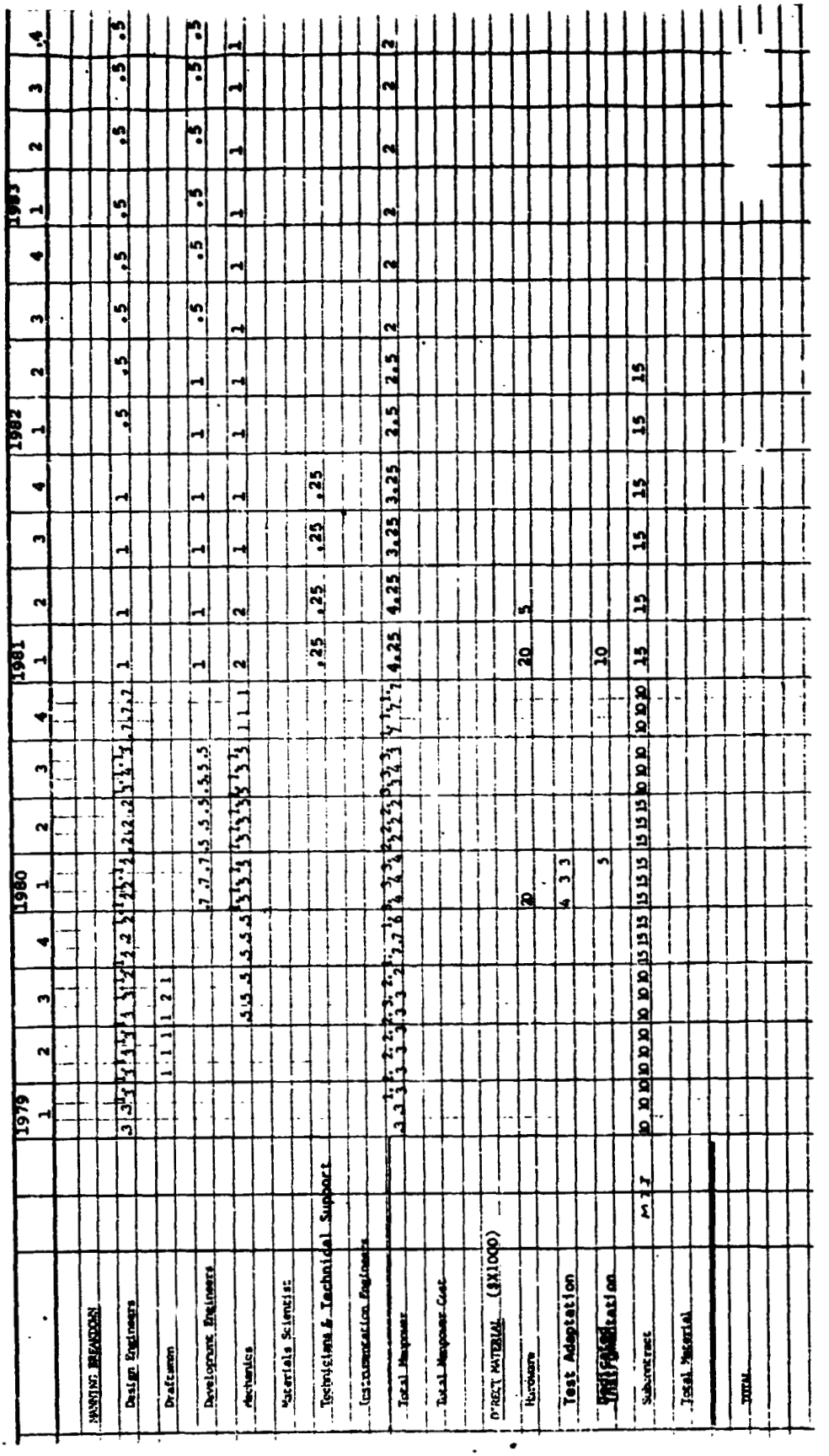

Figure 12C

APPENDIX C

Task 5 - Effort and Material Cost Estimates

Design and Develop CVT/Control System

Figure 13C

APPENDIX C

Task 6 - Effort and Material Cost Estimates

Develop and Utilize Improved Materials

	1979 1	2	3	4	1980 1	2	3	4	1981 1	2	3	4	1982 1	2	3	4	1983 1	2	3	4
MANNING BREAKDOWN																				
Design Engineers	2 2 2 1	1 1 1 1	1 2 2 2	3 3 3 3	2 2 2 1	1 1 1 2	2 2 1 1	1 2 2 2	2.5	2.5	2.5	2.5	1	1	3	3	3	2	3	3
Draftsmen	2 1 1	1 1	2 2	2 2 2	1	1 1 2	2 2 1		3	2	2									
Development Engineers	1 1 1 1	1 1 1 1	1 1 1 1	2 2 2 2	2 2 2 2	2 2 2 2	2 2 2 2	2 2 2 2	2	2	2	2	2	1.5	.5	.5				
Mechanics	1 1 1 1	1 1 1 1	2 2 2 2	2 2 2 2	3 3 3 3	3 3 3 3	3 3 3 3	1 1 1	4	4	4	4	4	4	4	4	2	2	2	2
Materials Scientist	4 4 4 4	4 4 4 4	4 4 4 4	4 4 4 4	4 4 4 4	4 4 4 4	4 4 4 4	4 4 4 4	6	6	6	6	6	6	6	6	6	6	6	6
Technicians* & Support	3 5 5 5	3 3 3	3 3 3	5 5 5	5 5 3	3 3 3	3 3 3	2 2 2 2	4	4	5,5	5,5	4	4	5,5	5,5	5,5	4	4	4
Instrumentation Engineers									1											
Total Manpower	16 15 15 13	12 12 11 10	12 15 15 14	18 18 18 18	17 16 14 13	17 17 18 18	17 15 13 13	11 11 10 10	22.5	20.5	22	20	17	16.5	19	19	16.5	14	15	15
Total Manpower Cost																				
DIRECT MATERIAL ($X1000)																				
Hardware	15	30			25	2 2 2	2 2 2	2 2 2	5	5	5	5	5	5	5	5				
Test Adaptation	5 5 5			10 10 5	5 5 1															
Dedicated Instrumentation	10			5 5																
Subcontracts - P&W RSR Wheel	20 20 20	20 20 20	20 20 20	20 20 20	20 20 20	20 20 20	20 20 20	20 20 20	120	120	120	120	120	120	120	120	30	30	30	30
Subcontracts - Carborundum	40 40 40	40 40 40	40 40 40	40 40 40	40 40 40															
Subcontracts - KBI	6 6 6	6 6 6	6 6 6	6 6 6																
Total Material																				
TOTAL																				

*Constant 3 man Technician Level for Dept. 9410 (4 man beginning FY 1981)

Figure 14C

APPENDIX C

Task 7 - Effort and Material Cost Estimates

Evaluate and Develop Workhorse Engine

Figure 15C

APPENDIX C

Task 8 - Effort and Material Cost Estimates

Develop IAGT Program Engine Regenerator System

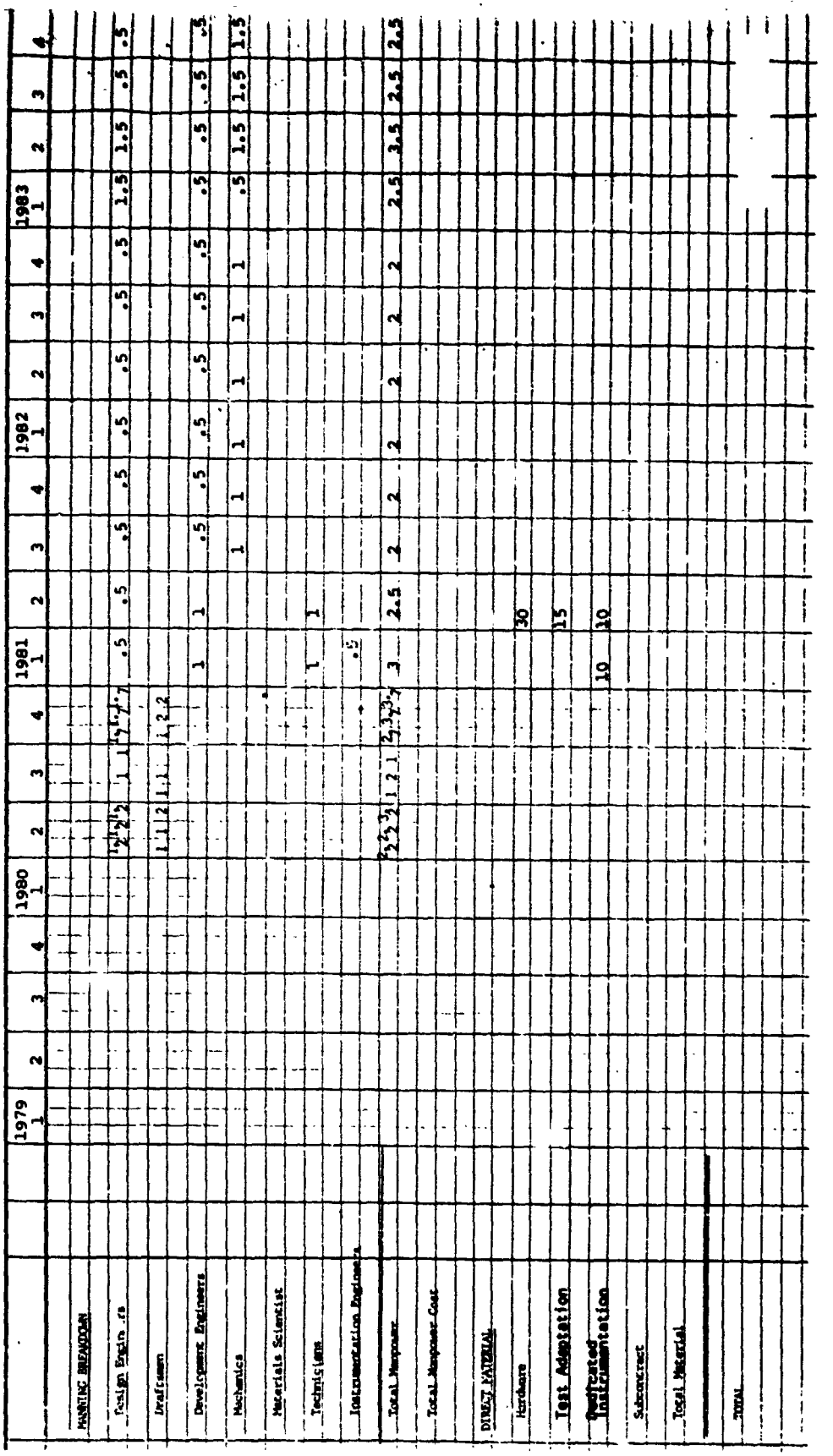

	1979 1	2	3	4	1980 1	2	3	4	1981 1	2	3	4	1982 1	2	3	4	1983 1	2	3	4
MANTNG BREAKDOWN																				
Design Engin..rs					2	2	1	1	.5	.5	.5	.5	.5	.5	.5	.5	.5	1.5	.5	.5
Draftsmen					1	1	1	1												
Development Engineers									1	1	.5	.5	.5	.5	.5	.5	.5	.5	.5	.5
Mechanics											1	1	1	1	1	1	.5	1.5	1.5	1.5
Materials Scientist																				
Technicians									1	1										
Instrumentation Engineers									.5											
Total Manpower					2	2	2	2	3	2.5	2	2	2	2	2	2	2.5	3.5	2.5	2.5
Total Manpower Cost																				
DIRECT MATERIAL																				
Hardware										30										
Test Adaptation										15										
Monitored Instrumentation									10	10										
Subcontract																				
Total Material																				
TOTAL																				

Figure 16C

APPENDIX C

Task 9 - Effort and Material Cost Estimates

Develop IAGT Program Engine Burner System

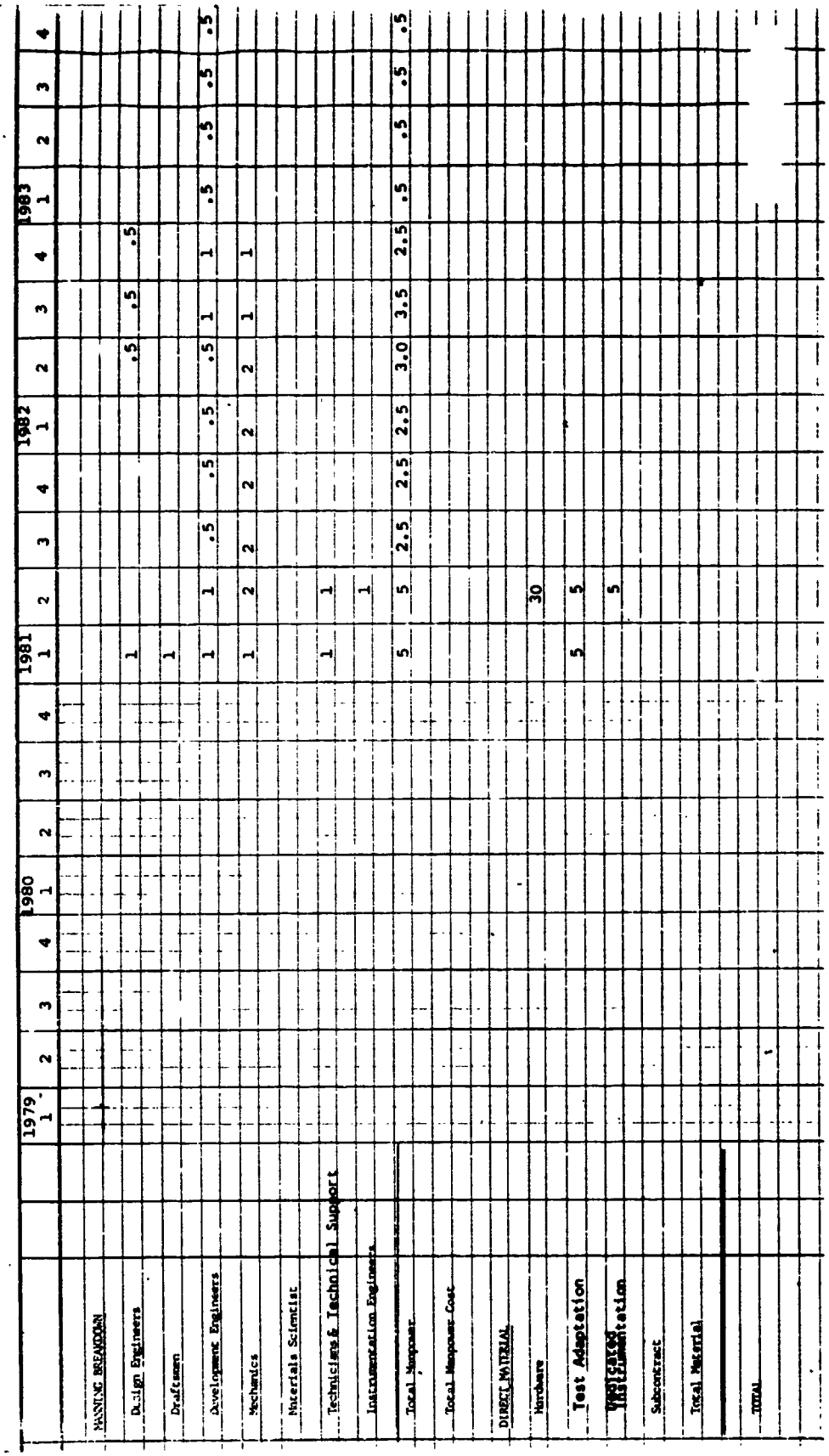

	1979 1	2	3	4	1980 1	2	3	4	1981 1	2	3	4	1982 1	2	3	4	1983 1	2	3	4
MANNING BREAKDOWN																				
Design Engineers									1					.5	1	1	.5	.5	.5	.5
Draftsmen									1											
Development Engineers									1	1	.5	.5	.5	.5	1	1	.5	.5	.5	.5
Mechanics									1	2	2	2	2	2	1	1				
Materials Scientist																				
Technicians & Technical Support									1	1										
Instrumentation Engineers										1										
Total Manpower									5	5	2.5	2.5	2.5	3.0	3.5	2.5	.5	.5	.5	.5
Total Manpower Cost																				
DIRECT MATERIAL																				
Hardware										30										
Test Adaptation									5	5										
Instrumentation										5										
Subcontract																				
Total Material																				
TOTAL																				

Figure 17C

APPENDIX C

Task 10 - Effort and Material Cost Estimates

Design IAGT Program Engine

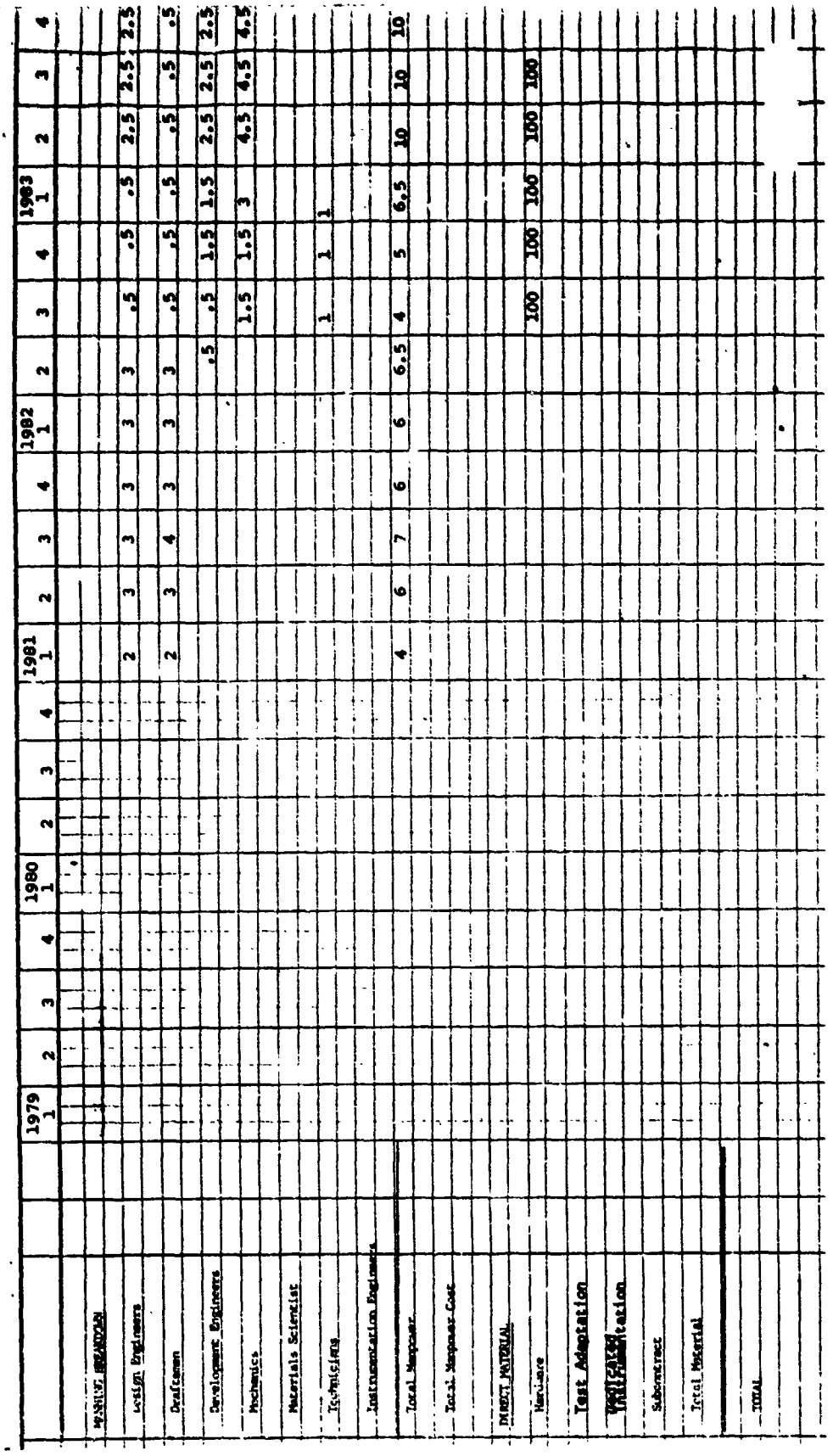

	1979 1	2	3	4	1980 1	2	3	4	1981 1	2	3	4	1982 1	2	3	4	1983 1	2	3	4
MANPOWER BREAKDOWN																				
Design Engineers									2	3	3	3	3	3	.5	.5	.5	2.5	2.5	2.5
Draftsmen									2	3	4	3	3	3	.5	.5	.5	2.5	.5	.5
Development Engineers														.5	.5	1.5	1.5	2.5	2.5	2.5
Mechanics															1.5	1.5	3	4.5	4.5	4.5
Materials Scientist																				
Technicians															1	1	1			
Instrumentation Engineers																				
Total Manpower									4	6	7	6	6	6.5	4	5	6.5	10	10	10
Total Manpower Cost																				
DIRECT MATERIAL																				
Hardware															100	100	100	100	100	
Test Adaptation																				
Modification																				
Subcontract																				
Total Material																				
TOTAL																				

Figure 18C

APPENDIX C

Task 11 - Effort and Material Cost Estimates

Design IAGT Program Engine Vehicle Installation

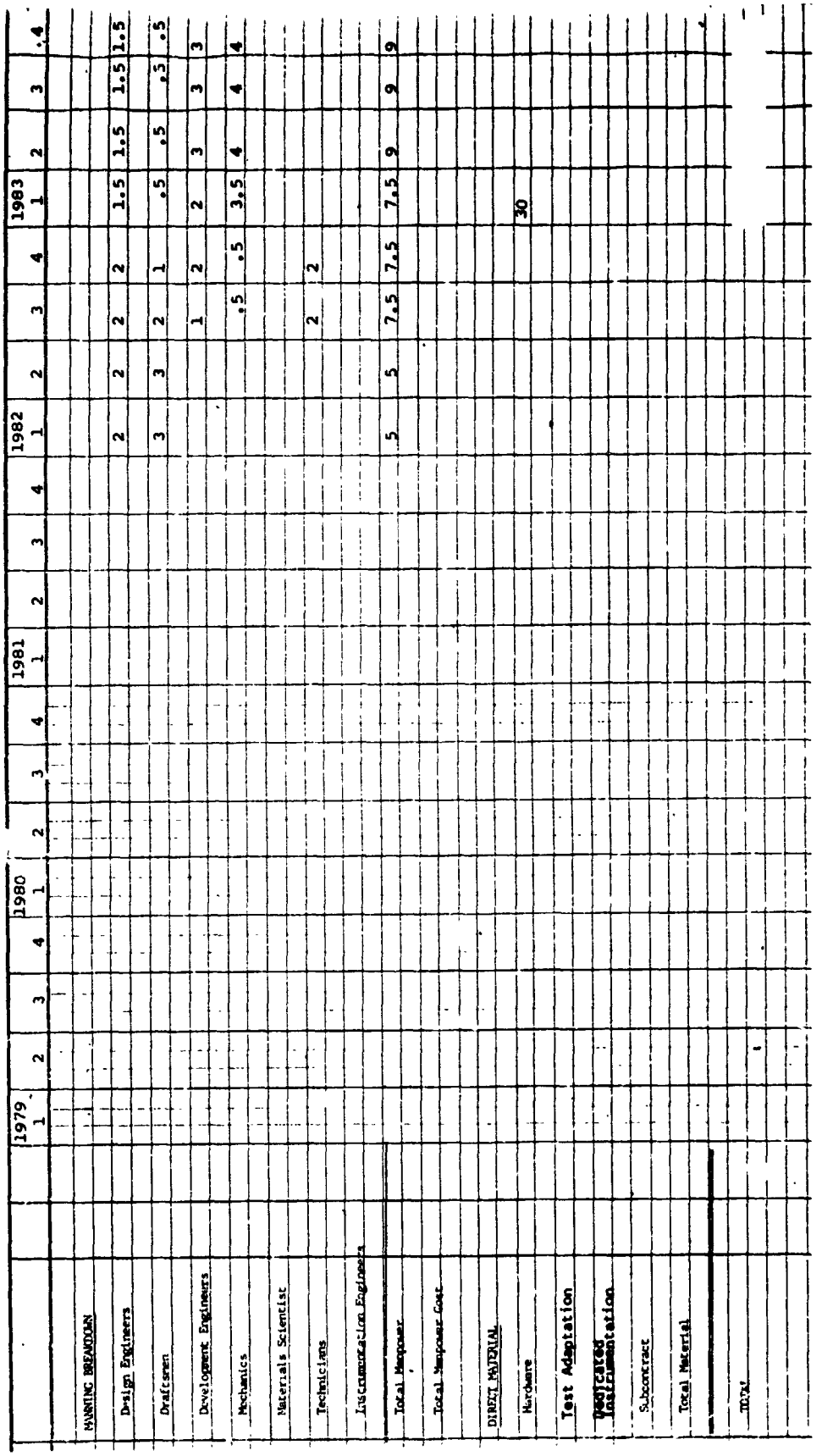

	1979 1	2	3	4	1980 1	2	3	4	1981 1	2	3	4	1982 1	2	3	4	1983 1	2	3	.4
MANNING BREAKDOWN																				
Design Engineers													2	2	2	2	1.5	1.5	1.5	1.5
Draftsmen													3	3	2	1	.5	.5	.5	.5
Development Engineers															1	2	2	3	3	3
Mechanics															.5	.5	3.5	4	4	4
Materials Scientist																				
Technicians															2	2				
Instrumentation Engineers																				
Total Manpower													5	5	7.5	7.5	7.5	9	9	9
Total Manpower Cost																				
DIRECT MATERIAL																				
Hardware																	30			
Test Adaptation																				
Dedicated Instrumentation																				
Subcontract																				
Total Material																				
TOTAL																				

Figure 19C

APPENDIX C

IAGT Program Manning and Material Cost Summary

	1979												1980												1981				1982				1983			
	CONTRACT MONTHS																								QUARTERS											
	1	2	3	4	5	6	7	8	9	10	11	12	13	14	15	16	17	18	19	20	21	22	23	24	1	2	3	4	1	2	3	4	1	2	3	4
Program Eng.	1	1	1	1	1	1	1	1	1	1	1	1	1	1	1	1	1	1	1	1	1	1	1	1	1	1	1	1	1	1	1	1	1	1	1	1
Design Eng.	10	10	9	9	9	9	9	9	10	10	9	9	9	9	9	9	9	9	8	8	8	8	8	8	11	11	11	11	11	11	11	11	11	11	11	11
Draftsmen	5	5	6	7	7	6	6	6	4	4	4	4	4	4	4	4	5	5	5	5	5	5	5	5	7	5	7	5	7	7	2.5	1.5	1	1	1	1
Development Engineer	5.5	5.5	5.5	5.5	5.5	5.5	5.5	5.5	5.5	5.5	6.5	6.5	8	8	8	8	8	8	8	8	8	8	8	8	11	11	11	11	11	11	11	11	11	11	11	11
Machanics	6	6	6	6	6	6	7	7	8	8	8	9	12	12	12	12	12	12	12	12	12	12	12	12	12	18	18	18	18	18	18	18	18	18	18	18
MaterialScientist	4	4	4	4	4	4	4	4	4	4	4	4	4	4	4	4	4	4	4	4	4	4	4	4	6		6	6	6	6	6	6	6	6	6	6
Technicians & Technical Supt	5	7	7	5	5	6	6	6	6	7	7	7	8	8	4	4	4	4	4	4	4	3	3	3	8	7.25	6.75	6.5	4.75	4.5	9	9	7	4.25	4.25	4.25
Instrument Engineer										2	2	2	2	.5											3.5	3	2									
Total	36.5	38.5	38.5	37.5	37.5	37.5	38.5	38.5	38.5	42.5	41.5	42.5	48	46.5	42	42	43	43	42	42	42	41	41	41	64.5	62.25	62.75	58.5	58.75	58.5	58.5	57.5	55	52.25	52.25	52.25
Manpower Cost x $1000																																				
Total Material Cost x $1000	40.5	35	20	15	6	36	56	36	6	51	10	10	84	33	9			30							75	120	75	145	25	25	115	105	135	100	100	
Subcontracts	104	104	104	104	104	104	104	104	104	109	109	109	103	103	103	103	103	103	103	103	103	103	103	103	219	219	219	219	219	219	204	204	204	204	204	204
Total Contract x $1000																																				

Figure 20C